Advances in Global Change Research 46

Sergio M. Vicente-Serrano
Ricardo M. Trigo *Editors*

Hydrological, Socioeconomic and Ecological Impacts of the North Atlantic Oscillation in the Mediterranean Region

Springer

Hydrological, Socioeconomic and Ecological Impacts of the North Atlantic Oscillation in the Mediterranean Region

ADVANCES IN GLOBAL CHANGE RESEARCH

VOLUME 46

For other titles published in this series, go to
www.springer.com/series/5588

Sergio M. Vicente-Serrano · Ricardo M. Trigo
Editors

Hydrological, Socioeconomic and Ecological Impacts of the North Atlantic Oscillation in the Mediterranean Region

Springer

Editors
Sergio M. Vicente-Serrano
Spanish National Research Council (CSIC)
Pyrenean Institute of Ecology
Avda. Montañana 1005
50059 Zaragoza
Spain
svicen@ipe.csic.es

Ricardo M. Trigo
Campo Grande
Faculdade de Ciencias
Instituto Dom Luiz, Universidade de Lisboa
Edificio C8
Piso 3
1749-016 Lisbon
Portugal
rmtrigo@fc.ul.pt

ISSN 1574-0919
ISBN 978-94-007-1371-0 e-ISBN 978-94-007-1372-7
DOI 10.1007/978-94-007-1372-7
Springer Dordrecht Heidelberg London New York

Library of Congress Control Number: 2011929639

Contents

Contributors

Marta Angulo-Martínez Estación Experimental de Aula Dei, Spanish National Research Council (CSIC), Zaragoza, Spain, mangulo@eead.csic.es

Cesar Azorin-Molina Instituto Pirenaico de Ecología, Spanish National Research Council (CSIC), Zaragoza, Spain, cazorin@ipe.csic.es

Carles Barriocanal Departament de Geografia, Universitat de Girona, Girona, Spain, carles.barriocanal@udg.edu

Santiago Beguería Estación Experimental de Aula Dei, Spanish National Research Council (CSIC), Zaragoza, Spain, sbegueria@eead.csic.es

Martin Beniston C3i-Climate Change and Climate Impacts Group, University of Geneva, Geneva, Switzerland, martin.beniston@unige.ch

Jesús Julio Camarero ARAID-Instituto Pirenaico de Ecología, Spanish National Research Council (CSIC), Zaragoza, Spain, jjcamarero@ipe.csic.es

Anna Dalla Marta Department of Plant, Soil and Environmental Science, University of Florence, Florence, Italy, anna.dallamarta@unifi.it

Uri Dayan Department of Geography, The Hebrew University of Jerusalem, Jerusalem, Israel, msudayan@mscc.huji.ac.il

Ahmed El Kenawy Instituto Pirenaico de Ecología, Spanish National Research Council (CSIC), Zaragoza, Spain, kenawy@ipe.csic.es

Oscar Gordo Departamento de Zoología y Antropología Física, Universidad Complutense de Madrid, Madrid, Spain, ogordo@bio.ucm.es

Célia Gouveia Faculty of Sciences, Instituto Dom Luiz (IDL), University of Lisbon, Lisbon, Portugal; EST, Polytechnic Institute of Setubal, Setúbal, Portugal, cmgouveia@fc.ul.pt

Daniele Grifoni Institute of Biometeorology, National Research Council, Florence, Italy, d.grifoni@ibimet.cnr.it

Ercan Kahya Istanbul Technical University, Istanbul, Turkey, kahyae@itu.edu.tr

Vicente Lara-Fanego Department of Physics, University of Jaén, Jaén, Spain, vlara@ujaen.es

Juan I. López-Moreno Instituto Pirenaico de Ecología, Spanish National Research Council (CSIC), Zaragoza, Spain, nlopez@ipe.csic.es

Jorge Lorenzo-Lacruz Instituto Pirenaico de Ecología, Spanish National Research Council (CSIC), Zaragoza, Spain, jlorenzo@ipe.csic.es

Marco Mancini Department of Plant, Soil and Environmental Science, University of Florence, Florence, Italy, marco.mancini@unifi.it

Francesc Maynou Institut de Ciències del Mar, Spanish National Research Council (CSIC), Barcelona, Spain, maynouf@icm.csic.es

Enrique Morán-Tejeda Instituto Pirenaico de Ecología, Spanish National Research Council (CSIC), Zaragoza, Spain, emoran@ipe.csic.es

Simone Orlandini Department of Plant, Soil and Environmental Science, University of Florence, Florence, Italy, simone.orlandini@unifi.it

Tim J. Osborn Climatic Research Unit, School of Environmental Sciences, University of East Anglia, Norwich, UK, t.osborn@uea.ac.uk

Edmond Pasho Instituto Pirenaico de Ecología, Spanish National Research Council (CSIC), Zaragoza, Spain, mondipasho@gmail.com

David Pozo-Vazquez Department of Physics, University of Jaén, Jaén, Spain, dpozo@ujaen.es

David Robson Institut Català d'Ornitologia, Barcelona, Spain, drbn@yahoo.com

Jose Antonio Ruiz-Arias Department of Physics, University of Jaén, Jaén, Spain, jararias@ujaen.es

Francisco Javier Santos-Alamillos Department of Physics, University of Jaén, Jaén, Spain, fsantos@ujaen.es

Joaquín Tovar-Pescador Department of Physics, University of Jaén, Jaén, Spain, jtovar@ujaen.es

Ricardo M. Trigo Instituto Dom Luiz, Universidade de Lisboa, Campo Grande, Faculdade de Ciencias, Edificio C8, Piso 3, 1749-016 Lisbon, Portugal, rmtrigo@fc.ul.pt

Sergio M. Vicente-Serrano Instituto Pirenaico de Ecología, Spanish National Research Council (CSIC), Zaragoza, Spain, svicen@ipe.csic.es

Javier Zabalza Instituto Pirenaico de Ecología, Spanish National Research Council (CSIC), Zaragoza, Spain, jzabalza@ipe.csic.es

José Luís Zêzere Centre for Geographical Studies, Institute of Geography and Spatial Planning, University of Lisbon, Lisboa, Portugal, zezere@campus.ul.pt

Introduction

Sergio M. Vicente-Serrano and Ricardo M. Trigo

This book is a collection of the main contributions in a thematic workshop devoted to the hydrological, socioeconomic, and ecological impacts of the NAO in the Mediterranean area that was held in Zaragoza (Spain), in May 2010, in the framework of the European Science Foundation (ESF) Mediterranean Climate Variability and Predictability (MedCLIVAR) program (http://www.medclivar.eu/).

According to the latest IPCC report, the Mediterranean basin represents one of the most important "hot spots" of climate change in the world, with recent trends towards a hotter and drier climate being related to changes in atmospheric circulation patterns. Previous work has shown that the interannual variability of Mediterranean climate is mostly associated to changes in certain relevant atmospheric circulation patterns (Dünkeloh and Jacobeit, 2003; Zorita et al., 1992; Xoplaki et al., 2003, 2004; Pauling et al., 2006; Trigo et al., 2006). Such changes can have significant impacts in the climate of this region but also on the natural environment and several socioeconomic activities. Among these patterns, the North Atlantic Oscillation (NAO) is the only one which shows a clear signal throughout the whole year, although with stronger intensity and extension during winter due to the stronger meridional gradients (Lamb and Peppler, 1987; Hurrell et al., 2003). During this season changes in the NAO phase lead to shifts in the location of the centers of action and in the associated storm tracks (Trigo, 2006).

The NAO is responsible for most of the climatic variability in the North Atlantic, modifying direction and intensity of the westerlies, the track of the polar depressions and the location of the anticyclones (Hurrell, 1995; Wanner et al., 2001). During the positive phases, the Azores subtropical high is reinforced, leading to sunny and dry weather in the Mediterranean region (Trigo et al., 2002). On the contrary, during the negative winters, cyclones move southward increasing precipitation on the western Mediterranean (Hurrell and Van Loon, 1997; García-Herrera et al., 2001; Moses et al., 1987). Cloudiness, temperature and solar radiation are also highly modulated by the NAO index (Trigo et al., 2002).

S.M. Vicente-Serrano (✉)
Instituto Pirenaico de Ecología, Spanish National Research Council (CSIC), Zaragoza, Spain
e-mail: svicen@ipe.csic.es

S.M. Vicente-Serrano, R.M. Trigo (eds.), *Hydrological, Socioeconomic and Ecological Impacts of the North Atlantic Oscillation in the Mediterranean Region*, Advances in Global Change Research 46, DOI 10.1007/978-94-007-1372-7_1,

The NAO behavior is characterized by a remarkable interannual variability, which is evident in long instrumental (Jones et al., 1997) but equally in paleo records (Cook et al., 2002; Luterbacher et al., 2002). In the instrumental period, the NAO has shown important decadal variability and a decreasing trend between 1940 and 1970. Nevertheless, the most unusual period was observed between the 1970s and 1990s when the NAO showed an increasing tendency towards positive phases (Osborn et al., 1999), coincident with severe drought conditions in the Mediterranean (López-Moreno and Vicente-Serrano, 2008; Sousa et al., 2011) and a reinforced NAO influence on climate (Vicente-Serrano and López-Moreno, 2008a). High variability has been recorded during the first decade of the twenty-first century, including extreme seasonal values of the NAO index. As usual, extreme winter NAO values are at the root of large climate impacts on different natural hazards (e.g. floods, droughts, landslides) but also several important socio-economic areas such as agriculture, renewable energies production, water resources. Thus the winter 2001 (2005) was characterised by several monthly negative (positive) values of NAO inducing an abnormally wet (dry) year in western Mediterranean (García-Herrera et al., 2007). However, the recent winter 2010 was characterised by the most negative NAO winter value ever recorded, and it has caused notable climate anomalies and impacts namely a colder than usual central Europe (Cattiaux et al., 2010) and a wetter than usual Western Mediterranean region (Vicente-Serrano et al., 2011).

The complexity of the NAO behaviour and their impact has attracted the attention of a wide variety of scientific communities, with more than 3800 papers published on different NAO features during the last decade (SCOPUS database, visit: 15/11/2010). The association between the NAO and the Mediterranean climate variability has been well documented, showing that it is one of the main forcing factors in the region. Its impact on extreme events such as droughts, severe precipitations or heat and cold waves has been well established (e.g. Gallego et al., 2006; Garcia-Herrera et al., 2007; Della-Marta et al., 2007; López-Moreno and Vicente-Serrano, 2008). These changes have also an impact on the availability of water resources throughout the entire basin, affecting, not only river flows but also storage availability in lakes and reservoirs and snow cover (Trigo et al., 2004; Karabörk et al., 2005; López-Moreno et al., 2007; Küçük et al., 2009). The ecological dynamics of the region is also greatly affected, as has been shown through satellite imagery and tree rings (Gouveia et al., 2008; Vicente-Serrano and Heredia, 2004; Roig et al., 2009). This has an impact on the quality and quantity of crops and in the migration and welfare of animal populations (Gimeno et al., 2002; Rubolini et al., 2007). The marine environment is also affected by NAO through changes in sea level and fisheries dynamics (Woolf et al., 2003; Lloret et al., 2001; Maynou, 2008). Other reported impacts are landslides (Zêzere et al., 2008), air pollution and human health (Dayan and Lamb, 2008).

Current climate change scenarios obtained with state-of-the-art General Circulation Models (GCMs) predict large modifications in the NAO behaviour in the next decades, however a clear change towards more positive or negative NAO values has not been yet universally established (Solomon et al., 2007). Nevertheless,

the majority of the GCMs indicate as the most probable outcome an increase of the NAO values, with a decreased gradient of the Sea Level Pressures and more frequent positive NAO phases (Osborn et al., 1999; Osborn, 2004; Demuzere et al., 2009). However, the increase likelihood of positive NAO mode does not eliminate the high inter-annual variability, thus the possibility of occurrence of extreme negative values, which can trigger large impacts (Vicente-Serrano et al., 2011). In addition, GCMs predict a more robust and stable link between NAO and surface climate variables (Raible et al., 2006; Vicente-Serrano and López-Moreno, 2008b), suggesting that future climate variability, and their related impacts in the Mediterranean region might be controlled even more by the NAO pattern under a warmer world.

The NAO impacts on Northern Europe have been well reviewed and compiled (Hurrell et al., 2003), but no similar work has been attempted for the Mediterranean, which is the other key area impacted by NAO (Trigo et al., 2006). The aim of the book "Hydrological, socioeconomic and ecological impacts of the North Atlantic Oscillation in the Mediterranean region" is to serve as an updated reference text that covers the wide range of evidences on the NAO impacts in the Mediterranean regions and from a multidisciplinary perspective. We hope that this volume constitutes a unique document to present the state of the art of the numerous studies undertaken on the Hydrological, Socioeconomic and Ecological impact of the NAO, collecting the expertise of researchers from several complementary earth science fields (Geography, Hydrology, Remote-sensing, Climatology, Agriculture, Energy), but that have been lacking a common ground.

The first book chapter provides an updated overview on the internal spatial and temporal variability of the NAO and how external forcing factors may affect the future NAO pattern. Tim J. Osborn shows how multi-model ensemble of simulations under increasing anthropogenic forcing strengthens earlier findings of a shift in the mean state of the winter atmospheric circulation towards positive NAO conditions, but he indicates that if a shift towards positive NAO conditions is a realistic response to increasing anthropogenic forcing, then this signal has not yet emerged from the natural variability. He discuss that anthropogenic forcing could be altering the temporal or spatial character of the interannual NAO variability, though only relatively small changes in pattern are evident when considering a multi-model ensemble.

Some of the book chapters focus on the NAO impacts on climate extreme events, like droughts, which will also have subsequent environmental, hydrological and socioeconomic impacts. The paper by Sergio M. Vicente-Serrano and co-authors show the influence of the NAO on droughts in the entire Mediterranean region, focussing on the use of the Standardized Precipitation Evapotranspiration Index, a multi-scale drought indicator that allows to determine how the effects of the winter NAO are propagated for further months when long time scales of drought are analysed.

In terms of the hydrological impacts of the NAO, Ricardo M. Trigo presents that the strong control exerted by NAO on precipitation is very significant between October and March, being extensive to the river flow of major Iberian rivers, such as Douro/Duero, Tejo/Tagus and Guadiana. Correlation coefficient values computed between Iberian winter river flow and contemporaneous (and lagged) winter NAO

index show that the large inter-annual variability of the rivers flow is largely modulated by the NAO phenomena. In fact this mode controls inter-annual and decadal variability of both precipitation and river flow of large sectors of Iberia. In the East of the Mediterranean region the hydrological variability of river discharges and lake levels is also determined by the NAO. Ercan Kahya documents the impact of the NAO on the hydrology of eastern Mediterranean countries, such as Turkey, Iran, Kuwait, Oman, and Israel from a general perspective. Patterns of precipitation, streamflow, and lake levels in Turkey are discussed to show the NAO impacts. He devotes special attention to the NAO influences on the formation of streamflow homogeneous region and on the probability distribution functions of critical droughts. The results of his analyses clearly shows that the NAO signals are quite identifiable in various hydrologic variables in Turkey.

The NAO also affects the water stored in the form of snow with evident hydrological but also tourist implications, since the winter snow tourism represents an important income source for several mountain chains located around the Mediterranean basin. Juan I. López-Moreno and collaborators analyse the influence of NAO on the interannual evolution of winter temperature, precipitation and snowpack in these Mediterranean mountains. They show that the snow cover response to winter NAO may differ spatially as a consequence of the different influence of winter NAO on precipitation and temperature. In Switzerland, they show how the influence of NAO on snow is significant at the lowest elevation areas, where temperature is the main control on snowpack accumulation, but in the Pyrenees the highest correlation with snow is found at high elevations where precipitation controls mainly the accumulation of snow related to the NAO control of the interannual variability of precipitation.

Primary activities over land and sea are also being largely affected by NAO. On the one hand, several Mediterranean fisheries reveal inter-annual variations closely related to the NAO variability. Francesc Maynou shows that the NAO explains a large part of the variability in population abundance of red shrimp *Aristeus antennatus* in the western Mediterranean Sea, with a lag of 2–3 years. Moreover, the stocks of hake also respond to the NAO since positive NAO years enhance hake fishery production through increasing the individual size of recruits, as well as the individual weight and abundance of adult hake. The NAO signal is also observed in the crop productions as Simone Orlandini and collaborators illustrate. They stress that besides common meteorological information supplied by local stations, the use of the NAO may allow to forecast agricultural yields and production quality in regions of the Mediterranean basin.

The dynamic of ecosystems of the Mediterranean region is also largely determined by the NAO. In their chapter, Célia Gouveia and Ricardo Trigo analyse the relationship between NAO, vegetation dynamics and carbon absorption over Iberian Peninsula. They provides strong evidence that positive (negative) values of winter NAO induce low (high) vegetation activity in the following spring and summer seasons. These features are mainly associated with the impact of NAO on winter precipitation, together with the strong dependence of the spring and summer vegetation activity on water availability during the previous winter. Jesus J. Camarero

quantified the tree growth responses to NAO index across a climatic gradient in Northeastern Spain, considering ten tree species with contrasting habitats and plausibly different growth responses to climate. He shows that climatic variables and NAO indices explained on average 40.1 and 15.9% of the growth variance, respectively. He also shows how the growth responses to climate and NAO also changed through time, illustrating how long tree-ring chronologies of different species may serve as valuable monitors of the responses of forests to winter NAO. In terms of animal communities, Oscar Gordo and collaborators review more than 60 studies that have demonstrated the effects of the NAO on both terrestrial and aquatic Mediterranean ecosystems. They show how the NAO affects the condition and diet of mammals and disease-related mortality in amphibians and how the birds communities are affected by NAO impacts on the availability and extent of their habitat and by influencing dispersal decisions of individuals. Thus, they illustrate how the NAO plays an essential role in the migration of birds throughout the Mediterranean basin, and it is probably a reason for the observed advance of arrival dates during the spring in Europe.

Moreover, the environmental NAO impacts are also evident in terms of air quality and contaminants dispersion. Uri Dayan presents simulations of transport of anthropogenic CO for high and low phases of the NAO. He shows the different spatial and temporal influence played by the positive and negative phases of the NAO mode when controlling the dust tranport to the Mediterranean: the positive phase during summer over the western region and the negative one regulating dust transport over the Eastern Mediterranean in winter. He indicates that positive phases imply a reduced import of European trace gases, an enhancement of long range transport of air pollutants from North American sources and conditions in favor of mobilization and transport of North African dust mainly to the western part of this fragile basin.

Geomorphological processes in the Mediterranean region are also being largely affected by the NAO. The erosive capacity of rainfall is the factor that triggers different surface processes that finally determine soil erosion. Marta Angulo-Martínez and Santiago Beguería illustrate in a western Mediterranean area how the erosive power of rainfall is stronger during the negative phase of NAO and weaker during positive NAO conditions, a finding very useful in the implementation of soil conservation strategies. In addition, soil intensity and magnitude also triggers mass movements and landslides. José Luís Zêzere and Ricardo Trigo show that NAO have an impact on the landslide events that have occurred in the region located just north of Lisbon between 1956 and 2010. Thus, they show how many months with landslide activity are characterized by negative average values of the NAO index and high values of average precipitation (above 95 mm/month).

The volume ends showing the influence of the NAO on a key economic sector that at present is increasing its economic importance. David Pozo-Vazquez and collaborators explore the influence of the NAO on the solar and wind energy resources in the Mediterranean area, in particular, and over the whole North Atlantic area, in general. They show that interannual variability of the solar and wind energy resources in the Mediterranean area can reach values above 20% in winter and 10% in the annual case associated with changes in the NAO phase. They results are of interest

regarding the estimation of the expected interannual variability of the wind farms and solar plants production in the study region.

The set of chapters of this books provides the most complete overview about the impacts of the NAO in the Mediterranean region, highlighting the importance of this phenomenon not only in terms of the understanding of climate processes in the region, but also to know in depth the derived impacts that are affecting our environment, economy and natural resources.

Acknowledgements The scientific workshop that made possible this book was supported by the European Science Foundation, in the framework of the Mediterranean Climate Variability and Predictability (MedCLIVAR) program, the Spanish Ministry of Science and Innovation and the Aragón Government (Spain).

References

Cattiaux J, Vautard R, Cassou C, Yiou P, Masson-Delmotte V, Codron F (2010) Winter 2010 in Europe: a cold extreme in a warming climate. Geophys Res Lett 37. doi:10.1029/2010GL044613

Cook E, D'Arrigo RD, Mann ME (2002) A well-verified, multiproxy reconstruction of the winter North Atlantic Oscillation Index since A.D. 1400. J Clim 15:1754–1764

Dayan U, Lamb D (2008) Influence of atmospheric circulation on the variability of wet sulfate deposition. Int J Climatol 28:1315–1324

Della-Marta PM, Luterbacher J, von Weissenfluh H, Xoplaki E, Brunet M, Wanner H (2007) Summer heat waves over western Europe 1880–2003, their relationship to large-scale forcings and predictability. Clim Dyn 29:251–275

Demuzere M, Werner M, van Lipzig NPM, Roeckner E (2009) An analysis of present and future ECHAM5 pressure fields using a classification of circulation patterns. Int J Climatol 29: 1796–1810

Dünkeloh A, Jacobeit J (2003) Circulation dynamics of mediterranean precipitation variability 1948–98. Int J Climatol 23:1843–1866

Gallego MC, García JA, Vaquero JM, Mateos VL (2006) Changes in frequency and intensity of daily precipitation over the Iberian Peninsula. J Geophys Res D: Atmos 111:D24105. doi:10.1029/2006JD007280

García-Herrera R, Paredes D, Trigo RM, Trigo IF, Hernández H, Barriopedro D, Mendes MT (2007) The outstanding 2004–2005 drought in the Iberian Peninsula: the associated atmospheric circulation. J Hidrometeorol 9:483–498

García-Herrera R, Gallego D, Hernández E, Gimeno L, Ribera P (2001) Influence of the North Atlantic Oscillation on the Canary Island precipitation. J Clim 14:3889–3903

Gimeno L, Ribera P, Iglesias R, de la Torre L, Garcia R, Hernandez E (2002) Identification of empirical relationships between indices of ENSO and NAO and agricultural yields in Spain. Clim Res 21:165–172

Gouveia C, Trigo RM, DaCamara CC, Libonati R, Pereira JMC (2008) The North Atlantic Oscillation and European vegetation dynamics. Int J Climatol 28:1835–1847

Hurrell J (1995) Decadal trends in North Atlantic Oscillation and relationship to regional temperature and precipitation. Science 269:676–679

Hurrell JW, Kushnir Y, Ottersen G, Visbeck M (2003) The North Atlantic Oscillation: climate significance and environmental impact. Geophysical monograph series, vol 134. American Geophysical Union, Washington, DC

Hurrell J, Van Loon H (1997) Decadal variations in climate associated with the North Atlantic Oscillation. Clim Change 36:301–326

Jones PD, Jónsson T, Wheeler D (1997) Extension to the North Atlantic Oscillation using early instrumental pressure observations from Gibraltar and South-West Iceland. Int J Climatol 17:1433–1450

Karabörk MÇ, Kahya E, Karaca M (2005) The influences of the southern and North Atlantic Oscillations on climatic surface variables in Turkey. Hydrol Process 19:1185–1211

Küçük M, Kahya E, Cengiz TM, Karaca M (2009) North Atlantic Oscillation influences on Turkish lake levels. Hydrol Process 23:893–906

Lamb PJ, Peppler RA (1987) North Atlantic Oscillation: concept and application. Bull Am Meteorol Soc 68:1218–1225

Lloret J, Lleonart J, Solé I, Fromentin J-M (2001) Fluctuations of landings and environmental conditions in the north-western Mediterranean sea. Fisheries Oceanogr 10:33–50

Luterbacher J, Xoplaki E, Dietrich D, Jones PD, Davies TD, Portis D, González-Rouco JF, von Storch H, Gyalistras D, Casty C, Wanner H (2002) Extending North Atlantic Oscillation reconstructions back to 1500. Atmos Sci Lett 2:114–124

López-Moreno JI, Beguería S, Vicente-Serrano SM, García-Ruiz JM (2007) The influence of the NAO on water resources in Central Iberia: precipitation, streamflow anomalies and reservoir management strategies. Water Resour Res 43:W09411. doi:10.1029/2007WR005864

López-Moreno JI, Vicente-Serrano SM (2008) Extreme phases of the wintertime North Atlantic Oscillation and drought occurrence over Europe: a multi-temporal-scale approach. J Clim 21:1220–1243

Maynou F (2008) Influence of the North Atlantic Oscillation on Mediterranean deep-sea shrimp landings. Clim Res 36:253–257

Moses T, Kiladis N, Díaz H, Barry R (1987) Characteristics and frequency of reversals in mean sea level pressure in the north Atlantic sector and their relationship to long term temperature trend. J Climatol 7:13–30

Osborn TJ (2004) Simulating the winter North Atlantic Oscillation: the roles of internal variability and greenhouse gas forcing. Clim Dyn 22:605–623

Osborn TJ, Briffa KR, Tett SFB, Jones PD, Trigo RM (1999) Evaluation of the North Atlantic Oscillation as simulated by a coupled climate model. Clim Dyn 15:685–702

Pauling A, Luterbacher J, Casty C, Wanner H (2006) Five hundred years of gridded high-resolution precipitation reconstructions over Europe and the connection to large-scale circulation. Clim Dyn 26:387–405

Raible CC et al (2006) Climate variability-observations, reconstructions, and model simulations for the Atlantic-European and Alpine region from 1500–2100 AD. Clim Change 79:9–29

Roig FA, Barriopedro D, Herrera RG, Patón Domínguez D, Monge S (2009) North Atlantic Oscillation signatures in western Iberian tree-rings. Geogr Ann 91:141–157

Rubolini D, Ambrosini R, Caffi M, Brichetti P, Armiraglio S, Saino N (2007) Long-term trends in first arrival and first egg laying dates of some migrant and resident bird species in northern Italy. Int J Biometeorol 51:553–563

Solomon S, Qin D, Manning M, Chen Z, Marquis M, Averyt KB, Tignor M, Miller HL (2007) Climate change 2007: the physical science basis. Cambridge University Press, Cambridge, UK and New York, NY

Sousa P, Trigo RM, Aizpurua P, Nieto R, Gimeno L, Garcia-Herrera R (2011) Trends and extremes of drought indices throughout the 20th century in the Mediterranean. Nat Hazards Earth Syst Sci 11:33–51

Trigo IF (2006) Climatology and interannual variability of storm-tracks in the Euro-Atlantic sector: a comparison between ERA-40 and NCEP/NCAR reanalyses. Clim Dyn 26:127–143

Trigo RM et al (2006) Relations between variability in the Mediterranean region and Mid-Latitude variability. In: Lionello P, Malanotte-Rizzoli P, Boscolo R (eds) The Mediterranean climate: an overview of the main characteristics and issues. Elsevier, Amsterdam, pp. 179–226

Trigo RM, Osborn TJ, Corte-Real JM (2002) The North Atlantic Oscillation influence on Europe: climate impacts and associated physical mechanisms. Clim Res 20:9–17

Trigo RM, Pozo-Vazquez D, Osborn TJ, Castro-Diez Y, Gamiz-Fortis S, Esteban-Parra MJ (2004) North Atlantic Oscillation influence on precipitation, river flow and water resources in the Iberian Peninsula. Int J Climatol 24:925–944

Vicente-Serrano SM, Heredia A (2004) NAO influence on NDVI trends in the Iberian Peninsula (1982–2000). Int J Remote Sens 25:2871–2879

Vicente-Serrano SM, López-Moreno JI (2008a) The nonstationary influence of the North Atlantic Oscillation on European precipitation. J Geophys Res Atmos 113:D20120. doi:10.1029/2008JD010382

Vicente-Serrano SM, López-Moreno JI (2008b) Differences in the nonstationary influence of the North Atlantic Oscillation on European precipitation under different scenarios of greenhouse gases concentrations. Geophys Res Lett 35:L18710. doi:10.1029/2008GL034832

Vicente-Serrano SM, Trigo RM, López-Moreno JI, Liberato MLR, Lorenzo-Lacruz J, Beguería S, Morán-Tejeda E, El Kenawy A (2011) Extreme winter precipitation in the Iberian Peninsula in 2010: anomalies, driving mechanisms and future projections. Clim Res 46:51–65

Wanner H et al (2001) North Atlantic Oscillation—concepts and studies. Surv Geophys 22:321–382

Woolf DK, Shaw AGP, Tsimplis MN (2003) The influence of the North Atlantic Oscillation on sea-level variability in the North Atlantic region. Global Atmos Ocean Syst 9:145–167

Xoplaki E, González-Rouco JF, Luterbacher J, Wanner H (2003) Mediterranean summer air temperature variability and its connection to the large-scale atmospheric circulation and SSTs. Clim Dyn 20:723–739

Xoplaki E, González-Rouco JF, Luterbacher J, Wanner H (2004) Wet season Mediterranean precipitation variability: influence of large-scale dynamics and trends. Clim Dyn 23:63–78

Zêzere JL, Trigo RM, Fragoso M, Oliveira SC, Garcia RAC (2008) Rainfall-triggered landslides in the Lisbon region over 2006 and relationships with the North Atlantic Oscillation. Nat Hazards Earth Syst Sci 8:483–499

Zorita E, Kharin V, Von Storch H (1992) The atmospheric circulation and sea surface temperature in the North Atlantic area in winter: their interaction and relevance for Iberian precipitation. J Clim 5:1097–1108

Variability and Changes in the North Atlantic Oscillation Index

Tim J. Osborn

Abstract Most – or perhaps even all – of the observed variations in the winter North Atlantic Oscillation (NAO) index can be explained as internally-generated climate variability. The influence of external forcing factors on the observed NAO behaviour is still an open question. Two sea level pressure datasets yield different results for the strength of the winter NAO trend from the 1960s to the 1990s, though these trends from both datasets lie outside the 90% range of trends generated by the internal variability of climate models, and the latter is more precisely known now that over 8000 years of simulation under constant forcing is available for analysis. Similarly, a much expanded, multi-model ensemble of simulations under increasing anthropogenic forcing strengthens earlier findings of a shift in the mean state of the winter atmospheric circulation towards positive NAO conditions. There is considerable inter-model spread in both the magnitude of this response to increased forcing and in its regional structure, but of the 21 climate models analysed here, none showed an overall decrease in the mean level of the NAO index. If a shift towards positive NAO conditions is a realistic response to increasing anthropogenic forcing, then this signal has not yet emerged from the natural variability: observations since the 1990s show a return to lower values, and the 2009/2010 winter had the record negative NAO index in a record lasting almost two centuries. It is possible that anthropogenic forcing could be altering the temporal or spatial character of the interannual NAO variability, though only relatively small changes in pattern are evident when considering the multi-model ensemble as a whole and there is only weak evidence for an increase in the interannual variance.

Keywords Internal variability · External forcing · North Atlantic Oscillation index · Temperature

T.J. Osborn (✉)
Climatic Research Unit, School of Environmental Sciences, University of East Anglia, Norwich, UK
e-mail: t.osborn@uea.ac.uk

S.M. Vicente-Serrano, R.M. Trigo (eds.), *Hydrological, Socioeconomic and Ecological Impacts of the North Atlantic Oscillation in the Mediterranean Region*, Advances in Global Change Research 46, DOI 10.1007/978-94-007-1372-7_2,

1 Introduction

The interannual variability of the North Atlantic Oscillation (NAO) represents between 20 and 30% of the Northern Hemisphere winter atmospheric sea-level pressure (SLP) variance, and an even greater part of the variance in the Atlantic-European sector (e.g. Hurrell and Deser, 2009). For example, defining the NAO index as the leading principal component of winter (December to February or December to March, as here, are typically used) SLP in the domain 15–90°N and 110°W–70°E represents around 40% of the variance in this domain (Figs. 1a and 2a), updated from Osborn (2004). Taking instead a station-based index – simply the difference between standardised or raw SLP records near the Azores High and Iceland Low pressure systems can yield a longer record, but captures slightly less variance (because the principal component was optimised to maximise the variance captured). The Gibraltar minus Iceland record first developed by Jones et al. (1997) and updated here (Fig. 1b) now contains 187 complete winters (only those since 1887 are shown here).

This is all well established, as are the links between the NAO and some aspects of surface climate (Trigo et al., 2002; López-Moreno and Vicente-Serrano, 2008; and

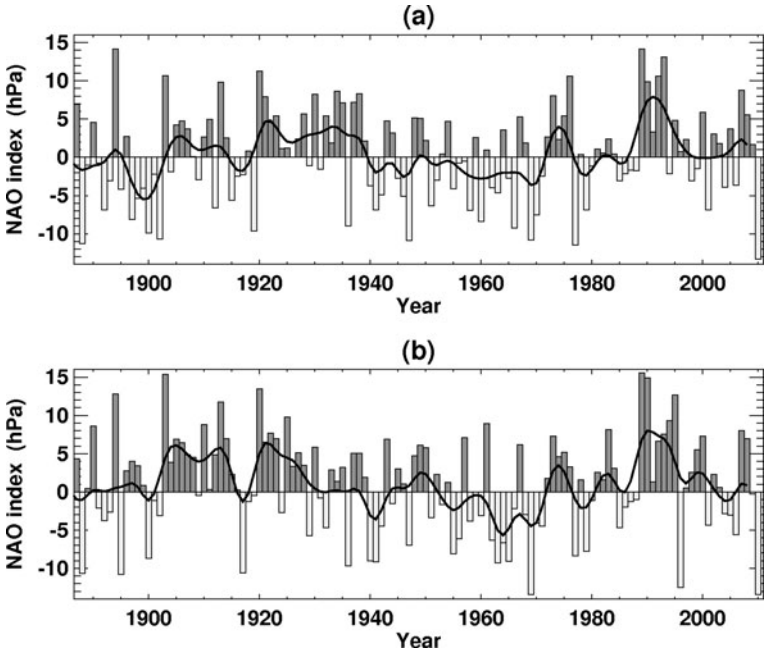

Fig. 1 Two alternative observed timeseries of the winter NAO index. (**a**) The leading principal component timeseries of Atlantic-European SLP, using the HadSLP2r dataset (Allan and Ansell, 2006). (**b**) The difference between Gibraltar and southwest Iceland SLP observations. The values represent the absolute pressure difference (hPa) between winter-mean values (**a**) from the maxima and minima of the EOF pattern, and (**b**) from Gibraltar and Iceland

many others). More recent research, coupled with longer observational records that enable empirical relationships to be better established, is increasing this knowledge and also extending it to new areas such as the consequences of NAO variability for various natural and societal systems. See the rest of this volume for many examples. What is considerably more uncertain is the link between internally-generated variability and externally-forced change, and whether the signature of the latter is evident in the observed record. The positive trend in the NAO index from the 1960s to the 1990s, evident in Fig. 1, has been a particular focus of such work (Osborn et al., 1999; Gillett et al., 2003; Osborn, 2004), though more general changes in the mean level of the NAO index have also been considered (Selten et al., 2004).

Others have investigated changes in the spatial structure of the NAO pattern (Fig. 2a). For example, a tendency for an eastward shift or extension of the NAO signature is apparent during part of the observed record (1978–1997 compared with 1958–1977; Jung et al., 2003) and also in the response to increased greenhouse gas concentrations simulated by some climate models (Ulbrich and Christoph, 1999). Multi-model analyses (Osborn, 2004; Kuzmina et al., 2005) suggest that such a result is model dependent, though the multi-model mean response in both cases did show a small north-eastward shift (Fig. 2b–d). A reconsideration of this is worthwhile using more recent climate models that typically have finer resolution and increasingly sophisticated representations of some physical and dynamical processes.

In addition to possible shifts in the mean level of the NAO index – i.e. corresponding to a change in the mean atmospheric circulation that has a structure that correlates positively with the NAO pattern (Fig. 2a) – or in the pattern of interannual NAO variability, it is feasible that external forcing could influence the *amplitude* of temporal variability. This is of topical interest because the winter 2009–2010 NAO index had a record low value in the 187-year record (Osborn, 2011). Though this could simply be a random event arising from internal variability, it is also important to assess the evidence for externally-forced changes in NAO variance which could alter the likelihood of such extreme events.

This chapter is structured as follows: Section 2 provides a brief description of the observed and climate model simulated datasets used in this study, while Section 3 compares the observed record with the range of internal variability simulated by the

Fig. 2 Spatial patterns of SLP variability associated with the winter NAO, estimated from the regression coefficients between local SLP and the NAO principal component index. (**a**) Observed pattern using HadSLP2r (Allan and Ansell, 2006). (**b**) Average simulated pattern from 7 older climate models used by Osborn (2004), using pre-industrial or twentieth-century control runs. (**c**) As (**b**), but using the 2050–2099 period under a scenario with increasing CO_2 concentrations (1% year^{-1}). (**d**) Difference (**c**) minus (**b**). (**e**) Average simulated pattern from 22 CMIP3 climate models, using the 1922–1999 period under historic forcing (anthropogenic only or anthropogenic and natural). (**f**) As (**e**), but using the 2050–2099 period under the SRES A1B scenario of increasing anthropogenic forcing. (**g**) Difference (**f**) minus (**e**). Note that the contour interval is 4 times smaller in *panel* (**d**) than in *panels* (**b**) and (**c**), and is 10 times smaller in *panel* (**g**) than in *panels* (**e**) and (**f**)

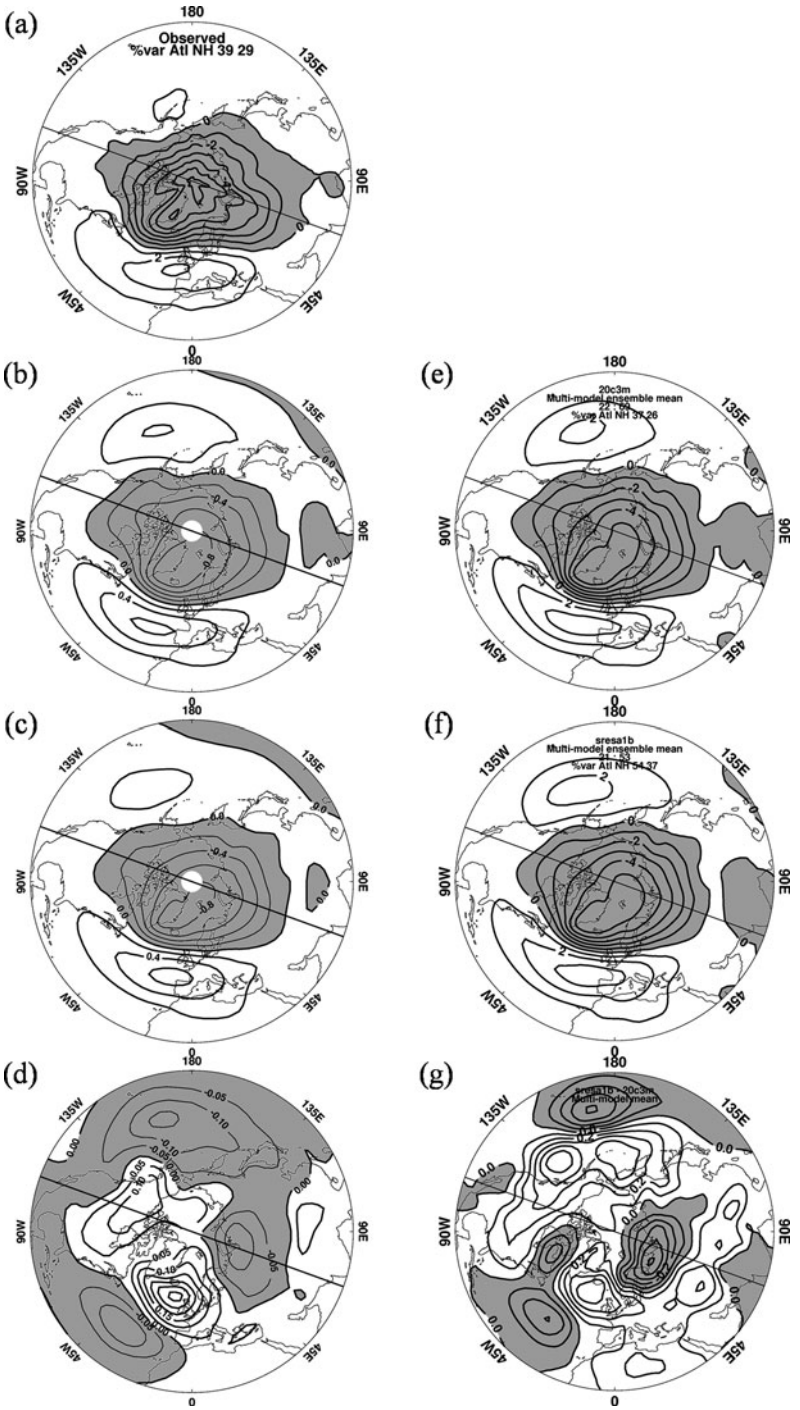

Fig. 2 (continued)

climate models. Then the simulated response to increasing greenhouse gases and other anthropogenic forcings is described, for the mean circulation (Section 4), the pattern of interannual variability (Section 5) and the amplitude of temporal variance (Section 6), before some concluding remarks in Section 7.

2 Observed and Simulated Data

2.1 Observed Data, NAO Pattern and NAO Index

Monthly-mean SLP fields from 1850 to 2010 from the HadSLP2r dataset (Allan and Ansell, 2006) were used. These consist of fields on a 5° latitude by 5° longitude grid based on ship and weather station observations till 2004, with near-real-time updates from 2005 to 2010 using NCEP/NCAR reanalysis data adjusted so that its climatological average matches the observed data. The EOF analysis used to define the NAO index was applied to the period from 1922 to 1999, because 1922 is the first year in the record when at least 20% of the Northern Hemisphere grid boxes contain at least 30 observations per month (Allan and Ansell, 2006). Note that the HadSLP2r dataset falls back below this threshold from 1941 to 1948; the dataset is spatially complete because it is based on interpolation from the available observations, but nevertheless the values of the NAO index prior to 1922 and between 1941 and 1948 should be considered with more caution.

The spatial pattern of the NAO (Fig. 2a, the leading EOF of the December-to-March seasonal mean SLP) is similar to the pattern found by Hurrell and Deser (2009) who used a longer period, a smaller spatial window focussed on the North Atlantic, and a different SLP dataset (Trenberth and Paolino, 1980, dataset with updates). One difference is in the relative strengths of the northern and southern parts of the dipole, which are more equal in Hurrell and Deser's pattern (bottom panel of their figure 8) compared with that shown in Fig. 2a here, perhaps because the EOF has not been calculated with area-weighting of the SLP data here. Hurrell and Deser (2009) also show that using the shorter December-to-February season (compare the top-left panel of their figure 6 with their figure 8) results in stronger loadings over the North Pacific – which is of interest because most climate models show an EOF pattern with that feature.

The observed NAO index obtained by projecting the HadSLP2r seasonal mean data fields onto the leading EOF is quite similar to the Gibraltar minus Iceland index (Fig. 1). This is in contrast to the earlier analysis of Osborn (2004), where the trend from the 1960s to the 1990s was more pronounced and the early 1990s values were distinctly higher than the preceding century. Osborn (2004) used SLP data based on the UK Met Office analyses, updated from Jones (1987). Hurrell and Deser (2009) use the leading EOF of the Trenberth and Paolino (1980) SLP data to obtain an NAO index that shows a more intermediate result. Although these NAO indices are highly correlated, they do have different characteristics (e.g. the strength of multi-decadal variations compared with shorter term variability) that can influence the statistical significance of trends. Further investigation is needed of the differences between

these SLP datasets (e.g. whether the reduced-space optimal interpolation algorithm used for HadSLP2r affects the amplitude of long-term variations).

2.2 Simulated Data and NAO Patterns

Osborn (2004) reported an analysis of the NAO as simulated by seven climate models whose primary references were published between 1997 and 2000 (table 1 of Osborn, 2004). Here, I report results of similar analyses applied to models that have been developed or improved more recently, using 22 models from the World Climate Research Programme's (WCRP's) Coupled Model Intercomparison Project phase 3 (CMIP3) multi-model dataset (Meehl et al., 2007). The focus is on the multi-model-mean results; detailed results from individual models will be presented elsewhere. The 22 models used here are listed in Table 1. The simulations used are control runs under constant pre-industrial forcings, those under historic transient forcing, beginning between 1850 and 1900 and extending to between 1999 and 2003, and those

Table 1 CMIP3 simulated data used in the analyses presented here

Model	Control run (year)	Historic forcing	Runs	Future forcing (SRES A1B)	Runs
bcc_cm1	–	1871–2003	4	–	–
bccr_bcm2_0	250	1850–1999	1	2000–2099	1
cccma_cgcm3_1	1001	1850–2000	5	2001–2200	5
cccma_cgcm3_1_t63	350	1850–2000	1	2001–2200	1
cnrm_cm3	390	1860–1999	1	2000–2200	1
csiro_mk3_0	380	1871–2000	3	2001–2200	1
gfdl_cm2_0	500	1861–2000	3	2001–2200	1
gfdl_cm2_1	500	1861–2000	3	2001–2200	1
giss_aom	502	1850–2000	2	2001–2100	2
giss_model_e_h	400	1880–1999	5	2000–2099	4
giss_model_e_r	500	1880–2003	9	2004–2200	5
iap_fgoals1_0_g	150	1850–1999	3	2000–2199	3
inmcm3_0	331	1871–2000	1	2001–2200	1
ipsl_cm4	–	1860–2000	1	2000–2100	1
miroc3_2_hires	100	1900–2000	1	2001–2100	1
miroc3_2_medres	500	1850–2000	3	2001–2200	1
				2001–2100	2
mpi_echam5	506	1860–2000	3	2001–2200	3
				2001–2100	1
mri_cgcm2_3_2a	350	1851–2000	5	2001–2200	1
				2001–2100	4
ncar_ccsm3_0	830	1870–1999	8	2000–2199	1
				2000–2099	3
ncar_pcm1	350	1890–1999	3	2000–2200	2
				2000–2099	2
ukmo_hadcm3	341	1860–1999	2	2000–2199	1
ukmo_hadgem1	–	1860–1999	2	2000–2099	1

under the SRES A1B future scenario of increasing greenhouse gas concentrations and other anthropogenic forcing to 2100. For most models, the SRES A1B simulations are extended beyond 2100 with fixed forcings, and model output up to 2200 is used here.

Multiple simulations under the same forcing, but different initial conditions and hence different realisations of internal variability, are available in some cases. These initial-condition ensembles are used by analysing the individual ensemble members separately, and then averaging the results to produce an ensemble mean. Table 1 indicates the availability of simulations, including the size of initial-condition ensembles, for each of the models used here.

Osborn (2004) explained the advantages of regridding all datasets to a common grid prior to analysis, so here all simulated data are regridded to the grid of the HadSLP2r observational data. The same methods described in Osborn (2004) for calculating and scaling the principal component NAO index time series from an EOF analysis of each model simulation are used here – refer to that paper for a detailed description.

The simulated spatial pattern of the NAO, when averaged across the 22 climate models with twentieth century simulations (Fig. 2e), bears a very close resemblance to the observed NAO pattern (Fig. 2a). As with the earlier models (Fig. 2b), the teleconnection between the NAO and the North Pacific is stronger than observed, resembling the Northern Annular Mode more closely (Miller et al., 2006). Note that the NAO is defined here from an EOF analysis of only the Atlantic half of the hemisphere, but the pattern shown in the maps is from the pattern of regression coefficients between the principal component NAO index and SLP from across the entire northern hemisphere. With this exception, the similarity with the observed pattern provides some justification for using these model experiments to investigate NAO behaviour.

3 Comparing the Observed Record with Internally-Generated Climate Variability

The detection of climate changes that might be caused by some external forcing requires the comparison of an observed record with an estimate of the variations that might typically be expected to arise from internal variability. In most cases, the amplitude of internal variability increases with decreasing timescale, so that even where a real climate change is present the likelihood of detecting it is rather small within a short (e.g. sub-decadal) record. But longer-term trends must be compared with an estimate of internally-generated variability on multi-decadal timescales, and a multi-century record is required to provide an adequate sample of such variations. The instrumental record is not long enough and is also "contaminated" by any responses to natural or anthropogenic forcings, rather than being a "pure" representation of internal variability. In most detection studies, therefore, the internal climate variability is estimated from climate model simulations, using

a multi-century control run (i.e., a simulation in which the external forcings are constant).

Detection results are thus completely dependent on whether the climate model(s) adequately simulate climate variability on the timescale of interest (e.g. multi-decadal fluctuations). These simulations can be evaluated by comparison with the observational record, but the focus is of course on the shorter timescales that are sampled within the limited length of the observations. Studies that go beyond detection and include an attempt to attribute some of the observed changes to particular external forcings also check for consistency between the observed changes and a combination of internal variability and attributed external effects. Although this can identify instances where the internal variability simulated by the climate model is inconsistent with the observed evidence, the power of the test is again limited for the crucial multi-decadal timescales.

Osborn (2004) compared the sub-decadal variance of simulated and observed NAO indices and found that three of the models had variances that were significantly higher than observed, while the other four were similar. Detection analyses were repeated, therefore, after scaling the simulated NAO indices to have the same sub-decadal variance as observed. This scaling step profoundly alters the meaning of the detection exercise, as noted by Osborn (2004), because the climate models are then only being used to estimate the *spectral shape* of the NAO indices, rather than the absolute magnitude of NAO variability.

The analysis of Osborn (2004) is repeated here using the CMIP3 pre-industrial control runs (Table 1), together with the NAO index from the HadSLP2r dataset. The 30-year trends evident in this observed NAO index, calculated using a sliding window, are compared with the distributions of 30-year trends simulated by these climate models with fixed, unchanging forcings (Fig. 3). These distributions are calculated from all the 30-year trends in the simulated NAO indices from the 19 climate models with pre-industrial control run data. The 5–95% ranges of these simulated trends are then determined either for each climate model separately (Fig. 3b) or after all the trends have been pooled together over the multi-model ensemble (Fig. 3a). This represents a considerable extension to the analysis of Osborn (2004), with 19 rather than 7 models, and total simulation time of over 8000 years rather than under 3000 years; in addition, many of the models are more sophisticated or have higher spatial and temporal resolution.

The results show that when the simulated NAO indices are scaled to have the same sub-decadal variance as the observed winter NAO index, the 30-year trends centred around 1980 (e.g. 1965–1994) lie outside the 90% range of internal variability simulated by these climate models. The result is the same whether the models are pooled together (Fig. 3a) or whether they are considered separately (Fig. 3b), even for the models with the strongest multi-decadal variability (relative to their sub-decadal variance). Note that Osborn (2004) showed the 95% range (from 2.5 to 97.5%) of the control run variability, whereas here I have used the 90% range (from 5 to 95%) because previous analysis of multi-model ensembles (e.g. Osborn, 2004; Kuzmina et al., 2005) now yields the a priori expectation of an increase in the NAO index, and thus 95% confidence in detecting an externally-forced trend can be

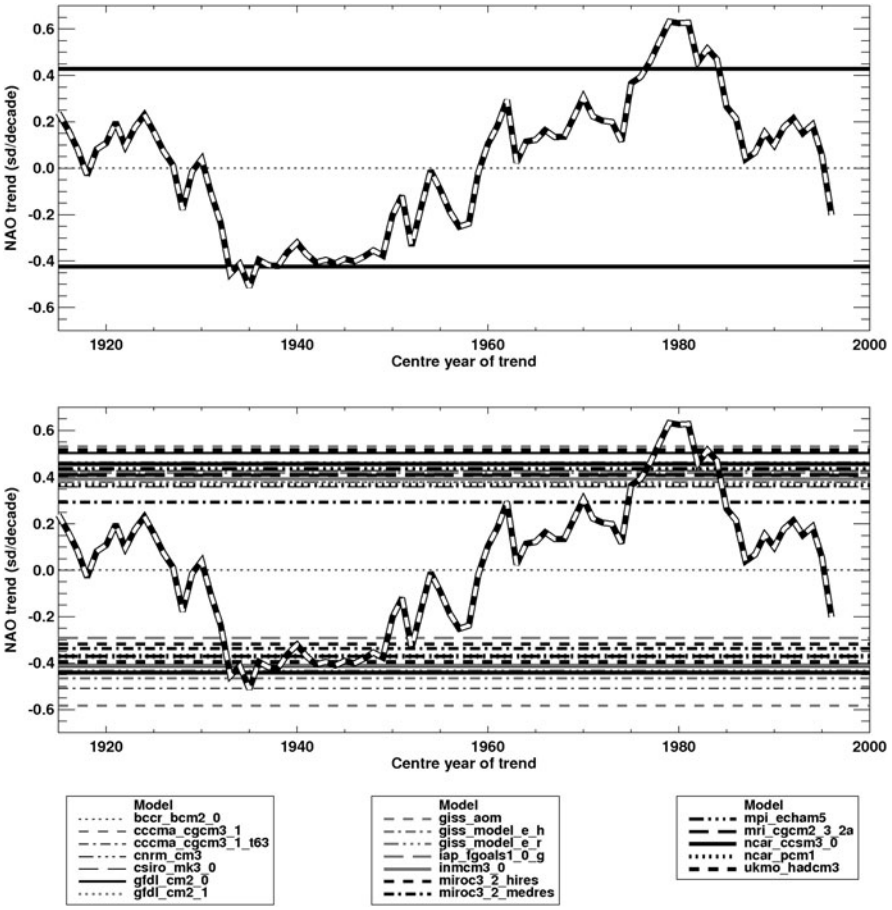

Fig. 3 Thirty-year trends in the observed NAO index, calculated in a sliding window and plotted against the central year of each window (*black dashed curve*), compared with the 5 and 95 percentiles of 30-year NAO index trends arising from the internal variability simulated by 19 climate models (*horizontal lines*). (**a**) The 5 and 95 percentiles of the overall multi-model ensemble; (**b**) the 5 and 95 percentiles of the individual model pre-industrial control runs (see legend). All NAO indices are calculated from the leading EOF pattern of each dataset; all simulated NAO indices were scaled to have the same sub-decadal variance as the observed NAO index; 30-year trends are expressed as a trend in standard deviations per decade

assessed using a one-tailed test. The observed trend also exceeds the 97.5 percentile (not shown) of the CMIP3 control run variability (for all individual models as well as for the multi-model ensemble), so this difference in choice of range is not critical.

The degree to which the observed trend exceeds the simulated internal variability is less in this study than found by Osborn (2004). This is mostly because the NAO index obtained from the HadSLP2r dataset has a considerably weaker trend than that found by Osborn (2004); the former peaks just above 0.6 standard deviations per decade, whereas the latter peaked just over 1.1 standard deviations per decade.

This was noted in Section 2.1. As a result, the behaviour of the observed NAO index might be compatible with the internal variability of the models, since we would expect the 95 percentile to be exceeded 5% of the time purely by chance. The lower NAO values since 1995 also suggest that any contribution to the earlier increase in the winter NAO index from continuing greenhouse gas forcing is likely to be small (see the discussion in Osborn, 2004). The most recent 30-year trend (1981–2010) is still comfortably within the range of internal variability, but analysing 15- or 20-year trends in the same way (not shown) shows that the most recent trends over these shorter periods fall below the 5 percentile of the climate model internal variability.

4 Changes in the Mean Circulation and the Mean NAO Index

The response of the Northern Hemisphere atmospheric circulation in winter to increasing anthropogenic forcing is quite varied between different climate models, though a feature common to all but one (GISS AOM) of the CMIP3 models analysed here is that SLP decreases over most of the Arctic. Most of these climate models also simulate an increase in SLP over parts of the subtropics, though there is less consistency in the location of these increases. The multi-model average change in winter SLP (Fig. 4) displays these consistent or semi-consistent features: decreases in SLP over the Arctic and surrounding high latitudes, and increases over parts of the subtropics, especially the Mediterranean, but also the Pacific and Atlantic. This is in agreement with Miller et al. (2006), who examined the behaviour of the Northern Annular Mode in these models. The multi-model mean pattern of SLP change is stronger and more consistent in the CMIP3 models than in the earlier ensemble analysed by Osborn (2004), and indicates strengthened mean westerly circulation around the mid-latitudes, including across the Atlantic and into northern Europe.

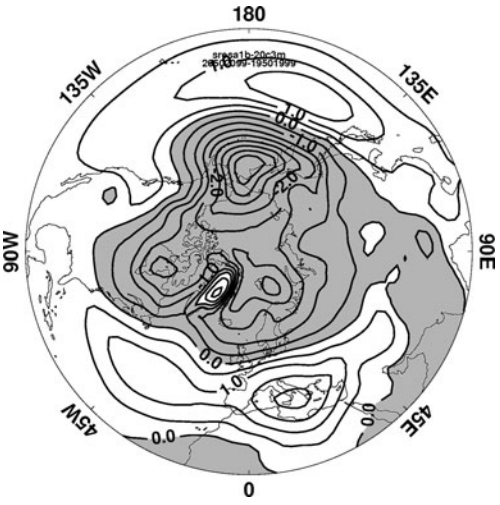

Fig. 4 Differences in long-term mean December-to-March SLP (hPa) simulated during the 1950–1999 period of the historic simulations and the 2050–2099 of the simulations under the SRES A1B scenario, averaged across all available model simulations

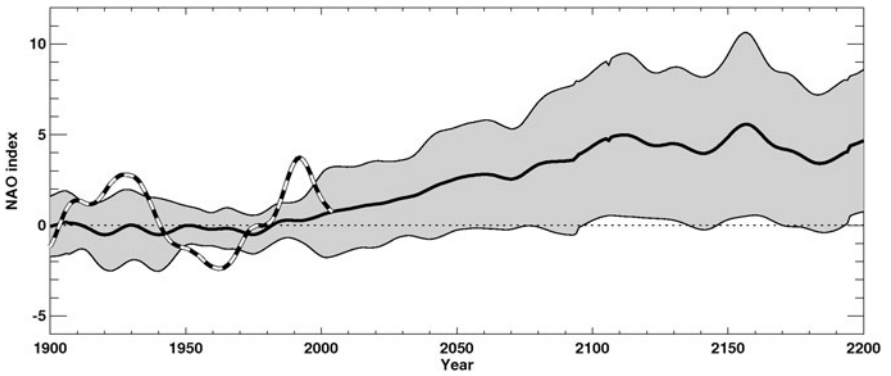

Fig. 5 Timeseries of observed (*black dashed line*) and simulated December-to-March NAO index, smoothed with a 30-year low-pass filter. Only the mean and estimated 5–95% range of the ensemble of individual climate model results are shown, indicated by the *thick black line* and the *grey shading*. The simulations are driven by historic forcing estimates up to around 2000, then by the increasing anthropogenic forcing of the SRES A1B scenario to 2100, followed by constant forcings to 2200. The NAO indices are calculated from the leading EOF pattern of each dataset, and then scaled to represent the change in absolute pressure difference (hPa) between the maximum and minimum of the EOF pattern

There are also strong changes in the western North Pacific, though they are not relevant to the current paper.

Given this multi-model pattern of SLP change, and some consistency between models in the large-scale structure (though not in the regional details for individual models – not shown here), it is not surprising that the simulated NAO indices show a long-term shift towards positive values (Fig. 5). The individual model results (not shown) provide a large range of future projections, from almost no change up to values in excess of a 5 hPa increase in the pressure difference between the locations of maximum and minimum of the EOF patterns (note that these do not correspond exactly with the maximum and minimum in the present-day SLP in this region). The GISS AOM model simulates the lowest NAO index during the twenty-first century, but even for this model there is no statistically significant decrease in the NAO index. The inter-model spread is used to estimate a 5–95% range of NAO projections from the CMIP3 ensemble, and this is shown in Fig. 5. The observed NAO index is also shown, though it is not strictly comparable because some of the model results are based on the mean of an initial-conditions ensemble (Table 1), which reduces the spread arising from internal variability.

5 Changes in the Pattern of Interannual NAO Variability

Previous work (summarised in Section 1) identified the possibility that the spatial pattern of interannual variability represented by the NAO might change when the mean climate changes (e.g. Jung et al., 2003; Ulbrich and Christoph, 1999; Osborn,

2004; Kuzmina et al., 2005). In particular, an eastward (or possibly north-eastward) shift or extension of the main centres of action, especially the northern anomalies associated with the Iceland Low pressure system, might accompany an increase in the mean state of the NAO. Hurrell and Deser (2009) also discuss how this might be related to circulation regimes on shorter timescales, with regimes associated with positive NAO conditions tending to extend further eastward in the subpolar region.

Here, I have only considered the CMIP3 models as a whole ensemble (i.e., they have not been stratified or selected according to the strength of the shift in the mean NAO index, which might have led to different results). For the whole ensemble, the EOF patterns calculated from the last 50 years of the twentieth century and the twenty-first century (under the SRES A1B scenario) are compared in Fig. 2e, f. There is very little difference between the multi-model average of the individual EOFs during the two periods. The difference between the EOF patterns (Fig. 2g) shows some minor differences (note that the contour interval in Fig. 2g is ten times smaller than in 2e and 2f). The small negative changes (shaded) in the loadings over Scandinavia and north-west Russia, coupled with the small positive changes (unshaded) south of Iceland, represent a minor eastward shift in the northern centre of action. The change in the multi-model mean EOF pattern is, however, considerably smaller than obtained by Osborn (2004) from the smaller ensemble of older climate models (Fig. 2b–d).

6 Changes in the Amplitude of Interannual NAO Variability

Few changes in the amplitude of NAO variability simulated by individual CMIP3 climate models are statistically significant. This is not surprising, however, because higher-order statistics, such as the temporal standard deviation, are associated with greater sampling variability and changes in those statistics are, therefore, more "difficult" to detect than changes in the mean climate (i.e. even when a real change in variability is present, the likelihood of detecting it is smaller than for an equivalent change in the mean). Treating them as a multi-model ensemble can help to identify relatively small changes, providing the changes are consistent across models. In this case, however, there is little consistency between models. Comparing the intradecadal standard deviations of the simulated NAO indices during the last 50 years of the twentieth century with the last 50 years of the twenty-first century (under the SRES A1B scenario), seven models show an increase of at least 10%, three show a decrease of at least 10%, and 11 show changes of less than 10%. Averaging across all 21 models shows a minor increase of 4% in the standard deviation of the NAO index under the SRES A1B scenario.

Another measure of interest is the fraction of overall SLP variability that is associated with the NAO. Within the Atlantic half of the hemisphere, and over the same periods used above, there is also little change under increased anthropogenic forcing. Averaged across all 21 models, the SLP variance associated with the leading EOF increases from 39 to 41%. However, when assessed for individual models, there are nearly as many that show a decrease in the variance explained as show an increase.

7 Conclusions

Fluctuations in atmospheric circulation related to the North Atlantic Oscillation are an important driver of climate variability over Europe and the Mediterranean region. Yet it is rather uncertain whether anthropogenic forcings might cause a shift in the mean atmospheric circulation that resembles the NAO, or in some way alter the characteristics of the internal variability of the NAO (e.g. the spatial pattern or the temporal variance). This cannot be confidently determined solely from an empirical analysis of the observed record, due to difficulties in separating the response to individual external forcings from internal variability within the available observational record. Other approaches to learning more about NAO behaviour include examining processes within the atmosphere (e.g. stratosphere-troposphere interactions, Perlwitz and Harnik, 2004) that might influence the NAO.

An alternative approach, taken in this study, is to analyse ensembles of multiple climate models (based on general circulation models of the atmosphere and oceans). Here the CMIP3 ensemble of around 20 climate models shows that increasing anthropogenic forcings (principally greenhouse gases) might drive a shift of the mean circulation towards positive NAO conditions, with enhanced westerly flow across the Atlantic and into northern Europe. The magnitude of the simulated shift is very model dependent, and whether such an externally-forced response is needed to explain the observed NAO record is uncertain. The observed increase in the winter NAO index from the 1960s to the 1990s is large compared with the models' internally-generated variability, but the dependence of the magnitude of this trend on the sea level pressure dataset used, plus the return to lower values of the NAO index since the early 1990s, reduce the likelihood that a strong influence of greenhouse gas forcing is already evident in the observed NAO record. This study significantly extends earlier multi-model analyses of NAO behaviour (Osborn, 2004; Kuzmina et al., 2005) by using many more climate models, including some with finer resolution and more sophisticated representations of physical and dynamical processes. It also complements multi-model studies of related atmospheric circulation features such as the annular modes (Miller et al., 2006).

Acknowledgements This work was supported by a Research Councils UK Academic Fellowship. The modelling groups, the Program for Climate Model Diagnosis and Intercomparison (PCMDI) and the WCRP's Working Group on Coupled Modelling (WGCM) are acknowledged for their roles in making available the WCRP CMIP3 multi-model dataset. Support for CMIP3 dataset is provided by the Office of Science, U.S. Department of Energy.

References

Allan RJ, Ansell TJ (2006) A new globally complete monthly historical mean sea level pressure data set (HadSLP2): 1850–2004. J Clim 19:5816–5842

Gillett NP, Graf HF, Osborn TJ (2003) Climate change and the North Atlantic Oscillation. In Hurrell JW, Kushnir Y, Ottersen G, Visbeck M (eds) North Atlantic Oscillation: climatic significance and environmental impact. Geophysical Monograph, vol 134. American Geophyscial Union, Washington, DC, pp 193–209

Hurrell JW, Deser C (2009) North Atlantic climate variability: the role of the North Atlantic Oscillation. J Mar Syst 78:28–41

Jones PD (1987) The early twentieth century Arctic high—fact or fiction? Clim Dyn 1:63–75. doi:10.1007/BF01054476

Jones PD, Jonsson T, Wheeler D (1997) Extension to the North Atlantic Oscillation using early instrumental pressure observations from Gibraltar and South-West Iceland. Int J Climatol 17:1433–1450

Jung T, Hilmer M, Ruprecht E, Kleppek S, Gulev SK, Zolina O (2003) Characteristics of the recent eastward shift of interannual NAO variability. J Clim 16:3371–3382

Kuzmina SI, Bengtsson L, Johannessen OM, Drange H, Bobylev LP, Miles MW (2005) The North Atlantic Oscillation and greenhouse-gas forcing. Geophys Res Lett 32:L04703. doi:10.1029/2004GL021064

López-Moreno JI, Vicente-Serrano SM (2008) Positive and negative phases of the winter-time North Atlantic Oscillation and drought occurrence over Europe: a multitemporal-scale approach. J Clim 21:1220–1243

Meehl GA, Covey C, Delworth T, Latif M, McAvaney B, Mitchell JFB, Stouffer RJ, Taylor KE (2007) The WCRP CMIP3 multi-model dataset: a new era in climate change research. Bull Am Meteorol Soc 88:1383–1394

Miller RL, Schmidt GA, Shindell DT (2006) Forced annular variations in the 20th century Intergovernmental Panel on Climate Change Fourth Assessment Report models. J Geophys Res 111:D18101. doi:10.1029/2005JD006323

Osborn TJ (2004) Simulating the winter North Atlantic Oscillation: the roles of internal variability and greenhouse gas forcing. Clim Dyn 22:605–623

Osborn TJ (2011) Winter 2009/2010 temperatures and a record-breaking North Atlantic Oscillation index. Weather 66:19–21

Osborn TJ, Briffa KR, Tett SFB, Jones PD, Trigo RM (1999) Evaluation of the North Atlantic Oscillation as simulated by a coupled climate model. Clim Dyn 15:685–702

Perlwitz J, Harnik N (2004) Downward coupling between the stratosphere and troposphere: the relative roles of wave and zonal mean processes. J Clim 17:4902–4909

Selten FM, Branstator GW, Dijkstra HA, Kliphuis M (2004) Tropical origins for recent and future Northern Hemisphere climate change. Geophys Res Lett 31:L21205. doi:10.1029/2004GL020739

Trenberth KE, Paolino DA (1980) The Northern Hemisphere sea level pressure data set, trends, errors and discontinuities. Mon Wea Rev 108:855–872

Trigo RM, Osborn TJ, Corte-Real J (2002) The North Atlantic Oscillation influence on Europe: climate impacts and associated physical mechanisms. Clim Res 20:9–17

Ulbrich U, Christoph M (1999) A shift of the NAO and increasing storm track activity over Europe due to anthropogenic greenhouse gas forcing. Clim Dyn 15:551–559

The NAO Impact on Droughts in the Mediterranean Region

Sergio M. Vicente-Serrano, Juan I. López-Moreno, Jorge Lorenzo-Lacruz, Ahmed El Kenawy, Cesar Azorin-Molina, Enrique Morán-Tejeda, Edmond Pasho, Javier Zabalza, Santiago Beguería, and Marta Angulo-Martínez

Abstract This chapter shows the influence of the North Atlantic Oscillation (NAO) on droughts in the entire Mediterranean region between 1901 and 2006. The analysis has been based on identification of positive and negative NAO winters and also detection of the anomalies of drought severity by means of the Standardized Precipitation Evapotranspiration Index (SPEI). The analysis is focussed on the winter NAO. Nevertheless, given that the SPEI drought indicator can be obtained at different time-scales, the study shows how the effects of the winter NAO on droughts are propagated for the following months when long time scales are considered. In general, during the positive phases, the negative SPEI averages are recorded in Southern Europe (the Iberian Peninsula, Italy and the Balkans), areas of Turkey and northwest Africa. On the contrary, the SPEI averages are found positive in northeast Africa. The opposite configuration, but with some differences in the spatial patterns and the magnitude of the SPEI averages, is found during the negative NAO years. The findings of this study should be of great applicability in terms of developing early warning systems. The established relationships between NAO phases and drought indices seem appropriate for drought prediction over large areas of the Mediterranean basin.

Keywords Standardized Precipitation Evapotranspiration Index (SPEI) · Drought index · Drought trends · Time-scales · Potential evapotranspiration · North Atlantic Oscillation (NAO)

1 Introduction

Droughts are first-order hazards of high frequency and intensity in the Mediterranean region. They are one of the main natural causes of agricultural, economic and environmental damage (Burton et al., 1978; Wilhite, 1993). In contrast to other extreme events such as floods, which are typically restricted to small

S.M. Vicente-Serrano (✉)
Instituto Pirenaico de Ecología, Spanish National Research Council (CSIC), Zaragoza, Spain
e-mail: svicen@ipe.csic.es

S.M. Vicente-Serrano, R.M. Trigo (eds.), *Hydrological, Socioeconomic and Ecological Impacts of the North Atlantic Oscillation in the Mediterranean Region*, Advances in Global Change Research 46, DOI 10.1007/978-94-007-1372-7_3,

regions and well-defined temporal intervals, droughts are difficult to pinpoint in time and space. In particular, droughts can affect wide areas over long periods of time. It is also very difficult to determine the beginning of a drought event until human activities, or the environment, are affected. Moreover, the influences of a drought can persist over longer periods after it has ended (Changnon and Easterling, 1989). Although droughts are complex phenomenon related to a multitude of factors (Wilhite and Glantz, 1985), they always have a climatic origin. This has promoted scientific research to investigate the behaviour and characteristics of climatic droughts in the Mediterranean region, including their driving mechanisms (Van del Schrier et al., 2006).

In the Mediterranean region, droughts are a climatic risk that have severe consequences for agriculture and natural vegetation (Austin et al., 1998; Lázaro et al., 2001; Reichstein et al., 2002; Iglesias et al., 2003), increasing the frequency of fires (Colombaroli et al., 2007; Pausas, 2004) and significantly reducing water availability for urban and tourist consumption (Morales et al., 2000). Droughts are frequent, but not spatially uniform in the Mediterranean region (Briffa et al., 1994; López-Moreno and Vicente-Serrano, 2008), with significant spatial differences, even at regional scale (Vicente-Serrano et al., 2004; Vicente-Serrano, 2006).

The North Atlantic Oscillation (NAO) is the primary atmospheric circulation mode that determines the climate of the Mediterranean region (Hurrell et al., 2003), with large and well known impacts on temperature, precipitation, cloudiness, etc. (e.g., Hurrell et al., 2003; Hurrell and Van Loon, 1997; Trigo et al., 2002). Different studies have focused on analysing the role of the NAO on droughts in South of Europe and the Mediterranean region (Briffa et al., 1994; Lloyd-Hughes and Saunders, 2002; Van del Schrier et al., 2006). These studies made significant contributions to literature in terms of analyzing the spatial and temporal patterns of drought using one of the most widely used drought indices: the Palmer Drought Severity Index (PDSI; Palmer, 1965).

In addition, drought is widely accepted as a multi-scalar phenomenon. McKee et al. (1993) clearly illustrated this essential characteristic of droughts through consideration of usable water resources including: soil moisture, ground water, snowpack, river discharges, and reservoir storages. The time period from the arrival of water inputs to availability of a given usable resource differs considerably. Thus, the time scale over which water deficits accumulate becomes extremely important, and functionally separates hydrological, environmental, agricultural and other droughts. For example, the response of hydrological systems to precipitation can markedly vary as a function of time (Changnon and Easterling, 1989; Elfatih et al., 1999; Pandey and Ramasastri, 2001). This is determined by the different frequencies of hydrologic/climatic variables (Skøien et al., 2003). For this reason, drought indices must be associated with a specific timescale to be useful for monitoring and management of different usable water resources. Thus, the 9–12-month fixed time scale considered by the PDSI (Guttman, 1998) limits the ability of the user to analyze certain characteristics of droughts. This is mainly because the response of different water sources to drought is very sensitive to the chosen time scale. López-Moreno and Vicente-Serrano (2008) used the Standardised Precipitation

Index (SPI; McKee et al., 1993) to determine the impact of the NAO on drought conditions, quantified at different time-scales, in Europe. They found that the response of droughts to the NAO varies spatially, and differs largely according to the month of the year and the time scale of the analysis.

At present there is no study that analyses the role of the NAO on droughts at different time scales across the entire Mediterranean region. In this regard, the study conducted by López-Moreno and Vicente-Serrano (2008) only focussed on the Mediterranean Europe employing the SPI, which neglects the role of other variables different to precipitation, to determine drought severity. Different empirical studies have shown that temperature rise markedly affects the severity of droughts and their derived impacts (e.g., Abramopoulos et al., 1988; Breshears et al., 2005; Ciais et al., 2005; Cai and Cowan, 2008; Gerten et al., 2008). Owing to its general increase in the Mediterranean region (0.5–2°C) during the last past 150 years (Jones and Moberg, 2003), it is reasonably expected to have adverse consequences of temperature on drought conditions, with an increase in water demand due to evapotranspiration (Sheffield and Wood, 2008). For this purpose, and to analyse the NAO impact on drought at different time-scales, we have used a new drought index (the Standardized Precipitation Evapotranspiration Index; SPEI). This index is advantageous in that it is sensitive to changes in evaporation demand and can also be obtained at different time-scales.

The objective of this chapter is to show the influence of NAO phases on drought conditions in the Mediterranean region both spatially and temporally, and also to include the influence on different time-scales of drought.

2 Methods

To analyse the NAO impact on droughts throughout the Mediterranean basin, we used the SPEIbase, which is based on the Standardised Precipitation Evapotranspiration Index (SPEI). The data set covers the period 1901–2006 considering time-scales of drought from 1 to 24 months at a spatial resolution of 0.5°, which represent the variability of a variety of water usable sources (Szalai et al., 2000; Sims et al., 2002; Vicente-Serrano and López-Moreno, 2005; Patel et al., 2007; Khan et al., 2008; Lorenzo-Lacruz et al., 2010) and may have very different impacts on natural ecosystems and crops (Ji and Peters, 2003; Vicente-Serrano, 2007; Quiring and Ganesh, 2010). More details about the SPEI and the corresponding data set can be found in Vicente-Serrano et al. (2010), Beguería et al. (2010) and Vicente-Serrano et al. (2010b). From the SPEIbase we selected the area comprised between 25.5–48.5°N and 10°W–45.5°E.

The analysis of the NAO impact on droughts was based on a composite procedure by means of the selection of the positive and negative NAO winters. In the present study, we used the NAO index calculated from the difference between the standardized pressure anomalies measured at Gibraltar (south of Spain) and Reykjavík (Iceland). The advantage of using these stations is discussed in depth by Jones et al. (1997), who noted that Gibraltar appears to better represent the southern

part of the NAO dipole than other commonly used stations, such as Lisbon or Ponta Delgada in the Azores. The NAO index was compiled by the Climate Research Unit (CRU), University of East Anglia (http://www.cru.uea.ac.uk/cru/data/nao.htm). We calculated the average wintertime NAO index for months from December to March (DJFM) because the NAO has higher activity at this time of the year (Hurrell et al., 2003). Interdecadal variability of the NAO appears to be the most coherent when the December–March season is used, rather than using other months (Osborn et al., 1999). Since the NAO index is calculated by the CRU using data from the beginning of the nineteenth century and using the period 1950–1980 as reference, the average of the winter NAO index for the period 1901–2006 is not 0. Therefore, in order to have the same number of positive and negative winters and a magnitude comparable, the resulting winter NAO series obtained from the average of the monthly values was standardised to have an average of 0 and a standard deviation equal to 1. Based on the obtained series, we identified the positive and negative NAO winters as those with values that differed from the average by at least $\pm\sigma$. Consequently, 16 years were identified as having positive phases and 16 as having negative phases. The positive phases are found in 1903, 1905, 1910, 1913, 1920, 1925, 1957, 1961, 1967, 1983, 1989, 1990, 1992, 1994, 1995, and 2000; while the negative phases occur in 1917, 1936, 1940, 1941, 1947, 1955, 1956, 1963, 1964, 1965, 1969, 1971, 1977, 1979, 1996 and 2006.

For both positive and negative phases of the NAO, we calculated the average values of the SPEI at different time scales for each 0.5° series. We then used the Wilcoxon–Mann–Whitney rank-sum test (Siegel and Castelan, 1988; Wilks, 2006) to determine whether contrasted NAO phases (positive/negative) lead to statistically significant differences in SPEI averages (dry/humid conditions) at different time scales. The Wilcoxon–Mann–Whitney rank-sum test is based on ranks that do not require normally distributed samples; it is slightly less powerful than parametric tests such as the t test (Helsel and Hirsch, 1992). Although the SPEI is a normalized variable for the entire series, the normality of the sample cannot be guaranteed, and the distribution may be biased when a sample of years is extracted (i.e., the SPEI values during positive and negative years). For this reason, the use of a non-parametric test is more convenient. The sample that comprised SPEI values for each of the months of the positive/negative years was compared with the values of SPEI for months of normal years (those years within the rank $+\sigma > \text{NAO} < -\sigma$) and months of years with the opposite sign. The significance level was established at $\alpha < 0.05$.

Given that SPEI anomalies for the positive and negative NAO years were obtained for a range of time scales and months for each 0.5° series, we summarised the information by means of Principal Component Analysis (PCA) applied to the matrix of month/time-scale SPEI anomalies for each series. PCA has been widely used to determine the general temporal and spatial patterns of climatic variables. It allows common features to be identified and specific local characteristics to be determined (Jolliffe, 1990). In this case, the purpose was to identify the general patterns of the month/time-scale SPEI anomaly matrixes for the positive and negative NAO phases. The areas represented by each mode (component) were identified

by mapping the factorial loadings. The number of components was selected in accordance with the criteria of an eigenvalue larger than 1.

3 Results

Figure 1 shows, as a representative example, the evolution of the SPEI at the time scales of 3-, 6-, 9-, 12-, 18- and 24-month in a region of central France (46.5°N, 8°E). Negative SPEI index values indicate higher severity of droughts. On the shorter time scales (3 or 6 months), the dry and humid periods are short and occur with high-frequency. At a time scale of 12 months, droughts were less frequent, but they lasted longer. At longer time scales (18 or 24 months), droughts lasted longer, but were less frequent, with very few dry or humid periods recorded. The index allows to identify the main drought periods affected this region in the decades of 1940, 1990 and 2000.

Figure 2 shows the SPEI anomalies corresponding to the entire Mediterranean region from the average Mediterranean SPEI series in the positive and negative NAO phases. The pattern is very different among both phases, with general negative (positive) SPEI anomalies across time scales and months during the positive (negative) NAO phases. The most negative anomalies recorded for the positive

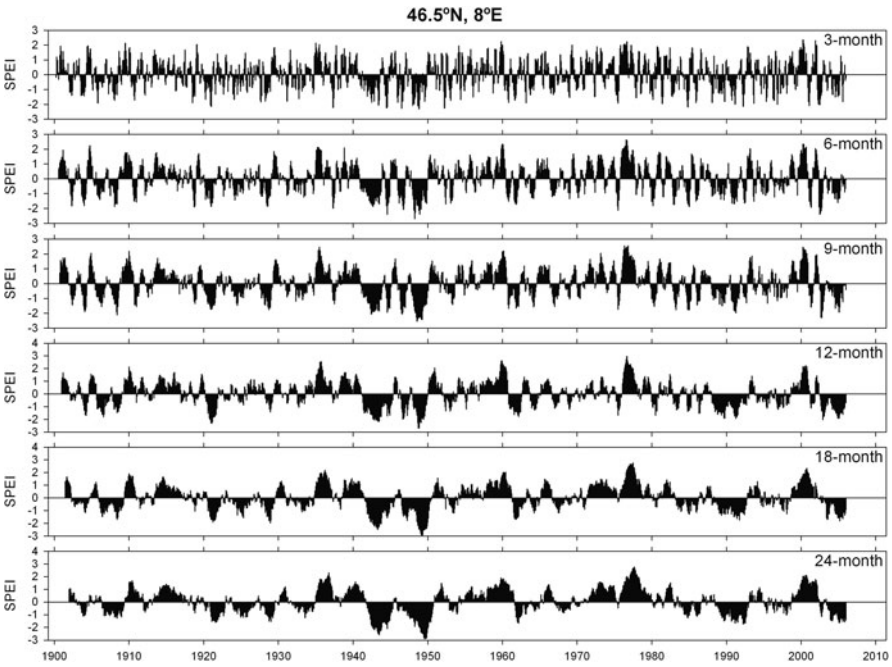

Fig. 1 Evolution of the 3-, 6-, 9-, 12-, 18- and 24-month SPEI in central France (46.5°N, 8°E)

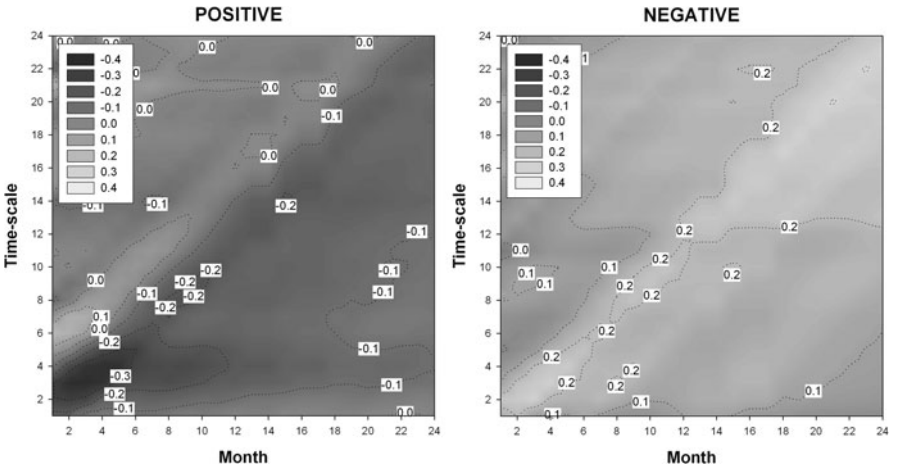

Fig. 2 Average SPEI anomalies for the entire Mediterranean region corresponding to the positive and negative years of the NAO. The month 1 corresponds to December of the NAO phase and the month 24 is November of two months after

NAO phases is observed at the time scales of 2- to 5-month considering the period between February and June. Nevertheless, although not so intense as observed in late winter and early spring, the negative anomalies are propagated throughout longer SPEI time-scales several months further. On the contrary, the negative NAO phases show general positive SPEI anomalies in most of the months and time-scales, even at the longest time-scales (e.g., 24 months). We should also remark that although both phases show opposite pattern, the magnitude of SPEI anomalies are not so high, probably due to the large spatial variability existing in the role of NAO on the precipitation and temperature across the Mediterranean basin. Figure 3 shows the average SPEI at various time-scales in different months of the year during the year of the NAO event and the following year for the positive NAO phases. It also shows the standard deviations of the SPEI values recorded during the events. The first relevant conclusion is the important spatial differences in the impact of the NAO positive phases across the Mediterranean basin. As expected, when the time-scale is higher, the effects of the positive NAO events are smoothed. Nevertheless, independently of this pattern, it is clearly observed that the strongest negative SPEIs are recorded in the Iberian Peninsula, Morocco, Algeria, Italy and the Balkans. The negative anomalies have a lower magnitude and a patchy configuration in Turkey and South France. Moreover, in the Northeast Africa the SPEI anomalies are positive, and the difference of the SPEI values in relation to the negative and normal years is statistically significant for most of the months and time-scales.

Figure 3 shows how at short time scales (3- and 5-months) during the spring immediately after the winter NAO, the SPEI averages are very strong: negative in the north and southwest and positive in the southeast of the basin. In most of the

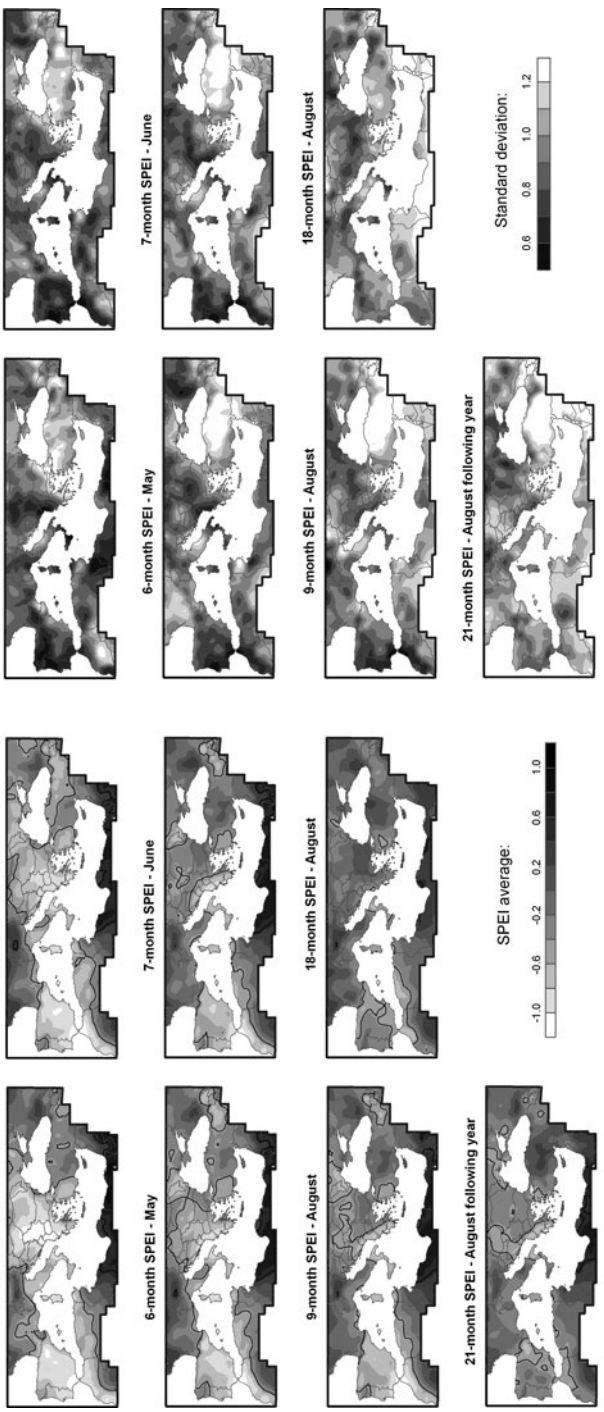

Fig. 3 *Left*: Spatial distribution of the average SPEI at different time-scales for some months of the positive NAO years and in August of the following year. *Black lines* isolate areas in which the average SPEI for the positive NAO years is significantly different to the rest of the years. *Right*: Standard deviation of the SPEI values during the positive NAO winters

basin these averages show statistically significant differences regarding to the SPEI averages recorded during the negative or normal years. Thus, in most of the Iberian Peninsula and large regions of the Balkans the anomalies indicate very strong dry conditions. On the contrary, very humid conditions, on average, are identified in northeast Africa during the positive NAO winters. Droughts quantified at longer time-scales also show how the effect of the positive winter NAO propagates several months after. Thus, in August negative 9-month SPEI values are still recorded in large areas, whereas positive values are identified in Northeast Africa. Even during the summer of the following year (see the chart of August of the following year considering the time-scale of 21 months), the same pattern is identified, and large areas show significant differences in the average SPEI values regarding negative and normal years. Therefore, the results show how the NAO signal may be evident in the drought conditions several months after the winter.

Figure 3 also shows the standard deviation values of the SPEI calculated for the 16 positive NAO years. Low standard deviations would indicate low variability among the positive years. Independently of the time scale and the month of the year, regions with strong SPEI anomalies commonly show low variability. The Iberian Peninsula, Northwest Africa and areas of the Balkans show, in general, a low variability among events. On the contrary, Turkey and the eastern sectors of the Balkans, the Iberian Peninsula, and of Italy show very high variability of the SPEI values corresponding to the positive years.

Figure 4 shows the spatial distribution of the SPEI average and standard deviation for the negative NAO years. In the majority of the region, and independently of the time-scale and the month of the year, the SPEI anomalies tend to be positive. Thus, the magnitude of the average anomalies, regardless of their sign, tends to be much higher for the positive than for the negative NAO years. Moreover, the effect of the negative phases is propagated for longer, with a stronger magnitude, than the observed for the positive phases. The two regions with droughts during positive NAO phases are the Northeast Africa and the near East. In these areas, the NAO effects are recorded for several months further, showing significant differences with the SPEI values of the positive and normal years. The standard deviations of the SPEI values are, in general, lower than the observed for the positive phases, which indicates that the humid conditions associated with the negative phases show a low variability among events.

The different average values of the SPEI found between the positive and the negative NAO years clearly indicate a very different risk in the occurrence of drought conditions across the Mediterranean basin. Figure 5 shows the percentage of years in which negative SPEI values, associated to dry conditions, have been found for the positive and negative NAO years. The analysis covers the same months and time scales shown in Figs. 3 and 4. During the positive phases, high probabilities of dry conditions occurrence are recorded in most of South Europe, Turkey and Northwest Africa, mainly during the spring and summer of the positive winters. In March, at a time scale of 3 months, the majority of the Iberian Peninsula, Italy, western Turkey, the Balkans and Morocco show a percentage higher than 90% of dry conditions during positive NAO winters. In France, northern Italy, Turkey and Algeria the

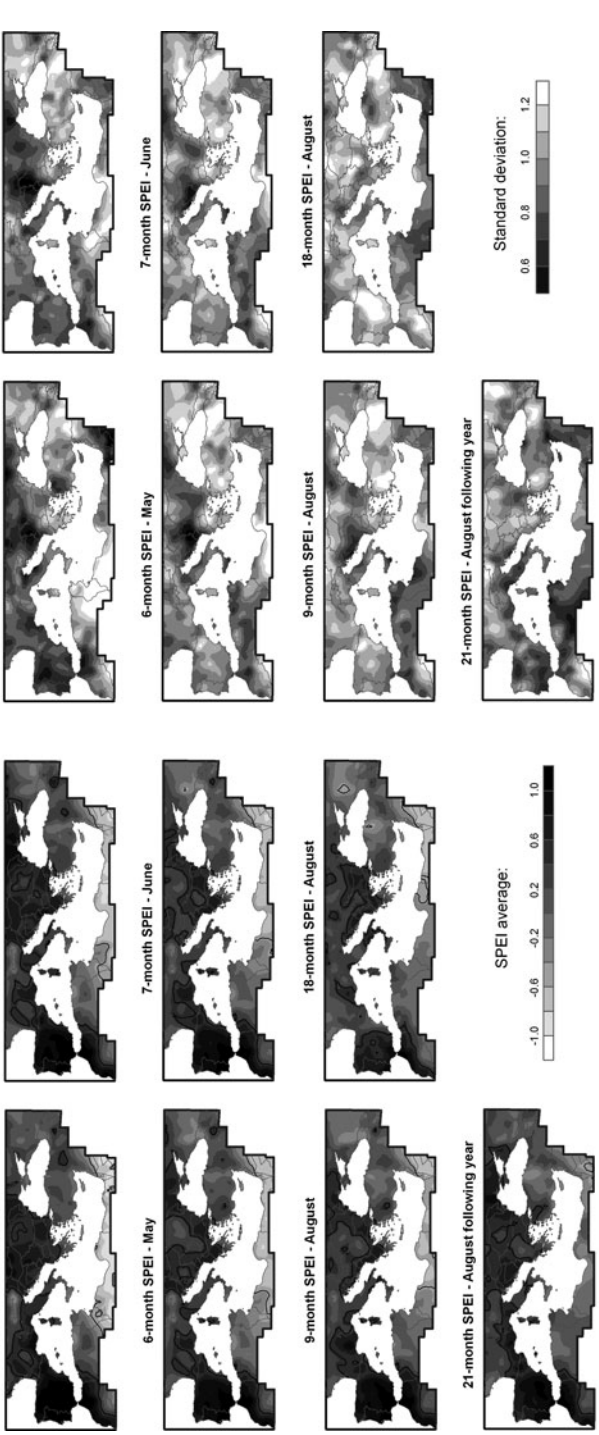

Fig. 4 *Left*: Spatial distribution of the average SPEI at different time-scales for some months of the negative NAO years and in August of the following year. *Black lines* isolate areas in which the average SPEI for the negative NAO years is significantly different to the rest of the years. *Right*: Standard deviation of the SPEI values during the negative NAO winters

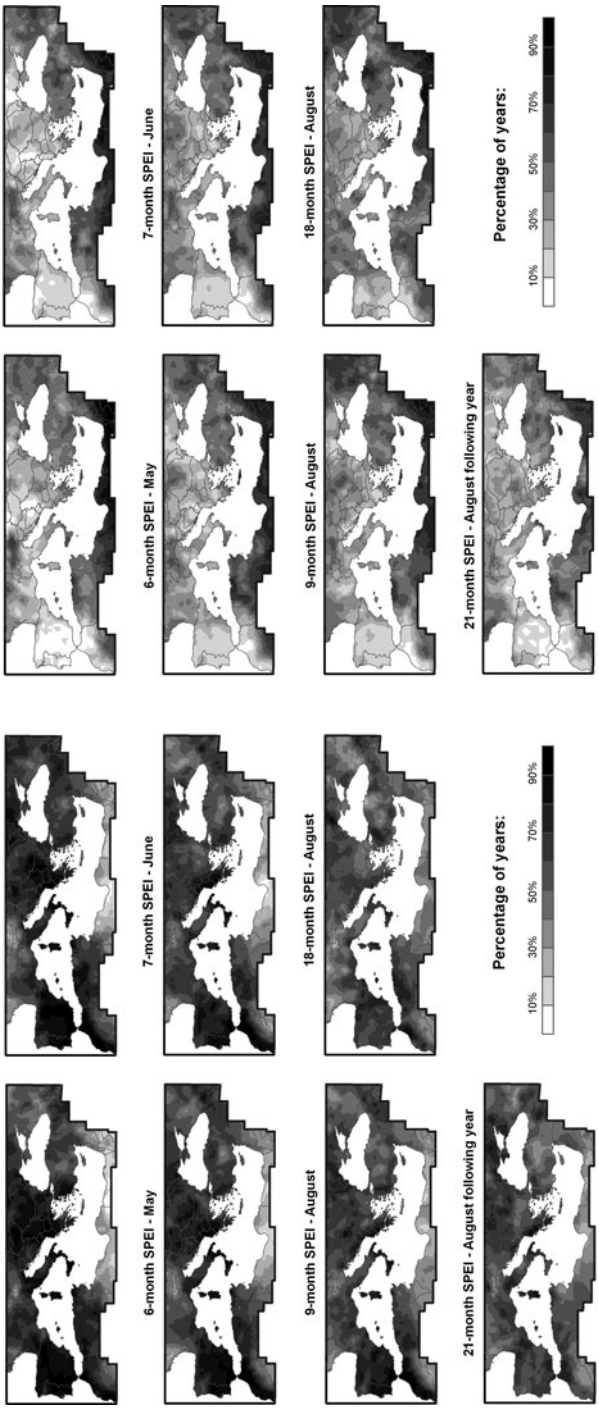

Fig. 5 Percentage of years with negative SPEI values. *Left*: Positive NAO years. *Right*: Negative NAO years

probability is lower but still relatively high (> 65%). On the contrary, in Northeast Africa the probability of having dry conditions at this time scale is close to 0. In April, and at the time-scale of 5-months, the spatial pattern of probability is similar to March. Thus, until June the probability of having dry conditions is higher than 80% in the Iberian Peninsula and North of Morocco considering a time-scale of 7 months. During the negative NAO years (Fig. 5 left) the probability of having dry conditions is very low in the majority of the basin; thus in some areas of southwestern Iberian Peninsula the value is close to 0 during the spring and summer. Only in the Northeast Africa and the Near East the probability is high (>80%) for most of the months of the year and time-scales.

We have summarised the information of the entire Mediterranean region by means of a principal component analysis (see methods) for the positive and the negative NAO years. The purpose was to determine the most general time-scale/month matrices of the SPEI anomalies corresponding to both phases, in addition to the regions represented by each pattern. The results of the matrix are shown in standardised units (PC-scores), comparable to the SPEI magnitudes.

Figure 6 shows the results for the positive phases. Three PCs were extracted, which account for 69.3% of the total variance. The component 1 shows some resemblance with the average pattern indicated in Fig. 2: negative SPEI anomalies at the time scales of 2–6 months between January and August of the positive year. Moreover, the negative values, indicative of dry conditions, propagate for further months and are dominant until, at least, 24 months after the positive NAO winter. According to the loadings of the first PC, this pattern of time-scale/month anomalies mainly represents the entire Iberian Peninsula, the southern coastland of France, most of Italy, the majority of the Balkans, the Anatolian Peninsula and the northwest Africa. Therefore, in these regions the positive NAO years are associated with a propagation of the dry conditions for most of the months and SPEI time scales. In northeast Africa the PC-loadings are dominantly negative and close to –1, which indicates that these areas are represented by the inverse of the obtained matrix during the positive NAO years. The second and third components represent the northernmost areas of France, Italy, the Balkans; and the northern basin of the Black Sea, and the near East and parts of North Africa, respectively. They contribute to a lower portion of the total variance (15.5 and 9.7%, respectively). In the northernmost areas of the basin (Component 2) the positive NAO phases are also related to the generalised negative SPEI values during the winter and spring, but there is no clear propagation throughout time-scales and months.

For the negative NAO years, the first PC explains 49.2% of the total variance, and represents most of the Iberian Peninsula, south of France, Italy, Morocco, south of the Balkans and western Turkey (Fig. 7). The pattern of the time-scale/month SPEI anomalies reveals the first pattern of the positive NAO phases, but with opposite signs to SPEI values. Thus, the negative NAO phases tend to cause humid conditions, which are propagated to the SPEI values several months after the winter. This pattern shows negative loadings in northeast Africa and the near East, suggesting the opposite behaviour in these areas: a propagation of the dry conditions. The

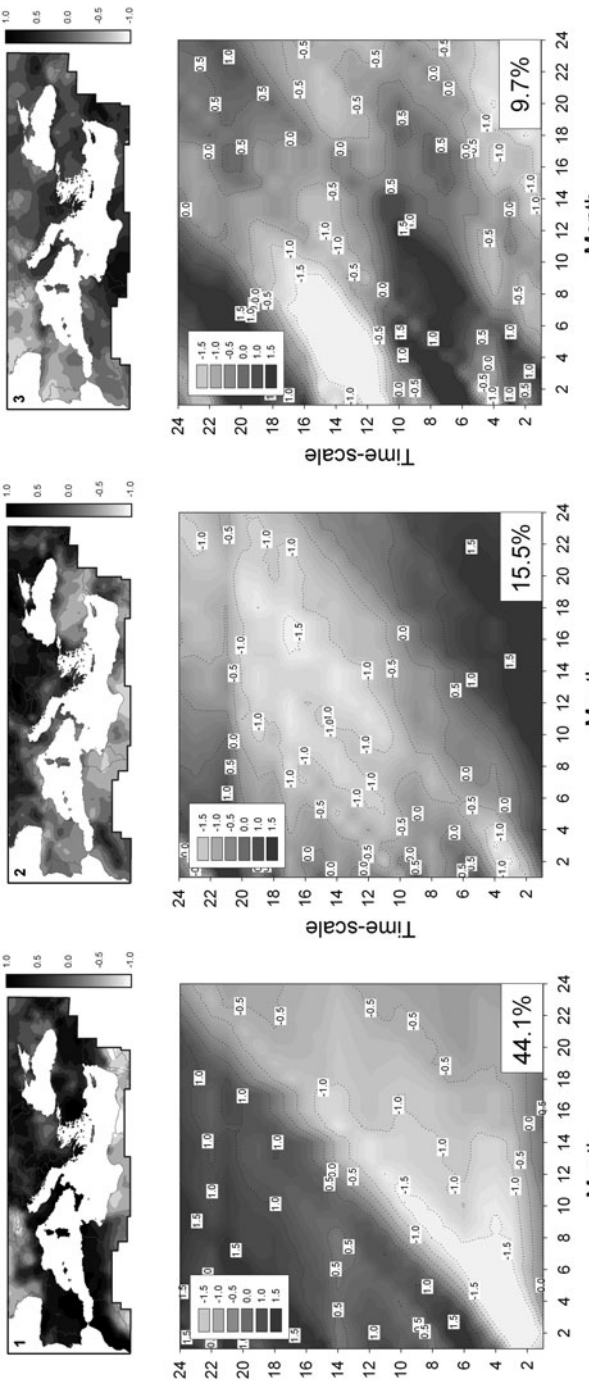

Fig. 6 Results of the principal component analysis for the positive NAO years. The *upper figures* represent the PC loadings of each component. The *lower figures* represent the principal components that summarise the matrix of NAO-SPEI correlations at different time-scales and months

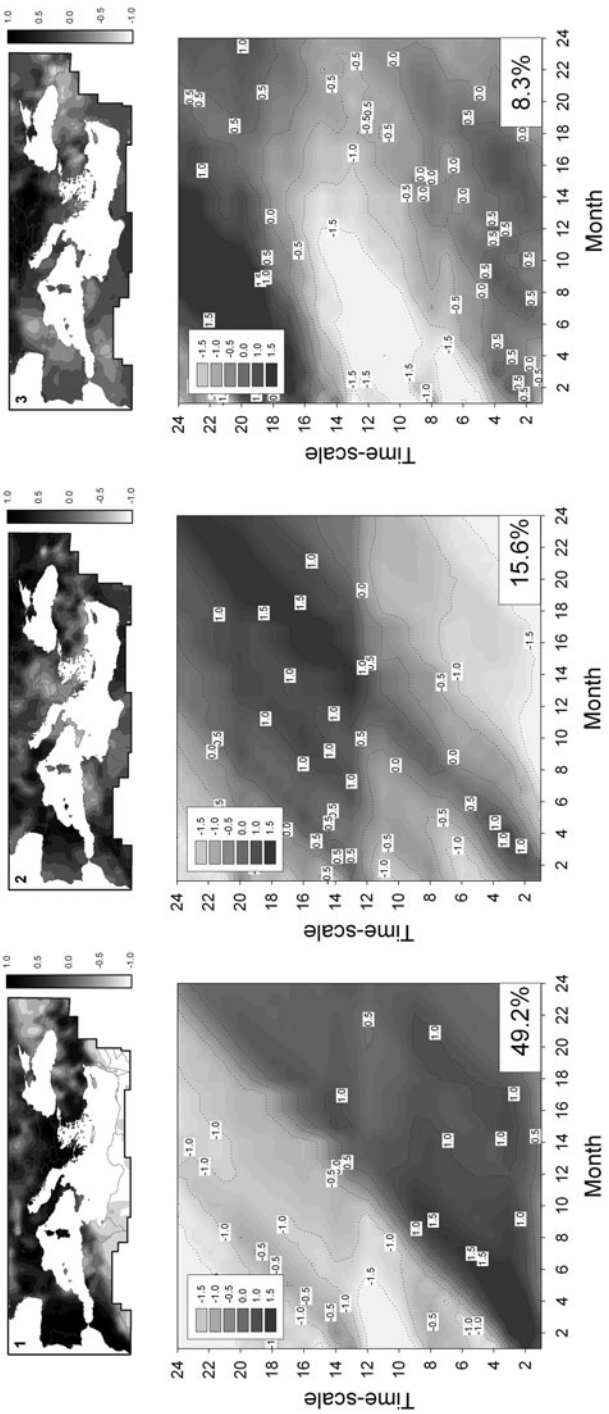

Fig. 7 Results of the principal component analysis for the negative NAO years. The *upper figures* represent the PC loadings of each component. The *lower figures* represent the principal components that summarise the matrix of NAO-SPEI correlations at different time-scales and months

components 2 and 3 represent a lower percentage of the total variance, including areas in which the influence of the negative NAO phases is lower than the observed for the component 1.

4 Conclusions

The results of this study have demonstrated that the response of droughts to positive and negative phases of the NAO varies spatially and also depends greatly on the time scale of drought. In general, during the positive phases, negative SPEI averages are recorded in southern Europe (mainly in the Iberian Peninsula, Italy and the Balkans), parts of Turkey and northwest Africa. On the contrary, in northeast Africa the SPEI averages are positive. The opposite configuration, but with some differences in the spatial patterns and the magnitude of the SPEI averages, is found for the negative years. This observation is in agreement with the general and widely known behaviour of the effects of the NAO on precipitation and temperature throughout the Mediterranean region (e.g., Hurrell and Van Loon, 1997; Trigo et al., 2002).

This study highlights the outstanding influence of positive and negative phases of the wintertime NAO on drought conditions during the succeeding months, quantified by means of a multi-scalar drought indicator. This index gives indication of the important role of positive and negative phases of the wintertime NAO on usable water sources throughout the year. We have found that there is a prevalence of either maximum or minimum values of the SPEI along the diagonal that summarised the principal component analysis in Figs. 6 and 7, with some differences depending on the regions. This fact is related to the importance of winter climate in terms of the total annual amounts. In the Mediterranean region, where the bulk of the precipitation comes mostly during winter, differences in winter precipitation between positive and negative phases are very important, and this behaviour has a noticeable impact on drought condition during the succeeding months.

Previous studies have shown that the time scales of droughts have a direct relationship with usable water sources, such as soil moisture, river discharge, and reservoir storage (Vicente-Serrano and López-Moreno, 2005; Lorenzo-Lacruz et al., 2010). In general, long time scales of the SPI are related to reservoir storage and river discharge, whereas short time scales are connected with variability in soil moisture. Therefore, positive phases of the NAO could lead to drought conditions in terms of soil moisture during winter and spring and hydrological droughts (reduction in river discharge and the levels of reservoir storages) in summer and autumn over southern Europe and northwest Africa. On the contrary, in northeast Africa and the near East the deficits will be mainly driven by the negative phases of the NAO. The above results are in agreement with the observed response of hydrological systems to the NAO in different Mediterranean regions. Trigo et al. (2004) documented a lag time of 2–3 months in the response of river discharge to NAO positive and negative phases in the Atlantic basins of the Iberian Peninsula. Also, in a study of the Tagus basin within the Iberian Peninsula, López-Moreno et al. (2007) reported that the impact of positive and negative phases of the NAO on river discharge and levels

of storage in reservoirs is neither instantaneous nor restricted to the winter months. Thus, the decrease in the amount of water stored in the reservoirs during negative phases of the NAO is especially severe during the next summer and autumn, whereas in winter and spring the amount of stored water is similar to that of normal years.

Nevertheless, the expected impact is not only restricted to the direct usable water resources since different natural systems and crops show a response to longer drought time scales. Vicente-Serrano (2007) found a high correlation between the vegetation activity in semi-arid regions of northeast Spain and drought time-scales between 6 and 12 months. Within dry-lands of this region, crop production of early summer responded considerably at time-scales between 6 and 12 months (Vicente-Serrano et al., 2006). Therefore, in these regions the NAO variability will have a great impact on the vegetation activity, directly driven by the soil moisture availability (Vicente-Serrano and Heredia-Laclaustra, 2004; Gouveia et al., 2008). In this way, in the coastland areas of Egypt and the near East, where large agricultural areas depend on winter rainfall, crop productions will be driven by drought variability, which is highly conditioned by the NAO positive phases.

Finally, we must highlight that although teleconnection indices such as the NAO have been widely used to predict drought conditions with a high degree of reliability (e.g., Rodwell, 2003), they may be useful only in those regions in which a general stability of the SPEI values for the positive or negative SPEI phases is found (Figs. 3 and 4). In other areas (mainly in Turkey and South France), the large variability among events observed during the positive NAO phases does not make the prediction and management of droughts an easy task, particularly those based solely on the wintertime NAO index. Given that the NAO configurations and the NAO-climate connectivity have had large changes in the last decades (Vicente-Serrano and López-Moreno, 2008), the regions less affected by the direct influences of the NAO dipole show a large variability among events (Massei et al., 2007).

The findings reported here should be of great use in the development of early warning systems and in mitigating the effects of drought in an area that is especially prone to such phenomena. The development of measures for drought planning and preparedness is a priority to reduce drought hazards (Wilhite, 1996; Wilhite et al., 2007; Prabhakar and Shaw, 2008). A critical component in drought planning is the provision of timely and reliable climate information on which management decisions are made (Svoboda et al., 2004). Hence, drought monitoring is crucial for the implementation of drought plans and the use of the results found here, in terms of the lagged impacts of NAO events throughout different time-scales and months, offers a unique mechanism for drought prediction. The established relationships between NAO phases and drought indices therefore seem appropriate for drought prediction over large areas of the Mediterranean basin.

Acknowledgements This work has been supported by the research projects CGL2008-01189/BTE and CGL2006-11619/HID financed by the Spanish Commission of Science and Technology and FEDER, EUROGEOSS (FP7-ENV-2008-1-226487) and ACQWA (FP7-ENV-2007-1- 212250) financed by the VII Framework Programme of the European Commission, and "La nieve en el Pirineo aragonés: Distribución espacial y su respuesta a las condiciones climáticas" Financed by "Obra Social La Caixa" and the Aragón Government.

References

Abramopoulos F, Rosenzweig C, Choudhury B (1988) Improved ground hydrology calculations for global climate models (GCMs): soil water movement and evapotranspiration. J Clim 1: 921–941

Austin RB, Cantero-Martínez C, Arrúe JL, Playán E, Cano-Marcellán P (1998) Yield-rainfall relationships in cereal cropping systems in the Ebro river valley of Spain. Eur J Agron 8:239–248

Beguería S, Vicente-Serrano SM, Angulo M (2010) A multi-scalar global drought data set: the SPEIbase: a new gridded product for the analysis of drought variability and impacts. Bull Am Meteorol Soc 91:1351–1354

Breshears DD, Cobb NS, Rich PM et al (2005) Regional vegetation die-off in response to global-change-type drought. PNAS 102:15144–15148

Briffa KR, Jones PD, Hulme M (1994) Summer moisture variability across Europe, 1892–1991: an analysis based on the Palmer drought severity index. Int J Climatol 14:475–506

Burton I, Kates RW, White GF (1978) The environment as hazard. Oxford University Press, New York, 240 pp

Cai W, Cowan T (2008) Evidence of impacts from rising temperature on inflows to the Murray-darling basin. Geophys Res Lett 35:L07701. doi:10.1029/2008GL033390

Changnon SA, Easterling WE (1989) Measuring drought impacts: the Illinois case. Water Resour Bull 25:27–42

Ciais Ph, Reichstein M, Viovy N et al (2005) Europe-wide reduction in primary productivity caused by the heat and drought in 2003. Nature 437:529–533

Colombaroli D, Marchetto A, Tinner W (2007) Long-term interactions between Mediterranean climate, vegetation and fire regime at Lago di Massaciuccoli (Tuscany, Italy). J Ecol 95:755–770

Elfatih A, Eltahir B, Yeh PJF (1999) On the asymmetric response of aquifer water level to floods and droughts in Illinois. Water Resour Res 35:1199–1217

Gerten D, Rost S, von Bloh W, Lucht W (2008) Causes of change in 20th century global river discharge. Geophys Res Lett 35:L20405. doi:10.1029/2008GL035258

Gouveia C, Trigo RM, DaCamara CC, Libonati R, Pereira JMC (2008) The North Atlantic Oscillation and European vegetation dynamics. Int J Climatol 28:1835–1847

Guttman NB (1998) Comparing the Palmer drought index and the Standardized Precipitation Index. J Am Water Resour Assoc 34:113–121

Helsel DR, Hirsch RM (1992) Statistical methods in water resources. Elsevier, New York, 522 pp

Hurrell JW, Kushnir Y, Ottersen G, Visbeck M (2003) An overview of the North Atlantic Oscillation. In Hurrell JW, Kushnir Y, Ottersen G, Visbeck M (eds) The North Atlantic Oscillation: climate significance and environmental impact. Geophysical Monograph Series, vol 134, pp 1–36

Hurrell J, Van Loon H (1997) Decadal variations in climate associated with the North Atlantic Oscillation. Clim Change 36:301–326

Iglesias E, Garrido A, Gomez-Ramos A (2003) Evaluation of drought management in irrigated areas. Agric Econ 29:211–229

Ji L, Peters AJ (2003) Assessing vegetation response to drought in the northern Great Plains using vegetation and drought indices. Rem Sens Environ 87:85–98

Jolliffe IT (1990) Principal component analysis: a beginner's guide. Part I: Introduction and application. Weather 45:375–382

Jones PD, Jónsson T, Wheeler D (1997) Extensions to the North Atlantic Oscillation using early instrumental pressure observations from Gibraltar and southwest Iceland. Int J Climatol 17:1433–1450

Jones PD, Moberg A (2003) Hemispheric and large-scale surface air temperature variations: an extensive revision and an update to 2001. J Clim 16:206–223

Khan S, Gabriel HF, Rana T (2008) Standard precipitation index to track drought and assess impact of rainfall on watertables in irrigation areas. Irrigat Drain Syst 22:159–177

Lloyd-Hughes B, Saunders MA (2002) A drought climatology for Europe. Int J Climatol 22:1571–1592

Lorenzo-Lacruz J, Vicente-Serrano SM, López-Moreno JI, Beguería S, García-Ruiz JM, Cuadrat JM (2010) The impact of droughts and water management on various hydrological systems in the headwaters of the Tagus River (central Spain). J Hydrol 386:13–26

Lázaro R, Rodrigo FS, Gutiérrez L, Domingo F, Puigdefábregas J (2001) Analysis of a 30-year rainfall record (1967–1997) in semi-arid SE spain for implications on vegetation. J Arid Environ 48:373–395

López-Moreno JI, Beguería S, Vicente-Serrano SM, García-Ruiz JM (2007) The influence of the NAO on water resources in central Iberia: precipitation, streamflow anomalies and reservoir management strategies. Water Resour Res 43:W09411. doi: 10.1029/2007WR005864

López-Moreno JI, Vicente-Serrano SM (2008) Extreme phases of the wintertime North Atlantic Oscillation and drought occurrence over Europe: a multi-temporal-scale approach. J Clim 21:1220–1243

Massei N, Durand A, Deloffre J, Dupont JP, Valdes D, Laignel B (2007) Investigating possible links between the North Atlantic Oscillation and rainfall variability in Northwestern France over the past 35 years. J Geophys Res 112:D09121. doi:10.1029/2005JD007000

McKee TBN, Doesken J, Kleist J, (1993) The relationship of drought frequency and duration to time scales. 8th conference on applied climatology, Anaheim, CA. Amer Meteor Soc, pp 179–184

Morales A, Olcina J, Rico AM (2000) Diferentes percepciones de la sequía en España: adaptación, catastrofismo e intentos de corrección. Investigaciones Geográficas 23:5–46

Osborn TJ, Briffa KR, Tell SFB, Jones PD, Trigo RM (1999) Evaluation of the North Atlantic Oscillation as simulated by a climate model. Clim Dyn 15:685–702

Palmer WC (1965) Meteorological droughts. U.S. Department of Commerce Weather Bureau Research Paper 45, 58 pp

Pandey RP, Ramasastri KS (2001) Relationship between the common climatic parameters and average drought frequency. Hydrol Process 15:1019–1032

Patel NR, Chopra P, Dadhwal VK (2007) Analyzing spatial patterns of meteorological drought using standardized precipitation index. Meteorol Appl 14:329–336

Pausas JG (2004) Changes in fire and climate in the eastern Iberian Peninsula (Mediterranean basin). Clim Change 63:337–350

Prabhakar SVRK, Shaw R (2008) Climate change adaptation implications for drought risk mitigation: a perspective for India. Clim Change 88:113–130

Quiring SM, Ganesh S (2010) Evaluating the utility of the Vegetation Condition Index (VCI) for monitoring meteorological drought in Texas. Agr Forest Meteoro 150:330–339

Reichstein M, Tenhunen JD, Roupsard O, Ourcival J-M, Rambal S, Miglietta F, Peressotti A, Valentini R (2002) Severe drought effects on ecosystem CO_2 and H_2O fluxes at three Mediterranean evergreen sites: revision of current hypotheses? Global Change Biol 8:999–1017

Rodwell MJ (2003) On the predictability of the North Atlantic climate. In: Hurrell JW, Kushnir Y, Ottersen G, Visbeck M (eds) The North Atlantic Oscillation: climate significance and environmental impact. Geophysical Monograph Series, American Geophysical Union (AGU), Washington DC, vol 134, pp 173–192

Sheffield J, Wood EF (2008) Projected changes in drought occurrence under future global warming from multi-model, multi-scenario, IPCC AR4 simulations. Clim Dyn 31:79–105

Siegel S, Castelan NJ (1988) Nonparametric statistics for the behavioral sciences. McGraw-Hill, New York

Sims AP, Nigoyi DS, Raman S (2002) Adopting indices for estimating soil moisture: a North Carolina case study. Geophys Res Lett 29:1183. doi:10.1029/2001GL013343

Skøien JO, Blösch G, Western AW (2003) Characteristic space scales and timescales in hydrology. Water Resour Res 39:1304. doi:10.1029/2002WR001736

Svoboda MD, Hayes MJ, Wilhite DA, Tadesse T (2004) Recent advances in drought monitoring. 14th conference on applied climatology, Seattle, WA, Jan 12–16. American Meteorological Society, pp 5237–5240

Szalai S, Szinell CS, Zoboki J (2000) Drought monitoring in Hungary. In: Early warning systems for drought preparedness and drought management. World Meteorological Organization, Lisbon, pp 182–199

Trigo RM, Osborn TJ, Corte-Real JM (2002) The North Atlantic Oscillation influence on Europe: climate impacts and associated physical mechanisms. Clim Res 20:9–17

Trigo RM, Pozo-Vazquez D, Osborn TJ, Castro-Diez Y, Gamiz-Fortis S, Esteban-Parra MJ (2004) North Atlantic Oscillation influence on precipitation, river flow and water resources in the Iberian Peninsula. Int J Climatol 24:925–944

Van del Schrier G, Briffa KR, Jones PD, Osborn TJ (2006) Summer moisture variability across Europe. J Clim 19:2818–2834

Vicente-Serrano SM (2006) Spatial and temporal analysis of droughts in the Iberian Peninsula (1910–2000). Hydrol Sci J 51:83–97

Vicente-Serrano SM (2007) Evaluating the impact of drought using remote sensing in a mediterranean, semi-arid region. Nat Hazards 40:173–208

Vicente-Serrano SM, Beguería S, López-Moreno JI (2010) A multi-scalar drought index sensitive to global warming: the standardized precipitation evapotranspiration index – SPEI. J Clim 23:1696–1718

Vicente-Serrano SM, Beguería S, López-Moreno JI, Angulo M, El Kenawy A (2010b) A new global 0.5° gridded dataset (1901–2006) of a multiscalar drought index: comparison with current drought index datasets based on the Palmer Drought Severity Index. J Hydrometeorol 11:1033–1043

Vicente-Serrano SM, Cuadrat JM, Romo A (2006) Early prediction of crop productions using drought indices at different time scales and remote sensing data: application in the Ebro valley (North-East Spain). Int J Remote Sens 27:511–518

Vicente-Serrano SM, González-Hidalgo JC, de Luis M, Raventós J (2004) Spatial and temporal patterns of droughts in the Mediterranean area: the Valencia region (East–Spain). Clim Res 26:5–15

Vicente-Serrano SM, Heredia-Laclaustra A (2004) NAO influence on NDVI trends in the Iberian Peninsula (1982–2000). Int J Remote Sens 25:2871–2879

Vicente-Serrano SM, López-Moreno JI (2005) Hydrological response to different time scales of climatological drought: an evaluation of the standardized precipitation index in a mountainous Mediterranean basin. Hydrol Earth Syst Sci 9:523–533

Vicente-Serrano SM, López-Moreno JI (2008) The nonstationary influence of the North Atlantic Oscillation on European precipitation. J Geophys Res Atmos 113:D20120. doi:10.1029/2008JD010382

Wilhite DA (1993) Drought assessment, management and planning: theory and case studies. Kluwer, Boston, MA

Wilhite DA (1996) A methodology for drought preparedness. Nat Hazards 13:229–252

Wilhite DA, Glantz MH (1985) Understanding the drought phenomenon: the role of definitions. Water Int 10:111–120

Wilhite DA, Svoboda MD, Hayes MJ (2007) Understanding the complex impacts of drought: a key to enhancing drought mitigation and preparedness. Water Resour Manag 21:763–774

Wilks DS (2006) Statistical methods in the atmospheric sciences. Academic Press, San Diego, CA, 648 pp

The Impacts of the NAO on Hydrological Resources of the Western Mediterranean

Ricardo M. Trigo

Abstract The present study analyses the impact of the North Atlantic Oscillation (NAO) on the precipitation and river flow regime of the western Mediterranean region. The spatial pattern of the NAO impact over western Europe and the Mediterranean is evaluated on a monthly basis showing that the NAO impact is well apparent and significant between December and March, and not so well defined between October and November. I have focused the attention on the impact of the NAO pattern on the river flow regimes for the three largest transboundary Iberian river basins, namely the Douro (north), the Tejo (centre) and the Guadiana (south). Results show that the large inter-annual variability of these three rivers flow is largely modulated by the NAO phenomena. Moreover, the magnitude of the relationship between NAO and river discharges increases substantially for the last period considered (1973–1998), with values being statistically significant at the 1%. Major changes in the precipitation regime of Iberia have occurred in the last 5 decades, with an outstanding decrease in precipitation being noticed in March since the 1960s, which is significantly associated with increasing probabilities of positive values of the NAO index. It is also shown that this decline of precipitation is inducing a significant decrease of river flow for the three Iberian river basins considered. Finally, it is well known that the precipitation and river flow regimes in Iberia present large values of inter-annual variability, being characterised by large disparities between wet and dry years. These characteristics will probably exacerbate in the coming decades as, according to modelling results, the entire Mediterranean basin is bound to become hotter and drier under an increased frequency of positive NAO winters. Therefore, if we consider the rising use of water in both Iberian countries (Portugal and Spain) for agricultural, touristic, hydroelectricity production and urban purposes, one can foresee an increasing stressed situation for the water resources management in the region directly driven by the NAO conditions.

Keywords NAO · Precipitation · Water resources · River flow · Iberian Peninsula · Trends

R.M. Trigo (✉)
Instituto Dom Luiz, Universidade de Lisboa, Campo Grande, Faculdade de Ciencias, Edificio C8, Piso 3, 1749-016 Lisbon, Portugal
e-mail: rmtrigo@fc.ul.pt

S.M. Vicente-Serrano, R.M. Trigo (eds.), *Hydrological, Socioeconomic and Ecological Impacts of the North Atlantic Oscillation in the Mediterranean Region*, Advances in Global Change Research 46, DOI 10.1007/978-94-007-1372-7_4,

1 Introduction

The western Mediterranean region is roughly positioned at the southern edge of the North Atlantic storm tracks. Thus this sector is particularly susceptible to interannual shifts in the trajectories of mid-latitude cyclones and associated fronts that can lead to remarkable anomalies of precipitation and, to a lesser extent, of temperature (Trigo et al., 2006). Given the seasonal characteristics of the Atlantic storm-tracks, this is particularly true in winter when the influence of mid-latitude variability is at its greatest. Storm-track variability impacts primarily the western Mediterranean, but it has also a signature clearly present in the eastern Mediterranean (e.g. Türkeş and Erlat, 2003; Xoplaki et al., 2004). The Iberian Peninsula orography has a strong influence on the way that most low pressure systems affect the climate at a more local scale, as mountain ranges shield regions from oceanic moisture advection (Gimeno et al., 2010). Thus the precipitation regime in the northern and western sectors of the Iberian Peninsula is mostly controlled by the mean annual cycle of the location of the Atlantic storm track, while the interior and the eastern sectors of Iberia are partially affected by large-scale synoptic systems with Atlantic origin, but also by convective precipitation with Mediterranean influence (Trigo et al., 1999, 2000). The amount and distribution of precipitation in the Iberian Peninsula is highly irregular in both the spatial and temporal dimensions (Esteban-Parra et al., 1998; Serrano et al., 1999; Trigo and DaCamara, 2000).

The variability of precipitation over large sectors of Iberia are known to be closely connected to the large-scale atmospheric circulation modes, including the North Atlantic Oscillation (von Storch et al., 1993; Serrano et al., 1999; Trigo and Palutikof, 2001; López-Moreno et al., 2007). The North Atlantic Oscillation (NAO) has been described since the pioneering works of Walker (1924) in the early twentieth century and corresponds to one of the major patterns of atmospheric variability in the Northern Hemisphere (Wallace and Gutzler, 1981; Barnston and Livezey, 1987). This important circulation mode was poorly studied in the following decades until relatively recently when it has been characterised in more detail (e.g., Wallace and Gutzler, 1981; Barnston and Livezey, 1987; Hurrell, 1995; Hurrell et al., 2003). In simple terms, the NAO corresponds to a large-scale meridional oscillation of atmospheric mass between the subtropical anticyclone near the Azores and the subpolar low pressure system near Iceland (Hurrell, 1995; Trigo et al., 2002). Recently, a number of different studies have shown the relevance of the NAO to the winter surface climate of the Northern Hemisphere in general and over the Atlantic/European sector in particular (Hurrell, 1995; Hurrell and van Loon, 1997; Trigo et al., 2002). Furthermore several studies have established links between different NAO modes and changes in the associated activity of North-Atlantic storm tracks (Osborn et al., 1999; Trigo et al., 2006). The existence of two contemporaneous and possibly related winter-time trends over the last 3 decades: a trend towards the positive phase of the NAO and a trend towards warmer Northern Eurasian land temperatures has now been established (Hurrell and van Loon, 1997). Nevertheless it should be noted that the influence of the NAO pattern in the Mediterranean is considerably higher for precipitation

than for temperature, where it plays a relatively minor role (Castro-Díez et al., 2002).

The strong control exerted by the NAO on precipitation over the Mediterranean basin is bound to be reflected in the seasonal flow of rivers across the region. It should be noted that the river basin system acts as an effective spatial and temporal integrator of precipitation (rain and snow), temperature, and related evapotranspiration over a specific region. Therefore, seasonal to interannual streamflow variability in many river-basins can be controlled by corresponding changes in large scale atmospheric circulation patterns. The relationship between these climatic regimes and its hydrological response, through its streamflow, presents different grades of complexity according to the physical characteristics of the basin (e.g. topography, land cover, soil types, lithology, etc.). Thus, the spatial variability in the response of river discharges to the NAO can be very high, with strong differences between neighbour rivers as a consequence of the basin characteristics (Morán-Tejeda et al., 2011).

During the last decade several works have been published focusing on the impact of the NAO pattern on river flow regimes of many Mediterranean river basins (e.g. Struglia et al., 2004; Trigo et al., 2004; López-Moreno et al., 2007) but also for adjacent Middle Eastern rivers, including the Tigris, Euphrates and Jordan (Cullen and deMenocal, 2000; Cullen et al., 2002), and the large central European river Danube (Rîmbu et al., 2002). While the statistical significance of results varies among river basins, these studies show that river flow tends to be lower (higher) when the NAO index is in its positive (negative) phase.

The main objective of this chapter is to summarize different impacts of the NAO investigated by the author in the last decade, namely on the European/Mediterranean climate (Trigo and Palutikof, 2001, 2002, 2004, Trigo et al., 2006), with a particular emphasis on the Iberian water resources (Trigo et al., 2004; Trigo, 2008), but also on changes of precipitation and river flow regime (Paredes et al., 2006; Trigo et al., 2008).

2 Results

2.1 Impact in Large-Scale Circulation and Precipitation

There are a number of NAO indices available in the literature and provided by researchers that have implemented different methodological approaches (e.g. Barnston and Livezey, 1987; Hurrell, 1995; Jones et al., 1997). Results presented here were based on the NAO index developed at the Climatic Research Unit (University of East Anglia, UK) and defined, on a monthly basis, as the difference between the normalized surface pressure at Gibraltar (southern tip of Iberian Peninsula) and Stykkisholmur in Iceland (Jones et al., 1997). Taking into account that the NAO index for winter months presents a positive trend during the last 3 decades of the twentieth century its distribution is dominated by positive values,

with monthly averages above zero (Jones et al., 1997). Therefore it is advisable to normalize the entire winter NAO index (average of DJFM values) so it has zero mean (for the normal period 1961–2000) and standard deviation one. Finally, we defined the seasonal high NAO composite to be a combination of all winters with NAO index greater than 0.5, while the low NAO composite corresponds to all winters characterised with an NAO index value smaller than –0.5.

Following the approach adopted in Trigo et al. (2004), we show the large-scale impact of winter NAO on atmospheric circulation and precipitation for the North Atlantic and European sector (Fig. 1). This is performed using monthly average values of sea level pressure (SLP) and precipitation rate fields obtained from the NCEP/NCAR (National Centers for Environmental Prediction/National Center for Atmospheric Research) reanalyses dataset (Kalnay et al., 1996) for the period spanning between 1961 and 2000. Anomaly fields of SLP and precipitation rate for winter (DJFM) months characterized by high (NAO index > 0.5) and low (NAO index < –0.5) values are shown in Fig. 1a, b, respectively. The spatial signature of the NAO is given by the difference in SLP between composites (Fig. 1c). The corresponding precipitation rate anomalies are also represented (grey scale), wherever those anomalies are significantly different (at the 5% level) from climatology (Fig. 1a, b) or between composites (Fig. 1c). Several aspects in this figure are worth to be mention, namely:

(a) The typical NAO pattern can be recognised in the SLP anomalies obtained for both the positive (Fig. 1a) and negative (Fig. 1b) composites that reveal the expected dipole between the Iceland and the Azores regions so well depicted when the difference between composites is computed (Fig. 1c). However, it should be noted that the southern centre of action is not located over the strait of Gibraltar (where the station used for computing the NAO index is placed), because the variance of SLP is lower there than over the Azores, and thus the magnitude of the composite anomaly is greater over the Azores (Trigo et al., 2002);
(b) The impact of the NAO on the North Atlantic winter precipitation field, for both phases of the NAO index, is not restricted to the European continent but extends considerably over large sectors of the, mostly uninhabited, North Atlantic. In fact Fig. 1c shows quasi-zonal bands of opposite anomaly signs, with large positive differences concentrated in the northern latitudes, extending from eastern Greenland to Scandinavia. At lower latitudes, a significant band of negative differences extends from south of Newfoundland crosses the Azores archipelago and extends throughout the northern Mediterranean basin until Turkey, with larger differences located west of Iberia.

Interestingly, the vast majority of works that have been published evaluating the impact of NAO in Europe/Mediterranean have been performed on a seasonal basis, usually confined to the winter months (e.g. DJF of DJFM). Following the approach adopted in Trigo et al. (2008) the monthly spatial correlation pattern between the European precipitation and the corresponding monthly NAO pattern is presented

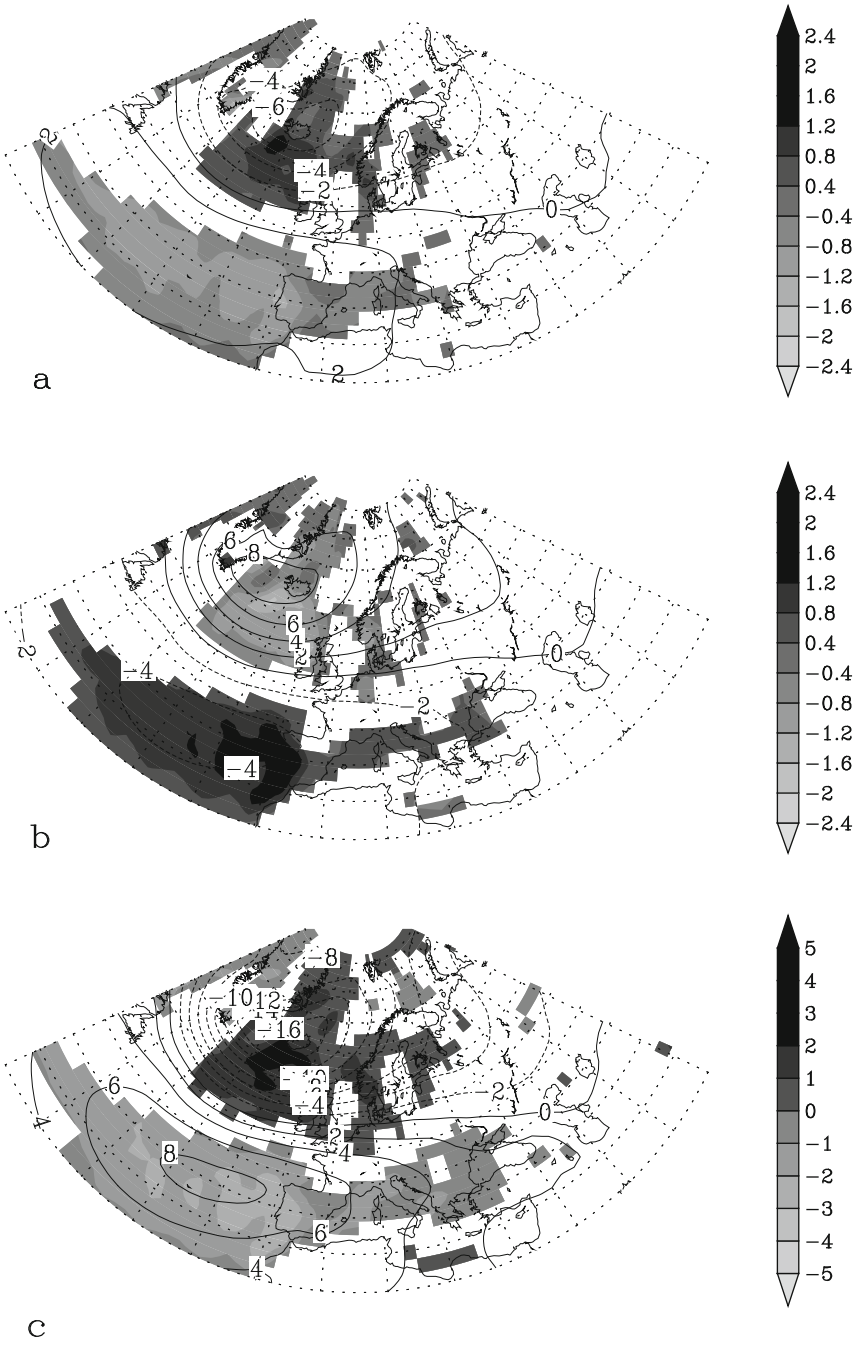

Fig. 1 Precipitation rate anomaly fields (mm/day) from the NCEP/NCAR reanalysis for winter months with (**a**) high NAO index > 0.5, (**b**) low NAO index < –0.5 and, and, (**c**) their difference. Precipitation anomalies are represented only if significant at the 5% level. Positive (*solid*) and negative (*dashed*) isolines of the sea level pressure anomaly field (hPa) are also represented

here (Fig. 2). This assessment is obtained using the high resolution (0.5°) dataset from the Climate Research Unit – CRU – of the University of East Anglia (Mitchell and Jones, 2005), between 1961 and 2000, and only restricted to those grid boxes that present a correlation value statistically significant at the 10% significance level. Naturally, no precipitation information is available over the oceans as this data set

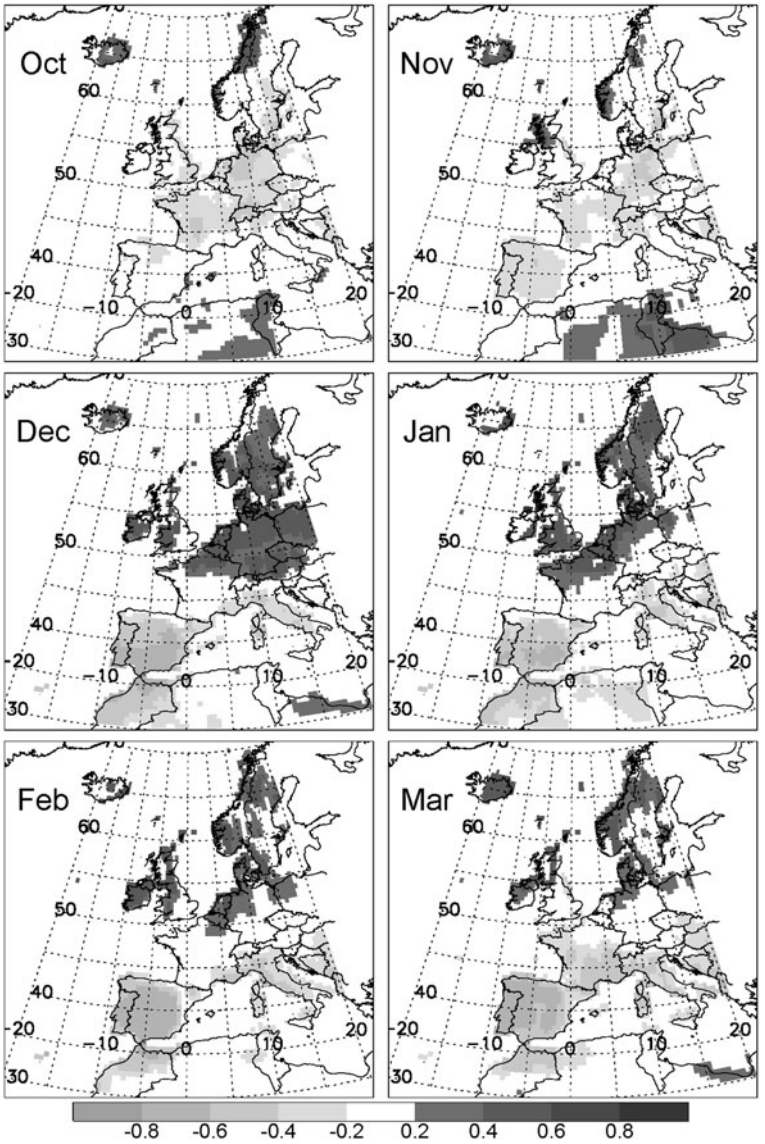

Fig. 2 Spatial pattern of correlation values between monthly European precipitation (CRU data set) and the corresponding monthly value of NAO index for the period 1961–2000

is constructed with precipitation values observed in rain gauges. The typical winter NAO-precipitation pattern shown in Fig. 2 confirms that the most prominent correlations can be observed between the core winter months that span December and March, with large negative values over Iberia ($r < -0.7$), northern Africa and central Mediterranean, while positive values dominate over northern Europe, albeit with a smaller magnitude ($r < 0.6$). A slightly different pattern emerges between October and November with weak, but still statistically significant, negative correlation values covering most of Europe between Iberia and southern Scandinavia, while positive values remained confined to small-scattered patches of UK and Scandinavia and most of northern Africa.

2.2 Impact in Western Mediterranean Water Resources

As stated in the introduction, it is expectable that the strong impact of the NAO on the precipitation regime over the western and central sectors of the Mediterranean should be also observed on the stream flow of rivers located within these sectors. This section focuses on three large transboundary Iberian rivers (Douro, Tejo and Guadiana) that correspond almost to 50% of the entire Iberian surface (Fig. 3) and flow westwards, i.e. from Spain to Portugal. It should be stressed that water resources in this south-western European region are characterised by present and future challenges, namely:

- As a consequence of high interannual precipitation variability most Iberian rivers show relatively high coefficients of interannual stream flow variation, that decrease from rivers located in the north (∼50% for Douro) to those in the southern sector (∼100% for Guadiana).
- There has been a steady decline of Iberian precipitation in late winter (February) and early spring (March) since the 1960s (González-Hidalgo et al., 2010). This decrease is driven by latitudinal shifts of storm-tracks over the Atlantic that are ultimately associated with an increasing trend of the NAO index (Paredes et al., 2006; Trigo et al., 2008). This trend in precipitation is noticeable in river flow in March and April and diminishes the soil water moisture available in the following spring and summer seasons.
- Both Iberian countries present an increasing demand of water supply in recent decades. Besides hydroelectricity production, the touristic (e.g. golf courses) and agricultural sectors correspond to the two main socio-economic activities responsible for this increment. The strong socio-economic impacts of the recent extreme drought observed during the 2004/2005 hydrological year further emphasises the necessity to develop long-term planning tools (García-Herrera et al., 2007).
- The latest IPCC report (Solomon et al., 2007) confirms what many studies based on global and regional climate models have been suggesting in the last decade; i.e. that the Mediterranean area will register a general trend towards less precipitation during the twenty-first century (e.g. Giorgi and Lionello, 2008;

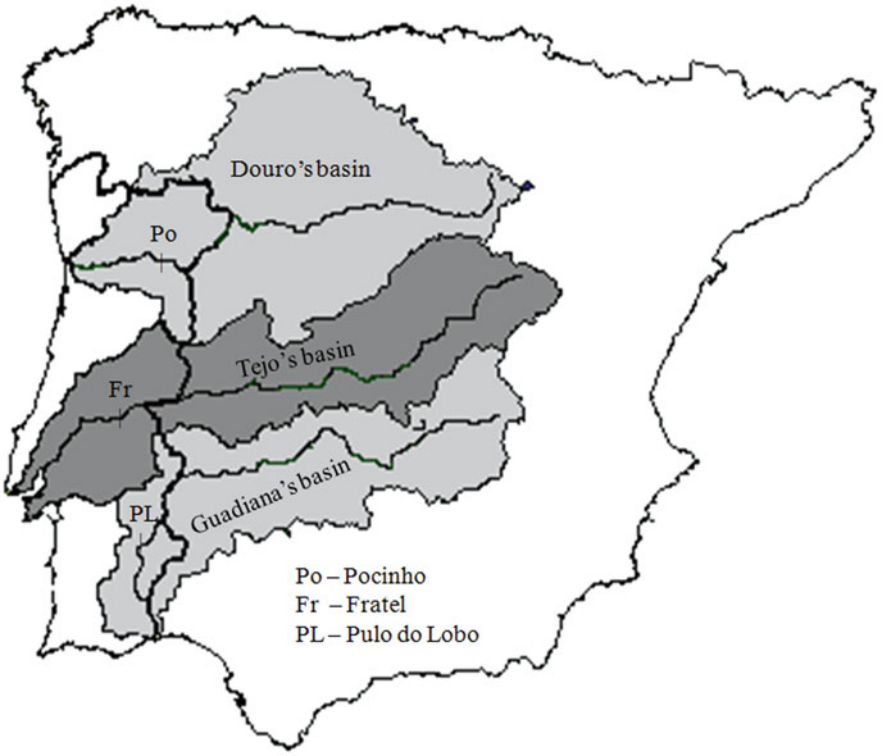

Fig. 3 Location of the three Iberian river basins considered. Small vertical lines show the location of river flow gauges used in each basin

López-Moreno et al., 2009). The combined effects of this future precipitation decrease and the widely accepted future increment in the surface temperature on the Mediterranean will bear important changes in the region's water cycle (Mariotti et al., 2008).

Following the work developed in Trigo et al. (2004) and updated in Trigo (2008) we used monthly river flow data for the three rivers depicted in Fig. 3, namely the Guadiana, the Tejo (Tagus or Tajo) and the Douro (or Duero). The datasets were kindly provided by the Portuguese Institute of Water (INAG). The location of the river gauges, corresponds to large dams located within the Portuguese section of the rivers as shown in Fig. 3. Monthly river flow anomalies during and following winters with high (low) NAO index values are represented by black (grey) bars in Figs. 4a, 5a and 6a for the Douro, Tejo and Guadiana rivers, respectively. Taking into account the very dry months that characterize Iberia between July and September we show results using the hydrological year, i.e. between October and September of the following year. It is clear that all three cases are characterized by a clear separation of river flow between the high and low winter NAO composites

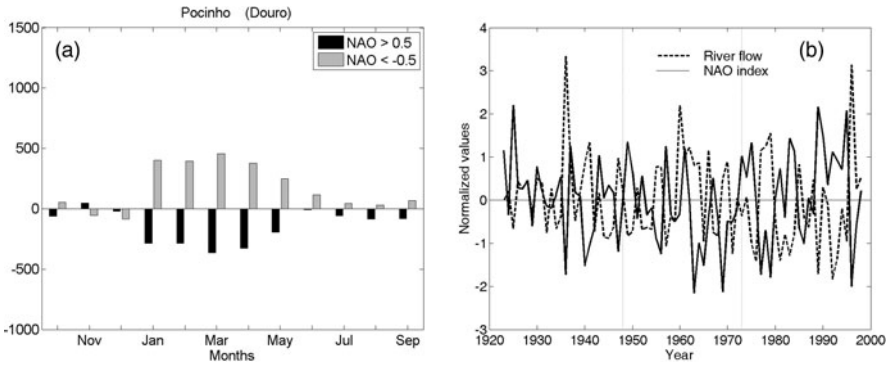

Fig. 4 (**a**) Monthly river flow anomalies (hm^3/month) of river Douro at Pocinho during and following winters with high NAO index (*black bars*) and winters with low NAO index (*grey bars*), (**b**) Interannual variability of the mean winter (JFM) river flow (*solid curve*), for river Douro at Pocinho, and the lagged winter (DJF) NAO index. Both *curves* have been normalised

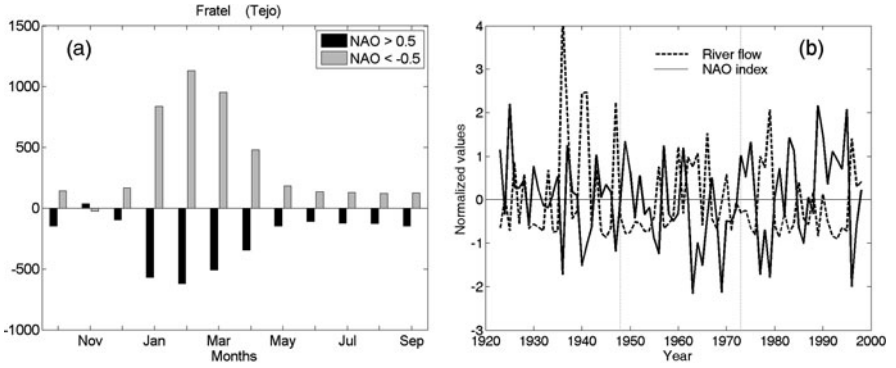

Fig. 5 The same as in Fig. 4 but for river Tejo at Fratel

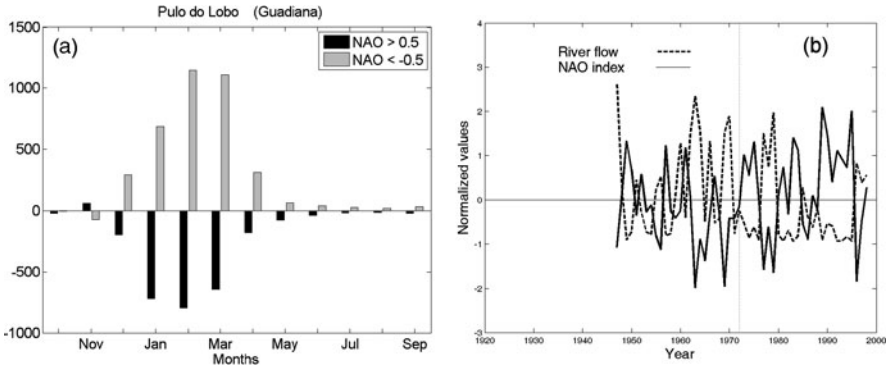

Fig. 6 The same as in Fig. 4 but for river Guadiana at Pulo do Lobo

and that such impact is not restricted to the winter months but extends considerably to the following seasons. Moreover, these changes increase as we move southwards with successive larger ranges of positive (black) and negative (grey) bars size. Thus for river Douro these differences are significant (at the 5% significance level) only between January and April, while for rivers Tejo and Guadiana these differences are significant between January and September. Lagged and non-lagged correlation coefficients were computed between winter river flow (DJF) and contemporaneous winter NAO index, using the full period of data available for each river.

The 1-month lagged correlation values were computed considering the NAO index for DJF and the river flow for JFM. In order to evaluate how stationary results are correlation coefficients were computed for three consecutive sub-periods; 1923–1947, 1948–1972 and 1973–1998 for rivers Tejo and Douro rivers while, due to shorter time series availability, results for Guadiana have to be restricted for the two most recent sub-periods (Table 1). The inter-annual variability of winter (JFM) river flow against the winter (DJF) NAO index is represented in Figs. 4b, 5b and 6b for the Douro, Tejo and Guadiana rivers, respectively. Sub-periods are delimited by vertical dotted lines, additionally both curves (river flow and NAO index) were normalized (for the total period of available data for each river) and represented between 1920 and 2000 to facilitate comparisons between all three rivers. These figures (and correlation values shown in the companying Table 1) provide some considerations:

(1) Generally speaking the 1 month-lagged correlation coefficient values are consistently higher than the corresponding non-lagged ones. In fact, when considering the entire period of data available for all three rivers, the correlation coefficient values increase when the NAO index is lagged by 1 month. Considering the last sub-period (i.e. 1973–1998) the 1-month lagged correlation

Table 1 Seasonal 1-month lagged (lag 1) and simultaneous (lag 0) correlation coefficients between winter NAO index and river flow in Pulo do Lobo (Guadiana), Fratel (Tejo) and Pocinho (Douro). Statistically significant results at the 5% level are highlighted in bold

		River flow Lag 1 NAO (DJF), flow (JFM)	River flow Lag 0 NAO (DJF), flow (DJF)
Guadiana	1948–1972	**–0.60**	**–0.45**
	1973–1998	**–0.79**	**–0.67**
	1948–1998	**–0.69**	**–0.57**
Tejo	1923–1947	**–0.56**	**–0.54**
	1948–1972	–0.37	–0.25
	1973–1998	**–0.77**	**–0.61**
	1923–1998	**–0.52**	**–0.45**
Douro	1923–1947	**–0.48**	–0.27
	1948–1972	–0.29	–0.10
	1973–1998	**–0.76**	**–0.58**
	1923–1998	**–0.55**	–0.35

coefficients achieve very significant values, namely; –0.76 for Douro, –0.77 for Tejo and –0.79 for Guadiana. These results have opened promising prospects for the use of these relationships for constructing monthly to seasonal forecasting models.

(2) The longer time series available for the Douro and Tejo rivers allow further insight on the long term behavior of these link between NAO and river flow. Interestingly, both rivers reveal a certain decrease between the first and the second sub-periods that is followed by a major increment between the second and third sub-periods. The long term evolution of this relationship can be also appreciated by the change in coherence between both time series (Figs. 4b, 5b and 6b).

The increase in the strength of the impact of NAO in the river flow since the 1970s reflects most probably two different aspects that contribute to such an outcome. On the one hand the link between precipitation and the NAO patterns is not stationary, but changes at decadal scale, having increased significantly between the mid-twentieth century to the last few decades (e.g. Trigo et al., 2004; Vicente-Serrano and López-Moreno, 2008). Additionally, it has been suggested that part of this increment in strength is related to the increase in water storage volume associated with the construction of major dams in the 1950s and 1960s (Trigo et al., 2004), given that there are evidences that variability in the water stored by reservoirs of the Tagus basin is more determined by NAO than river discharges, both in the duration and magnitude of the anomalies (López-Moreno et al., 2007). In fact, results obtained in Table 1 show that the correlation increase is larger at 1-month lag than it is for simultaneous correlations.

2.3 Precipitation and River Flow Trends Associated with the NAO

A number of studies has shown that winter (DJFM) precipitation has been decreasing steadily since the 1960s over western Mediterranean, particularly for the month of March (e.g. Trigo and DaCamara, 2000; Paredes et al., 2006; González-Hidalgo et al., 2010), with latter analysis showing that such decline is becoming to be extensive to the month of February (Trigo et al., 2008). These authors show that March monthly-accumulated precipitation for the central and western regions of the Iberian Peninsula presents a very significant decline of circa 50% during the 1960–2000 period. Naturally these changes are not confined to Iberia but correspond to the most visible aspect of a larger phenomenon affecting the entire North-Atlantic/European sector. In fact, while Iberia and the majority of the western sector of the Mediterranean experiences this decreasing trend in March, the northern regions of Scandinavia and British Isles present a remarkable increase (Trigo et al., 2008). It should be notice that the significance of these trends varies according to the period of data considered.

As expected such trends are bound to be connected with changes of the atmospheric circulation over the North Atlantic and European sectors. In this regard a

number of different approaches were used to quantify the links with large-scale and smaller scale features (Paredes et al., 2006; Trigo et al., 2008). Based on the Iberian Weather Types (WTs) classification developed by Trigo and DaCamara (2000) it was shown that, at the synoptic scale, the major contributors towards the March decline are associated with a corresponding decrease in the frequency of a few specific WTs. These "wet" WTs are characterized by higher than average values of daily precipitation and include the cyclonic (C), the western (W) and south-western (SW). On the contrary, March is also characterized by a notorious increment in the frequency of "dry" anticyclonic (A) type. In contrast the corresponding "wet" WTs for the British Isles display increasing frequencies justifying the increment of Precipitation observed in England and Scotland (Paredes et al., 2006). Within a larger context, a Lagrangean approach, based on the analysis of storm-tracks over the entire North Atlantic region, reveals dramatic changes in the location of cyclones since the early 1960s that coincides with the corresponding precipitation trends in Europe (Trigo et al., 2008). It is of no surprise that the NAO is somehow related with both phenomena, i.e. changes in the preferred path of most low pressure perturbations and contemporaneous changes of monthly precipitation totals for March. In fact, for Iberia, the region displaying the maximum correlation values between NAO and March precipitation is almost exactly coincident with the region presenting the largest decreases in precipitation. Using data for the 1960–2000 period the spatially averaged series of precipitation shows a correlation value of –0.60, that decreases to –0.48 when computed with the detrended series (Paredes et al., 2006).

It should be emphasised that the region with significant NAO induced decline of precipitation in March encloses the three major international Iberian river basins referred in the previous section, i.e. rivers Douro (North), Tejo (Center) and Guadiana (South). Thus, it is highly expectable that such a significant change in precipitation must have an imprint on the long-term evolution of monthly river flow for these rivers. That is precisely what can be seen for rivers Douro and Guadiana (Fig. 7), with both cases exhibiting very strong declines (significant at 1%) of river flow in March, computed between 1956 and 2000, similar results were obtained for river Tejo (not shown). Moreover, this decline is not restricted to the month of

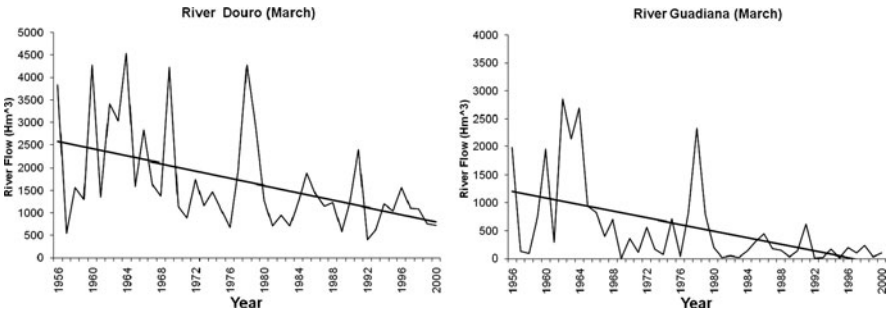

Fig. 7 Inter-annual variability of March river flow for Douro and Guadiana rivers. The corresponding linear regression trend is also represented

March but can be observed also in the following months of April and May (albeit less pronounced) due to the relatively high values of persistence that characterize river flow time series.

Finally it must be stressed that these changes can have significant socio-economic impacts for both Portugal and Spain economies. Large amounts of water from these three rivers are used for various economic activities as well as for water supply to urban areas. As an example, these three rivers together account for a very significant amount of hydroelectric production in both Iberian countries, with roughly 55% (70%) of Spanish (Portuguese) annual average (Trigo et al., 2004).

3 Conclusions

Western Mediterranean precipitation regime is strongly influenced by the NAO pattern with roughly 40% of the winter precipitation being related to the NAO index. Because this large-scale atmospheric circulation phenomenon is characterized by a marked interannual variability, it implies that the Iberian Peninsula is particularly prone to large inter-annual variability of precipitation. Therefore NAO is a key component of the relatively high frequency of wet and drought periods observed in Iberia (Vicente-Serrano, 2006; Sousa et al., 2011). Two recent extreme years exemplify perfectly this dichotomy, the extreme dry hydrological year of 2004/2005 and the wet winter of 2009/2010. The year of 2004–2005 was considered the driest for many stations in Iberia (including Lisbon and Madrid) since the beginning of the twentieth century (García-Herrera et al., 2007). This extreme event was induced by several favoring atmospheric circulation anomalies including positive values of the NAO index between November 2004 and February 2005. On the contrary the winter of 2009/2010 was characterized by record breaking negative values of the NAO index at the monthly and seasonal scales (Cattiaux et al., 2010; Wang et al., 2010). This anomalous circulation triggered particularly cold temperatures over central and northern Europe (Cattiaux et al., 2010) and simultaneously, large parts of the Iberian Peninsula (including Gibraltar and Lisbon) have registered the highest amounts of winter precipitation since the beginning of regular measurements in the second half of the nineteenth century (Vicente-Serrano et al., 2011).

As shown here the influence of NAO on the winter Iberian precipitation is extensive to the river flow of major Iberian rivers. Moreover it is possible to state that the magnitude of the NAO impact is considerably larger for Iberian rivers than what has been obtained by other authors for rivers Tigris and Euphrates (Cullen and deMenocal, 2000) and the Danube (Rîmbu et al., 2002). In fact, according to the results obtained by Struglia et al. (2004) for many river basins in the Mediterranean there are very few European rivers presenting a seasonal correlation coefficient value with – either with NAO or other large-scale circulation mode – similar to the values obtained here (~0.75). Recent results obtained by Spanish colleagues have extended the results presented here to many more gauges of Douro and Tejo, including several subsidiaries (López-Moreno et al., 2007; Morán-Tejeda et al., 2011). These authors showed that the impact of positive and negative phases of the NAO on river

discharge and levels of storage in reservoirs is neither instantaneous nor restricted to the winter months, extending well into the rest of the year. Thus, the decrease in the amount of water stored in the reservoirs during positive phases of the NAO is especially severe during the following summer and autumn, whereas in winter and spring the amount of stored water is similar to that of normal years. In this regard it is now clear that the NAO during winter months holds a significant capacity to constrain the observed river flow and water capacity for most of the year in most Iberian rivers, thus representing an important factor to be accounted for all water resources managers in general, and by agricultural and hydroelectric power production companies in particular.

Acknowledgements This work was supported by the Portuguese Science Foundation (FCT) through project ENAC (Evolution of North Atlantic Climate; the role of Blocking and Storm-tracks in the Past, Present and Future climate of Southern Europe) PTDC/AAC-CLI/103567/2008. Many thanks to Pedro Sousa for helping with the editing of this chapter.

References

Barnston AG, Livezey RE (1987) Classification, seasonality and persistence of low-frequency atmospheric circulation patterns. Mon Wea Rev 115:1083–1127

Castro-Díez Y, Pozo-Vázquez D, Rodrigo FS, Esteban-Parra MJ (2002) NAO and winter temperature variability in southern Europe. Geophys Res Lett 29. doi:10.1029/2001GL014042

Cattiaux J, Vautard R, Cassou C, Yiou P, Masson-Delmotte V, Codron F (2010) Winter 2010 in Europe: a cold extreme in a warming climate. Geophys Res Lett 37:L20704. doi:10.1029/2010GL044613

Cullen HM, Kaplan A, Arkin PA, DeMenocal PB (2002) Impact of the North Atlantic Oscillation on the Middle Eastern climate and streamflow. Clim Change 55:315–338

Cullen HM, deMenocal PB (2000) North Atlantic influence on Tigris-Euphrates streamflow. Int J Climatol 20:853–863

Esteban-Parra MJ, Rodrigo FS, Castro-Díez Y (1998) Spatial and temporal patterns of precipitation in Spain for the period 1880–1992. Int J Climatol 18:1557–1574

García-Herrera R, Paredes D, Trigo RM, Trigo IF, Hernández E, Barriopedro D, Mendes MA (2007) The outstanding 2004/05 drought in the Iberian Peninsula: associated atmospheric circulation. J Hydrometeorol 8:483–498

Gimeno L, Drumond A, Nieto R, Trigo RM, Sthol A (2010) On the origin of continental precipitation. Geophys Res Lett 37:L13804. doi:10.1029/2010GL04371

Giorgi F, Lionello P (2008) Climate change projections for the Mediterranean region. Glob Planet Change 63:90–104

Gonzalez-Hidalgo JC, Brunetti M, de Luis M (2010) Precipitation trends in Spanish hydrological divisions, 1946–2005. Clim Res 43:215–228

Hurrell JW (1995) Decadal trends in the north Atlantic oscillation: regional temperatures and precipitation. Science 269:676–679

Hurrell JW, Kushnir Y, Ottersen G, Visbeck M (2003) The North Atlantic Oscillation: climate significance and environmental impact. Geophysical Monograph Series, vol 134. American Geophysical Union, Washington, DC

Hurrell JW, van Loon H (1997) Decadal variations in climate associated with the north Atlantic Oscillation. Clim Change 36:301–326

Jones PD, Jónsson T, Wheeler D (1997) Extension to the North Atlantic Oscillation using early instrumental pressure observations from Gibraltar and South-West Iceland. Int J Climatol 17:1433–1450

Kalnay E, Kanamitsu M, Kistler R, Colins W, Deaven D, Gandin L, Iredell M, Saha S, White G, Wollen J, Zhu Y, Leetmaa A, Reynolds R, Chelliah M, Ebisuzaki W, Higgins W, Janowiak J, Mo KC, Ropelewski C, Wang J, Jenne R, Joseph D (1996) The NCEP/NCAR 40-years reanalyses project. Bull Am Meteorol Soc 77:437–471

López-Moreno JI, Beguería S, Vicente-Serrano SM, García-Ruiz JM (2007) The influence of the NAO on water resources in Central Iberia: precipitation, streamflow anomalies and reservoir management strategies. Water Resour Res 43:W09411. doi: 10.1029/2007WR005864

López-Moreno JI, Vicente-Serrano SM, Gimeno L, Nieto R (2009) The stability of precipitation regimes in the Mediterranean region: observations since 1950 and projections for the twenty-first century. Geophys Res Lett 36:L10703

Mariotti A, Zeng N, Yoon JH, Artale V, Navarra A, Alpert P, Li L (2008) Mediterranean water cycle changes: transition to drier 21st century conditions in observations and CMIP3 simulations. Environ Res Lett 3(4):044001. doi:10.1088/1748-9326/3/4/044001

Mitchell TD, Jones P (2005) An improved method of constructing a database of monthly climate observations and associated high-resolution grids. Int J Climatol 25:693–712

Morán-Tejeda E, López-Moreno JI, Ceballos-Barbancho A, Vicente-Serrano SM (2011) Evaluating Duero's basin (Spain) response to the NAO phases: spatial and seasonal variability. Hydrol Process 25:1313–1326

Osborn TJ, Briffa KR, Tett SFB, Jones PD, Trigo RM (1999) Evaluation of the North Atlantic Oscillation as simulated by a climate model. Clim Dyn 15:685–702

Paredes D, Trigo RM, Garcia-Herrera R, Trigo IF (2006) Understanding precipitation changes in Iberia in early Spring: weather typing and storm-tracking approaches. J Hydrometeorol 7:101–113

Rîmbu N, Boroneanţ C, Carmen B, Mihai D (2002) Decadal variability of the Danube river flow in the lower basin and its relation with the North Atlantic Oscillation. Int J Climatol 22:1169–1179

Serrano A, García JA, Mateos VL, Cancillo ML, Garrido J (1999) Monthly modes of variation of precipitation over the Iberian Peninsula. J Clim 12:2894–2919

Solomon S, Qin D, Manning M, Alley RB, Berntsen T, Bindoff NL, Chen Z, Chidthaisong A, Gregory JM, Hegerl GC, Heimann M, Hewitson B, Hoskins BJ, Joos F, Jouzel J, Kattsov V, Lohmann U, Matsuno T, Molina M, Nicholls N, Overpeck J, Raga G, Ramaswamy V, Ren J, Rusticucci M, Somerville R, Stocker TF, Whetton P, Wood RA, Wratt D (2007) Technical summary. In: Solomon S, Qin D, Manning M, Chen Z, Marquis M, Averyt KB, Tignor M, Miller HL (eds) Climate change 2007: the physical science basis. Contribution of Working Group I to the 4th assessment report of the Intergovernmental Panel on Climate Change. Cambridge University Press, Cambridge, UK and New York, NY, USA

Sousa P, Trigo RM, Aizpurua P, Nieto R, Gimeno L, Garcia-Herrera R (2011) Trends and extremes of drought indices throughout the 20th century in the Mediterranean. Nat Hazards Earth Syst Sci 11:33–51. doi:10.5194/nhess-11-33-2011

Struglia MV, Mariotti A, Filograsso A (2004) River discharge into the Mediterranean Sea: climatology and aspects of the observed variability. J Clim 17:4740–4751

Trigo IF, Davies TD, Bigg GR (1999) Objective climatology of cyclones in the Mediterranean region. J Clim 12:1685–1696

Trigo IF, Davies TD, Bigg GR (2000) Decline in Mediterranean rainfall caused by weakening of Mediterranean cyclones. Geophys Res Lett 27:2913–2916

Trigo RM et al (2006) Relations between variability in the Mediterranean region and Mid-latitude variability. In: Lionello P, Malanotte-Rizzoli P, Boscolo R (eds) The Mediterranean climate: an overview of the main characteristics and issues. Elsevier, Amsterdam, pp 179–226

Trigo RM (2008) Quantifying the impact of the North Atlantic Oscillation on western Iberia. In: Soares A, Pereira MJ, Dimitrakopoulos R (eds) geoENV VI – geostatistics for environmental applications. Springer, Berlin, pp 235–246

Trigo RM, DaCamara C (2000) Circulation weather types and their impact on the precipitation regime in Portugal. Int J Climatol 20:1559–1581

Trigo RM, Osborn TJ, Corte-Real JM (2002) The North Atlantic Oscillation influence on Europe: climate impacts and associated physical mechanisms. Clim Res 20:9–17

Trigo RM, Palutikof JP (2001) Precipitation scenarios over Iberia: a comparison between Direct GCM output and different downscaling techniques. J Clim 14:4422–4446

Trigo RM, Pozo-Vazquez D, Osborn TJ, Castro-Diez Y, Gámis-Fortis S, Esteban-Parra MJ (2004) North Atlantic Oscillation influence on precipitation, river flow and water resources in the Iberian Peninsula. Int J Climatol 24:925–944

Trigo RM, Valente MA, Trigo IF, Miranda PM, Ramos AM, Paredes D, García-Herrera R (2008) North Atlantic wind and cyclone trends and their impact in the European precipitation and Atlantic significant wave height. Ann NY Acad Sci 1146:212–234. doi:10.1196/annals.1446.014

Türkeş M, Erlat E (2003) Precipitation changes and variability in Turkey linked to the North Atlantic Oscillation during the period 1930–2000. Int J Climatol 23:1771–1796

Vicente-Serrano SM (2006) Spatial and temporal analysis of droughts in the Iberian Peninsula (1910–2000). Hydrol Sci J 51:83–97

Vicente-Serrano SM, López-Moreno JI (2008) The nonstationary influence of the North Atlantic Oscillation on European precipitation. J Geophys Res Atmos 113:D20120. doi:10.1029/2008JD010382

Vicente-Serrano SM, Trigo RM, Liberato MLR, López-Moreno JI, Lorenzo-Lacruz J, Beguería S, Morán-Tejeda H, El Kenawy A (2011) Extreme winter precipitation in the Iberian Peninsula, 2010: anomalies, driving mechanisms and future projections. Clim Res 46:51–65. doi:10.3354/cr00977

von Storch H, Zorita E, Cubasch U (1993) Downscaling of global climate change estimates to regional scales: an application to Iberian rainfall in wintertime. J Clim 6:1161–1171

Walker GT (1924) Correlations in seasonal variations of weather, IX. Mem Indian Meteorol Dept 24:275–332

Wallace JM, Gutzler DS (1981) Teleconnections in the geopotential height field during the Northern Hemisphere winter. Mon Wea Rev 109:784–812

Wang C, Liu H, Lee S (2010) The record-breaking cold temperatures during the winter of 2009/2010 in the Northern Hemisphere. Atmos Sci Lett 11:161–168

Xoplaki E, González-Rouco JF, Luterbacher J, Wanner H (2004) Wet season Mediterranean precipitation variability: influence of large-scale dynamics. Clim Dyn 23:63–78

The Impacts of NAO on the Hydrology of the Eastern Mediterranean

Ercan Kahya

Abstract The impacts of the NAO on the hydrology of eastern Mediterranean countries, such as Turkey, Iran, Kuwait, Oman, and Israel, are documented here from a general perspective. Results for the eastern Mediterranean countries differ from one location to another in terms of consistent NAO signal. Patterns of precipitation, streamflow, and lake levels in Turkey are discussed to show the NAO impacts. A special attention is devoted to the NAO influences on the formation of streamflow homogeneous region and on the probability distribution functions of critical droughts. The results of all these analyses clearly showed that the NAO signals are quite identifiable in various hydrologic variables in Turkey. For example, the NAO during winter was found to influence precipitation and streamflow patterns. In contrast temperature patterns appeared to be less sensitive to the NAO. The results of wavelet analysis showed that the Tuz, Sapanca, and Uluabat lakes reflect strong NAO influences. In southwest Iran, the October–December season is influenced mostly by the NAO in both dry and wet spells. Positive significant correlation values were found between the NAO and the total rainfall in the centre and southern Israel and with some of the rainfall categories. High correlations between the winter mode of the NAO and temperature and sea level pressure in Israel were also noted. In conclusion, current evidences have shown that the NAO has detectable influences on the hydrology of eastern Mediterranean countries with different magnitudes.

Keywords NAO · Eastern Mediterranean · Middle East · Hydrology · Climate

1 Introduction

The intensification hypothesis of the hydrologic cycle at the global scale was reported by climate modellers; however, knowledge of these changes will provide little guidance for developing long-term strategies in water resources management from a water resources perspective. Most water resources issues are regional in nature, and decisions are often made at river basin to catchment scales. Therefore,

E. Kahya (✉)
Istanbul Technical University, Istanbul, Turkey
e-mail: kahyae@itu.edu.tr

S.M. Vicente-Serrano, R.M. Trigo (eds.), *Hydrological, Socioeconomic and Ecological Impacts of the North Atlantic Oscillation in the Mediterranean Region*, Advances in Global Change Research 46, DOI 10.1007/978-94-007-1372-7_5,

it is import to note that future climate impacts are appropriately observed and studied at regional scales to make relevant and accurate information available for decision-making purposes (Sorooshian et al., 2003).

Studies in recent decades have shown that the North Atlantic Oscillation (NAO), a dominant mode of Atlantic sector climate variability, has the far-field influence on interannual to decadal variations of main climate and hydrological variables (i.e., temperature, precipitation and streamflow) in the eastern Mediterranean region. The Middle East (ME) region is commonly neglected in North Atlantic studies because of its proximity to the monsoonal region and the relatively scarceness of hydrological data. However the form of the NAO signature, with enhanced precipitation in the western Europe during its high index phases, and in the eastern Mediterranean during its low index phases, has been noted. A relationship between the eastern Mediterranean and Atlantic sector is expected since the NAO controls Atlantic heat and moisture fluxes into the Mediterranean region. In this context, it was shown that the first principal component of December through March streamflow variability reflects changes in the NAO using a sea surface temperature (SST) based index of the NAO and available streamflow data from some Middle Eastern rivers (Cullen et al., 2002).

A summary of climate characteristics of the ME where a complicated relation between land and climate exists is worthwhile to mention here. The ME region is known to experience a Mediterranean climate type (Csa in the Köeppen classification) with wet winters and dry summers in most parts; however, spatial gradients in climate are sharper than in the broad prototype Csa region to the west (Evans et al., 2004). That is, northward transition from desert through steppe to cool highland climate all take places within 400 km along the 40°N meridian. Presence of many coastlines and mountain ranges function in the modification of local climates in the ME elsewhere. Specifically speaking, upslope seasonal precipitation occurs in mountain ranges of southern the Black and Caspian Seas, and eastern coast of the Mediterranean Sea. Similarly orographic precipitation in the Taurus and Zagros Mountains feeds the Euphrates and Tigris Rivers, a source integrated watershed system for the Mesopotamia region. As prevailing sources of water vapour, the Red Sea and Persian Gulf activate little precipitation locally owing to descending air mass in the Hadley cell. Interior steppe and deserts extending Syria, Iraq, Jordan and Saudi Arabia, cause drier climate conditions by means of surrounding mountain ranges. Dry summers render only winter rainfall (which is highly changeable) possible for source of renewable water in the eastern Mediterranean region. Developing economies in the region heavily depend upon water, so they are extremely vulnerable to droughts. Krichak et al. (2002) proclaimed that the NAO and the East Atlantic-West Russian oscillation (EA-WR) have a combined effect, so that when they are both in their positive phase, a rainy season occurs in the southeastern region, and vice versa.

For regional atmospheric patterns governing rainfall in Israel, Ziv et al. (2006) explained that the synoptic-scale system affecting the eastern Mediterranean that is responsible for most of the annual rainfall is an extratropical cyclone, known as the Cyprus Low. Rainfall is formed within cold air masses originated from Europe, entering the region from the northwest. Air masses gain moisture from warm water

and become conditionally unstable. The strong thermal affects significantly cyclone dynamics over this region, in turn, resulting in intensive rainfall over Israel.

A relationship between the eastern Mediterranean and Atlantic sector is to be expected since the NAO controls Atlantic heat and moisture fluxes into the Mediterranean region (Türkes, 1996). Since these winter cyclones are the dominant source of Middle Eastern rainfall and streamflow, changes in Atlantic westerly heat/moisture transport and Atlantic/Mediterranean SSTs in relation to the NAO are expected to influence the ME climate (Cullen et al., 2002). Thus both fundamental climatic processes and their critical socio-economical consequences are manifested in the eastern Mediterranean region, and offer the motivation for this chapter. Presentation of typical pictures of the NAO impacts on the country and regional scales in the eastern Mediterranean region is the purpose of this chapter.

2 Results

In the last 2 decades, climate modelling studies have been undertaken to simulate the climate of the Middle East/eastern Mediterranean region. For example, Evans et al. (2004) had the same aim and showed that processes controlling the seasonality of precipitation differ in different subregions and are often different from the processes controlling interannual variability in the Middle East. More recently, in a regional climate modelling study of the winter climate of Central–Southwest Asia (CSWA), focusing on the mean model climatology of temperature and precipitation, Syed et al. (2010) analysed the simulated storm characteristics and the effects of ENSO and NAO on storm activity and precipitation. Their detailed storm analysis demonstrated that they are mostly associated with an intensification of western disturbances originating in the eastern Mediterranean and Middle East regions and moving eastward across a mid-troposphere (500 hPa) trough situated over the CSWA during the positive NAO and warm ENSO phases. The NAO and ENSO signals are reinforced by enhanced moisture sources from the Mediterranean, Caspian and Arabian Seas.

To overview the NAO signals on two essential hydrologic variables (precipitation and streamflow) in the eastern Mediterranean region, it would be reasonable to address the issue at both regional and country scale under the lights of some major studies. For the first scale, we prefer to rely on our review on two diagnostic studies by Cullen and her colleagues in this section. For the second scale, the order of naming country in the region is selected according to clockwise direction starting from the north.

2.1 Regional Scale Review: NAO Impacts on the Hydrology of Middle East Region

2.1.1 Precipitation Variability Associated with the NAO

Cullen et al. (2002) described the influence of the NAO on interannual to decadal precipitation variability in the Middle East by computing composite

precipitation anomalies using the 21-year CMAP monthly data set over the region (90°W–60°E; 20°N–70°N) extending from the east coast of the U.S. to the Middle East for months with positive and negative values of the NAO index for the complete period 1979–1998. Their composite analysis clearly showed evident appearance of the expected signature of the NAO in the form of enhanced precipitation in north Europe during high index periods and in the Mediterranean region during low index periods (Fig. 1). Another important clue visualised in this figure is said to be an axis of enhanced monthly wintertime precipitation that is clearly observable during low index periods extending from southeastern U.S. across the Atlantic to the Iberian Peninsula having negative anomalies more or less parallel to the north and south. In contrast a reversed pattern with departures from strict linearity is virtually evident during high index periods. More specifically this pattern comprises of the enhanced precipitation axis during low index months extending across the northern Mediterranean nearly to the Caspian Sea with an enhanced secondary maximum along the west coast of Spain and Portugal and over Turkey.

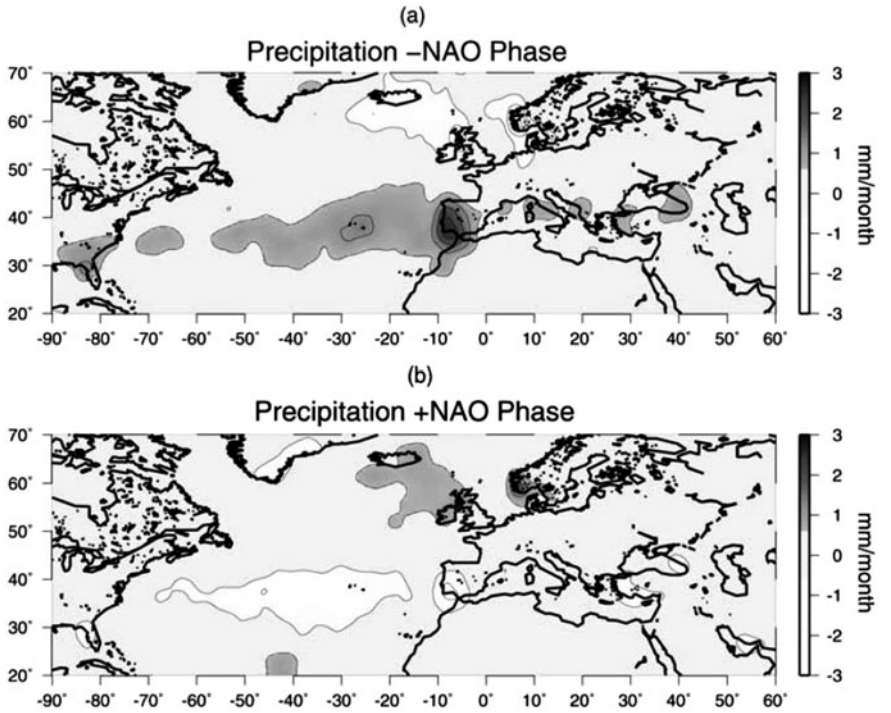

Fig. 1 (**a**) Composite of the most negative quartile of NAO index years (negative NAO phase) and (**b**) the most positive quartile of NAO index years (positive NAO phase) (adopted from Cullen et al., 2002)

2.1.2 Streamflow Variability Associated with the NAO

Cullen et al. (2002) examined streamflow data in relation to the NAO from five Middle Eastern rivers, namely Ceyhan (Turkey), Euphrates (Turkey), Karun (Iran), Tigris (Iraq), and Yarmouk (Jordan). They demonstrated that the first principal component of December through March streamflow variability reflects changes in the NAO. The hydrology of these rivers revealed two primary flooding periods: the first due to rainfall-driven runoff from December through March, regulated on interannual to decadal timescales by the NAO, and the second period due to spring snowmelt from April through June, contributing in excess of 50% of annual runoff. They also noted that the latter witness no significant NAO teleconnection and a less direct relationship with local climatic factors.

2.2 NAO Impacts on the Hydrology of Turkey

Climate response in Turkey to variability of the NAO, in particular, has been a major concern in last decade. The results of Türkeş and Erlat (2003) indicated that negative correlation coefficients between Turkish precipitation and the NAO indices were stronger in winter and autumn, and weaker in spring and almost non-existent in summer. They stated that annual and seasonal composite precipitation means were mostly characterized by wetter than longterm average during the weak NAO phase, whereas the strong NAO responses mostly exhibited drier than long-term average annually and in all seasons except summer. Spatially coherent and statistically significant changes in precipitation amounts during the extreme NAO phases were more evident in western and middle Turkey.

Henceforth this section will emphasize on the findings of the author and his colleagues' earlier and current works in regard to the NAO impacts on hydrological surface variables in Turkey. As a first start of presenting our results based upon basic statistical analyses, we examined Turkish climatic variables (precipitation, streamflow and maximum and minimum temperatures) in association with the NAO using correlation analysis with various lag combinations (Karabörk et al., 2005). In this study, we used monthly precipitation totals (compiled from 94 climate stations with a period 1951–1993), monthly streamflow (compiled from 76 streamflow gauging stations with a period 1964–1994) and monthly maximum and minimum temperature (compiled from 54 climate stations with a period 1951–1994) observations. In general, simultaneous and lag cross-correlation analyses showed that precipitation, streamflow, maximum temperature and minimum temperature patterns over Turkey have significant negative correlations with the NAO index. The results of some lag correlations also indicated a considerable prediction potential for precipitation and streamflow variables. A portion of this potential for streamflow could be readily explained by the carry-on effects of catchments, nevertheless there is a need for further investigation to elucidate the NAO and precipitation relationship that has been identified to be valid for the time lag of several months in some cases. Correlation analysis revealed less sensitive characteristics of Turkish temperature

patterns against the NAO. The consequences of the present study verify far reaching influences of the NAO in eastern Mediterranean basin and the Middle East region. Moreover, we stated that the SOI series was negatively correlated with both Turkish precipitation and streamflow patterns; however, these correlations were not as significant when compared with those between the NAO and precipitation and streamflow separately.

Of particular interest in Hurrell (1996) is said to be the contribution of the NAO variability to the recent trend in global hemispheric mean wintertime temperature. It was shown that both the NAO and SO extremes are linearly related to the climate trend, with the NAO dominating a larger land area than the SO. When he used only the NAO and the SO indices in his regression models, more confidence was observed in the estimated coefficients and 44% of the variance of the extra-tropical Northern Hemisphere temperatures was explained.

This diagnosis also appeared, to some extent, in the results of our next investigation (Kalayci and Kahya, 2006), involving the systematic modes of spatial and temporal variation in monthly streamflow records in Turkey using the principal components (PCs) analysis. The PC1 reproduces 38.2% of the total variance of the entire streamflow data set. In other words, 142 of 372 observed anomaly map patterns during the study period 1964–1994 have a similar map pattern to that of PC1 loadings (Fig. 2), illustrating only positive sign across the study domain. It represents a basic streamflow anomaly pattern having above-normal streamflow anomalies everywhere when the PC1 scores are positive or below-normal streamflow anomalies everywhere when the scores are negative values. The homogeneous appearance of PC1 is a common feature of the PC analysis. The contoured values in Fig. 2 are the PC1 loadings, corresponding to the values of correlation coefficients between streamflow and the PC values. It is important to note that strongest loadings indicate greatest departures from the mean streamflow (Lins, 1985). We then targeted seasonal correlations between the PC scores and the indices of large-scale atmospheric circulation (i.e., the NAO and SO) to elucidate the physical meaning of the components. For this purpose, we carried out various correlation analyses between the scores of each PC and the series of the NAO index at the annual and seasonal bases. The relation between PC1 scores and NAO index was witnessed as –0.491 (significant at 99% level) for annual average; –0.424 (significant at 95% level) for DJF seasonal average; –0.387 (significant at 95% level) for MAM seasonal average; and –0.506 (significant at 99% level) for JFM seasonal average. There were no similar significant correlations for other PCs. For the JFM season, Karabörk et al. (2005) also found a highly significant relation in conjunction with the NAO in the western Turkey. These indications clearly imply the sensitivity of the Turkish streamflow climatology to the NAO variations.

More recently we considered the NAO impacts on the hydrology of Turkey using different variables through new but uncommon perspectives and arrived to following interesting results. Let's consider first drought variables, representing complex events which may impair social, economic, agricultural, and other activities in a society. We were concerned in Şarlak et al. (2009) with a hydroclimatological study, which shed light on the NAO impacts on regional drought characteristics in Turkey,

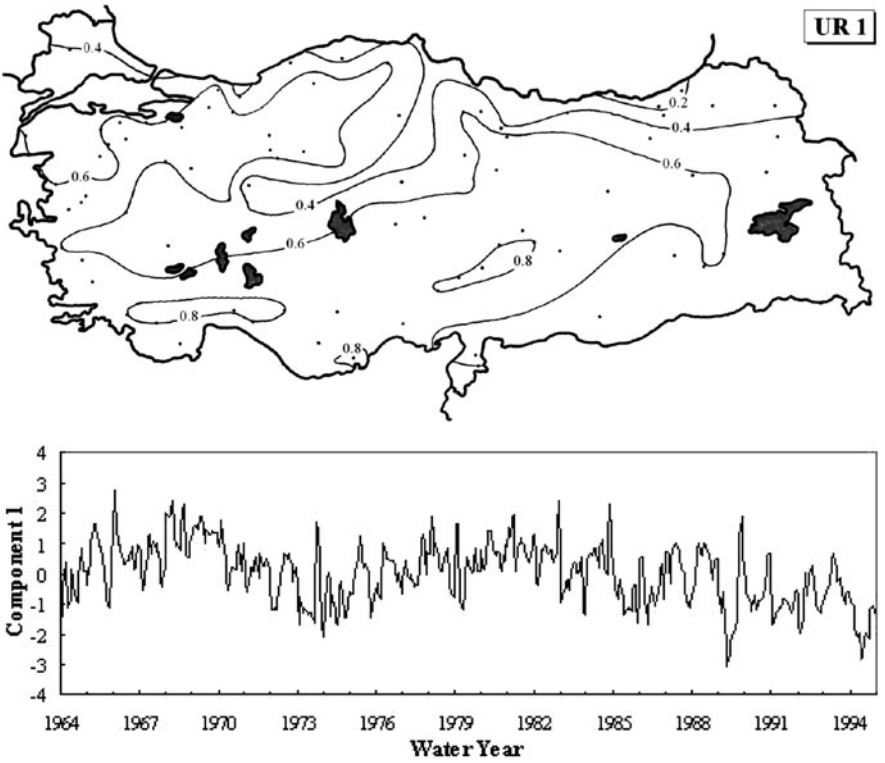

Fig. 2 The map pattern of the first component loadings and time series of the first component scores (adopted from Kalayci and Kahya, 2006)

consisting of three stages: first a Markov chain model based on annual flows at Göksu river (located in the mid-southern Turkey); second a critical drought analysis; and third the influences of the NAO on the probability distribution functions (PDFs) of critical droughts. Drought duration was taken as a key parameter in our Markov chain model. It is noteworthy to recall that the critical drought duration is the possible maximum duration likely to occur over the economic life of any water resources system. The expectations of the critical drought duration are provided for different transitional probabilities. We examined the influences of NAO on the PDFs of critical droughts for two opposite phases; namely, the period dominated by negative NAO index values (1936–1971) and the period controlled by positive NAO index values (1972–2000). The analysis of results clearly indicated that the NAO mode has quantifiable influences on the transition probabilities and expectation of the critical drought duration for annual flows at Göksu River. For example, the probability *P(d/d)* corresponding to the characteristic of negative anomaly followed by another negative anomaly, takes on a remarkably high value of 0.81 for the period of positive NAO index phase causing dry conditions in Turkey. It is striking that this

value resided at a magnitude as low as 0.40 for the period of negative NAO index phase causing wet conditions in Turkey.

Currently it is not certain as to whether this conclusion can be generalized for other rivers in Turkey. It would not be illogical to expect similar results with varying spatial and temporal response for the other parts of the country. A justification for such expectation can be made through the indications of López-Moreno and Vicente-Serrano (2008) who studied droughts using the standardized precipitation index at different time scales for Europe over a period of a century. They stated that the responses of droughts to the phases of the NAO vary spatially; however, the response depends on the month of the year *and* the time scale of the analysis.

In our other study we were concerning lake-level variations in relation to the NAO using the wavelet transform technique. The use of this approach is rather limited in the literature, therefore we investigated the variability of lake levels in seven lakes mostly scattered around western Turkey using continuous wavelet transforms and global spectra methods (Küçük et al., 2009). In their analysis, long winter (DJFM) lake-level series and the NAO index series were subjected to the wavelet transform. In most cases, the global wavelet spectrum (energy spectrum of periodicities) of lake levels and winter NAO index anomalies revealed a significant correlation. It was shown that Tuz, Sapanca, and Uluabat lakes reflect much stronger influences of the NAO than the other four lakes. In contrast, weak correlations were found in the coastal areas of the Mediterranean and eastern Turkey. The periodic structures of Turkish lake levels in relation to the NAO revealed a spectrum between the 1-year and 10-year scale level. They stated that the periodicities of more than 10-year scale levels were detected; however, explanation of such significant relations between the NAO and these long-term periodicities still remains a challenging task.

Since we were curious about different aspects of the NAO impacts on different hydrological variables in Turkey and have been releasing the relevant results from our previous studies, we later wondered whether or not it is possible to discover a noticeable difference due to the NAO forcing on hydrological regionalization in Turkey. This might be thought as an aggregate hydrologic response to the NAO; consequently we have started to conduct a research based on cluster analysis of streamflow data in order to depict maps related to positive and negative phase of the NAO. Following a similar logic used by Şarlak et al. (2009) and after rigorous inspection of available continuous streamflow series, we were able to form two different data sets; one with a period 1962–1971 and other with a period 1970–1997. Needless to say, the former period represents the negative phase period of the NAO whereas the latter stands for the opposite phase. The number of stations included for the analysis of each case is not the same; that is, 40 stations come out for the negative phase period as 83 stations were selected for the positive phase period. The results of analysis for monthly streamflow means are illustrated in Fig. 3. Differences between the two maps could be highlighted as follows: (i) elongated regions in the middle and east Turkey for the negative phase of the NAO and (ii) additional small region appearance (located in western Black Sea coast shown by pink colour) and

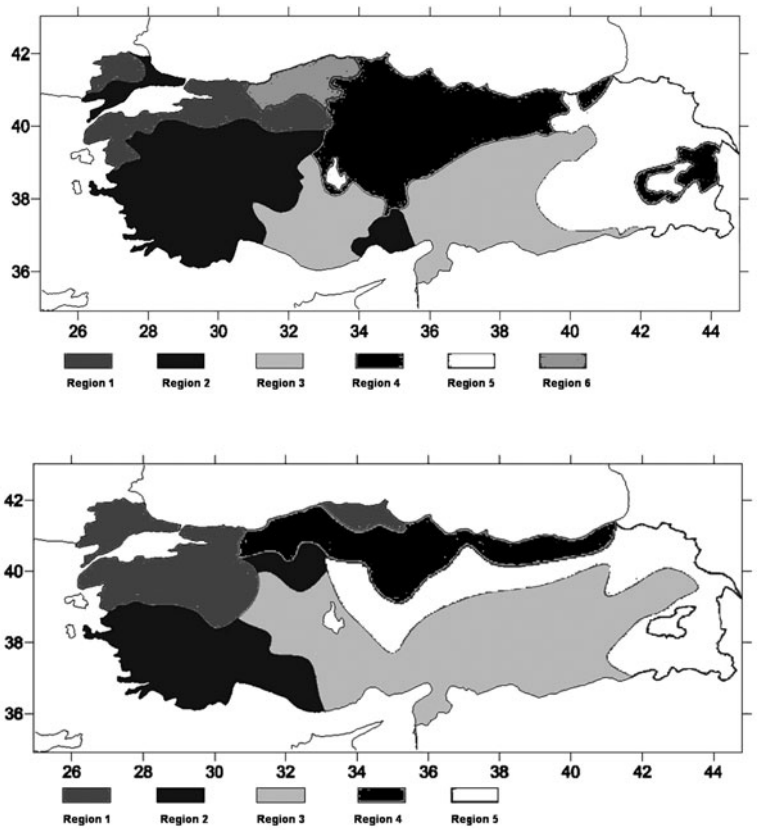

Fig. 3 The map patterns of hydrological regionalization based on the positive phase of NAO (*top panel*) and the negative phase of NAO (*lower panel*)

patchy form of Marmara region for the positive phase of the NAO. As a result this comparison shows a potential of the NAO in controlling mechanisms for hydrologic regionalization in Turkey.

2.3 NAO Impacts on the Hydrology of Iran

The influence of the NAO on historically observed rainfed crop yields of both barley and wheat in the northeast of Iran was investigated by Bannayan et al. (2010a) for the period 1983–2005. In central part (Mashhad), the NAO provided a firm basis for a measurable teleconnection between crop yields and climate factors. They noted significant correlation between the NAO and wheat only during October, but no such significant relationship for barley was detected for any month in Mashhad. During the period of positive NAO index, yields increased whereas the reverse happened

during the opposite phase. In other words, it is likely to expect a higher wheat yield in Mashhad when the NAO index is negative. Moreover Bannayan et al. (2010b) studied that the relationship between aridity index (AI) and detrended crop yield of selected crops (wheat and barley) and the influence of three climate indices (AO, NAO and NINO-3.4) were assessed for Khorasan province in northeast of Iran. They observed a significant correlation between the NAO and NINO-3.4 with AI. Precipitation is one of the components of AI, in turn; the AI response to the NAO and NINO-3.4 can be related to the observed association between this index and precipitation. It seems that these climate indices could be used to construct useful tools to monitor drought patterns and subsequent yield variability in some regions of Khorasan province. Owing to the importance of reference evapotranspiration (ET_o) in determining crop water demand, some studies were conducted to assess the impacts of different climate factors that are known to account for important fraction of climate variability in many areas of the world. For example, Sabziparvar et al. (2010) stated the following two important points: (i) the teleconnection impact of El Nino/Southern Oscillation (ENSO) phenomenon on ET_o in warm arid regions (southern parts of Iran), in general, was more significant than that in warm humid regions, and (ii) the modulation of the ENSO impacts by the NAO variability might also cause complex interactions on ET_o process in some sites in the north coasts of Iran.

Besides analyzing recent trends in streamflow, precipitation and temperature in mountainous, semiarid Karkheh River basin (which is located in the western part of Iran), Masih et al. (2010) studied also the relationship between the NAO index with the local climate variable (e.g., precipitation and temperature). Some earlier studies for the Middle East have demonstrated the NAO influences on temperature and precipitation regime during winter and early spring (e.g. Cullen et al., 2002; Mann, 2002; Evans et al., 2004). Following these works Masih et al. (2010) examined the magnitude of correlation values between monthly NAO index and the monthly precipitation and temperature during the winter months from December to March. Their findings regarding precipitation appeared to be different than those of Cullen et al. (2002) who found strong impact of changes in the NAO on the streamflow, precipitation and temperature during December–March for the Euphrates-Tigris River system. However, the results of Masih et al. (2010) confirmed those of Evans et al. (2004) who indicated that the NAO index alone could not be a predictor of the local climate in the Zagros Mountains, Iran.

In order to make more reliable decisions in water resources management, information on regional characteristics of drought duration and intensity is thought to provide critical insights in arid and semiarid regions. In this regard, determination of appropriate predictors for seasonal rainfall is important in regional analyses of meteorological droughts, since rainfall is the sole variable to quantify the characteristics of such drought. Dezfuli et al. (2010) concerned the regional rainfall relationships with the SOI and NAO at the seasonal time scale to find the appropriate regional drought predictors over southwest Iran. They found that the NAO is negatively correlated with autumn rainfall such that it is least likely for an extreme autumn drought to occur when June–August NAO is negative. A spring drought

is usually preceded by an October–December NAO greater than 0.5. In contrast winter droughts were not lag-correlated with either NAO or SOI. In addition to the findings for droughts, these indices considerably influenced wet seasons. A wet autumn tends to occur when either May–July SOI is less than −0.5 or June–August NAO is less than about −0.3. It is also noted that the extreme wet springs were absent during positive October–December NAO. This season is influenced most by NAO in both dry and wet spells. Finally, Defluzi et al. concluded that, similar to droughts, the wet winter seasons were not in association with either SOI or NAO.

Ghasemi and Khalili (2006), who studied the impact of the Arctic Oscillation (AO) on the winter surface air temperature (SAT) over Iran, found a significant relationship between the NAO index and the winter SAT for about 53% of 51 stations in Iran. Significant correlation coefficients between the NAO index and the winter SAT vary from –0.34 in Tabriz to –0.58 in Abadan. Using seasonal average of the NAO, there were some attempts to develop a forecasting model for climate variables in Iran. A model developed by Setoodeh et al. (2004) was able to predict rainfall and temperature one season ahead with reasonable error based on neural network-based models in Shiraz.

2.4 NAO Impacts on the Hydrology of Kuwait, Oman and Israel

Because of small geographical extent and limitation in data coverage and length country wise, there is no ample amount of studies that could reflect different aspects of NAO signals in Oman and Kuwait. However recent results introduced by Marcella and Eltahir (2008) may shed light on possible teleconnection between the NAO and Kuwait's hydrology. Kuwait, surrounded by the Syrian and Arabian Deserts to the west and the Persian Gulf to the east, is located in a semiarid climate zone. Its location lies in a transitional area between the tropics and midlatitudes; hence, the contributions of both climate zones to Kuwait's rainfall intrigues for answer to how sensitive the country and the surrounding region's rainfall is to large-scale circulation indices. Among other issues in their study, Marcella and Eltahir (2008) attempted to explain changes in the strength of the NAO in affecting Kuwait's annual rainfall. Nevertheless their investigation revealed no significant correlation on a monthly or yearly time scale for the relationship between Kuwait rainfall and NAO. These results are similar to those of Evans et al. (2004), who did not find a significant correlation between the NAO and rainfall in the Middle East. As far as it can be seen from their paper, the authors have used normalized annual rainfall anomalies in Kuwait from CRU (Climate Research Unit: 1976–2001) and GPCP (Global Precipitation Climatology Project: 1979–2001). The use of gridded datasets (that have used with few original stations in their assemblage) casts some doubts on the significance of these results and might explain why these are fundamentally different from the relatively well established impacts of NAO over Turkey, Iran and Oman.

A recent work by Charabi and Al-Hatrushi (2010) provides some evidence for Oman, having studied the relation between winter rainfall in Oman and the large-scale circulation as well as synoptic activity on a monthly basis. Their investigation focused on wet and dry spells that occurred during the period 1984–2007 based on composite analysis and the role of the main Eurasian oscillations; the EA/WR and the NAO in controlling the Oman winter rainfall. Charabi and Al-Hatrushi obtained the best results for the NAO in such a way that the wet spells are negatively correlated with NAO. The negative NAO phase corresponds to enhanced westerly flow (850-hPa up to 200-hPa), bringing moisture from the Atlantic ocean across the Mediterranean area towards Oman. However, the correlation detected between dry spells and positive phase of the NAO was relatively weak. The teleconnection showed that the extreme wet spells in northern Oman during winter correspond to the extreme negative index of NAO. Such prominent examples were noted in December 1989 (regional rainfall index = 1.45 vs. NAO index = −1.15) and in December 1995 (regional rainfall index = 3.32 vs. NAO index = −1.67). It is also worth to note that the influence of a weak NAO in winter precipitation may tend to cause a widespread wet event rather than an expected widespread drought condition in northern Oman during some winter months (e.g., December 1991, December 1992, January 1998, January 2001, February 1993, and March 1987). The bulk of rainfall in northern Oman occurs in the winter *seif* season from November/December to April and accounts for 58–83% of the average annual rainfall. These are caused by midlatitude westerly depression by polar front jet stream (Andy et al., 2009). An essential conclusion drew by Charabi and Al-Hatrushi (2010) was that the winter rainfall in Oman showed, in general, some linkages with the negative phase of NAO.

Israel is located on a climatic border, between the temperate and the arid regions. There have been extensive studies to put forward detailed aspects of the NAO impacts on hydrology and climatology of Israel and some major works in the context of this section are reviewed here. Ziv et al. (2006) aimed to find a linkage between the interannual variations of the rainfall measured in twelve stations in the northern half of Israel (the southern Levant) and regional to global scale atmospheric circulations. For the relation between the southern Levant rainfall and NAO, they pointed out that weak correlation found between the rainfall and the NAO by Ben-Gai et al. (2001) and in this study is inconsistent with Eshel and Farrell (2000, 2001), who found that the rainfall variability over the EM is explained through the modulations of a North Atlantic/Mediterranean teleconnectivity. Other than rainfall variable, Ben-Gai et al. (2001) showed high correlations between the winter mode of the NAO and temperature and sea level pressure (SLP) in Israel with a magnitude of –0.8 and +0.9, respectively. However, none of these studies witnessed any significant correlation between NAO and the rainfall over the southern Levant.

Categorized rainfall intensity in different regions of Israel could be put on the table for searching the NAO signals. Yosef et al. (2009) examined rainfall intensity trends and searched NAO signals at the same time. Their results included that a positive significant correlation was found with the total rainfall in the centre and south and with some of the rainfall categories.

3 Conclusions

The findings in terms of consistent NAO signal for the eastern Mediterranean countries differ from one location to another. The following aspects are the articled highlights of the NAO signals in the eastern Mediterranean countries.

Highlights for Turkey;

1. The results of some lag correlations indicated a considerable prediction potential for precipitation and streamflow variables.
2. Correlation analysis revealed less sensitive characteristics of Turkish temperature patterns with the NAO.
3. The relation between the NAO index and streamflow PC1 scores (representing a basic streamflow anomaly pattern in the entire Turkey) was determined highly significant for annual average and various seasonal averages.
4. The NAO has quantifiable influences on the transition probabilities and expectation of the critical drought duration for annual flows at Göksu River.
5. Tuz, Sapanca, and Uluabat lakes demonstrated much stronger influences of the NAO than the other four lakes.
6. The NAO was shown as a factor affecting the form of hydrological regionalization depending on its positive and negative phases.

Highlights for Iran;

1. In the central part of Iran (Mashhad), the NAO provided a firm basis for a measurable teleconnection between crop yields and climate factors. It is likely to expect a higher wheat yield in Mashhad when the NAO index is negative.
2. Aridity index series compiled from Khorasan province in northeast of Iran revealed significant correlations between the NAO and NINO-3.4.
3. The NAO index alone could not be a predictor of the local climate in the Zagros Mountains, Iran. Similar to droughts, the wet winter seasons were not in association with the NAO in the same area.
4. In southwest Iran, the October–December NAO season was influenced most by the NAO in both dry and wet spells.
5. Significant relationship between the NAO index and winter surface air temperature was found in about 53% of 51 stations throughout Iran.

Highlights for Kuwait, Oman and Israel;

1. No significant correlation on a monthly or yearly time scale for the relationship between the NAO and Kuwait rainfall was noted.
2. During the period 1984–2007, the wet spells in Oman winter rainfall were negatively correlated with the NAO.
3. Extreme wet spells in northern Oman during winter corresponded to the extreme NAO negative index.

4. Poor correlation was found between the NAO and rainfall in the northern half of Israel.
5. High correlations were detected between the winter mode of the NAO and temperature and sea level pressure in Israel.
6. Positive significant correlation was found with the total rainfall in the centre and south and with some of the rainfall categories.

It will be a good practice to close this chapter by a rare NAO related indication for Iraq. Recalling preliminary research showing that the band of drying and cooling during the positive NAO phase extends from Spain through northern Africa and Italy to Turkey and the Middle East, this signal for temperature in Iraq was exceptionally strong, with the NAO explaining nearly 50% of the variance in wintertime temperatures according to the study by Sorooshian et al. (2003). Such a strong signal level is not common among climate studies, therefore it provides a potential for accurate seasonal forecasts.

Acknowledgements The author is grateful to the efforts of organizers of ESF-MedCLIVAR Workshop (Hydrological, socioeconomic and ecological impacts of the North Atlantic Oscillation in the Mediterranean region, Zaragoza, Spain, May 24–27, 2010) Drs. García-Herrera, Trigo and Vicente-Serrano. This work has been funded through support by TUBITAK Research Project, No: ÇAYDAG 108Y165.

References

Andy YK, Dorvlo AS, Kumar GTV (2009) Analysis of a 27-year rainfall data (1977–2003) in the Sultanate of Oman. Int J Climatol 29:605–617

Bannayan M, Lotfabadi SS, Sanjani S, Mohamadian A, Aghaalikhani M (2010a) Effects of precipitation and temperature on crop production variability in northeast Iran. Int J Biometeorol 55(3):387–401

Bannayan M, Sanjani S, Alizadeh A, Lotfabadi SS, Mohamadian A (2010b) Association between climate indices, aridity index, and rainfed crop yield in northeast of Iran. Field Crops Res 118:105–114

Ben-Gai T, Bitan A, Manes A, Alpert P, Kushnir Y (2001) Temperature and surface pressure anomalies in Israel and the North Atlantic Oscillation. Theor Appl Climatol 69:171–177

Charabi Y, Al-Hatrushi S (2010) Synoptic aspects of winter rainfall variability in Oman. Atmos Res 95:470–486

Cullen HM, Kaplan A, Arkin PA, Demenocal PB (2002) Impact of the north Atlantic oscillation on the Middle Eastern climate and streamflow. Clim Change 55:315–338

Dezfuli AK, Karamouz M, Araghinejad S (2010) On the relationship of regional meteorological drought with SOI and NAO over southwest Iran. Theor Appl Climatol 100:57–66

Eshel G, Farrell BF (2000) Mechanisms of Eastern Mediterranean rainfall variability. J Atmos Sci 57:3219–3232

Eshel G, Farrell BF (2001) Thermodynamics of Eastern Mediterranean rainfall variability. J Atmos Sci 58:87–92

Evans JP, Smith RB, Oglesby RJ (2004) Middle East climate simulation and dominant precipitation processes. Int J Climatol 24:1671–1694

Ghasemi R, Khalili D (2006) The influence of the Arctic oscillation on winter temperatures in Iran. Theor Appl Climatol 85:149–164

Hurrell JW (1996) Influence of variation in extratropical wintertime teleconnections on Northern Hemisphere temperature. Geophys Res Lett 23:665–668

Kalayci S, Kahya E (2006) Assessment of streamflow variability modes in Turkey: 1964–1994. J Hydrol 324:163–177

Karabörk MÇ, Kahya E, Karaca M (2005) The influences of the Southern and North Atlantic Oscillations on climatic surface variables in Turkey. Hydrol Process 19:1185–1211

Krichak SO, Kishcha P, Alpert P (2002) Decadal trends of main Eurasian oscillations and the Eastern Mediterranean precipitation. Theor Appl Climatol 72:209–220

Küçük M, Kahya E, Cengiz TM, Karaca M (2009) North Atlantic oscillation influences on Turkish lake levels. Hydrol Process 23:893–906

Lins HF (1985) Streamflow variability in the United States: 1931–1978. J Clim Appl Climatol 24:463–471

López-Moreno JI, Vicente-Serrano SM (2008) Positive and negative phases of the wintertime north Atlantic oscillation and drought occurrence over Europe: a multitemporal-scale approach. J Clim 21:1220–1242

Mann ME (2002) Large-scale climate variability and connections with the Middle East in the past centuries. Clim Change 55:287–314

Marcella MP, Eltahir EAB (2008) The hydroclimatology of Kuwait: explaining the variability of rainfall at seasonal and interannual time scales. J Hydrometeorol 9:1095–1105

Masih I, Uhlenbrook S, Maskey S, Smakhtin V (2010) Streamflow trends and climate linkages in the Zagros Mountains, Iran. Clim Change 104(2):317–338

Sabziparvar AA, Mirmasoudi SH, Tabari H, Nazemosadat MJ, Maryanajic Z (2010) ENSO teleconnection impacts on reference evapotranspiration variability in some warm climates of Iran. Int J Climatol 31(6)

Şarlak N, Kahya E, Bég AO (2009) Critical drought analysis: a case study of Göksu River (Turkey) and north Atlantic oscillation influences. J Hydrol Eng 14:795–802

Setoodeh P, Safavi A, Nazemosadat MJ (2004) Intelligent forecasting of rainfall and temperature of Shiraz city using neural networks. Iran J Sci Technol 28:165–174

Sorooshian S, Imam B, Mahani S, Pagano T, Whitaker M (2003) Hydrologic sciences and water resources management issues in a changing world. In: Alsharhan AS, Wood WW (eds) Water resources perspectives: evaluation, management and policy. Developments in water science, vol 50. Elsevier Science, Amsterdam, pp 83–92

Syed FS, Giorgi F, Pal JS, Keay K (2010) Regional climate model simulation of winter climate over Central–Southwest Asia, with emphasis on NAO and ENSO effects. Int J Climatol 30:220–235

Türkeş M (1996) Spatial and temporal analysis of annual rainfall variations in Turkey. Int J Climatol 16:1057–1076

Türkeş M, Erlat E (2003) Precipitation changes and variability in Turkey linked to the North Atlantic Oscillation during the period 1930–2000. Int J Climatol 23:1771–1796

Yosef Y, Saaroni H, Alpert P (2009) Trends in daily rainfall intensity over Israel 1950/1-2003/4. Open Atmos Sci J 3:196–203

Ziv B, Dayan U, Kushnir Y, Roth C, Enzel Y (2006) Regional and global atmospheric patterns governing rainfall in the southern Levant. Int J Climatol 26:55–73

Influence of Winter North Atlantic Oscillation Index (NAO) on Climate and Snow Accumulation in the Mediterranean Mountains

Juan I. López-Moreno, Sergio M. Vicente-Serrano, Enrique Morán-Tejeda, Jorge Lorenzo-Lacruz, Javier Zabalza, Ahmed El Kenawy, and Martin Beniston

Abstract This work analyses the influence of NAO on the interannual evolution of winter temperature, precipitation and snowpack in the Mediterranean mountains. Due to lack of snow data in many mountain areas, the occurrence of four different winter modes are used as a proxy of the amount of accumulated snow. Winter modes are defined on the basis of combined precipitation and temperature thresholds: warm and wet (WW), warm and dry (WD), cold and wet (CW), and cold and dry (CD). The study focuses on 15 relevant mountain areas located in the Mediterranean Europe, Morocco, Turkey and Lebanon. Moreover, we present the relationship between winter NAO and snow depth data in the Swiss Alps and the Spanish Pyrenees. It has been demonstrated that snowpack accumulation in a given year is closely related to the occurrence of these winter modes. However, such relationship is variable among mountain areas and also there are differences depending on elevation in a particular mountain range. Results show that occurrence of different winter modes is strongly related to the winter NAO for the majority of the mountain chains under study, although these relationships are weaker in the easternmost part of the Mediterranean basin. Moreover, it has also been proven that the snow cover response to winter NAO may differ spatially as a consequence of the different influence of winter NAO on precipitation and temperature. In Switzerland, NAO is correlated more with temperature than with precipitation. Therefore, the influence of NAO on snow is significant at the lowest elevation areas, where temperature is the main control on snowpack accumulation. On the other hand, over the Spanish Pyrenees the NAO mainly controls the interannual variability of precipitation. In this region, the highest correlation with snow is found at high elevations where the interannual variability of temperature does not significantly influences snowpack, whereas precipitation controls mainly the accumulation of snow.

Keywords Snow · North Atlantic Oscillation (NAO) · Precipitation · Temperature · The Mediterranean

J.I. López-Moreno (✉)
Instituto Pirenaico de Ecología, Spanish National Research Council (CSIC), Zaragoza, Spain
e-mail: nlopez@ipe.csic.es

S.M. Vicente-Serrano, R.M. Trigo (eds.), *Hydrological, Socioeconomic and Ecological Impacts of the North Atlantic Oscillation in the Mediterranean Region*, Advances in Global Change Research 46, DOI 10.1007/978-94-007-1372-7_6,

1 Introduction

In the Mediterranean mountains snow cover exerts a strong control over ecology, agriculture, availability of water resources, feasibility of a diverse range of economic activities, and associated risks in mountainous and high-latitude regions (Beniston, 2003; Breiling and Charamza, 1999; López-Moreno and García-Ruiz, 2004; López-Moreno, 2005; De Jong et al., 2009). The climate in the Mediterranean region is markedly characterized by a strong seasonality, with relatively low annual precipitation and high interannual variability (Lionello et al., 2006). Winter is the most humid season of the year, with a large proportion of the annual precipitation. Thus, climate anomalies during winter may have major implications for the annual water budget (López-Moreno et al., 2008).

Previous research has identified the North Atlantic Oscillation as one of the main atmospheric circulation modes that determines the temporal evolution of winter precipitation and temperature in the Mediterranean area (Hurrell, 1995; Corte-Real et al., 1995; Hurrell and van Loon, 1997). Thus, it can be expected to exert a strong control on snowpack variability in many mountain areas. However, such a hypothesis is difficult to verify owing to the scarcity of snow data in most of the Mediterranean mountain ranges. In this study, we investigated the possible effects of the NAO on winter precipitation and temperature in 15 mountain ranges in the Mediterranean Europe, Morocco, Turkey and Lebanon during the period 1950-2005 Moreover, snow data from the Swiss Alps and the Spanish Pyrenees has also enabled to analyze the direct influence of the NAO on the variability of snow depth in two contrasted regions in terms of winter NAO influences on climate. In this context, a special emphasis was given to analyze the effect of NAO on combined winter precipitation and temperature modes. Winter modes were identified according to possible combinations of cold-warm and dry-wet conditions. The occurrence of different winter modes is closely related to the amount of accumulated snow; although such a relation is highly determined by the elevation of the mountainous area. Thus, Beniston et al. (in press) concluded that cold and wet years in the Swiss Alps significantly favor the development of a thick snow pack in mountain areas, although during warm and wet years the potential for snow accumulation is essentially restricted to high altitude sites. On the other hand, the association between warm and dry years often results in low snow accumulation at all elevations, and particularly on the lowest slopes.

Although the effect of the NAO on precipitation and temperature has been widely analyzed in the Mediterranean area (e.g. Hurrell and van Loon, 1997; Krichak and Alpert, 2005; López-Bustins et al., 2008), there have not been previous studies focusing on the main mountain areas, and only a few studies have considered the local influence of the NAO on combined temperature and precipitation modes or snow depth.

2 Data and Methods

The CRU TS3.0 monthly gridded (latitude/longitude resolution = 0.5°) precipitation and temperature database was used for the entire Mediterranean region for the period 1950-2005. It was compiled by the Climate Research Unit at the University of East Anglia (http://www.cru.uea.ac.uk; Mitchell and Jones, 2005). In addition, climate and snow data was provided for the Alps by the national meteorological service (Meteoswiss). The climate data of the Spanish Pyrenees was also provided by the Spanish Meteorological Agency (AEMET). Snow depth data in the Pyrenees was obtained from 106 snow poles placed in the area since 1985. The poles and the collection of data are managed by the ERHIN Programme (*Estudio de los Recursos Hídricos INvernales*: Study of winter water resources), run by the Spanish Ministry of Environment. Measurements are taken regularly three times each year, although weather conditions slightly modify the measurement dates. In this study, only snow depths measured in March were considered. Snowpack at this time is determined by the climate of the previous winter (López-Moreno, 2005) and, hence, it adequately determines the accumulated role of the winter NAO conditions. The snow depth series for the period 1985–2005 showed a high correlation with the winter precipitation and temperature. These high correlations allowed the prediction of a regional series for snow pack in March between 1950 and 1999. More details about snow measurements and the methodology of building the snow depth series is found in López-Moreno (2005).

From the CRU database, only those series corresponding to the grid cells that cover the 15 selected mountain areas (see Fig. 1), were used in the study. All the mountain ranges selected for the current analysis experience some level of Mediterranean climatic influence, or drain to the Mediterranean Sea (or the Caspian Sea in the case of northern Turkey and the Caucasus). This included four mountain systems in the Iberian Peninsula (the Pyrenees, the Cantabrian Range, the Central System and the Sierra Nevada); the Atlas Mountains in Morocco; the Apennines in Italy; the Alps, the Carpathian, the Balkan and the Pindos mountains, and Dynaric Alps in the Balkan Peninsula; the Taurus and northern mountains in Turkey; the Caucasus in Armenia and Georgia and the Lebanese mountains.

We used the NAO index defined by Jones et al. (1997), which is based on the difference in anomalies of the sea level pressure measured at the Gibraltar (southwest Iberian Peninsula) and Reykjavik (southwest Iceland) stations. The NAO index was compiled by the Climatic Research Unit, University of East Anglia (http://www.cru.uea.ac.uk/cru/data/nao.htm) for the period 1821 to the present. Prior to correlating series of winter temperature and precipitation (from December to March; DJFM) with the winter NAO (DJFM), we linearly de-trended the time series for autocorrelation. This approach minimized the influence of time series trends and multi-year to decadal signal variability on the strength and significance of the computed correlations and the deduced NAO predictability.

To assess the impact of the winter NAO on combined precipitation and temperature, we used the joint quantile approach described by Beniston and Goyette (2007). New insights on statistics that integrate mutual feedbacks between temperature and

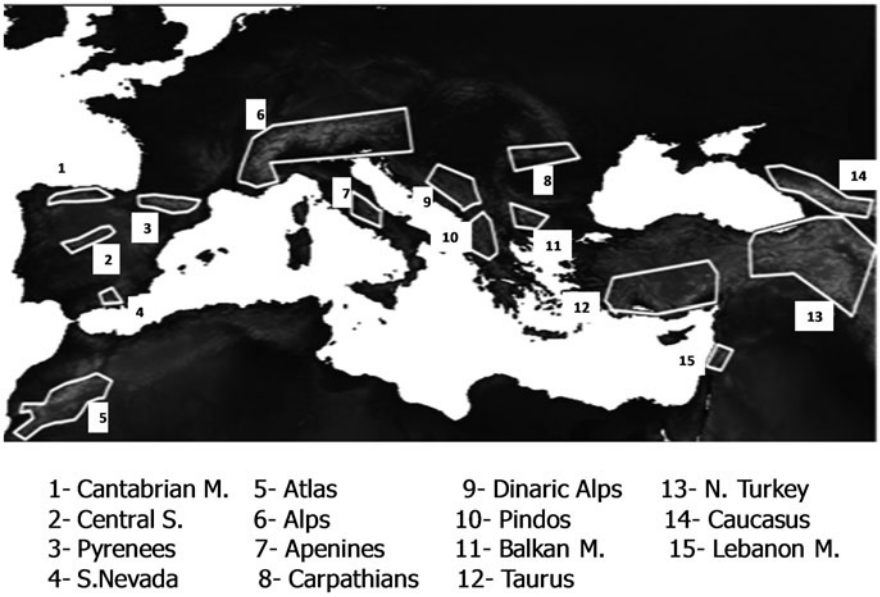

Fig. 1 Study area

moisture are possible when temperature and precipitation records are combined (Beniston, 2009). The 40 and 60% joint quantiles were used to define particular winter modes: (i) cold/dry (CD; when the joint quantiles were equal to or below $T_{40}p_{40}$; the subscript refers to the quantile threshold); (ii) cold/wet (CW; $T_{<40}p_{>60}$); (iii) warm/dry (WD; $T_{>60}p_{<40}$); and (iv) warm/wet (WW; $T_{>60}p_{>60}$). The winter NAO values for individual years belonging to each of the four winter modes were analyzed and compared with the other three modes. The 40 and 60 percentiles were selected, as opposed to the more restrictive percentiles used in previous research (Beniston, 2009). This was principally done to have a sufficient number of years for each winter mode to assess if differences in NAO among winter modes were statistically significant. The non-parametric Wilcoxon-Mann-Whitney rank test (Siegel and Castelan, 1988) was applied to determine whether differences in the NAO during the various winter modes were significant ($\alpha < 0.05$).

3 Results

3.1 Effects of the Winter Modes on Snow Accumulation in Mountain Areas

As an example, Fig. 2 shows how the occurrence of different winter modes affects the annual patterns of snow accumulation at four different locations in the Swiss

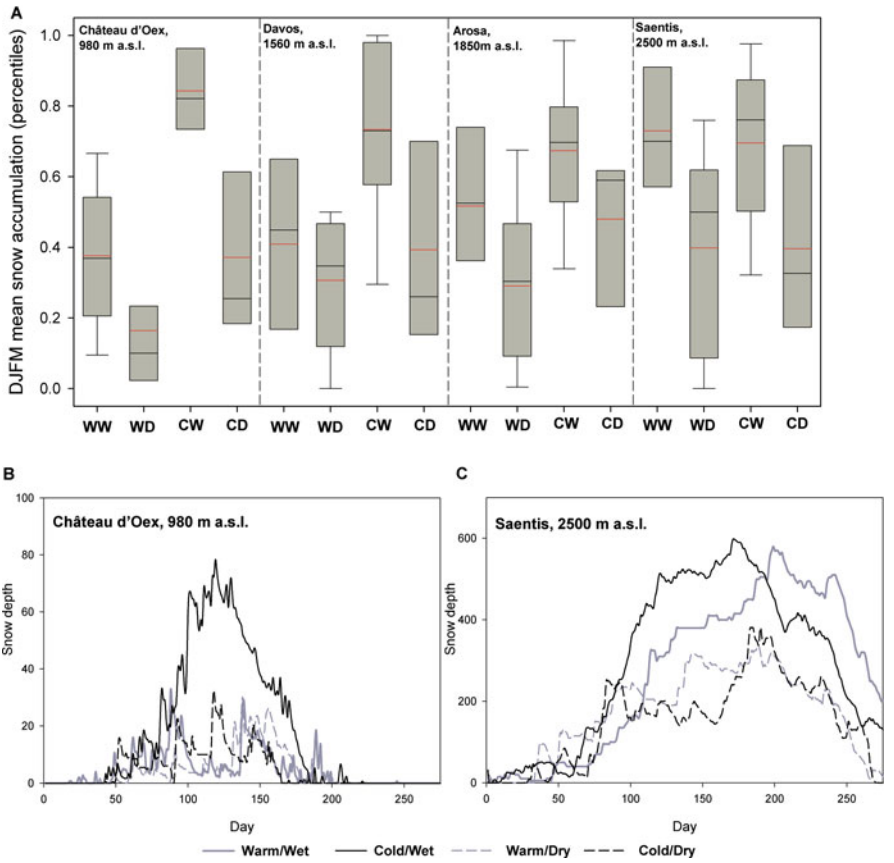

Fig. 2 (**a**) Mean snow accumulation (in cm) in four locations of the Swiss Alps during years that belong to different winter modes: warm and wet (WW), warm and dry (WD), cold and wet (CW) and cold and dry (CD). (**b**) Snow accumulation and melting patterns on Château d'Oex (**b**, 980 m a.s.l.) and Saentis (**c**, 2500 m a.s.l.). Day 1 is October 1st

Alps. Although this example is only based on data collected within the Swiss Alps, the results can be considered to be representative of the other mountainous areas because it depicts the absence of temperature influences on snow accumulation as elevation increases. This behavior can typically be expected in all mountain regions. Thus, the relation between winter modes and snow accumulation varies noticeably according to the elevation of the observatory. Figure 2a indicates the variability in mean snow accumulation from December to March according to different winter modes. Snow amounts have been standardized according to the value of their percentile, thereby enabling comparison between the impacts of the occurrence of winter modes on snow accumulation, independently of the magnitude of snowpack in each site. At high elevation sites (e.g. Saentis [2500 m a.s.l.] and Arosa [1850 m a.s.l.]), the occurrence of high accumulation is mainly related to the occurrence

of wet winters regardless of whether conditions are warm or cold. While warm and dry winters record a thinner snow pack, cold and dry winters record a low snow accumulation. As elevation declines, temperature plays a greater role in terms of snow accumulation. A typical example is Davos (1560 m a.s.l.), where cold and wet winters accumulate the deepest snowpack, whereas in contrast warm and dry years record the least amount of snow. Warm and wet and cold and dry years exhibit a similar amount of accumulated snow. At the lowest elevation site (Chateau d'Oex, 980 m a.s.l.), cold/wet and warm/dry years exhibit the largest differences between the highest and lowest snow accumulation respectively, while warm/wet winters show intermediate snow accumulation.

To assess whether there are significant differences in snow accumulation among years with different winter characteristics, the mean daily snow evolution in Château d'Oex (980 m a.s.l.) and Saentis (2500 m a.s.l.) for years belonging to different winter modes is presented in Fig. 2b. In Château d'Oex (980 m a.s.l.), years of warm winters are mainly characterized by very irregular snow cover during the whole season, with possibility to have melting events in any time of the snow season. On the contrary, snow remains constant over the ground for several months during cold and wet winters. This long period of snow accumulation is likely followed by a month of steady melting of snowpack. In Säntis (2500 m a.s.l.), the high elevation reduces the possible influence of winter type on snow accumulation. In particular, differences are mainly related to the amount of precipitation. Thus, during warm and wet years snow depth is practically the same to the observed during cold and wet years.

3.2 Influence of Winter NAO on Winter Precipitation, Temperature and Combined Modes in the Mediterranean Mountains

Figure 3 shows the correlation between the winter NAO (DJFM) and average temperature and precipitation for the 1950–2005 period in the Mediterranean region. It demonstrates that the NAO exerted marked control over both climate variables in the Mediterranean basin, with large areas with high and statistically significant correlation ($\alpha < 0.05$). Clearly, winter precipitation was negatively correlated with the NAO index over most of the Mediterranean basin. In particular, statistically significant negative correlations were found over large areas of Morocco and Tunisia, most of the Iberian Peninsula, southeastern France, Italy, the Balkan Peninsula, and large areas of central and northern Turkey. Nevertheless, exceptions were found along the coastal areas of Egypt and Libya, where the correlations were positive. With respect to temperature, a general positive correlation pattern was evident in the European Mediterranean. In contrast, a negative correlation was found in large areas of Turkey and the Middle East, whereas a non-significant correlation prevailed in north Africa (from Morocco to Egypt). The greatest positive correlations were found in northern Europe (r-values approximately 0.8); the correlations tended to decrease southward and eastward. Nonetheless, significant correlations were found over most of the Iberian Peninsula, France and the northernmost areas of Italy and the Balkan

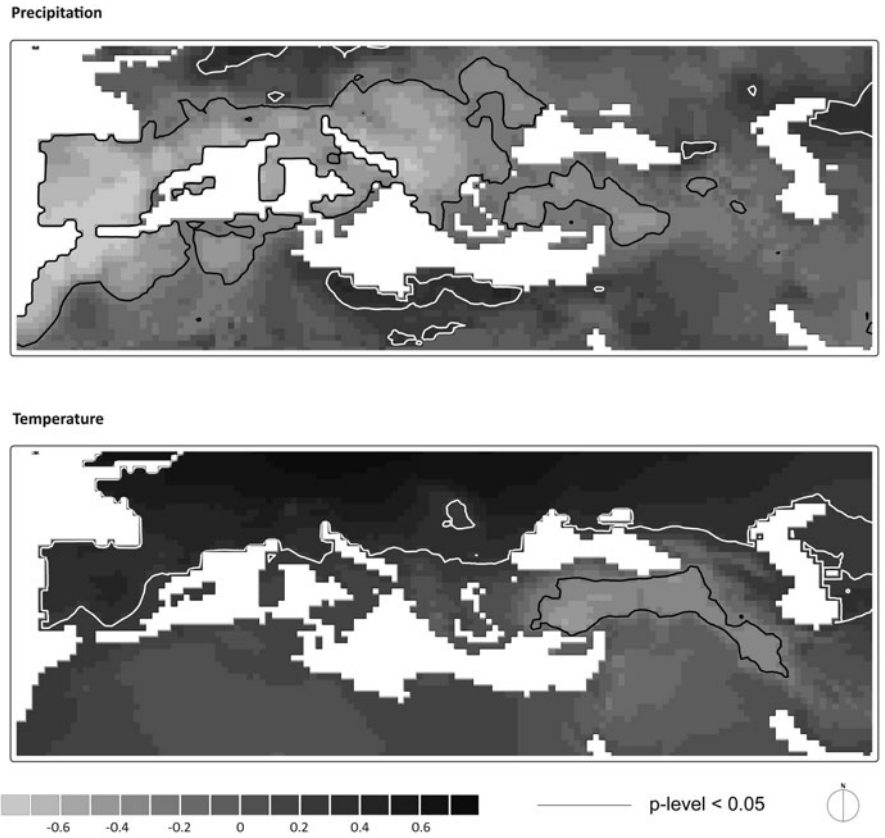

Fig. 3 Pearson's correlation coefficients between the winter (DJFM) NAO and precipitation and temperature for the period 1950–2005

Peninsula. In contrast, southern Italy, Greece and western Turkey exhibited low and non-significant correlations. These results are in good agreement with previous works describing the overall impact of NAO in European and Mediterranean temperatures (e.g. Trigo et al., 2002).

Table 1 presents the mean, the 25th and 75th percentiles and the coefficient of variation in the correlation of winter temperature and precipitation with the NAO index in each mountain area. In the Iberian Peninsula, the influence of the NAO on precipitation and temperature was evident for the four analyzed mountain areas. The correlation with mean temperature is statistically significant ($\alpha < 0.05$) in the Cantabrian Mountains, the Central System and over most of the Pyrenees. The Sierra Nevada, southeast the Iberian Peninsula, was the only mountain area with statistically non-significant correlation between the NAO and temperature. On the other hand, winter precipitation was negatively correlated with the NAO in the four mountain areas. Temperature in the Atlas Mountains in Morocco was negatively but not significantly correlated with the NAO. However, precipitation over most

Table 1 Mean correlation, 25th and 75th percentiles (C25 and C75) and coefficient of variation between precipitation, temperature and NAO in the 15 mountain areas. Average significant correlations ($\alpha < 0.05$) are in bold

	Precipitation				Temperature			
	Mean	C25	C75	CV	Mean	C25	C75	CV
Cantabrian M.	**–0.61**	−0.65	−0.54	−0.11	**0.39**	0.38	0.39	0.02
Central S.	**–0.63**	−0.66	−0.62	−0.06	**0.39**	0.34	0.44	0.17
Pyrenees	**–0.53**	−0.60	−0.50	−0.17	**0.31**	0.27	0.31	0.17
S. Nevada	**–0.72**	−0.72	−0.71	−0.02	0.14	0.10	0.17	0.42
Atlas	**–0.45**	−0.57	−0.37	−0.38	0.15	−0.28	−0.04	1.03
Alps	**–0.3**	−0.44	−0.24	−0.74	**0.52**	0.47	0.57	0.14
Apenines	**–0.39**	−0.48	−0.32	−0.24	0.17	0.11	0.23	0.46
Carphatians	**–0.37**	−0.46	−0.31	−0.22	**0.29**	0.27	0.31	0.1
Dinaric Alps	**–0.62**	−0.66	−0.59	−0.09	0.22	0.17	0.26	0.25
Pindos	**–0.61**	−0.66	−0.58	−0.10	0.04	−0.10	0.02	2.03
Balkan M.	**–0.49**	−0.57	−0.42	−0.18	0.20	0.15	0.25	0.25
Taurus	**–0.29**	−0.36	−0.23	−0.28	**0.41**	−0.45	−0.37	0.13
N. Turkey	–0.19	−0.26	−0.14	−0.60	0.25	−0.31	−0.22	0.45
Caucasus	0.01	−0.11	0.08	3.2	0.11	−0.07	0.18	0.94
Lebanon	–0.12	−0.15	−0.11	−0.43	**0.43**	−0.46	−0.40	0.09

of this area showed a statistically significant correlation with the NAO, but with high spatial variability. Although the Alps exhibited statistically significant positive correlations with the mean temperatures, precipitation showed marked spatial variability, but on average there was a significant negative correlation. Nonetheless, coefficients of correlation were noticeably lower than those found for the Pyrenees, which is a consequence to be an area between Southern and Northern Europe where NAO correlations with temperature goes increasingly south or north of the Alps. The Apennines exhibited a positive but non-significant relationship with temperature, and a negative correlation with precipitation. A similar pattern was evident for the Dynaric Alps and the Carpathians. However, for the Carpathians, the correlation with temperature was close to or exceeded the significance threshold. There was no clear correlation between the NAO and temperature in the Pindos and Balkan mountains although showed a marked influence on the interannual variability of winter precipitation. For the Taurus Mountains, the NAO was significantly and negatively correlated with both precipitation and temperature. The correlation for the mountains of northern Turkey was similar to that observed for the Taurus Mountains, but the α-coefficients were slightly above the statistical significance threshold. The NAO had not a significant influence on winter precipitation or temperature in the Caucasus. In the Lebanon Mountains, the NAO only showed a statistically significant negative correlation with temperature.

In the mountains of the Iberian Peninsula, the winter NAO values were clearly distributed according to the joint quantiles of precipitation and temperature. In particular, the WD winters were associated with the highest NAO values (Fig. 4), while the WW and CW winters accompanied to the lowest NAO values. Also, the CD

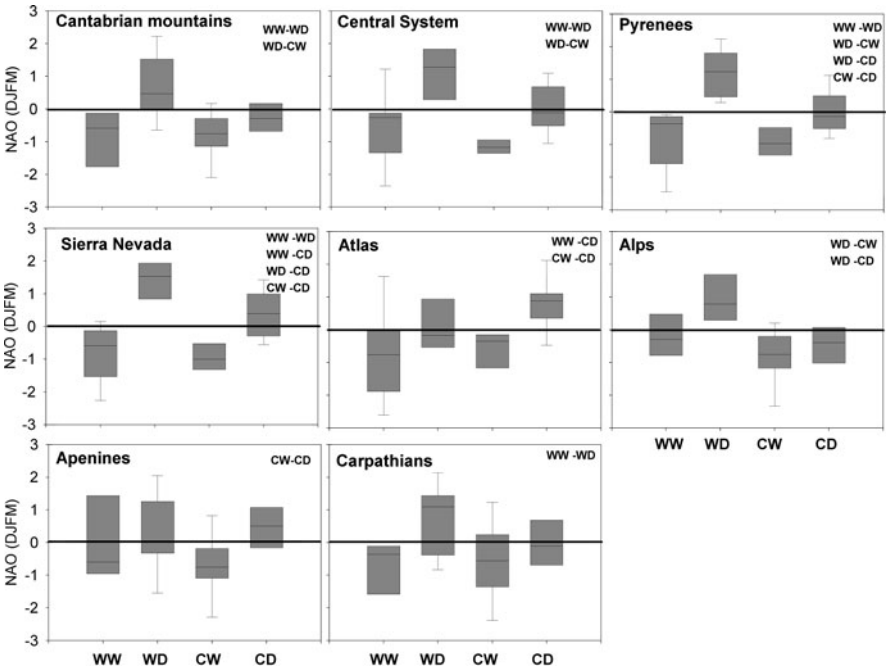

Fig. 4 Boxplots of the winter NAO values recorded during each winter mode in mountain areas of the Iberian Peninsula, Atlas, Alps, Apenines and the Carphatians. In each *panel* is depicted the pairs of winter modes in which NAO values has exhibited statistically significant differences according to the Mann-Whitney rank test

winters were related to the intermediate NAO values. The Mann-Whitney ranking indicated that the NAO values during the WD mode differed significantly from those observed during the wet modes (i.e. WW and CD).

Moreover, in the Sierra Nevada, the NAO values for the CD years were different from those of the CW and WD years. In the Pyrenees there were also significant differences between the NAO values during the WD and CD winters. In the Atlas Mountains (Morocco) precipitation is clearly affected by the NAO, which decreased from dry to wet winters. Thus, during the WW and CW winters, the NAO was much lower than those of the WD and CD winters. The differences between the CD winters and both the WW and CW winters were found statistically significant.

In the Alps the highest NAO values occurred during the WD winters. Significant differences in the NAO were identified between the CW and both CD and WD winters. For the Apennines there was no clear influence of the NAO on the winter modes; the only significant difference was between the CW and CD years.

In the Balkan Peninsula the NAO decreased from dry to wet years, with no clear pattern of influence on temperature. In the Carpathians (Fig. 4) the highest values of the NAO occurred during the WD years, which were statistically different from the WW years. In the Dinaric Alps (Fig. 5) there was a very similar pattern, but

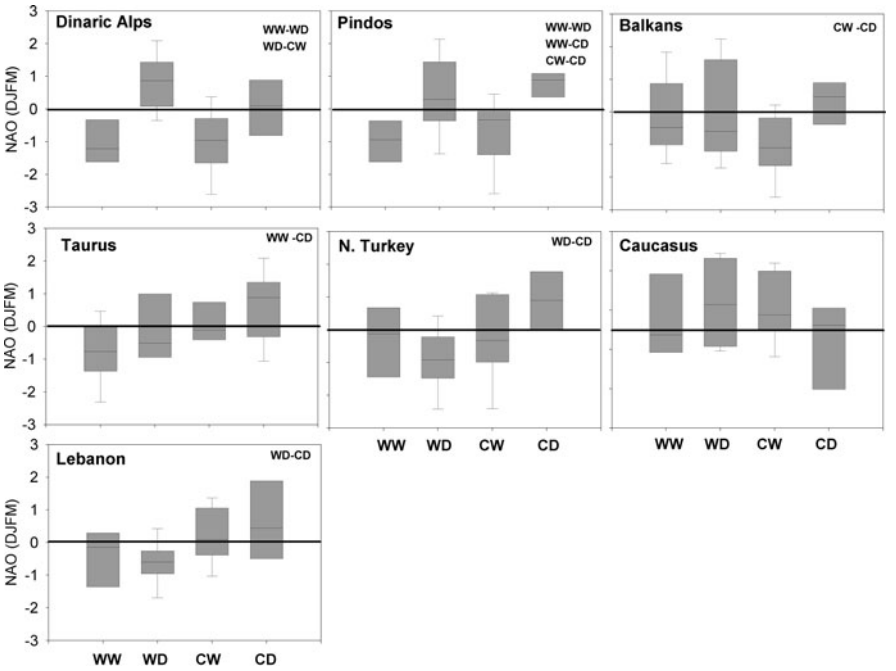

Fig. 5 Same as Fig. 4 but for the Dinaric Alps, Pindos, Balkans, mountain areas of Turkey and Lebanon

with statistically different WD years from both CW and WW winters. The Pindos Mountains had high NAO values during the WD and CD winters. However, in both cases the values were significantly different from those in the WW years. Moreover, the magnitude of the NAO during the CD years was significantly different to the CW years. Apart from the CW and CD years, the Balkan Mountains did not show clear differences in NAO values during the various winter modes.

The Taurus Mountains and the mountains of northern Turkey showed a negative NAO gradient as temperature increased. In the former there were significant differences between the WW and CD years, whereas in the later significant differences were found between the WD and CD years. In the Caucasus there was no evident signal in the magnitude of the NAO related to any of the four winter modes. In the Lebanese mountains, the NAO values varied with temperature, and significant differences were found between the WD and CD winters. Similarly, there were differences, but insignificant, in the mean NAO values between the WW and CW winters.

3.3 Influence of Winter NAO on Snow Accumulation in Switzerland

Table 2 shows the correlation between winter NAO and temperature, precipitation and snow indices (mean snow depth, days with snow over the ground and

Table 2 Correlation between winter NAO and winter temperature, precipitation, mean snow depth (Mean SD), days with snow (Days) and maximum snow accumulation (Max.snow)

	Elev. (m.a.s.l.)	Lat (°N)	Long (°E)	T_{max}	T_{min}	T_{avg}	Precip	Mean SD	Days	Max.snow
St Gallen	779	47.43	9.4	**0.52**	**0.52**	**0.52**	–0.15	**–0.49**	**–0.46**	**–0.40**
Saentis	2490	47.25	9.35	**0.51**	**0.48**	**0.51**	**0.45**	**0.25**	0.14	**0.24**
Neuchâtel	485	47.00	6.95	**0.60**	**0.50**	**0.55**	–0.19	**–0.4**	**–0.41**	**–0.41**
Lugano	273	46.00	8.97	**0.59**	**0.35**	**0.59**	**–0.37**	–0.19	–0.16	0.23
Geneva	420	46.25	6.13	**0.27**	**0.32**	**0.45**	**–0.24**	**–0.47**	**–0.49**	**–0.42**
Davos	1590	46.82	9.85	**0.41**	**0.33**	**0.55**	0.15	0.09	–0.04	0.13
Zurich	443	47.43	8.52	**0.55**	**0.52**	**0.55**	–0.05	**–0.41**	**–0.40**	**–0.40**
Arosa	1740	46.78	9.68	**0.43**	**0.46**	**0.47**	**0.25**	0.03	–0.10	0.05
Chateau D'Oex	981	46.28	7.08	**0.53**	**0.35**	**0.44**	0.00	–0.16	–0.10	–0.07

Bold numbers indicate significant correlations ($p < 0.05$).

maximum snow accumulation) in 9 locations across Switzerland. Following the results obtained for the Alps using the CRU dataset, average temperature exhibited a positive correlation with the NAO in all the considered locations, exceeding 0.44 in all cases. For precipitation, coefficients of correlation are markedly lower than for temperature; and they varied from negative (generally eastward) to positive (westward). In some cases contrasted correlations between the NAO and precipitation were found at very short distances. This was the case in St. Gallen ($r = –015$) and Saentis ($r = 0.45$), suggesting a more dominant influence of the complex topography of the region than an influence of large-scale atmospheric circulations on local precipitation. Given the response of temperature and precipitation to the NAO, interannual evolution of winter snow indices are only related to the NAO in those observatories located at low elevation (i.e. Zurich, Geneva, St Gallen and Neuchâtel). This is a consequence of the strong influence of the NAO on temperature, which determines not only the phase of precipitation (liquid or solid), but also the occurrence of melting events in those areas close to the 0°C winter isotherm. On the other hand, at highly elevated sites, temperature is always sufficiently cold for precipitation to fall essentially as snow during winter. In those areas, the interannual evolution of snowpack depends largely on winter precipitation amount, which is not generally controlled by the NAO in Switzerland. One exception is the Saentis weather station located at 2490 m a.s.l., where winter precipitation was clearly influenced by the NAO ($r = 0.45$), and snow indices accordingly exhibited a positive correlation with the NAO.

Figure 6 shows the temporal evolution of mean snow depth, days with snow cover and the NAO in Zurich (443 m a.s.l.) and Davos (1590 m a.s.l.). Both sites are located at a rather similar geographic position in the Swiss territory, but at a contrasted elevation. Both observatories have shown not only positive correlations between winter temperatures and the NAO, but also exhibited weak relationships between the NAO and precipitation. As previously mentioned, when the NAO only exerts a significant control on temperature as occurred in both sites, snow indices

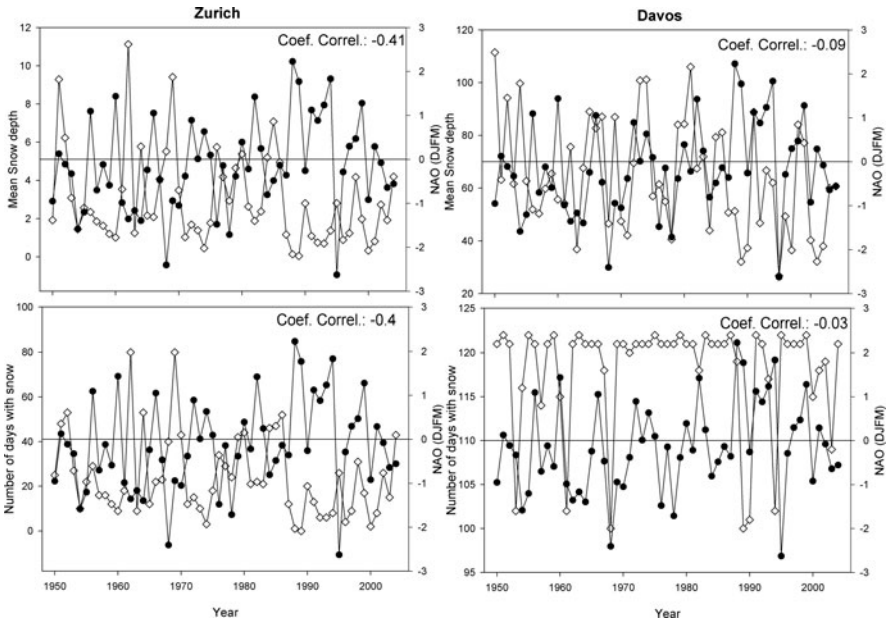

Fig. 6 Temporal evolution of mean snowdepth (in cm), days with snow cover and NAO in Zurich and Davos

were only correlated with the NAO at the lower elevation sites. Thus, mean snow depth and days with snow on the ground were significantly correlated with the NAO in Zurich ($r = –0.41$ and $r = –0.40$ respectively). On the other hand, both indices did not show any significant relationship in Davos. Indeed, we can observe how evolution of mean snow depth is independent of the winter NAO evolution. Likewise, the winter (DJFM) snow cover in Davos presents an inter-annual variability insensitive to the corresponding evolution of the winter NAO time series.

3.4 Influence of Winter NAO on Snow Accumulation in the Spanish Pyrenees

Previous studies using observational data in the Spanish Pyrenees (López-Moreno, 2005; López-Moreno and Vicente-Serrano, 2006) revealed that winter NAO had a positive but not significant correlation with the regional series of winter temperature ($r = 0.19$, $\alpha < 0.05$ for the 1950–2000 period), and a significant negative correlation with the regional precipitation ($r = –0.6$, $\alpha < 0.05$ for the 1950–2000 period). This strong relationship between the NAO and winter precipitation explains to large extent the negative correlation between the regional series of snow depth accumulated in March and winter NAO (Fig. 7).

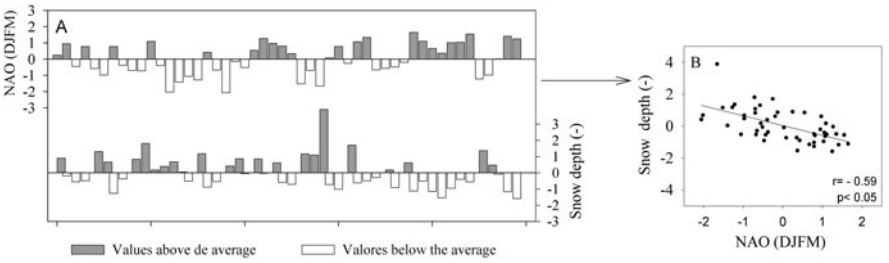

Fig. 7 (**a**) Temporal evolution of Winter (DJFM) NAO index and regional series of snow depth for the Pyrenees in March. (**b**) Correlation between NAO and snow depth series

Nonetheless, the weak relationship between winter NAO and temperature leads to a significant altitudinal gradient in the strength and significance of the correlation coefficients observed at individual sites in the Pyrenees. The differentiated influence of the NAO on snow depth depends on elevation. This is mainly a consequence of the necessity of low temperatures to ensure that precipitation falls as snow. At low elevation sites, interannual variability of winter precipitation is also controlled by the NAO. However, temperature determines the nature of precipitation (i.e. rain or snow) and also the occurrence of melting events during winter. In contrast, at high elevation sites, temperature is not the main control on snowpack and precipitation. Therefore, the NAO seems to be the principle factor governing the interannual variability of snow. Figure 8 shows the correlation coefficients between winter NAO

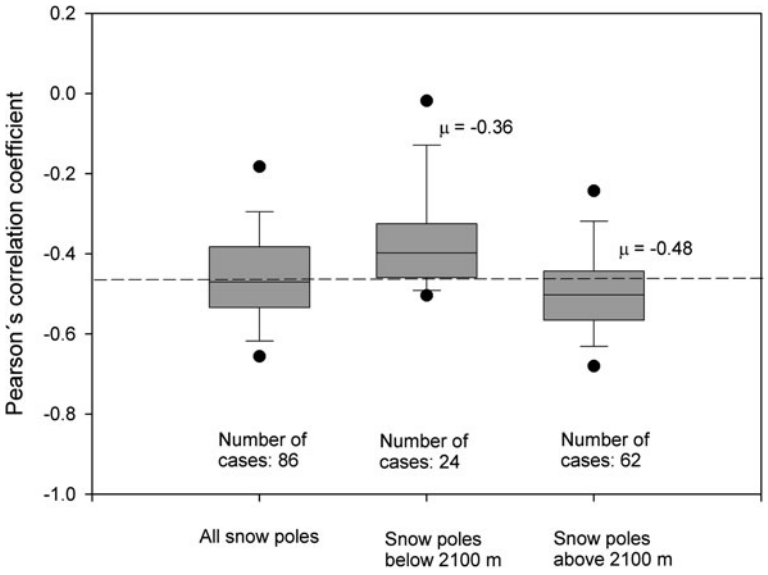

Fig. 8 Coefficient of correlation between winter NAO and snow depth measured in March in 86 locations at contrasted elevation. *Dashed line* indicate the threshold of statistical significance ($\alpha < 0.05$)

and snow depth measured at 86 snow poles located across the Pyrenees during the period 1986–2006. Depending on whether snow poles are located above or below 2100 m a.s.l., we can find statistical significant differences between both groups. Thus, snow depth measured at snow poles located below 2100 m a.s.l. showed a mean correlation of –0.36 with the NAO, which is statistically insignificant in the majority of cases. Conversely, snow depth measured above 2100 m a.s.l. exhibits a mean correlation of –0.48 with winter NAO, meeting the statistical significance threshold in most cases.

4 Discussion and Conclusions

The results of this study confirm the major influence of winter NAO on climate and snowpack in most of the Mediterranean mountains. Following the results obtained ion previous works we have identified large scale negative (positive) correlation with precipitation (temperature) (e.g., Trigo et al., 2002). However, there are noticeable spatial differences in the magnitude or sign of the correlations (Dunkeloh and Jacobeit, 2003). Thus, the negative correlation with precipitation tended to be higher in the western part of the Mediterranean basin (i.e. the Iberian Peninsula and northwestern Morocco), northern Italy, the western part of the Balkan Peninsula and some parts of central Turkey. Winter precipitation exhibited a close relationship with the NAO in the mountains of the Iberian Peninsula (the Cantabrian Mountains, Central System, Pyrenees and Sierra Nevada), the Atlas, the Pindos and the Balkan mountains, and the Dinaric Alps. Other mountains showed negative correlation with the NAO, but with lower coefficients. The exceptions were found in northern Turkey, the Caucasus and the Lebanese mountains, where no significant correlations were exhibited. The positive correlation between temperature and winter NAO tended to decrease southward in the Mediterranean basin. Only the Alps, the Cantabrian Mountains, the Central System, the Pyrenees and the Carpathians showed significant positive correlations. In the case of the Pyrenees, the correlation with temperature was positive but not statistically significant when the observational data was considered for analysis in the 1950–2000 period. In contrast to the general tendency, the mountains of Lebanon and some parts of the Caucasus and northern Turkey showed a significant negative correlation.

Spatial differences in the influence of the NAO on precipitation and temperature explain why there were differences in the response of the combined precipitation and temperature modes to winter NAO in the Mediterranean mountain areas. In most cases winters dominated by positive NAO conditions had warm and dry conditions, except for the eastern part of the Mediterranean basin, where NAO usually yields cold and dry winters. Negative NAO winters usually cause wet conditions in the Mediterranean mountains (except for those located in the eastern part of the basin), but generally there was no clear difference in their occurrence under warm or cold modes. Irrespective of the geographical location, the NAO had a statistically significant influence on the occurrence of winter modes in all the mountains, except the Caucasus and the Lebanese mountains. The NAO had a major influence

on the occurrence of various winter modes in the Pyrenees, the Sierra Nevada and the Pindos Mountains.

The occurrence of different winter modes has a major influence on the accumulation of snow in the mountain areas. Using snow depth data from the Swiss Alps, we have confirmed that snowpack varies noticeably depending on the occurrence of a given winter mode. However, the elevation of each specific mountain area or altitudinal gradients within a particular mountain sector often produces a contrasted response of snowpack to winter modes. In particular, the wet modes in the highly elevated sites of the Swiss Alps are associated with a deep snowpack, independently of whether the winters are warm or cold. As elevation decreases, the role of temperature increases. At the lowest altitudes, the cold and wet modes are exclusively associated to high snow accumulation. In all cases warm and dry modes are associated with winters that have an insufficient snowpack.

Given the relationship between the winter modes and snow pack, and also considering the large influence of the NAO on winter modes, it is not surprising that previous research has suggested the NAO pattern as an important driver of interannual variability of snowpack in mountain areas including: the Pyrenees (López-Moreno and Vicente-Serrano, 2006; García et al., 2009), the Alps (Beniston, 1997; Scherrer and Appenzeller, 2006; Schöner et al., 2009), the Romanian mountains (Micu, 2009), the Bulgarian Carpathians (Petkova et al., 2004). Following the results of this study, it can be concluded that the snow in mountain areas of the Iberian Peninsula (the Sierra Nevada, the Cantabrian Mountains, the Central System), the Atlas, the Pindos and Turkish mountains could also be markedly affected by the NAO in winter.

This research provides clear evidence of the role of elevation as an important variable in explaining the spatial variability of the impacts of the NAO on snowpack evolution within a specific mountain region. The Swiss and Spanish case studies have enabled to assess how coefficients of correlation between NAO and snow indices may exhibit opposite dependence with elevation. More specifically, winter NAO in Switzerland controls mainly temperature, with a variable influence on precipitation. Accordingly, the NAO does not explain interannual variability of snow at highly elevated areas, where temperature is generally below the freezing level. Similarly, snowpack is significantly influenced by the NAO in sites located at low altitudes. In the valley bottoms, temperature determines whether precipitation is solid or liquid, and the NAO controls the interannual characteristics of winter temperature. An opposite example is the Spanish Pyrenees, where the NAO mainly controls the interannual evolution of winter precipitation rather than temperature. Thus, at high elevation sites, where temperature is usually below the freezing point, the NAO explains to a larger extent the interannual variability of the snowpack. However, when elevation decreases, the influence of the precipitation on snowpack weakens, and temperature becomes the major control on snow pack duration and magnitude.

Nonetheless, under global warming conditions expected in the Mediterranean region during the next decades (Giorgi, 2006), the relationships obtained in this study may be different from those for past and current climates. For instance, the

frequency of cold modes is expected to dramatically decrease in favor of both the WD and WW modes in the Swiss Alps (Beniston et al., in press). Also, a higher frequency of warm modes is likely to occur in all mountain areas under study owing to the expected increase in the Mediterranean temperature. In large areas of the Mediterranean region winter precipitation is expected to decrease (López-Moreno et al., 2009). A higher frequency of warm and dry winters in those areas could negatively affect snow cover. In other areas where an increase in winter precipitation is expected, an increase in the WW winters could likely occur in several mountain areas. An increase in the WW winters will be favorable for snow accumulation only at very high altitudes, where precipitation falling as snow can remain in the solid state over a number of consecutive days, even under generally warmer conditions. This hypothesis coincides with numerous studies that have simulated future snowpack and predicted a general decrease in the Mediterranean mountains, especially for sites at low elevations (López-Moreno et al., 2008; Uhlmann et al., 2009).

Acknowledgements This work was supported by the research projects CGL2006-11619/HID, CGL2008-01189/BTE, and CGL2008-1083/CLI, financed by the Spanish Commission of Science and Technology and FEDER, EUROGEOSS (FP7-ENV-2008-1-226487) and ACQWA (FP7-ENV-2007-1-212250), financed by the VII Framework Programme of the European Commission; and "La nieve en el Pirineo Aragonés y su respuesta a la variabilidad climática", financed by "Obra Social La Caixa" and the Aragón Government.

References

Beniston M (1997) Variations of snow depth and duration in the Swiss Alps over the last 50 years: links to changes in large-scale climatic forcings. Clim Change 36:281–300

Beniston M (2003) Climatic change in mountain regions: a review of possible impacts. Clim Change 59:5–31

Beniston M (2009) Trends in joint quantiles of temperature and precipitation in Europe since 1901 and projected for 2100. Geophys Res Lett 36:L07707

Beniston M, Goyette S (2007) Changes in variability and persistence of climate in Switzerland: exploring 20th century observations and 21st century simulations. Glob Planet Change 57:1–20

Beniston M, Uhlmann B, Goyette S, Lopez-Moreno JI (in press) Will snow-abundant winters still exist in the Swiss Alps in a greenhouse climate? Int J Climatol. doi:10.1002/joc.2151

Breiling M, Charamza P (1999) The impact of global warming on winter tourism and skiing: a regionalised model for Austrian snow conditions. Reg Environ Change 1:4–14

Corte-Real J, Zhang X, Wang X (1995) Large-scale circulation regimes and surface climatic anomalies over the Mediterranean. Int J Climatol 15:1135–1150

De Jong C, Lawler D, Essery R (2009) Mountain hydroclimatology and snow seasonality and hydrological change in mountain environments. Hydrol Process 23:955–961

Dunkeloh A, Jacobeit J (2003) Circulation dynamics of Mediterranean precipitation variability 1948–98. Int J Climatol 23:1843–1866

García C, Martí G, Oller P, Moner I, Gavalda J, Martinez P, Peña JC (2009) Major avalanches occurrence at regional scale and related atmospheric circulation patterns in the Eastern Pyrenees. Cold Regions Sci Technol 59:106–118

Giorgi F (2006) Climate change hot-spots. Geophys Res Lett 33:L08707. doi:10.1029/2006GL025734

Hurrell J (1995) Decadal trends in the North-Atlantic Oscillation. Regional temperatures and precipitation. Science 269:676–679

Hurrell J, van Loon H (1997) Decadal variations in climate associated with the North Atlantic Oscillation. Clim Change 36:301–336

Jones PD, Jónsson T, Wheeler D (1997) Extensions to the North Atlantic oscillation using early instrumental pressure observations from Gibraltar and southwest Iceland. Int J Climatol 17:1433–1450

Krichak SO, Alpert P (2005) Decadal trends in the East Atlantic–West Russia pattern and Mediterranean precipitation. Int J Climatol 25:183–192

Lionello P, Malanotte-Rizzoli P, Boscolo R, Alpert P, Artale V, Li L, Luterbacher J, May W, Trigo R, Tsimplis M, Ulbrich U, Xoplaki E (2006) The Mediterranean climate: an overview of the main characteristics and issues. In: Lionello P, Malanotte-Rizzoli P, Boscolo R (eds) Mediterranean climate variability. Elsevier, Amsterdam, pp 1–26

López-Bustins J-A, Martin-Vide J, Sanchez-Lorenzo A (2008) Iberia winter rainfall trends based upon changes in teleconnection and circulation patterns. Glob Planet Change 63:171–176

López-Moreno JI (2005) Recent variations of snowpack depth in the Central Spanish Pyrenees. Arct Antarct Alpine Res 37:253–260

López-Moreno JI, García-Ruiz JM (2004) Influence of snow accumulation and snowmelt on streamflow in the Central Spanish Pyrenees. Int J Hydrol Sci 49:787–802

López-Moreno JI, García-Ruiz JM, Beniston M (2008) Environmental change and water management in the Pyrenees. Facts and future perspectives for Mediterranean mountains. Glob Planet Change 66:300–312

López-Moreno JI, Vicente-Serrano SM (2006) Atmospheric circulation influence on the interannual variability of snowpack in the Spanish Pyrenees during the second half of the twentieth century. Nordic Hydrol 38:38–44

López-Moreno JI, Vicente-Serrano SM, Gimeno L, Nieto R (2009) The stability of precipitation regimes in the Mediterranean region: observations since 1950 and projections for the twentieth-one century. Geophys Res Lett 36:L10703. doi:10.1029/2009GL037956

Micu D (2009) Snow pack in the Romanian Carpathians under changing climatic conditions. Meteorol Atmos Phys 105:1–16

Mitchell TD, Jones PD (2005) An improved method of constructing a database of monthly climate observations and associated higher resolution grids. Int J Climatol 25:693–712

Petkova N, Koleva E, Alexandrov V (2004) Snow cover variability and change in mountainous regions of Bulgaria, 1931–2000. Meteorologische Zeitschrift 13:19–23

Scherrer SC, Appenzeller C (2006) Swiss Alpine snow pack variability: major patterns and links to local climate and large-scale flow. Clim Res 32:187–199

Schöner W, Auer I, Böhm R (2009) Long term trend of snow depth at Sonnblick (Austrian Alps) and its relation to climate change. Hydrol Process 23:1052–1073

Siegel S, Castelan NJ (1988) Nonparametric statistics for the behavioral sciences. McGraw-Hill, New York

Trigo RM, Osborn TJ, Corte-Real JM (2002) The North Atlantic Oscillation influence on Europe: climate impacts and associated physical mechanisms. Clim Res 20:9–17

Uhlmann B, Gollete S, Beniston M (2009) Sensitivity analysis of snow patterns in Swiss ski resorts to shifts in temperature precipitation and humidity under condition of climate change. Int J Climatol 29:1048–1055

Impact of NAO on Mediterranean Fisheries

Francesc Maynou

Abstract The effect of the North Atlantic Oscillation (NAO) on fisheries production has received attention in the last 2 decades, especially in relation to the inter-annual fluctuation of the important North Atlantic cod fisheries. Results of these studies show that the effects of NAO on cod stocks vary geographically, with opposite patterns in the western and eastern North Atlantic and that NAO affects mainly the recruitment success of cod, especially on heavily fished stocks. In the Mediterranean sea the number of studies is much more limited, due in part to the paucity of sufficiently long and reliable data series for Mediterranean fisheries. A recent study on the interannual variation of landings of the red shrimp *Aristeus antennatus* in Catalonia shows that the NAO explains a large part of the variability in population abundance with a lag of 2–3 years. New results presented here show that, at the scale of the entire Mediterranean, stocks of hake (*Merluccius merluccius*) respond to the NAO with different trends in the northwestern and southeastern stocks. Analysis of detailed life history data of this species in the Spanish Mediterranean coast allows to postulate the hypothesis that positive NAO years enhance hake fishery production through increasing the individual size of recruits, as well as the individual weight and abundance of adult hake. No effect on other demographic parameters such as recruitment strength or natural mortality could be demonstrated.

Keywords Aristeus antennatus · Fisheries · Mediterranean · Merluccius merluccius · NAO

1 Introduction

Fisheries production depends on the interaction between human inputs (*fishing effort*) and the biomass of fish. While fishing effort may change over time due to socioeconomic factors, such as market interests, changing costs of effort or other reasons, fish biomass fluctuates over time due to environmental factors, such as biological productivity of its prey resources, or abiotic factors such as

F. Maynou (✉)
Institut de Ciències del Mar, Spanish National Research Council (CSIC), Barcelona, Spain
e-mail: maynouf@icm.csic.es

S.M. Vicente-Serrano, R.M. Trigo (eds.), *Hydrological, Socioeconomic and Ecological Impacts of the North Atlantic Oscillation in the Mediterranean Region*, Advances in Global Change Research 46, DOI 10.1007/978-94-007-1372-7_7,

changes in temperature or salinity (Bakun, 1996; Cushing, 1996; Ottersen et al., 2004).

The abundance of marine fish is difficult to determine and many different methods have been developed over time (Hilborn and Walters, 1992). Briefly, fish abundance can be estimated from two basic sources: fisheries dependent data (commercial catches) or fisheries-independent data. In the first case, data series of catches are relatively easy to obtain because most countries maintain relatively long data bases on fish production by species (Evans and Grainger, 2001). However, to interpret catch data it is often necessary to know the evolution of fishing effort and catchability, which are often not available or difficult to estimate (Hilborn and Walters, 1992). Fisheries-independent programmes are more reliable but expensive to maintain and rarely have the long time spans required to assess the relationship between environmental variations and fish abundance (Sparre and Venema, 1998). In the European North Atlantic, there exist data series derived from scientific trawl surveys longer than 40 years (International Bottom Trawl Survey: http://datras.ices.dk), but in the Mediterranean, the only continuous fisheries monitoring programme (MEDITS: Mediterranean International Trawl Surveys: http://www.ifremer.fr/Medits_indices) to cover all EU member states started in 1994 and the data series is thus considerably shorter than in the Atlantic (Bertrand et al., 2002). In any case both types of data sources, commercial and trawl surveys, have advantages and disadvantages and it is convenient to use the two types of data concurrently when possible.

It is known that the changes in total biomass of a fishery target species can be due to individual changes in (one or more) individual demographic parameters. For instance, the abundance of a given year class may fluctuate from year to year due to environmental factors that cause enhanced survival (or conversely, increased mortality) of the individuals of that particular year class (Cushing, 1996; Myers, 2002; Watanabe et al., 2003). This is specially important in the first age class recruited to the fishery (known as recruitment), and several studies have shown the relationship between interannual fluctuations in recruitment and environmental variability (e.g. Mendelsohn and Mendo, 1987; Watanabe et al., 1996; Stige et al., 2006). Other key life history parameters affected by environmental variability are the individual growth rate, the natural mortality or the reproductive success (Hänninen et al., 1999; Jobling, 2002).

It is often difficult to determine the causes of the relationship between large scale climatic indices and fisheries due to the paucity of data, but also due to the complexity of the mechanisms involved (Cushing, 1996). In recent years, the usefulness of employing large scale climatic indices such as the NAO index as a proxy for complex space-time variations in ecological variables has been suggested (Hallett et al., 2004; Stenseth and Mysterud, 2005) and indeed the relationship between climatic indices and fisheries is well documented in non-Mediterranean settings, particularly in upwelling ecosystems (e.g. anchovy/sardine substitutions in the Pacific Kuroshio and Humboldt Current ecosystems and teleconnections among fish populations, reviewed in Alheit and Bakun, 2010).

The effects of NAO on North Atlantic fisheries has received attention in recent decades, especially in the last 10 years (Reid et al., 2001; Beaugrand, 2004), with studies focused particularly on cod (*Gadus morhua*, Mann and Drinkwater, 1994; Beaugrand et al., 2003; Stige et al., 2006). The results of these studies show that the NAO affects cod fisheries mainly by modulating the strength of cod recruitment with a time lag of 2 years (Brodziak and O'Brien, 2005). It has been shown also that the effect is stronger when spawning stock biomass (SSB) is low (Brander, 2005). Most significantly, some of these studies showed that the effect of the NAO varies spatially across North Atlantic cod stocks (synthesized in the model by Stige et al., 2006): while cod recruitment is enhanced in Newfoundland, Greenland, Iceland, northern Norway and the Faroes during positive NAO years, it is decreased in the eastern US, around the British Isles, in the North sea and in the Baltic sea (figure 4 in Stige et al., 2006).

In many cases the relationship between the NAO and fisheries production has been shown to be mediated by changes in the composition and abundance of zooplankton (Fromentin and Planque, 1996; Ottersen and Stenseth, 2001; Reid et al., 2003; Molinero et al., 2008).

In the Mediterranean, the relationship between the NAO and fisheries has received less attention, probably because data series are generally shorter than in Atlantic fisheries. Lloret et al. (2001) assessed the relationship between river runoff in 13 coastal fishery species of the Catalan coasts. They found that catches per unit of effort were positively correlated with the wind mixing index in the Gulf of Lions and the runoff of local rivers, which varied synchronously with the NAO index: negative NAO indices were associated with higher river runoff (probably because during negative NAO years precipitation increases in the NW Mediterranean, Mariotti et al., 2002). Maynou (2008) showed that the detrended landings of the deepwater red shrimp *Aristeus antennatus* were positively correlated with the NAO index with time lags of 2 and 3 years. An ecological mechanism to explain this correlation was produced, based on current knowledge of the biology of this species and the water mass dynamics in the study area (NW Mediterranean): positive NAO years are correlated with decreased rainfall in the NW Mediterranean sea, especially in the Gulf of Lions, the Ligurian sea and adjacent hinterland (Mariotti et al., 2002). Decreased rainfall is linked to enhanced vertical mixing of the water masses in the Gulf of Lions (Demirov and Pinardi, 2002; Jordi and Hameed, 2009), due to the saltier (hence, more dense) surface water mass in low rainfall years. Knowing that food supply in winter is key to the reproductive success of *A. antennatus*, because during this period females switch from their normal generalist diet to a high-energy content diet based on zooplankton (Cartes et al., 2008; Maynou, 2008) postulated that positive NAO years would enhance egg production and higher abundance of recruits to the fishery.

The objective of this contribution is to assess the effects of NAO in another important Mediterranean demersal fishery resource, the hake *Merluccius merluccius* at the scale of the entire Mediterranean basin, in order to investigate whether ecological mechanisms linking the NAO with fisheries productivity demonstrated in local areas (Catalan sea, Ligurian sea) can be extrapolated to wider areas.

2 Results

European hake (*Merluccius merluccius*) is an important resource of the Mediterranean demersal fishery, with catches fluctuating between 20 and 50,000 t in recent decades (FAO Fisheries Department, 2000). The biology of this species is well-known (e.g. the review by Oliver and Massutí, 1995; Recasens et al., 1998). Hake is distributed mainly over the continental shelf between 50 and 200 m depth, although occasional large individuals are caught down to 800 m. It is a heavily exploited species and catches are at present mainly composed of juvenile individuals of age classes 0–2. The recruitment period of hake varies across Mediterranean subareas and is relatively protracted, but it occurs mainly in early summer (June–July) in the NW Mediterranean (Recasens et al., 1998).

I analyzed the annual data series of hake catches for the period 1970–2005 in the seven geographical areas of the Mediterranean used by the FAO for fisheries statistics purposes (Fig. 1) based on the FISHSTAT database (FAO Fisheries Department, 2000).

As shown in Fig. 2, the data series of hake catches are very noisy, although some general patterns emerge. First, hake catches increased from 1970 until the early 1990s in most areas (Gulf of Lions, Adriatic, Ionian and Aegean). In these areas, and also in the Levant, hake production decreased since the early 1990s to the present due probably to overfishing (Lleonart, 2008). In the Balearic area no overall trend can be distinguished, but periods of high catches and low catches can be discerned, while in the Sardinia area hake catches have been decreasing since the beginning of the time series (Fig. 2).

To analyze these data sets, a Generalized Additive Model (GAM) was set up for each statistical area, using *year* as the main effect (because it is expected that long-term trends in interannual variations in catches are mainly due to the observed

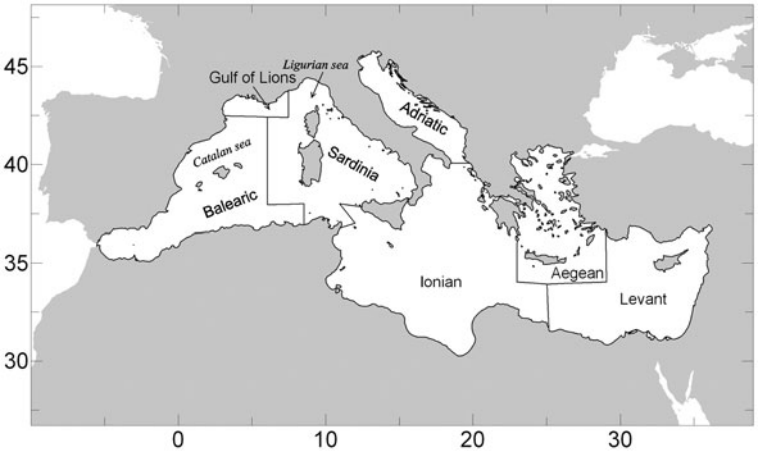

Fig. 1 FAO fisheries divisions in the Mediterranean and geographic names mentioned in the text (italics)

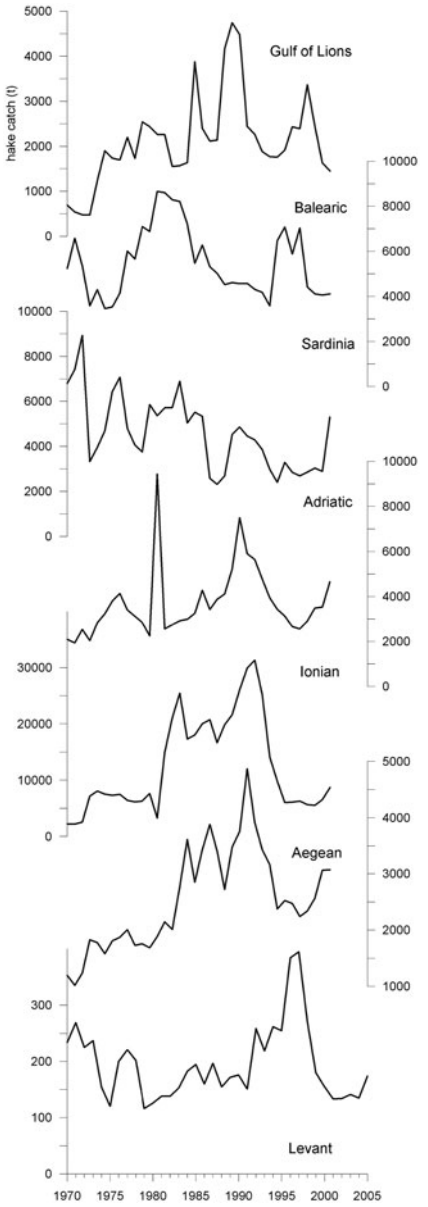

Fig. 2 Data series of hake (*Merluccius merluccius*) landings in the seven Mediterranean FAO fisheries divisions for the period 1970–2005 (data extracted from FISHSTAT, FAO Fisheries Department, 2000)

increase in fishing effort, Lleonart, 2008) and the NAO index as additional effect with time lags of 1 and 2 years (*nao1* and *nao2*). GAMs are a flexible class of statistical regression models which allow to assess linear or nonlinear relationships between a set of predictors (in our case, *year*, *nao1* and *nao2*) and a dependent variable (in our case hake *catch*) (Wood, 2006):

$$\log(catch) = \mathrm{s}(year) + \mathrm{s}(nao1) + \mathrm{s}(nao2) + \varepsilon,$$

where ε is a normally distributed error term.

I used smoothing splines to represent the possibly nonlinear effect of predictors and Generalized Cross Validation (GCV) to establish the optimal degree of the smooth terms. Model selection was achieved by means of Akaike's Information Criteria to assess the goodness of fit (Wood, 2006).

The GAM models fitted for hake catch in the seven statistical subareas for the period 1970–2005 helped explain between 62% (Gulf of Lions) and 96% (Aegean sea) of the deviance in the data series (Table 1). These results show that most of the variability in the catch data series can be attributed to the year effect, which mostly reflects changes in fishing effort over time. More interestingly, the results of the GAM analysis show that the lagged NAO index explains between 2 and 8% of the deviance of the models and that some of the functional non-parametric terms are statistically significant (Table 1). The shape of these nonparametric terms can be examined in Fig. 3, which shows that hake stocks in the western and northern Mediterranean areas (Gulf of Lions, Balearic and Adriatic) are positively correlated with the NAO index at lags 1 and 2 years, while hake stocks in the eastern Mediterranean (Aegean and Levant) would be negatively correlated with these NAO

Table 1 Results of the GAM analysis of hake (*Merluccius merluccius*) landings in the seven Mediterranean areas for fishery purposes defined by FAO

Area	Deviance explained by full model (%)	Deviance explained by term *year* (%)	Deviance explained by term *nao1*	Deviance explained by term *nao2*
Gulf of Lions	62.3	55.0	4.3%	3.0%
Balearic	87.5	81	5.7%	0.8% (NS)
Sardinia	69.1	62.6	2.1% (NS)	4.4%
Adriatic	66.8	44.9	1.2%	0.7% (NS)
Ionian	95.0	93.9	0.1% (NS)	1%
Aegean	96.2	89.7	4.2%	2.0%
Levant	81.5	77.2	3.7%	0.6% (NS)

Data series from FAO Fisheries Department (2000).
nao1 and *nao2* are the NAO index lagged 1 and 2 years, respectively.
NS: non-significant term, otherwise significant terms at $p < 0.1$ level.

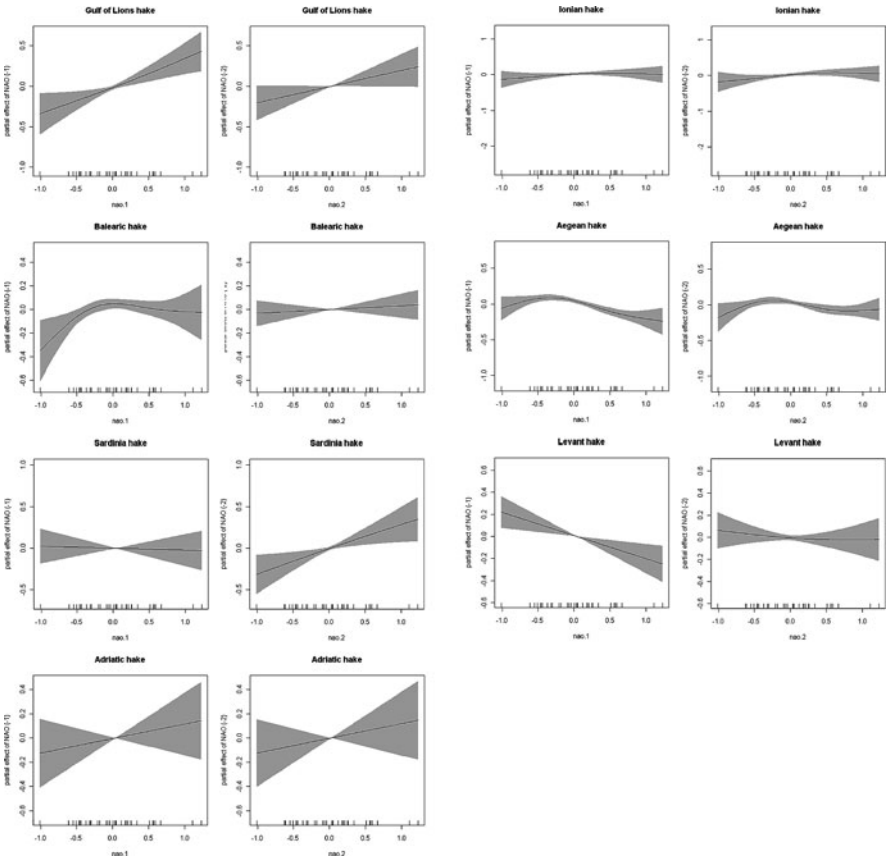

Fig. 3 Non-parametric smooth terms determined by the GAM analysis for hake (*Merluccius merluccius*) landings in the seven Mediterranean FAO fisheries divisions. *Left column*: effect of NAO index lagged 1 year. *Right column*: effect of NAO index lagged 2 years

indices (Fig. 3). Hake stocks in the central Mediterranean show weak correlations (Ionian) or of opposite sign (Sardinian).

To investigate the causes linking NAO with hake fisheries variability I analyzed the correlation between several life-history indicators derived from fisheries independent trawl surveys in the western Mediterranean (MEDITS surveys carried out along the continental coast of Spain, Bertrand et al., 2002) by means of autocorrelation function analysis (Venables and Ripley, 2002). The span of this data set (1994–2009) is shorter than the FAO production statistics, but includes a critical transitional period from positive values of the NAO index in the 1990s to negative or zero values later on. I extracted several demographic indicators from the

Table 2 Demographic indicators of hake (*Merluccius merluccius*) analyzed by autocorrelation functions. Indicators were derived from the annual MEDITS trawl surveys carried out along the Mediterranean continental coast of Spain (1994–2009)

	Age class	Result
Abundance indices	0 (recruits)	NS
No of individuals/km^2	1	NS
	2	NS
	Average for ages 3–6	S (lags 1 and 2)
Individual length (cm TL)	0 (recruits)	S (lag 1)
	1	NS
	2	NS
	Average for ages 3–6	NS
Individual weight (g)	0 (recruits)	NS
	1	NS
	2	NS
	Average for ages 3–6	S (lag 1)
Natural mortality (year^{-1})	0 (recruits)	NS
	1	NS
	2	NS
	Average for ages 3–6	NS
Biomass	Total population biomass	NS
	Spawning stock biomass (SSB)	NS

Data elaborated from http://www.ifremer.fr
S: significant; NS: Not Significant at $p<0.05$ level.

MEDITS database (http://www.ifremer.fr/Medits_indices): abundance by age class, natural mortality by age class, total biomass, spawning stock biomass, and average individual length and weight (Table 2).

The results of autocorrelation function analysis (Fig. 4) show that the mean length of recruits (hake of age class 0) is positively correlated with NAO at lag 1, i.e. recruits are larger than average after positive NAO years. Also the abundance of adults (age classes 3–6) of hake is increased 1 and 2 years after positive NAO years, while the average weight of adults is positively correlated with NAO at lag 1. Despite this increase in abundance and mean weight of adults, no increase in spawning stock biomass could be shown in positive NAO years, probably because the biomass of the adult fraction of the population is much lower than the juvenile fraction (age classes 0–2) in this heavily exploited population. Natural mortality was not correlated to the NAO. These results show that in the Balearic subarea, and probably also in the Gulf of Lions and Adriatic, positive NAO years have a positive effect in at least 3 critical indicators of the hake life history (length of recruits, abundance of adults and weight of adults) suggesting that the positive effects on the catches shown earlier from the FAO production data series can be related to increase size and weight of the hake population and not, for instance, to decreased natural mortality or increased reproductive success, as in the red shrimp (Maynou, 2008).

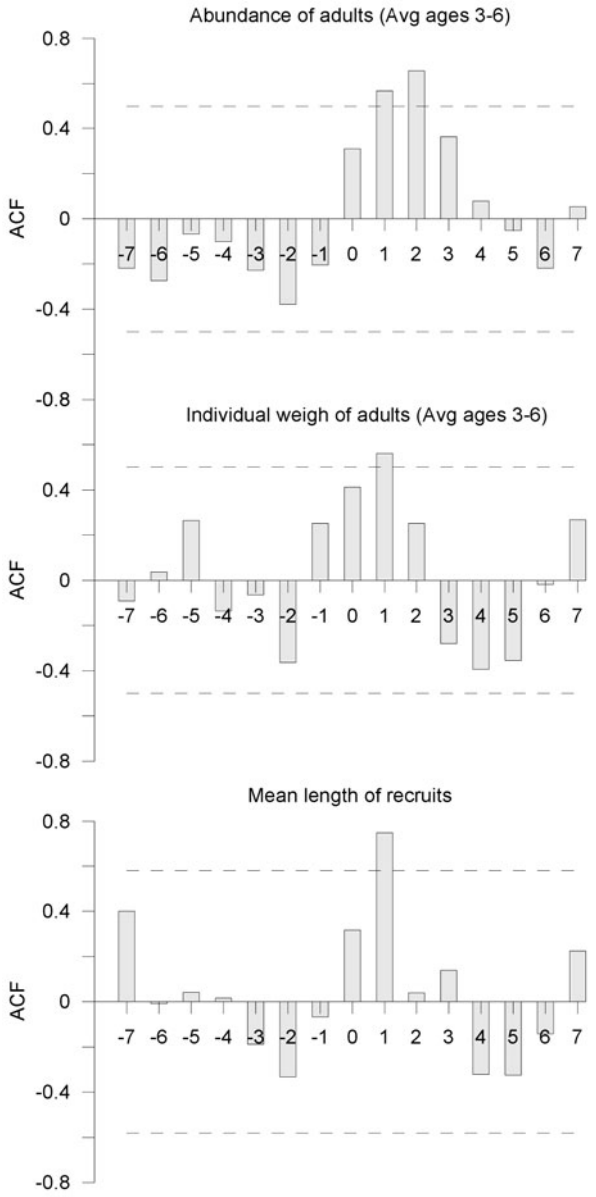

Fig. 4 Autocorrelograms of significant demographic indicators (Table 2) extracted from the MEDITS database for hake (*Merluccius merluccius*) in the Spanish Mediterranean coast (subarea 6). *Dotted lines* indicate significant correlation at the $p < 0.05$ level

3 Conclusions

The North Atlantic Oscillation has profound influences on fisheries productivity, mediated by complex dynamics of ocean processes and biological productivity, as shown in North Atlantic fish stocks (Ottersen and Stenseth, 2001; Reid et al., 2001, 2003; Stenseth and Mysterud, 2005; Stige et al., 2006), but also in the Mediterranean (Lloret et al., 2001; Maynou, 2008).

In fisheries research the influence of environmental variation on stock productivity may be difficult to detect due to the lack of long and consistent time series of the main oceanographic and ecological parameters at appropriate scales. Large-scale climatic indices such as the NAO are often better proxies of ecological processes than local weather variables, because they reduce the complexities of time and space variability in environmental phenomena to simple measures (Hallett et al., 2004; Stenseth and Mysterud, 2005), and are specially useful for fish abundance data where comparable environmental data sets are non existent or expensive to obtain (e.g. for deep-sea fishery resources, Maynou, 2008).

The influence of the NAO on fish stocks has been shown to vary geographically, with impacts of different sign in cod stocks of, broadly, the western Atlantic and the eastern Atlantic (Stige et al., 2006). In Mediterranean hake stocks, present results suggest also geographically varying impacts of the NAO. A N/S – W/E trend in the effects of NAO has been evidenced: in the N and W areas (Balearic sea, Gulf of Lions, Adriatic sea) the effect is close to linear and positive (enhanced hake catches at positive NAO values). In the E and S subareas (Aegean sea, Levantine sea) the effects is negative (enhanced catches at negative NAO values), while in the two central subareas (Sardinian seas and Ionian sea) the effect is weak but mainly positive. Focusing on the Balearic area, I used a shorter data set derived from fisheries independent surveys to investigate the possible biological causes of enhanced catches by NAO in this area. I showed that the positive relationship between NAO and catches of hake is related to the positive effect of NAO (with temporal lags of 1 or 2 years) on at least 3 critical indicators of the hake life history: length of recruits, abundance of adults and weight of adults. These results suggest that the positive effects of NAO on Mediterranean hake catches can be related to increased size and weight of the hake population and not, for instance, to decreased natural mortality nor increased reproductive success, as in the red shrimp (Maynou, 2008).

Although the effect of the NAO on fisheries of Mediterranean stocks has been shown in a few studies (Lloret et al., 2001; Maynou, 2008; present work for hake), further research is needed to investigate the relationships linking the North Atlantic Oscillation, Mediterranean oceanography and biological productivity. Although it is likely that the effect of the NAO on higher trophic levels (which constitute the fisheries target species) is mediated by the effects of NAO on zooplankton (Fromentin and Planque, 1996; Maynou, 2008; Molinero et al., 2008) the details of these relationships are often mere working hypotheses that need to be refined and tested.

References

Alheit J, Bakun A (2010) Population synchronies within and between ocean basins: apparent teleconnections and implications as to physical-biological linkage mechanisms. J Mar Syst 79:267–285

Bakun A (1996) Patterns in the ocean: ocean processes and marine population dynamics. California Sea Grant College System/Centro de Investigaciones Biológicas del Noroeste, La Paz, 323 pp

Beaugrand G (2004) The North Sea regime shift: evidence, mechanisms and consequences. Prog Oceanogr 60:245–262

Beaugrand G, Brander KM, Lindley JA, Souissi S, Reid PC (2003) Plankton effect on cod recruitment. Science 426:661–664

Bertrand JA, Gil de Sola L, Papaconstantinou C, Relini G, Souplet A (2002) The general specifications of the MEDITS surveys. Sci Marina 66:9–17

Brander K (2005) Cod recruitment is strongly affected by climate when stock biomass is low. ICES J Mar Sci 62:339–343

Brodziak J, O'Brien L (2005) Do environmental factors affect recruits per spawner anomalies of New England groundfish? ICES J Mar Sci 62:1394–1407

Cartes JE, Madurell T, Fanelli E, López-Jurado JL (2008) Dynamics of suprabenthos-zooplankton communities around the Balearic Islands (western Mediterranean): influence of environmental variables and effects on the biological cycle of *Aristeus antennatus*. J Mar Syst 71:316–335

Cushing DH (1996) Towards a science of recruitment in fish populations. International Ecology Institute, Oldendorf/Luhe

Demirov E, Pinardi N (2002) Simulation of the Mediterranean Sea circulation from 1979 to 1993: Part I. The interannual variability. J Mar Syst 33–34:23–50

Evans D, Grainger R (2001) Gathering data for resource monitoring and fisheries management. In: Hart PJB, Reynolds JD (eds) Handbook of fish biology and fisheries, vol 2, chapter 5. Blackwell Publishing, Oxford

FAO Fisheries Department (2000) *FISHSTAT plus: universal software for fishery statistical time series*. Version 2.30. FAO Fisheries Department, Fishery Information, Data and Statistics Unit

Fromentin JM, Planque B (1996) *Calanus* and environment in the eastern North Atlantic. II. Influence of the North Atlantic Oscillation on *C. finmarchicus* and *C. helgolandicus*. Mar Ecol Prog Ser 134:111–118

Hallett TB, Coulson T, Pilkington JG, Clutton-Brock TH, Pemberton JM, Grenfell BT (2004) Why large-scale climate indices seem to predict ecological processes better than local weather. Nature 430:71–75

Hänninen J, Vuorinen I, Hjelt P (1999) Climatic factors in the Atlantic control the oceanographic and ecological changes in the Baltic Sea. Limnol Oceanogr 45:703–710

Hilborn R, Walters CJ (1992) Quantitative fish stock assessment: choice, dynamics and uncertainty. Chapman and Hall, London

Jobling M (2002) Environmental factors and rates of development and growth. In: Hart PJB, Reynolds JD (eds) Handbook of fish biology and fisheries, vol 1, chapter 5. Blackwell Publishing, Oxford

Jordi A, Hameed S (2009) Influence of the Icelandic low on the variability of surface air temperature in the Gulf of Lion: implications for intermediate water formation. J Phys Oceanogr 39:3228–3232

Lleonart J (2008) Review of the state of Mediterranean and Black Sea fishery resources. In: Basurco B (ed) The Mediterranean fisheries sector. *Options méditerranéennes, Série B: Études et recherches*, n. 62. CIHEAM/FAO/GFCM, Rome, 179 pp

Lloret J, Lleonart J, Solé I, Fromentin J-M (2001) Fluctuations of landings and environmental conditions in the north-western Mediterranean Sea. Fish Oceanogr 10:33–50

Mann KH, Drinkwater KF (1994) Environmental influences on fish and shellfish production in the Northwest Atlantic. Environ Rev 2:16–32

Mariotti A, Struglia MV, Zeng N, Lau KM (2002) The hydrological cycle in the Mediterranean region and implications for the water budget of the Mediterranean Sea. J Clim 15:1674–1690
Maynou F (2008) Influence of the North Atlantic Oscillation on Mediterranean deep-sea shrimp landings. Clim Res 36:253–257
Mendelsohn R, Mendo J (1987) Exploratory analysis of anchoveta recruitment off Peru and related environmental series. In: Pauly D, Tsukuyama I (eds) The Peruvian anchoveta and its upwelling ecosystem: three decades of change. ICLARM studies and reviews, Instituto del Mar de Peru, Callao (Peru), vol 15. pp 109–116
Molinero JC, Ibanez F, Souissi S, Buecher E, Dallot S, Nival P (2008) Climate control on the long-term anomalous changes of zooplankton communities in the northwestern Mediterranean. Glob Change Biol 14:11–26
Myers R (2002) Recruitment: understanding density-dependence in fish populations. In: Hart PJB, Reynolds JD (eds) Handbook of fish biology and fisheries, vol 1, chapter 6. Blackwell Publishing, London
Oliver P, Massutí E (1995) Biology and fisheries of western Mediterranean hake (*M. merluccius*). In: Alheit J, Pitcher TJ (eds) Hake: biology, fisheries and markets. Chapman and Hall, London, pp 181–202
Ottersen G, Alheit J, Drinkwater K, Friedland K, Hagen E, Stenseth NC (2004) The responses of fish populations to ocean climate fluctuations. In: Stenseth NC, Ottersen G, Hurrell J, Belgrano A (eds) Marine ecosystems and climate variation: the North Atlantic. Oxford University Press, Oxford, pp 73–94
Ottersen G, Stenseth NC (2001) Atlantic climate governs oceanographic and ecological variability in the Barents Sea. Limnol Oceanogr 46:1774–1780
Recasens L, Lombarte A, Morales-Nin B, Torres GJ (1998) Spatiotemporal variation in the population structure of the European hake in the NW Mediterranean. J Fish Biol 53:387–401
Reid PC, Borges MF, Svendsen E (2001) A regime shift in the North Sea circa 1988 linked to changes in the North Sea horse mackerel fishery. Fish Res 50:163–171
Reid PC, Edwards M, Beaugrand G, Skogen M, Stevens D (2003) Periodic changes in the zooplankton of the North Sea during the 20th century linked to oceanic inflow. Fish Oceanogr 12:260–269
Sparre P, Venema SC (1998) Introduction to tropical fish stock assessment – Part 1: Manual. FAO Fisheries Technical Paper 306/1
Stenseth NC, Mysterud A (2005) Weather packages: finding the right scale and composition of climate in ecology. J Animal Ecol 74:1195–1198
Stige LC, Ottersen G, Brander K, Chan KS, Stenseth NC (2006) Cod and climate: effect of the Northa Atlantic Oscillation on recruitment in the North Atlantic. Mar Ecol Prog Ser 325:227–241
Venables WN, Ripley BD (2002) Modern applied statistics with S, 4th edn. Springer, Berlin
Watanabe Y, Kurita Y, Noto M, Oozeki Y, Kitagawa D (2003) Growth and survival of Pacific saury (*Cololabis saira*) in the Kuroshio-Oyashio transitional waters. J Oceanogr 59:403–414
Watanabe Y, Zenitani H, Kimura R (1996) Causes of population decline in the Japanese sardine (*Sardinops melanostictus*): overfishing or early mortality? In: Watanabe Y, Yamashita Y, Oozeki Y (eds) Survival strategies in early life stages of marine resources. Balkema, Rotterdam, pp 83–94
Wood S (2006) Generalized additive models: an introduction with R. Chapman and Hall/CRC, London, p 410

Impacts of the NAO on Mediterranean Crop Production

Simone Orlandini, Anna Dalla Marta, Marco Mancini, and Daniele Grifoni

Abstract Meteorological conditions can influence the main biological processes responsible of plant growth and development affecting vegetative growing, setting and ripening of different plant organs, onset and duration of phenological stages and the final production, exerting a strong impact on agricultural activities. In particular, the study of the variability of timing and length of the plants growing season is gaining importance because plant phenology is a sensitive indicator of climate change and has large impacts on terrestrial ecosystems through changes in productivity and in the annual carbon and water cycles. For many years, starting from meteorological information, mathematical descriptions of these effects have been formulated in order to provide users (farmers, technicians, extension services, researchers, etc.) with operational tools for improving management and planning activities. Besides common meteorological information supplied by local or synoptic weather stations, the use of large-scale climatic variables has also been investigated in order to forecast agricultural yields and production quality in several regions of the world. In Europe, the North Atlantic Oscillation (NAO) seems to be responsible for a large component of climate variability, particularly influencing winter and, through climate interactions on plants, crop production quality and quantity characteristics. The use of large-scale meteorological information showed great potential, particularly for the development of crop production forecasting systems.

Keywords Wheat · Grapevine · Growth · Development · Yield

1 Introduction

Observations of the physical and biological variables in the environment are essential in agricultural meteorology. Meteorological considerations enter in assessing the performance of a plant or animal because their development is a result of the combined effect of genetic characteristics and their response to environment. Without quantitative data, agrometeorological planning, forecasting, research and services by agrometeorologists cannot properly assist agricultural producers to meet

S. Orlandini (✉)
Department of Plant, Soil and Environmental Science, University of Florence, Florence, Italy
e-mail: simone.orlandini@unifi.it

S.M. Vicente-Serrano, R.M. Trigo (eds.), *Hydrological, Socioeconomic and Ecological Impacts of the North Atlantic Oscillation in the Mediterranean Region*, Advances in Global Change Research 46, DOI 10.1007/978-94-007-1372-7_8,

the ever-increasing demands for food and agricultural products. Such data are also needed to assess the impacts of agricultural activities and processes on the environment and climate.

Crop production is the result of a complex interaction among environmental conditions, agronomic management and plant characteristics. Soil, described by its chemical, biological and physical properties, and climate (i.e. degree days accumulation, rainfall, total solar radiation) are the main environmental factors affecting plant responses.

Crop production is influenced by meteorological conditions such as temperature, precipitation, solar radiation (intensity, photoperiod, and quality) and wind. As these variables correspond to the main driving factors of crops production spatial and temporal variability, they are commonly used for the analysis and simulation of crop yield.

A number of approaches have been used to describe crop yield based on weather parameters. In most statistical approaches, regressions are obtained correlating environmental variables and yield. The main problems with statistical approaches are that yield is more complex than growth simulation and that there is little confidence in extrapolating the results beyond the original limits of the data-sets. On the other hand, in using mechanistic approaches, difficult arises from numerous assumptions. Intermediate approaches between statistical and complex models are to use simplified mechanistic models which define crop behaviour by only few relationships (Bindi et al., 1997).

Agrometeorological stations can provide data to feed crop yield simulators. The quality of agrometeorological variables is the basis for a precise simulation and consequently for the processing of information that meets the needs of the end-users. However, ground weather stations often fail to satisfy these quality standards, both in terms of accuracy and precision of measured data and of spatial and temporal representativeness (WMO, 1981). The implementation of networks of weather stations could partly solve these problems, but would involve high installation and maintenance costs (Vose and Menne, 2004).

Moreover meteorological observations do not inform us about the state of the local atmosphere unless we know how the observations were made – the instrument, its installation height and exposure, used sampling and averaging times – and the way in which the measurements were processed. Specifications of all these links of the observation chain are called metadata, and their availability determines the value of measurements. Unfortunately they are not commonly available, making the use of station data unable to provide a realistic description of crop responses, particularly for application at meso or macroscale level.

The internet has increasingly been used to disseminate climate and meteorological data, given its rapid manipulation and displays of information, the interaction and feedback with the users, and the reduction of cost. The internet allows for finding suitable applications providing free access to meteorological information with different spatial domains and temporal resolutions.

Besides common meteorological information supplied by local or synoptic weather stations, the use of large-scale climatic variables has also been investigated

in order to forecast agricultural yields and production quality in several regions of the world (Atkinson et al., 2005). Among these indices that identify the large-scale distribution of pressures and temperatures over defined geographical areas, the North Atlantic Oscillation (NAO) is one of the most studied due to its significant impact on the climate over important production regions worldwide (Tables 1 and 2). In Spain, Gimeno et al. (2002) found that the yield of many crops (lemon, orange, tangerine, wheat, rye and olive) is affected by NAO, while in Italy the effect of NAO was related to the phenology of grapevine (Dalla Marta et al., 2010a) and quality of wine (Grifoni et al., 2006). Many studies demonstrated a relationship between the wheat yield and grain quality (Hagber falling number, specific weight and protein concentration) and the winter NAO in Italy (Dalla Marta et al., 2010b), Portugal (Gouveia and Trigo, 2008) and UK (Kettlewell et al., 1999; Wanner et al., 2001; Hurrell et al., 2003; Atkinson et al., 2005, 2008). According to Kettlewell et al. (2003) the winter NAO has an effect on cumulated precipitation in summer in England and Wales and, consequently, on wheat quality, while Colman (1997) suggested an association between Sea Surface Temperature (SST) and NAO in the UK.

Large-scale climate variability affects average conditions considerably and is therefore likely to influence the phenology of plants. In Europe, the North Atlantic Oscillation (NAO) seems to be responsible for a large component of climate variability (Post and Stenseth, 1999; Benestad, 2001; Wanner et al., 2001; Sivle, 2005), particularly influencing winter weather and, through climate interactions on plants, flowering time of many tree species (Klaveness and Wielgolaski, 1996; Gormsen et al., 2005; Avolio et al., 2008).

At the same time, winter meteorological conditions play an important role in processes controlling the termination of dormancy and bud-break, strongly affecting the onset of the growing season, spring flowering phenophases and pollen season of different woody plants in North and southern Europe (Fitter et al., 1995; Klaveness and Wielgolaski, 1996; D'Odorico et al., 2002; Gormsen et al., 2005; Avolio et al., 2008; Nordli et al., 2008).

Table 1 Example of NAO effect on vegetation, forest and trees

Ecological descriptor	Parameter	Correlation	Period	Variable affected	References
Europe vegetation	Timing of spring phenology	Negative	Jan–Mar	Temperature, precipitation	D'Odorico et al. (2002)
Europe vegetation	Timing of phenology	Negative	Winter	Temperature, precipitation	Gouveia et al. (2008)
Europe forests	Timing of phenology	Negative	N.A.	Temperature	Cook et al. (2005)
Norway trees	Timing of phenology	Negative	Winter	Temperature	Post et al. (1999)
Norway trees	Timing of phenology	Negative	Winter	Temperature	Nordli et al. (2008)
Germany trees	Timing of spring/ summer phenology	Negative	Jan–Mar Feb–Mar	Temperature	Menzel (2003)

Table 2 Example of NAO effect on crop responses

Ecological descriptor	Parameter	Effect	Period	Variable affected	References
Spain wheat, orange, lemon	Yield	Positive	Yearly	Temperature, precipitation	Gimeno et al. (2002)
Portugal wheat	Yield	N.A.	Feb–Mar	Temperature, precipitation	Gouveia et al. (2008)
UK wheat	Quality (specific weight)	Positive	Winter	Radiation, precipitation	Atkinson et al. (2005)
UK wheat	Quality (specific weight)	Positive	Jan	Radiation, precipitation	Atkinson et al. (2008)
UK wheat	Quality (specific weight, protein)	Positive	Jan–Feb	Radiation, temperature	Kettlewell et al. (1999)
UK wheat	Quality (specific weight)	Positive	Winter	Summer precipitation	Kettlewell et al. (2003)
Italy durum wheat	Quality (protein content)	Positive	Nov–Feb	Winter precipitation	Dalla Marta et al. (2010b)
Italy grapevine	Timing of phenology	Negative	Feb–Mar	Radiation and temperature	Dalla Marta et al. (2010a)
Italy grapevine	Quality (rating)	Negative	Apr–Jul	Temperature, precipitation	Grifoni et al. (2006)
Italy olives	Pollen season	Negative	Mar–Jun	Temperature	Avolio et al. (2008)

1.1 Objectives

The main objective of this chapter was to analyze the correlations between NAO index (Jones et al., 1997) and several Italian crop productions. Different case studies were considered, all taking into consideration high quality Mediterranean crops, such as wheat and grapevine. Local ground weather stations data were also analysed, to compare obtained results by using large scale indices. Different temporal scales were compared in order to propose a crop response analysis and forecasting method based on meteorological conditions observed several months before harvest. Results are discussed with the aim of evaluating the possibility of assessing crop production with the freely available data, solving the problems related to the use of ground weather stations.

2 Results

2.1 NAO and Grapevine Phenology

In this study, data series of phenological stages of Sangiovese grapevine were analysed for the productive area of Montepulciano wine. Bud-break (1979–2006),

flowering and harvest (1970–2006) dates were used for the analysis and related to the NAO index. The phenology is the scientific study of periodic biological phenomena such as flowering, breeding, and migration in relation to climatic conditions. Phenological data, expressed as the day of the year in which the phenological stage (bud-break, flowering, fruit set, etc.) was reached (Balloid and Baggiolini, 1993), were collected by skilled field operators and considered as the mean value of 20 vines.

Bud-break date was negatively correlated with NAO index for February ($r = –0.402$, $p \leq 0.05$) and for the period February–March ($r = –0.377$, $p \leq 0.05$) (Fig. 1), even if the month of March did not show a significant correlation when considered independently.

The negative correlation between February and March NAO index and bud-break data was due to the relation between NAO and weather conditions in the wine production area at the beginning of the grapevine vegetative season. Winter and early spring NAO has a strong and well-documented effect on precipitation and consequently on the cloudiness of the same period. The role of NAO, therefore, could be mainly due to a reduction in cloud cover and consequently greater insolation than average for the positive NAO index phase. Greater sunshine probably leads to an increased surface temperature and thus the heat requirement for various stages of plant development could be reached earlier (Avolio et al., 2008).

Flowering of grapevine in the study area usually occurs between mid-May and early June. The NAO index of single months showed no correlation with flowering stage (data not shown) but a significant negative correlation was found between the NAO index for February–March ($r = –0.397$, $p \leq 0.05$) (Fig. 2) and the phenological stage date. The effect of winter NAO on flowering stage was probably an indirect result beginning at the bud-break stage. In fact, the effect of NAO on meteorological conditions is strong during winter and decreases in the spring and early summer months. However, the two stages of bud-break and flowering are partially

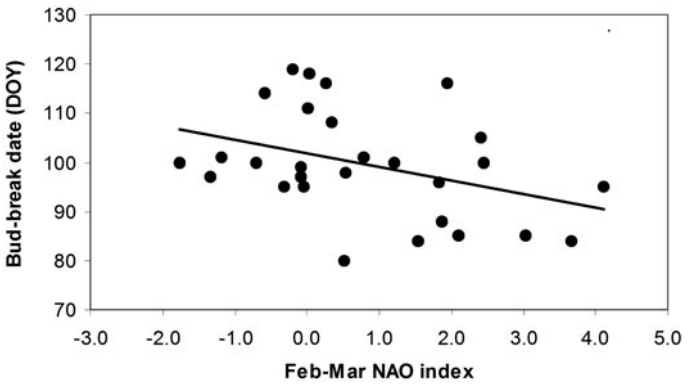

Fig. 1 Linear correlation between NAO index of the period February–March and grapevine bud-break phase date

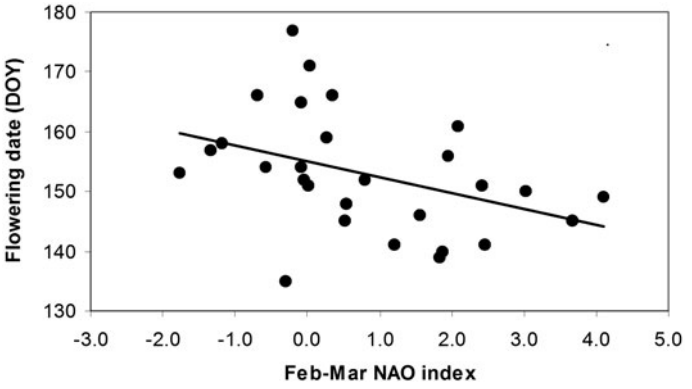

Fig. 2 Linear correlation between NAO index of the period February–March and grapevine flowering phase date

auto-correlated and the period in between is mainly determined by a thermal summation. Therefore, the anticipation of bud-break due to high values of winter NAO also has the indirect effect of anticipating flowering in late spring.

Harvest is usually conducted from mid-September to mid-October, depending on different environmental and physiological factors. The NAO index did not significantly affect harvest date, confirming that its effect on meteorological conditions is really evident in winter and, less strongly, in early spring.

2.2 NAO and Wheat Quality

The research was carried in Val d'Orcia (Siena, Italy) where durum wheat is considered an important quality production with a cultivated area of almost 135,000 ha, about 15% of the total cultivated surface. The quality of durum wheat grain was described by its protein content, expressed as the percentage of dry matter, due to its direct relation with the production of good quality pasta. Data were analyzed for the period 1997–2009. These results are not as robust as those obtained in the previous section due to the short time-series available (13-year), but the wheat quality was positively correlated with the NAO index for several months, in particular during the winter period. The higher correlations on a monthly basis were found for November ($r = 0.580$, $p \leq 0.05$) and February ($r = 0.546$, $p \leq 0.05$), but more significant results were obtained by aggregating NAO index on a multi-monthly basis when November and February are included. In particular, the best correlation was obtained for the November–February period ($r = 0.845$, $p \leq 0.001$) (Fig. 3) due to the contribution of the 2 months in between that are not significantly, but still positively, correlated to the final grain protein content. This result can be explained by the winter NAO index defining a specific atmospheric synoptic configuration over the Atlantic Ocean, strongly affecting winter precipitation over the Mediterranean sea and consequently over the study area (Hurrell and Van Loon, 1997; Bartolini et al.,

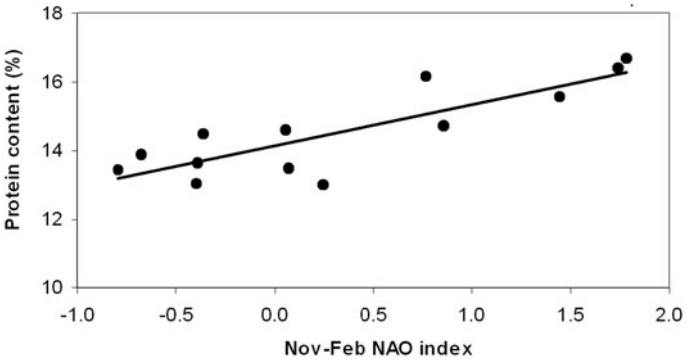

Fig. 3 Linear correlation between NAO index of the period November–February and durum wheat quality

2009). In turn, winter precipitation is negatively correlated with protein content. The negative effect of rainfall on grain quality is probably related to problems concerning crop management. In fact, abundant precipitations in November can create serious problems for field operations, even causing a significant delay in the sowing date. Nevertheless, even if wheat can be sown in time, a too high soil water content may give rise to asphyxia phenomena leading to further problems during crop development. Moreover, the negative effect of rainfall may be due to the losses of nitrogen applied with fertilization. Anyway, wheat protein resulted slightly more correlated with the NAO index than with cumulated precipitation, probably because the former is able to better describe the environmental conditions (being a consequence of atmospheric circulation) rather than just the precipitation.

To investigate the effect of NAO and common meteorological variables as a whole, a stepwise linear multiple regression analysis was performed. The model, based on an automatic procedure of variable inclusion/exclusion ($p \leq 0.05$ and $p \geq 0.10$ respectively), was tested by using the multi-monthly period for which the best correlation coefficients were obtained for each single meteorological variable. In particular, the variables used were February–June air temperature ($r = 0.609$, $p \leq 0.05$), November–May precipitations ($r = 0.732$, $p \leq 0.01$) and November–February NAO ($r = 0.845$, $p \leq 0.001$). Within the stepwise regression results, the simplest model was obtained using NAO index ($r = 0.845$, $p \leq 0.001$), while precipitation and air temperature were excluded since their addition to the model failed to improve its performance. This result is consistent with the previous considerations concerning the dependence of these variables on NAO, which already contains their partial contribution to the determination of wheat quality.

2.3 NAO and Wine Quality

This case study analyzed the relationships between NAO index and the quality of different important Italian wines for the period 1970–2002. The quality data

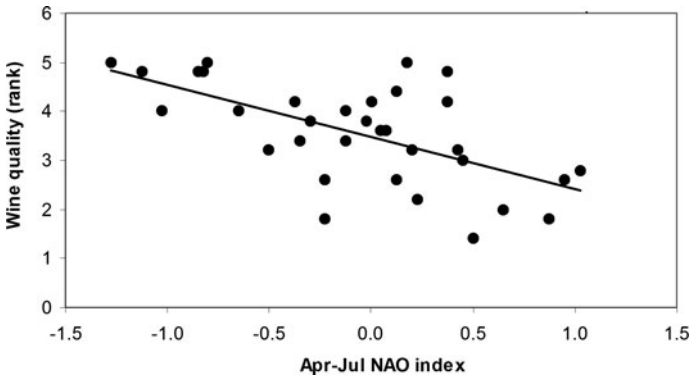

Fig. 4 Linear correlation between NAO index of the period April–July and Italian wine quality

series of the following six wines were used: Brunello di Montalcino, Nobile di Montepulciano and Chianti Classico (Tuscany region, central Italy), Barolo and Barbaresco (Piedmont region, north-western Italy), and Amarone (Veneto region, north-eastern Italy). Vintage ratings were used to define wine quality ranking. The rating of a given vintage is conducted in a single blind tasting of the individual varietals by a panel of experts. Although this rating does not consider variations in quality among the individual vineyards, it is the most comprehensive overall rating compiled for high-quality Italian wines (Corsi and Ashenfelter, 2001). This analysis allows for verifying whether the wine meets market expectations and represents a composite of all the quality elements of the wine. In production area, this ranking is based upon the collection of estimates from 1 to 5 classes (from insufficient to excellent) (Riou, 1994). The relationships between quality data of wines and NAO index were investigated through regression analysis on monthly and multi-monthly bases.

Wine quality rankings were inversely correlated with the NAO Index of several previous months (included in the growing season) and in particular, the higher negative correlations were obtained for April ($r = –0.439$, $p \leq 0.05$) and May ($r = –0.359$, $p \leq 0.05$).

More significant results were obtained by developing regression of the wine quality versus NAO Index aggregated on a multi-monthly basis including April and May. The best result, for some selected aggregations, was obtained for the April–July period ($r = 0.607$, $p \leq 0.001$) (Fig. 4). These results could be explained by the fact that the NAO index defines a specific atmospheric synoptic configuration over the Atlantic Ocean, affecting the regional rainfall and air temperature.

3 Conclusions

Obtained results are useful for agricultural communities when used to modify management decisions and to adopt practices that are better adapted to the expected

conditions. However the possible use of seasonal climate information for agricultural aims has been slower than expected for a number of reasons. The most significant is that the deterministic information requested by the farmers is beyond that elaborated by the NAO and other indices (ENSO, AO, etc.). As an example, the quality of short term forecast is not comparable with the information available from seasonal index. Recent development, however, provide some evidence of progress toward meeting user needs and forecast capabilities. This is due to the consideration that reliable sources of daily rainfall and temperature data are becoming more widely available for many parts of the world. Secondly, climate scientists are beginning to use these data to examine the observed statistics of climatic variables over the course of the season and how these statistics influence climatic indices. Further, investigations are being initiated to examine the ability of numerical weather models to replicate these statistics in analyses and forecasts (Baethgen et al., 2009).

Acknowledgements The authors wish to thank Fondazione Monte dei Paschi di Siena, Consorzio Agrario di Siena and COST734 Action for their support of this research.

References

Atkinson MD, Kettlewell PS, Hollins PD, Stephenson DB, Hardwik NV (2005) Summer climate mediates UK wheat quality response to winter North Atlantic Oscillation. Agri Forest Meteorol 130:27–37

Atkinson MD, Kettlewell PS, Poulton PR, Hollins PD (2008) Grain quality in the Broadbalk Wheat Experiment and the winter North Atlantic Oscillation. J Agric Sci 146:541–549

Avolio E, Pasqualoni L, Federico S, Fornaciari M, Bonofiglio T, Orlandi F, Bellocci C, Romano B (2008) Correlation between large-scale atmospheric fields and the olive pollen season in Central Italy. Int J Biometeorol 52:787–796

Baethgen WE, Carriquiry M, Ropelewski C (2009) Tilting the odds in maize yields. Bull Am Meteorol Soc 2:179–183

Balloid M, Baggiolini M (1993) Les stades repères de la vigne. Revue Suisse de Viticulture Arboriculture Horticulture 25:7–9

Bartolini E, Claps P, D'Odorico P (2009) Interannual variability of winter precipitation in the European Alps: relations with the North Atlantic Oscillation. Hydrol Earth Syst Sci 13:17–25

Benestad RE (2001) The cause of warming over Norway in the ECHAM4/OPYC3 GHG integration. Int J Climatol 21:371–387

Bindi M, Miglietta F, Gozzini B, Orlandini S, Seghi L (1997) A simple model for simulation of growth and development in grapevine (Vitis vinifera L.). I Model description. Vitis 36:67–71

Colman A (1997) Prediction of summer central England temperature from preceding North Atlantic winter sea surface temperature. Int J Climatol 17:1285–1300

Cook BI, Smith TM, Mann ME (2005) The North Atlantic Oscillation and regional phenology prediction over Europe. Glob Change Biol 11:919–926

Corsi A, Ashenfelter O (2001) Predicting Italian wines quality from weather data and experts' ratings, 18 pp. Cahier Scientifique de l'OCVE, n 4

Dalla Marta A, Grifoni D, Mancini M, Storchi P, Zipoli G, Orlandini S (2010a) Analysis of the relationships between climate variability and grapevine phenology in the Nobile di Montepulciano wine production area. J Agric Sci 148:657–666

Dalla Marta A, Grifoni D, Mancini M, Zipoli G, Orlandini S (2010b) The influence of climate on durum wheat quality in Tuscany, Central Italy. Int J Biometeorol 55:87–96

D'Odorico P, Yoo JC, Jaeger S (2002) Changing seasons: an effect of the North Atlantic Oscillation? J Clim 15:435–445

Fitter AH, Fitter RSR, Harris ITB, Williamson MH (1995) Relationship between first flowering date and temperature in the flora of a locality in Central England. Funct Ecol 9:55–60

Gimeno L, Ribera P, Iglesias R, de la Torre L, Garcia R, Hernandez E (2002) Identification of empirical relationships between indices of ENSO and NAO and agricultural yields in Spain. Clim Res 21:165–172

Gormsen AK, Hense A, Toldam-Andersen TB, Braun P (2005) Large-scale climate variability and its effects on mean temperature and flowering time of Prunus and Betula in Denmark. Theor Appl Climatol 82:41–50

Gouveia C, Trigo RM (2008) Influence of climate variability on wheat production in Portugal. In: Soares A, Pereira MJ, Dimitrakopoulos R (eds) geoENV VI – geostatistics for environmental applications. Springer, Berlin, pp 335–345

Gouveia C, Trigo RM, Da Camara CC, Libonati R, Pereira JMC (2008) The North Atlantic Oscillation and European vegetation dynamics. Int J Climatol 28:1835–1847

Grifoni D, Mancini M, Maracchi G, Orlandini S, Zipoli G (2006) Analysis of Italian wine quality using freely available meteorological information. Am J Enol Vitic 57:339–346

Hurrell JW, Kushnir Y, Ottersen G, Visbeck M (eds) (2003) The North Atlantic Oscillation: climatic significance and environmental impact. Geophys Monogr 134:1–35. Copyright 2003 by the American Geophysical Union 10.1029/134GM01

Hurrell JW, Van Loon H (1997) Decadal variations in climate associated with the North Atlantic Oscillation. Clim Change 36:301–326

Jones PD, Jonsson T, Wheeler D (1997) Extension to the North Atlantic Oscillation using early instrumental pressure observations from Gibraltar and South-West Iceland. Int J Climatol 17:1433–1450

Kettlewell PS, Sothern RB, Koukkari WLJ (1999) U.K. wheat quality and economic value are dependent on the North Atlantic Oscillation. J Cereal Sci 29:205–209

Kettlewell PS, Stephenson DB, Atkinson MD, Hollins PD (2003) Summer rainfall and wheat grain quality: relationships with the North Atlantic Oscillation. Weather 58:155–164

Klaveness D, Wielgolaski FE (1996) Plant phenology in Norway – a summary of past and present first flowering dates (FFDs) with emphasis on conditions within three different areas. Phenol Season 1:47–61

Menzel A (2003) Plant phenological anomalies in Germany and their relation to air temperature and NAO. Clim Change 57:243–263

Nordli Ø, Wielgolaski FE, Bakken AK, Hjeltnes SH, Måge F, Sivle A, Skre O (2008) Regional trends for bud burst and flowering of woody plants in Norway as related to climate change. Int J Biometeorol 52:625–639

Post E, Stenseth NC (1999) Climatic variability, plant phenology, and northern ungulates. Ecology 80:1322–1339

Riou C (1994) The effect of climate on grape ripening: application to the zoning of sugar content in the European Community. European Commission, Brussels, 319 pp

Sivle A (2005) Climatic oscillations in the period 1910–2004 (in Norwegian). Geophysical Institute, University of Bergen, Bergen

Vose RS, Menne MJ (2004) A method to determine station density requirements for climate observing networks. J Clim 17:2961–2971

Wanner H, Bronnimann S, Casty C, Gyalistras D, Luterbacher J, Schmutz C, Stephenson DB, Xoplaki E (2001) North Atlantic Oscillation – concepts and studies. Surv Geophys 22:321–381

World Meteorological Organization (1981) Guide to agricultural meteorological practices, 2nd edn. Secretariat of World Meteorological Organization, Geneva

The Impacts of the NAO on the Vegetation Activity in Iberia

Célia Gouveia and Ricardo M. Trigo

Abstract The present study analyses the relation between North Atlantic Oscillation (NAO) and satellite-based measures of vegetation dynamics (as obtained using Normalized Difference Vegetation Index, NDVI), carbon absorption by living plants (obtained by Net Primary Production, NPP estimates) over Iberian Peninsula and wheat yield in Portugal. There is a strong evidence that positive (negative) values of winter NAO induce low (high) vegetation activity in the following spring and summer seasons. Consequently, significant correlations patterns between NAO and NPP were also obtained, identifying a negative impact in spring and summer over southern Iberia. These features are mainly associated with the impact of NAO on winter precipitation, together with the strong dependence of the spring and summer vegetation activity on water availability during the previous winter. The different role played by NAO along the vegetative cycle of wheat yield in Portugal is also assessed and results obtained suggest using spring NDVI together with NAO in April and June to build up a simple model of wheat yield in Portugal. Results reveal to be satisfactory and are expect to be useful to estimate crop production and to perform agricultural monitoring.

Keywords NAO · Vegetation activity · NDVI · NPP · Wheat yield

1 Introduction

Recent global changes in vegetation dynamics have been continuously monitored from space and, additionally, significant connections with changes of surface climatic variables, such as temperature and precipitation, have been established (Myneni et al., 1997; Zhou et al., 2001; Nemani et al., 2003). In particular, the observed increment in temperature during spring and autumn over high latitude regions of the Northern Hemisphere leads to higher photosynthetic activity and larger growing seasons (Groisman et al., 1994; Boagert et al., 2002; Shabanov

C. Gouveia (✉)
Faculty of Sciences, Instituto Dom Luiz (IDL), University of Lisbon, Lisbon, Portugal; EST, Polytechnic Institute of Setubal, Setúbal, Portugal
e-mail: cmgouveia@fc.ul.pt

S.M. Vicente-Serrano, R.M. Trigo (eds.), *Hydrological, Socioeconomic and Ecological Impacts of the North Atlantic Oscillation in the Mediterranean Region*, Advances in Global Change Research 46, DOI 10.1007/978-94-007-1372-7_9,

et al., 2002). However, whereas in spring photosynthesis dominates respiration, the opposite takes place in autumn and therefore it is in spring that an increase in CO_2 sequestration is expected to occur (Piao et al., 2008). Accordingly, in a future warmer world, carbon sequestration capacity by northern hemisphere ecosystems may decrease faster than previously suggested due to a faster warming in autumn than in spring (Sitch et al., 2008). Nevertheless, changes in the seasonality of temperature and precipitation may have distinct impacts, depending on local characteristics. The strong dependence of vegetation dynamics on water availability in the Mediterranean regions has been now widely recognized (e.g. Gouveia et al., 2009; Vicente-Serrano, 2007; Lindner et al., 2010). It has been showed that the lack of precipitation over a certain period, combined with other climatic anomalies, such as high temperature, strong wind and low relative humidity over a particular area, may result in reduced green vegetation cover.

The above mentioned changes in the vegetation annual cycle can be detected, using satellite information, namely from observed changes in the most widely used vegetation-related satellite variable, the Normalised Difference Vegetation Index (NDVI) (Stöckli and Vidale, 2004; Vicente-Serrano and Heredia-Laclaustra, 2004). However, there is a strong need of long term studies of the impact of atmospheric circulation variability on vegetation greenness. In this context, special attention has been devoted to study the links between vegetation dynamics and the North Atlantic Oscillation (NAO). D'Odorico et al. (2002) showed that spring phenology and timing of pollen season in British Isles, Poland, Norway and Sardinia are influenced by NAO, with leaf unfolding occurring later (earlier) for negative (positive) phases of NAO. Stöckli and Vidale (2004) found that spring phenology over Europe, as obtained using AVHRR Pathfinder NDVI data, correlates well with anomalies in winter NAO index, as well as in winter temperature. More recently, Maignan et al. (2008) showed the strong impact of NAO on the vegetation onset over a large fraction of Northern Europe. The pattern of the NAO control on the vegetation dynamics is clearly apparent over a large extension of Europe revealing in general an evident North–South gradient.

On a more regional context, Vicente-Serrano and Heredia-Laclaustra (2004) analysed the NAO control on Iberian vegetation productivity trends, as represented by the annual integral of monthly AVHRR Pathfinder NDVI values. The NAO impact revealed to be stronger in southern Iberia that corresponds to areas of stable or decreasing vegetation productivity. On the other hand the NAO impact on vegetation greenness is weaker in the north of the peninsula, over areas where significant positive productivity trends occur. Gouveia et al. (2008) expanded the analysis on the relationship between vegetation greenness and NAO to the entire Europe. The authors relate the different vegetation behaviours particularly over Iberian Peninsula and Northeastern Europe, with a strong dependence of vegetation dynamics from water availability in Iberia and from winter temperature in Northeastern Europe.

Terrestrial Net Primary Production (NPP) is a measure of the amount of carbon fixed by the living plants and converted into plant biomass. Nemani et al. (2003) showed that changes in climate, related to increasing temperature and solar radiation, have eased several critical constrains to plant growth, leading to an upward

trend in global NPP from 1982 to 1999. However, they have also shown that NPP respond differentially with respect to latitude to major climate events, such as volcanic eruptions and El Niño episodes. Globally, NPP decreases during the three major El Niño events (particularly over tropical regions), while the decrease after Mount Pinatubo eruption was mostly restricted to northern hemisphere high latitudes. Recently, Zhao and Running (2010) showed that large-scale droughts have reduced NPP during the last decade, imposing a drying trend for the entire southern hemisphere, whereas an increased NPP can be found over the majority of the northern hemisphere.

Finally, climate is a key factor for the majority of agricultural systems, due to their dependence on interannual climate variability and in particular, their vulnerability to extreme events such as; droughts, floods and frost or hail occurrences. Important relations between regional distributions of temperature and precipitation and wheat yield for the European countries have been found (Cantelaube et al., 2004). In particular the winter NAO index has been associated with UK wheat crop and with better wheat, rye, oat and citrus yields in the Iberian Peninsula (Atkinson et al., 2005; Gimeno et al., 2002). Although not directly related to NAO, some authors have analysed in detail the links to climate variables that are ultimately related to this mode of variability. Iglesias and Quiroga (2007) evaluated over five sites in Spain the effects of climate variability on the final crop. Similarly drought indices and remote-sensed data were used to predict wheat and barley yields in the Ebro valley (Vicente-Serrano et al., 2006). Rodríguez-Puebla et al. (2007) have derived a model that integrates the effects of abundant precipitation together with dynamic aspects of the air masses during the maturation in order evaluate their effects on winter cereals productivity in Spain.

1.1 Objectives

Here we intend to provide a comprehensive assessment on the impact of NAO on various vegetation related variables, namely NDVI, NPP and crop yields. While some of these analyses were initially performed for other regions in northern Europe we opted here to focus only on the western Mediterranean sector.

1.2 Data

A number of restrictions on access to different types of dataset implied slightly distinct periods of analysis. The NPP monthly estimates were obtained in the frame of a Portuguese funded project entitled CARBERIAN, using the Carnegie Ames Stanford Approach (CASA) terrestrial biogeochemical model (Potter et al., 1993; Friedlingstein et al., 1999) for the period 1982–1999. The CASA simulates plant and soil processes allowing the estimation of both NPP and NEP (Net Ecosystem Productivity). Besides climate variables (precipitation, temperature and radiation)

the model incorporates information from vegetation and land cover types using satellite data, as well as soil texture and soil depth (Seixas et al., 2009).

The NDVI monthly anomalies, with 8 km of spatial resolution, were obtained from the Global Inventory Modeling and Mapping Studies (GIMMS) dataset. This dataset holds 24 values per year (i.e. twice a month) and corresponds to the most complete and longest remote sensing dataset covering the entire Mediterranean region. In the case of the assessment of the NAO impact on vegetation dynamics we have performed the analysis for the period 1982–2002. Finally, the evaluation of the NAO impact on Portuguese crop yields covers the period spanning between 1982 and 2005.

The NAO index used in this study is based on the one developed by the Climatic Research Unit (CRU), which was originally defined, on a monthly basis, as the difference between the normalized surface pressure at Gibraltar, in the southern tip of the Iberian Peninsula and Stykkisholmur, in Iceland (Jones et al., 1997). For each year covering the above mentioned periods, we have derived a late winter NAO index (hereafter referred only as NAO), defined as the average of the monthly values for January, February and March of the corresponding year.

2 Results

2.1 NAO and Vegetation Dynamics

Figure 1 displays the spatial patterns over Iberia of point correlation values of winter NAO and NDVI for spring ($NDVI_{MAM}$), summer ($NDVI_{JJA}$) and autumn ($NDVI_{SON}$) for the period between 1982 and 2002. Results show a negative correlation over the Iberian Peninsula in spring and summer, with some values reaching as low as –0.8. Positive correlations are found in northern and eastern Iberia, as well as in Murcia region in spring (values around 0.7). However in summer the positive

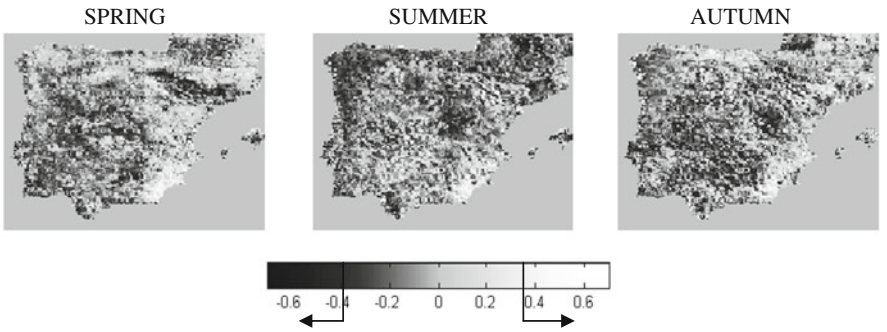

Fig. 1 Point correlation fields of NAO vs. $NDVI_{MAM}$ (*left panel*) and NAO vs. $NDVI_{JJA}$ (*middle panel*) and NAO vs. $NDVI_{SON}$ (*right panel*) for the period from 1982 to 2002. The *colorbar* identifies values of correlation and the *two arrows* indicate the ranges that are significant at 5% level

correlations are restricted to the Murcia region. A weaker pattern of correlations is found during autumn, presenting lower but still significant positive correlation (values around 0.4) spreading over eastern and Northern Iberia and presenting a negative pattern in Southern Iberia. These patterns are in good agreement with those obtained previously in the works of Buermann et al. (2003) and Vicente-Serrano and Heredia-Laclaustra (2004). This behaviour reflects the response of the annual variability of meteorological variables to large-scale atmospheric variability associated to the NAO mode, as well as the different response of vegetation to atmospheric variability, namely the changes induced by temperature and precipitation in the annual cycle of heat and moisture.

It should be stressed that other factors linked to the human influence can disturb the relationship between atmospheric parameters and vegetation, such as the nature and quality of the plant substrate, the over-use of agriculture land and the employment of irrigation (Gouveia et al., 2008). In order to isolate the NAO effect on vegetation dynamics, as obtained by NDVI, from factors related to the human influence, we have compared the NDVI anomalies for two subsets of years associated to extreme NAO indices: (i) higher than usual values of seasonal NAO index (whenever the NAO index is higher than the percentile 75 of its distribution) and (ii) lower than usual (whenever the NAO index is lower than the percentile 75 of its distribution). Figure 2 shows a comparison of seasonal NDVI anomalies for the two subsets of years associated with NAO– (upper panel) and NAO+ (lower panel). In the case of spring NDVI anomalies present well defined pattern over central and western Iberia. The southern anomaly center is particularly intense, positive (negative) anomalies being observed in spring NAO– (NAO+). The pattern is remaining in

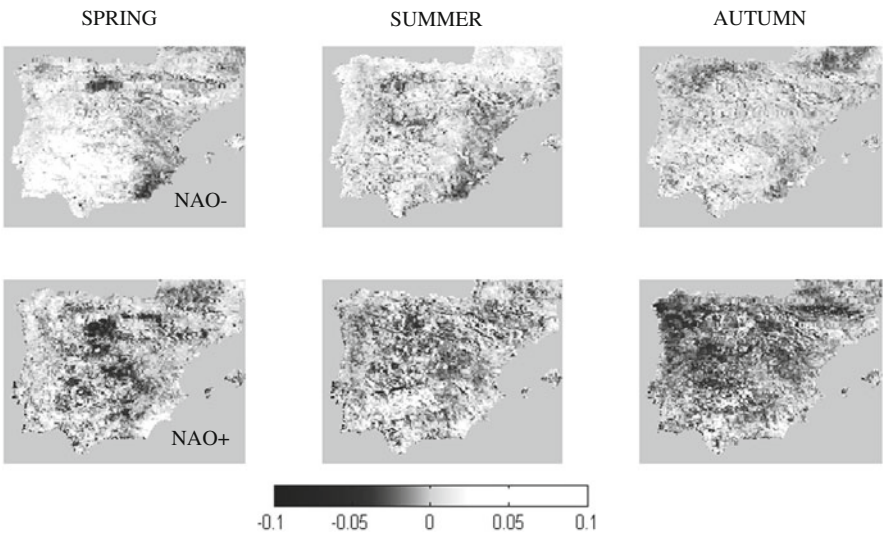

Fig. 2 Seasonal anomalies of NDVI for years of NAO– (*top panel*) and NAO+ (*bottom panel*) for spring (*left*), summer (*middle*) and autumn (*right*)

the following seasons, albeit with lower correlation values. Therefore, it means that for years characterised with positive winter NAO values, the vegetation is in vegetative stress, with lower than usual NDVI values, a feature that is common during drought years, like the recent 2004/2005 drought event (Gouveia et al., 2009).

In fact, Gouveia et al. (2008) have found significant correlations between winter NAO and contemporaneous late winter means of surface temperature and precipitation. For precipitation a well-developed meridional dipolar structure over Europe, delimiting two well-defined zonal bands of positive and negative correlation values along Northern Europe and Mediterranean region respectively. However it is also known that the connection between NAO and temperature over Iberia is not as clear-cut as for precipitation (Castro-Díez et al., 2002; Trigo et al., 2002). Although it is known that the impact of NAO on temperature and precipitation described above is especially prominent in winter (e.g. Vicente-Serrano and Heredia-Laclaustra, 2004; Trigo et al., 2004), such behaviour contrasts with that obtained for vegetation activity (Fig. 1), where the impact of NAO is clearly significant in spring, summer and autumn. Consequently the relationship between late winter temperature and precipitation with vegetation greenness in the following seasons are very important.

Additionally the work of Gouveia et al. (2008) showed that almost two thirds (64%) of the pixels that exhibit the highest (lowest) values of positive (negative) correlations of $NDVI_{MAM}$ and $NDVI_{JJA}$ with NAO correspond to areas of spring crops and about one sixth (17%) to forests and shrublands. The relative proportion of the two types undergoes a significant change in summer with only 29% relative to forest and shrubland, and an increase to 47% associated to cultivated areas. These results reflect the distinct responses of the various land cover types to moisture and heat conditions prevailing during the previous winter.

The Iberian Peninsula presents the same response of vegetation to precipitation in spring and summer, i.e. an increase (decrease) of vegetation greenness for NAO– (NAO+) years. A small dependence of vegetation greenness on temperature is also apparent in the case of spring (Gouveia et al., 2008). Additionally, Gouveia et al. (2008) have emphasized that the impact on precipitation is three times larger over Iberian Peninsula than the corresponding impact over Northern Europe. This feature is consistent with the specific dependence of NDVI on precipitation over Iberia, since vegetation growth is much more water-limited in Iberia than in Northern Europe, where temperature and snow cover play a major role (Trigo et al., 2002; Gouveia et al., 2008).

The remarkable differences in the response of vegetation to moisture and heat conditions, lead us to analyse the NDVI annual cycle for the highest (lowest) values of positive (negative) correlations of $NDVI_{MAM}$ and $NDVI_{JJA}$ with NAO over Iberia. Figure 3 shows the annual cycles of NDVI monthly values for the highest (lowest) values of positive (negative) correlations of $NDVI_{MAM}$ and $NDVI_{JJA}$ with winter NAO, for spring (left panel) and summer (right panel). The annual cycles of averages for the NAO+ (NAO–) subsets are identified by the thin solid (dashed) curves, while the annual cycles of mean NDVI for the entire period (1982–2002) are represented by thick solid lines.

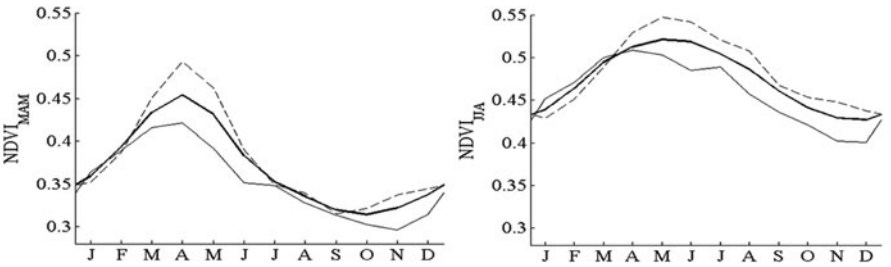

Fig. 3 Annual cycles of monthly values of NDVI for the highest (lowest) values of positive (negative) correlations of $NDVI_{MAM}$ and $NDVI_{JJA}$ with winter NAO, for spring (*left panel*) and summer (*right panel*), over Iberia. The annual cycles of averages for the NAO+ (NAO–) subsets are identified by the *thin solid (dashed) curves* and the annual cycles of mean NDVI for the entire period (1982–2002) are represented by *thick solid lines*

The highest impact of NAO is observed to occur during the periods of the year characterised by more intense vegetation activity (Ji and Peters, 2003), i.e. around April (June) in the case of highest correlated pixels for spring (summer). In the case of spring vegetation, two thirds of the pixels correspond to cultivated areas that are mostly associated to non irrigated crops, adapted to the relatively dry Iberian conditions. Vegetation has a short growth cycle, due to the generally observed high temperatures, starting as soon as water is available. This is a typical situation that can be favoured by NAO–. In the case of summer, the growing period of the most impacted vegetation starts later and therefore the response to precipitation tends to extend late in the year (Gouveia et al., 2008).

2.2 NAO and NPP Estimates

Figure 4 displays the spatial patterns over Iberia of point correlation values of winter NAO (NAO_{JFM}) and NPP for spring (NPP_{MAM}), summer (NPP_{JJA}) and autumn (NPP_{SON}) for the period between 1982 and 1999. This slightly shorter period results from the limited period of available data obtained with the CASA model by our colleagues within the CARBERIAN project that started in the early 2000s. Results show a negative correlation between NAO and NPP over the Iberian Peninsula in spring and summer, with values as low as –0.7 (Fig. 4, top panel). Positive correlations are found in northern and eastern Iberia and Northwestern Portugal. The highest positive correlations (values around 0.6) are found in Pyrenees and in coastal Mediterranean region of Murcia in spring. However in summer the positive correlations are mostly restricted to the Murcia region. A weaker pattern of correlations is found during autumn, presenting lower but still significant positive correlation (values around 0.4) spreading over eastern and Northern Iberia, Murcia region and southern Portugal. Interesting to notice the strong pattern of negative correlations located in the Southern interior of Iberia.

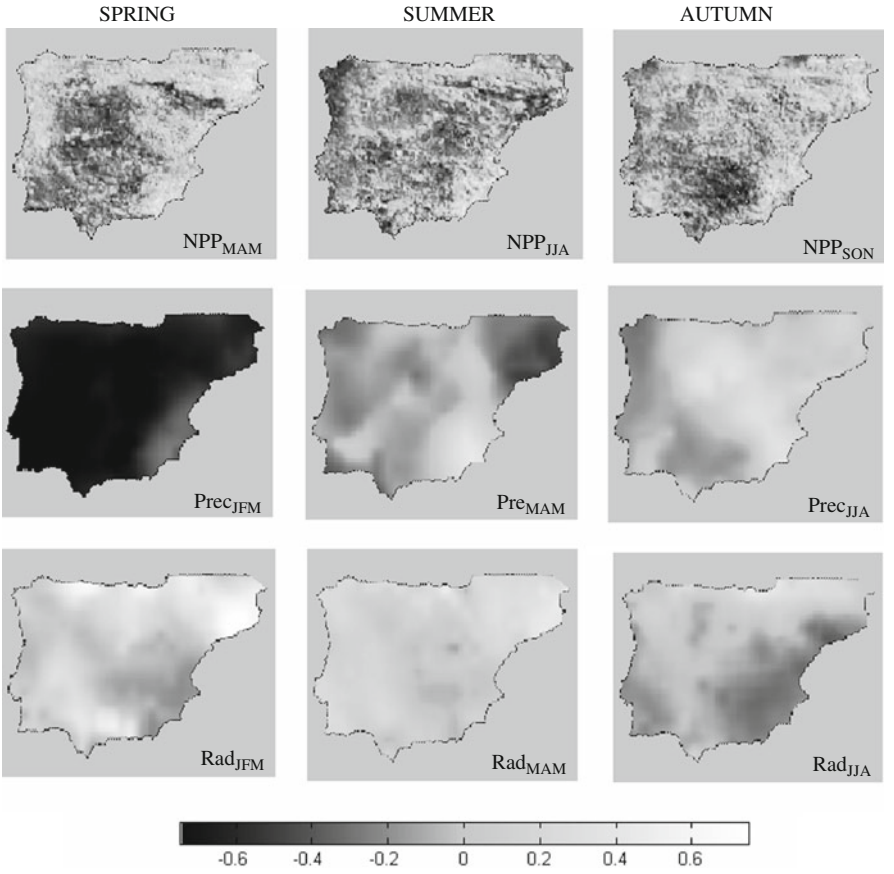

Fig. 4 Correlation fields of NAO vs. NPP, for spring (*left panel*), summer (*middle panel*) and autumn (*right panel*) over the period from 1982 to 1999 (*top panel*) and NAO vs. Precipitation (*middle panel*) and NAO vs. short wave radiation (*bottom panel*), for winter (*left panel*), spring (*middle panel*) and summer (*right panel*) over the period from 1982 to 1999

The impact of NAO in the previous winter, as well as in spring and summer in precipitation and short wave radiation is also provided in Fig. 4 (middle and bottom panels, respectively). As expected the negative pattern of correlations between NAO and NPP in spring is highly related to the corresponding impact of NAO on winter precipitation and short wave radiation. Thus, during the years characterised with a positive NAO mode in winter, lower precipitation and higher short-wave radiation (and fewer clouds) can be observed in the central Iberia, corresponding to lower NPP estimates. These results are in good agreement with the works of Nemani et al. (2003) and Zhao and Running (2010). This behaviour reflects the response of short-rooted grassland and croplands characteristic of the northern mid-latitudes, where water availability is a dominant control for plant growth. Accordingly to the analysis

undertaken by the above mentioned authors, NPP has a significant positive correlation with both total precipitation and Palmer Drought Severity Index (PDSI), which means that higher precipitation values and consequently lowers than usual NAO values, usually lead to higher NPP estimates. This result is compatible with the negative values of correlations between winter NAO and NPP that are prevailing during spring, summer and autumn. The exceptions for this behaviour are the forest areas typical over the Northwestern Iberia and higher altitude mountains in Pyrenees, that are more insensitive to precipitation and temperature and also the Murcia region where the NAO plays a negligible role.

The above mentioned differences in the response of vegetation to moisture and heat conditions prompted the analysis of the evolution (for NAO+ and NAO–) of NPP annual cycles for two sites over Iberia, used to calibrate and validate the CASA Model over Iberia (Seixas et al., 2009). Figure 5 (left panel) shows the annual cycles of monthly NPP for the above selected sites. The two selected sites correspond to two contrasting situations; one site being characterised mainly by negative correlation between NAO and NPP estimates located in the south of Iberia (site 1 in Fig. 5, top panel) while the other is characterised by positive correlations located in the North of Iberia (site 2 in Fig. 5, bottom panel). Moreover, while site 1 presents a maximum of NPP estimates during spring and site 2 corresponds to pixels with a maximum of NPP estimates during summer. Figure 5 (left panel) shows the annual cycles of NPP monthly anomalies for the above selected sites.

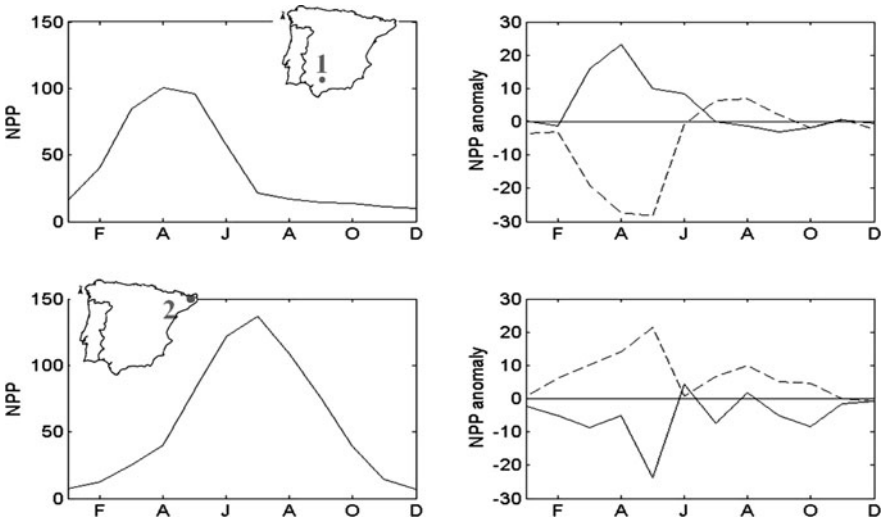

Fig. 5 *Left panel*: Annual cycles of monthly NPP estimates for site 1 located in the south of Iberia (*top panel*) and a site 2 located in the north of Iberia (*bottom panel*). *Right panel*: corresponding annual cycles of monthly anomalies of NPP estimates for the NAO– (*thin solid line*) and NAO+ (*thin dashed line*) subsets over site 1 (*top panel*) and site 2 (*bottom panel*)

The annual cycles of NPP anomalies for the NAO– (NAO+) subsets are identified by the thin solid (dashed) curves. The highest impact of NAO is observed to occur during spring and also in summer in the case of site 2. Differences in topography should be taken into account, as site 1 corresponds to low altitude areas while site 2 is located in a mountainous region. Moreover there are disparities in the main vegetation type characteristic of these sites; while site 1 are mainly grasses, cereal crops, site 2 is dominated by needleleaf forest. During years characterized by positive winter NAO, NPP estimates present low values during spring over site 1. This situation corresponds to years with considerably lower (higher) than usual precipitation (short wave radiation) that may inhibit the vegetation greenness and consequently low NPP estimates. This is the typical situation during drought events (García-Herrera et al., 2007). In the case of mountainous areas (site 2) where the vegetation activity is not dependent of the scarcity of water in part due to the lower temperature, the NPP estimates are relatively high during spring and even during summer although with relatively lower values than in spring. These features are in good agreement with the previously mentioned authors that related the climate variability and the carbon absorption from living plants (Nemani et al., 2003; Zhao and Running, 2010).

2.3 NAO and Wheat Yield

In order to quantify the climate impact on the wheat yield in Portugal it must be stressed that it is considerably smaller than the corresponding wheat yield obtained in the North-western European countries, with cold (but not too wet) winters and relatively wet summers (Gouveia and Trigo, 2008). During the grain filling until the complete grain ripening phase, the Mediterranean conditions may even get worse, due to the short period of time between frost episodes and relatively high temperatures at the end of spring (May/June). Another adverse situation, especially when compared with the same period for North-western European countries, consists in the low photoperiod (number of sun hours) and the high temperatures, which may occur at the end of the maturation phase. During this phase large values of potential evapotranspiration may lead to weak photosynthetic activity, since the plant mostly spends most of energy in the transpiration process in order to offset the warm season effects, thus reducing its capacity to produce dry matter. An excess of evapotranspiration may therefore lead to a decrease of wheat quality (Gouveia and Trigo, 2008).

In order to evaluate the seasonal evolution of the correlation between NAO and wheat yield we have performed a monthly evaluation (Table 1) reflecting the different role played by NAO along the vegetative cycle of wheat. In fact, the contrast between late winter/early spring and late spring/early summer is well apparent, with low correlations between NAO and yield in January to March being replaced by positive correlations for April and June (the last one significant at the 5% level). The role of NAO in June appears to be related to the need of warm temperatures during the wheat maturation phase, and simultaneously the absence of precipitation.

Table 1 Correlation coefficient values between annual wheat yield and monthly NAO (from January to June) for the pixels coded as arable land not irrigated. Bold values highlighted when significant at the 5% level

	Jan	Feb	Mar	Apr	May	Jun
NAO	0.06	0.08	–0.04	0.27	–0.06	**0.53**

The first and simplest assessment on the NAO effective impact on wheat production is shown in Fig. 6 (top panel) that depicts the inter-annual evolution of the NAO during April and June (NAO_{AJ}) and detrended wheat yield, considering the 24 year period between 1982 and 2005, presenting a correlation value of 0.49. With the aim of isolating the effect NAO on annual wheat yield from human-related factors we adopted the methodology described in Section 2.1, comparing the detrended wheat yield for two subsets of years associated to extreme NAO indices: (i) higher than usual values of seasonal NAO index (NAO > percentile 75) and (ii) lower than usual (NAO lower than percentile 25). Figure 6 (lower panel) shows a comparison of annual wheat yield for the three subsets of years associated with NAO+, NAO– and intermediate class. Generally speaking, years presenting positive (negative) anomalies for wheat yield are usually characterized by positive (negative) NAO index values in late spring. Therefore, it is possible to confirm that late spring correspond to an important moment for the wheat vegetative cycle in Portugal and that the NAO index controls, at least partially, what is happening in this moment of the vegetative cycle.

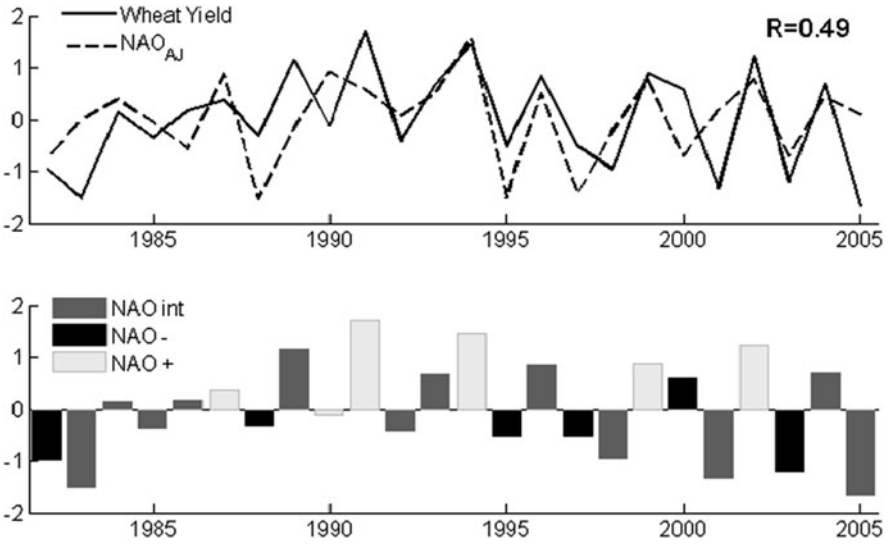

Fig. 6 *Top panel*: Inter-annual variability of spring NAO Index (*dashed line*) and wheat yield over the period 1982–2005. *Bottom panel*: Inter-annual evolution of annual wheat yield for years characterised by NAO_{AJ}+, NAO_{AJ}– and intermediate subsets

In summary, a good wheat yield usually corresponds to years characterized by positive NAO values in spring, particularly in April and June. This behaviour may be viewed as reflecting the integrated impact on radiation, temperature and precipitation fields of the large scale atmospheric circulation patterns associated to the different phases of NAO. The role of NAO in June could be especially related to the necessity of warm temperatures during the maturation phase of wheat.

Figure 7 (left panel) shows the grid point correlations between spring NDVI composites ($NDVI_{MAM}$) and detrended wheat yield, considering the 24 year period between 1982 and 2005. The highest positive and significant correlations (at the 1% level) are found over the southern region of Alentejo (Fig. 7, left panel). The analysis was restricted to the set of pixels that were coded, using Corine Land Cover Map (CLC2000) as non irrigated arable land. The average of spring NDVI for this subset of pixels holds a correlation value of 0.70 (significant at the 1% level). Results obtained above suggest using spring NDVI together with late spring NAO to build up a simple model of wheat yield for Portugal for the period 1982–2005. Spring NDVI is an indicator of the healthiness of wheat during the growing stage which in turn reflects the meteorological conditions in terms of radiation, temperature and

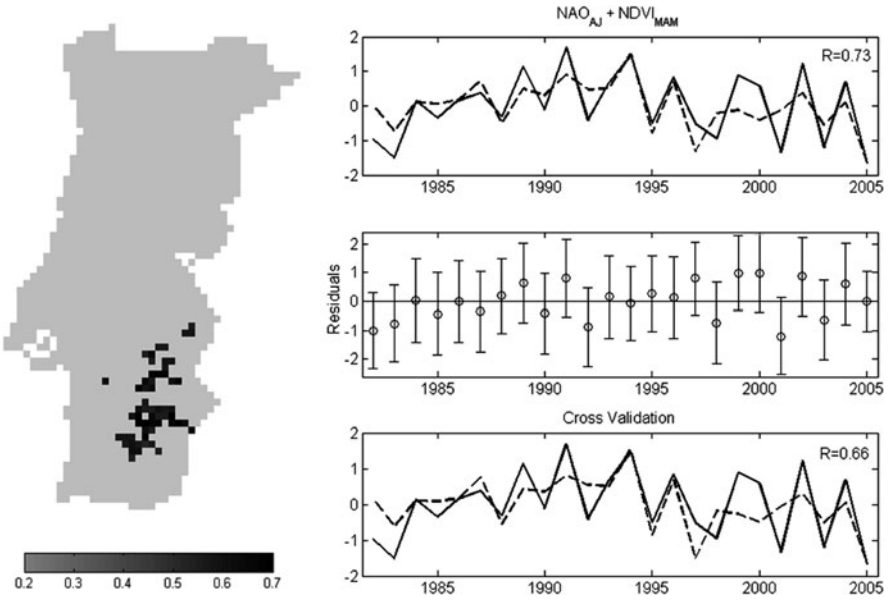

Fig. 7 *Left panel*: Patterns of simple correlation between spring NDVI composites and wheat yield in Portugal, for the period of 1982–2005, for pixels coded as arable land non-irrigated and significant at the 1% level. *Right panel*: Time series (1982–2005) of observed (*dark curve*) wheat yield in Portugal and of corresponding modelled values (*dashed curve*) when using a linear regression model based on spring NDVI and NAO in April and June (*upper panel*). Time series (1982–2005) of residuals and respective 95% level confidence intervals (*central panel*). Time series (1982–2005) of observed (*dark curve*) wheat yield in Portugal and of corresponding modelled values (*dashed curve*) as obtained from the leave-one-out cross-validation procedure

precipitation regimes. On the other hand late spring NAO is an indicator of the large-scale circulation affecting Portugal which in turn is related to regional conditions in terms of radiation, temperature and precipitation that have an important role in the wheat maturation process.

In fact a simple multi-linear regression model was calibrated and validated for the 24-year period of available data, using as predictors the spring $NDVI_{MAM}$ together with NAO_{AJ}. Figure 7 (right-upper panel) presents the time series of observed and modeled wheat yield. The overall agreement is worth being noted, with the two time-series presenting a correlation of 0.73. Figure 7 (right-central panel) shows the time series of residuals, defined as departures of observed values from modeled ones. The 95% confidence intervals relative to these residuals are plotted as error bars and it may be noted that there is not presenting any outlier since its error bar does not cross the zero reference line. Simple calibration approaches, using the entire period of available data, can lead to misleading results, namely over-fitting (Wilks, 2006). Therefore it is advisable to use more robust validation approaches, such as the leave-one-out cross validation (Fig. 7, right-lower panel). The good agreement between the modelled time series by the regression model (upper panel) and the one obtained by the cross validation indicate that the developed model is relatively robust with only a slight decrease (from 0.73 to 0.66) on the correlation between original and modelled time series. In summary, these results are statistically robust but also physically sound, revealing a very satisfactory performance and are expect to be useful to estimate crop production as well as to perform agricultural monitoring.

3 Conclusions

The behaviour of vegetation reflects the different response of surface climate to large-scale atmospheric variability associated to the NAO mode. Over Iberia there is strong evidence that positive (negative) values of winter NAO induce low (high) vegetation activity in the following spring and summer seasons. This feature is mainly associated with the impact of NAO on winter precipitation, together with the strong dependence of spring and summer NDVI on contemporary water availability. It is also related with the strong impact of climate variability in semi-arid areas, namely regarding effects of drought conditions on vegetation activity (Vicente-Serrano and Heredia-Laclaustra, 2004), in particular during the intense spring vegetation growth period.

In Iberia the NAO impact is greater on non-forested vegetation which responds rapidly to spatio-temporal variations in precipitation and soil moisture. During summer, forests and other dense vegetation areas display the highest sensitivity to NAO dynamics, as this type of vegetation shows slower response to precipitation, and therefore the NAO impacts are delayed until late in the year. Consequently, the NAO impact negatively on NPP estimates in southern and central Iberia and positively over the Northern mountainous areas. In fact, in Iberia the NAO impacts negatively the short-rooted grassland and croplands which responds rapidly to spatio-temporal

variations in precipitation and soil moisture. This type of vegetation is very sensitive to drought events.

It should be stressed that our lagged relationships between winter NAO and NDVI values for spring, summer and autumn already represent an added value since they allow formulating, by the end of March, simple outlooks of vegetation greenness for certain land cover types over the Iberian Peninsula that may provide useful information for a wide range of applications, including long-lead wildfire risk assessment and crop forecasts. It is within this context that we have evaluated the impact of NAO on cereal production over a specific region of Iberia with sufficient data. Accordingly, a strong negative correlation (range from 0.6 to 0.8) between NDVI and wheat yield for the 24 year-long period 1982–2005, over the southern part of Portugal (Alentejo) was obtained. A good year for wheat yield is usually characterized by positive NAO values for late spring. To obtain a good wheat yield, the NAO index signal in late spring should be positive, inducing higher values of short wave radiation and lower values of precipitation in the Iberian Peninsula. The low precipitation wheat requirements in this period allow a slow maturation to origin well formed grains and avoid the pests development and potential decrease of the wheat quality as mentioned before.

Acknowledgements This work was supported by the Portuguese Science Foundation (FCT) through project ENAC (Evolution of North Atlantic Climate; the role of Blocking and Storm-tracks in the Past, Present and Future climate of Southern Europe) PTDC/AAC-CLI/103567/2008. The authors would like to thank J. Seixas and N. Carvalhais for the NPP dataset derived in the frame of CARBERIAN project. The wheat yield was provided by Portuguese Statistical Institute (INE). The NDVI dataset was kindly supplied by Global Inventory Modeling and Mapping Studies (GIMMS, http://glcf.umiacs.umd.edu/data/gimms/) project.

References

Atkinson MD, Kettlewell PS, Hollins PD, Stephenson DB, Hardwick NV (2005) Summer climate mediates UK wheat quality response to winter North Atlantic Oscillation. Agri Forest Meteorol 130:27–37

Bogaert J, Zhou L, Tucker CJ, Myneni RB, Ceulemans R (2002) Evidence for a persistent and extensive greening trend in Eurasia inferred from satellite vegetation index data. J Geophys Res 107:4119. doi:10.1029/2001JD00107

Buermann W, Anderson B, Tucker CJ, Dickinson RE, Lucht W, Potter CS, Myneni RB (2003) Interannual covariability in Northern Hemisphere air temperatures and greenness associated with El Niño-southern oscillation and the Arctic Oscillation. J Geophys Res 108:4396. doi:10.1029/2002JD002

Cantelaube P, Terres J-M, Doblas-Reyes FJ (2004) Influence of climate variability on European agriculture – analysis of winter wheat production. Clim Res 27:135–144

Castro-Díez Y, Pozo-Vázquez D, Rodrigo FS, Esteban-Parra MJ (2002) NAO and winter temperature variability in southern Europe. Geophys Res Lett 29:1160. doi:10.1029/2001GL014042

D'Odorico P, Yoo JC, Jaeger S (2002) Changing seasons: an effect of the North Atlantic Oscillation? J Clim 15:435–445

Friedlingstein P, Joel G, Field CB, Fung IY (1999) Toward an allocation scheme for global terrestrial carbon models. Glob Change Biol 5:755–770

García-Herrera R, Paredes D, Trigo RM, Trigo IF, Hernández E, Barriopedro D, Mendes MA (2007) The outstanding 2004/05 drought in the Iberian Peninsula: associated atmospheric circulation. J Hydrometeorol 8:483–498

Gimeno L, Ribera P, Iglesias R, Torre L, Garcia R, Hernández E (2002) Identification of empirical relationships between indices of ENSO and NAO and agricultural yields in Spain. Clim Res 21:165–172

Gouveia C, Trigo RM (2008) Influence of climate variability on wheat production in Portugal. In: Soares A, Pereira MJ, Dimitrakopoulos R (eds) geoENV VI – geostatistics for environmental applications. Springer, Berlin, pp 335–345

Gouveia C, Trigo RM, DaCamara CC (2009) Drought and vegetation stress monitoring in Portugal using satellite data. Nat Hazards Earth Syst Sci 9:185–195

Gouveia C, Trigo RM, DaCamara CC, Libonati R, Pereira JMC (2008) The North Atlantic Oscillation and European vegetation dynamics. Int J Climatol 28:1835–1847

Groisman PY, Karl TR, Knight RW (1994) Observed impact of snow cover on the heat balance and the rise of continental spring temperatures. Science 263:198–200

Iglesias A, Quiroga S (2007) Measuring the risk of climate variability to cereal production at five sites in Spain. Clim Res 34:47–57

Ji L, Peters AJ (2003) Assessing vegetation response to drought in the northern Great Plains using vegetation and drought indices. Rem Sens Environ 87:85–98

Jones PD, Jónsson T, Wheeler D (1997) Extension to the North Atlantic Oscillation using early instrumental pressure observations from Gibraltar and south-west Iceland. Int J Climatol 17:1433–1450

Lindner M, Maroshek M, Netherer S, Kremer A, Barbati A, García-Gonzalo J, Seidl R, Delzon S, Corona P, Kolström M, Lexer M, Marchetti M (2010) Climate change impacts, adaptive capacity and vulnerability of European forest ecosystems. Forest Ecol Manag 259:698–709

Maignan F, Bréon F-M, Bacour C, Demarty J, Poirson A (2008) Interannual vegetation phenology estimates from global AVHRR measurements: comparison with in situ data and applications. Rem Sens Environ 112:496–505

Myneni RB, Keeling CD, Tucker CJ, Asrar G, Nemani RR (1997) Increase plant growth in the northern high latitudes from 1981–1991. Nature 386:698–702

Nemani RR, Keeling CD, Hashimoto H, Jolly WM, Piper SC, Tucker CJ, Myneni RB, Running SW (2003) Climate-driven increases in global terrestrial net primary production from 1982 to 1999. Science 300:1560–1563

Piao S, Ciais P, Friedlingstein P, Peylin P, Reichstein M, Luyssaert S, Margolis H, Fang J, Barr A, Chen A, Grelle A, Hollinger DY, Laurila T, Lindroth A, Richardson AD, Vesala T (2008) Net carbon dioxide losses of northern ecosystems in response to autumn warming. Nature 451: 49–52

Potter CS, Randerson JT, Field CB, Matson PA, Vitousek PM, Mooney HA, Klooster SA (1993) Terrestrial ecosystem production – a process model-based on global satellite and surface data. Global Biogeochem Cycles 7:811–841

Rodríguez-Puebla C, Ayuso SM, Frias MD, Garcia-Casado LA (2007) Effects of climate variation on winter cereal production in Spain. Clim Res 34:223–232

Seixas J, Carvalhais N, Nunes C, Benali A (2009) Comparative analysis of MODIS-FAPAR and MERIS-MGVI datasets: potential impacts on ecosystem modeling. Rem Sens Environ 113:2547–2559

Shabanov NV, Zhou L, Knyazikhin Y, Myneni RB (2002) Analysis of interannual changes in northern vegetation activity observed in AVHRR data during 1981 to 1994. IEEE Trans Geosci Rem Sens 40:115–130

Sitch S, Huntingford C, Gedney N, Levy PE, Lomas M, Piao SL, Betts R, Ciais P, Cox P, Friedlingstein P, Jones CD, Prentice IC, Woodward FI (2008) Evaluation of the terrestrial carbon cycle, future plant geography and climate-carbon cycle feedbacks using five Dynamic Global Vegetation Models (DGVMs). Glob Change Biol 14:2015–2039

Stöckli R, Vidale PL (2004) European plant phenology and climate as seen in a 20-year AVHRR land-surface parameter dataset. Int J Rem Sens 25:3303–3330

Trigo RM, Osborn TJ, Corte-Real JM (2002) The North Atlantic Oscillation influence on Europe: climate impacts and associated physical mechanisms. Clim Res 20:9–17

Trigo RM, Pozo-Vazquez D, Osborn TJ, Castro-Diez Y, Gámis-Fortis S, Esteban-Parra MJ (2004) North Atlantic Oscillation influence on precipitation, river flow and water resources in the Iberian Peninsula. Int J Climatol 24:925–944

Vicente-Serrano SM (2007) Evaluating the Impact of drought using remote sensing in a Mediterranean, semi-arid region. Nat Hazards 40:17–208

Vicente-Serrano SM, Cuadrat-Prats JM, Romo A (2006) Early prediction of crop production using drought indices at different time-scales and remote sensing data: application in the Ebro valley (North–East Spain). Int J Rem Sens 27:511–518

Vicente-Serrano SM, Heredia-Laclaustra A (2004) NAO influence on NDVI trends in the Iberian Peninsula (1982–2000). Int J Rem Sens 25:2871–2879

Wilks DS (2006) Statistical methods in the atmospheric sciences, International Geophysics Series, 2nd edn, vol 59. Academic, New York, NY, 627 pp

Zhao M, Running SW (2010) Drought-induced reduction in global terrestrial net primary production from 2000 through 2009. Science 20:940–943

Zhou L, Tucker CJ, Kaufmann RK, Slayback D, Shabanov NV, Myneni RB (2001) Variations in northern vegetation activity inferred from satellite data of vegetation index during 1981 to 1999. J Geophys Res 106:20069–20083

Direct and Indirect Effects of the North Atlantic Oscillation on Tree Growth and Forest Decline in Northeastern Spain

Jesús Julio Camarero

Abstract NAO effects on tree growth have not been assessed in the Northeastern Iberian Peninsula where: (i) Atlantic (NAO) and Mediterranean influences affect tree growth and (ii) contrasting climatic conditions determine very different forest types. It is hypothesized that positive (negative) values of winter NAO are linked to drier winter conditions and low (high) forest growth on the following spring. To understand the effects of climate and NAO on tree growth, first I quantified the growth responses to monthly and seasonal climatic variables (mean temperature, total precipitation and cloud cover) and NAO indices across a climatic gradient in Northeastern Spain. Dendrochronological methods are used and an extensive tree-ring network (48 sites, 687 trees) based on ten tree species with contrasting habitats and plausibly different growth responses to climate. Then, I focused on the longest tree-ring chronologies to estimate how unstable are the relationships between tree growth and NAO indices. Finally, the resultant findings are applied to understand how NAO has affected climatic variability during the last decades and how this may be related to the recent silver fir (*Abies alba*) decline in the Pyrenees. Climatic variables and NAO indices explained on average 40.1 and 15.9% of the growth variance, respectively. The maximum growth variance (52.1%) explained by NAO indices was found in a *Juniperus thurifera* forest under continental Mediterranean conditions. High NAO values during the previous December were linked to a reduction in precipitation and a low radial growth the following spring, but high February NAO values were also associated with warmer early-spring conditions and enhanced growth. The growth responses to climate and NAO also changed through time. In the case of silver fir, a shift in the positive relationship between growth and NAO indices of the previous winter (November, February) coincided with the triggering of decline in 1986 suggesting an alteration in the growth response to NAO and related climatic variables.

Keywords Atmospheric circulation patterns · Dendrochronology · Forest dieback · *Juniperus thurifera* · Tree ring-width

J.J. Camarero (✉)
ARAID-Instituto Pirenaico de Ecología, Spanish National Research Council (CSIC), Zaragoza, Spain
e-mail: jjcamarero@ipe.csic.es

S.M. Vicente-Serrano, R.M. Trigo (eds.), *Hydrological, Socioeconomic and Ecological Impacts of the North Atlantic Oscillation in the Mediterranean Region*, Advances in Global Change Research 46, DOI 10.1007/978-94-007-1372-7_10,

1 Introduction

Climatic projections foresee strong warming trends and a decrease in rainfall for the Mediterranean region during the twenty-first century (IPCC, 2007). Such tendencies toward drier conditions have been linked to an increasing anticyclonic activity associated with a northward shift of the north Atlantic storm track (Giorgi and Lionello, 2008). Thus, the predicted changes in atmospheric circulation and climatic conditions should affect forest growth in the Mediterranean basin directly through changes in large scale temperature but also indirectly through modifications in atmospheric patterns and proximate local climate factors such as wind patterns and precipitation (Hirschboeck et al., 1996; Girardin and Tardif, 2005).

Large-scale climatic indices may outperform local climatic conditions in explaining variation in ecological processes (Hallett et al., 2004). Such distinct results may be explained by the more spatially and temporally variable associations between local climate data (e.g., monthly temperature means or precipitation sums) and ecological process as compared with large-scale indices which can partially capture these processes giving insights on the underlying mechanisms (Garfin, 1998). However, few studies have assessed the influence of large-scale indices on tree growth in areas subjected to diverse climatic conditions, as is the case of the Iberian Peninsula, where climates range from mild to continental and from humid to semiarid resulting in diverse forest types subjected to different constraints for tree growth (Nahal, 1981).

In the Iberian Peninsula the climatic variability is under the influence of several large-scale atmospheric circulation patterns including the North Atlantic Oscillation (NAO), which is defined by a north-south dipole of sea level pressures and geopotential heights in the North Atlantic region (Hurrell et al., 2003). The NAO variability is related to changes in the position of the Iceland low-pressure and the Azores high-pressure systems, and to modifications in the direction and strength of westerly winds in southern Europe (Hurrell, 1995). The NAO has a strong effect on winter climate over the Iberian Peninsula Iberia where high (low) NAO values in winter are linked to low (high) precipitation (Hurrell and Van Loon, 1997), being these associations particularly strong in western Iberia (Rodó et al., 1997; Rodríguez-Puebla et al., 2001). The NAO does not exert a relevant influence on winter temperature variability in the western Mediterranean Basin (Sáenz et al., 2001).

Spatially heterogeneous and lagged effects of the previous winter NAO on tree growth of the following year have been described in mesic forests from western Spain (Roig et al., 2009; Rozas et al., 2009) and in drier locations from eastern Spain (Bogino and Bravo, 2008). However, few data exist in transitional areas closer to the Mediterranean Sea and subjected to xeric conditions, where the NAO influence on growth might differ as compared with western mesic areas. In this work, it is evaluated if high NAO values (increased westerlies, storms track towards Southern Europe) during the previous winter are linked to a reduction in tree radial growth through lower precipitation and water availability at the beginning of the growing season the following spring. The objectives of this study are: (i) to quantify the growth responses to monthly and seasonal climatic variables (mean temperature,

total precipitation and cloud cover) and NAO indices across a climatic gradient in Northeastern Spain using dendrochronological methods and an extensive tree-ring network (48 sites); (ii) to estimate how unstable are the relationships between tree growth and NAO indices, and (iii) to understand how NAO has affected climatic variability during the last decades and how this may be related to recent silver fir (*Abies alba*) decline episodes. Such decline events were observed in the Spanish Central Pyrenees since the 1980s and showed a marked geographical pattern characterized by a greater abundance of declining forests in more xeric sites from the western Pyrenees than elsewhere (Camarero et al., 2002).

2 Materials and Methods

2.1 Study Sites

In total 687 trees of ten tree species (*Abies alba* Mill., *Fagus sylvatica* L., *Juniperus oxycedrus* L., *Juniperus thurifera* L., *Pinus halepensis* Mill., *Pinus sylvestris* L., *Pinus uncinata* Ram., *Pistacia terebinthus* L., *Quercus faginea* Lam., *Quercus robur* L.) were sampled in 48 forests located in an area of approximately 150,000 km^2 within Northeastern Spain (Table 1). The studied species belong to diverse families (Anacardiaceae, Cupressaceae, Fagaceae, Pinaceae) and the studied forests occupy sites encompassing wide gradients of elevation (340–1800 m) and climatic types (mean annual temperature: 8.3–13.8°C; total annual precipitation: 317–2350 mm).

In Northeastern Spain, the rainfall decreases from north to south and from the coast towards inland sites resulting in diverse climatic conditions (González-Hidalgo et al., 2009). In the study area, Atlantic (e.g., higher winter and spring precipitation derived from the Atlantic storm track) and Mediterranean (e.g., higher autumn precipitation caused by cyclonic influence from the close Mediterranean Sea) influences increase westwards and eastwards, respectively. Such contrasting climatic conditions determine different forest types including Mediterranean coniferous forests growing under semi-arid continental climates (*J. thurifera*, *P. halepensis*), mesic Mediterranean shrub formations (*P. terebinthus*), sub-Mediterranean transitional oak forests (*Q. faginea*), humid temperate forests (*A. alba*, *Q. robur*), and cold mountain conifer forests (*P. sylvestris*, *P. uncinata*). Some of the studied sites corresponded to relict and isolated tree populations as is the case of *Q. robur* in the Moncayo site or *J. thurifera* in the Retuerta de Pina site. Other forests represent ecological limits near the "xeric" limit of the species distribution such as the *F. sylvatica* and *P. sylvestris* forests in the Monrepos site. Finally, the *P. uncinata* population in the Moncayo site was a plantation outside the main Iberian range of the species in the Pyrenees. Most sites are located on marls and limestones, which generate basic soils.

Table 1 Characteristics of the study sites

Species	Site (code)	Latitude (N)	Longitude	Elevation (m)	P (mm)[a]
Quercus robur	Bértiz (QrBE)	43° 09′	1° 36′ W	405	1677
Abies alba	Irati (AaIR)	42° 59′	1° 03′ W	1020	780
Quercus faginea	Luesia (QfLU)	42° 22′	1° 01′ W	950	684
Pinus sylvestris	Luesia (PsLU)	42° 22′	1° 01′ W	920	684
Quercus robur	Moncayo (QrMO)	41° 48′	1° 51′ W	1400	1020
Pinus uncinata	Moncayo (PuMO)	41° 47′	1° 49′ W	1850	1350
Fagus sylvatica	Monrepos (FsMR)	42° 19′	0° 25′ W	1290	1200
Pinus sylvestris	Monrepos (PsMR)	42° 19′	0° 25′ W	1300	1200
Abies alba	Declining sites – Pyrenees (AadPY)[b]	42° 44′	0° 45′ W	1196	1150
Abies alba	Non declining sites – Pyrenees (AanPY)	42° 35′	0° 23′ W	1390	1800
Juniperus oxycedrus	Agüero (JoAG)	42° 18′	0° 47′ W	750	635
Pistacia terebinthus	Mediano (PtME)	42° 19′	0° 14′ E	488	732
Pinus halepensis	Peñaflor (PhPE)	41° 47′	0° 43′ W	345	340
Juniperus thurifera	Peñaflor (JtPE)	41° 47′	0° 43′ W	340	340
Juniperus thurifera	Retuerta de Pina (JtRE)	41° 27′	0° 16′ W	350	395
Juniperus thurifera	Olmedilla (JtOL)	40° 19′	0° 44′ W	1400	700
Juniperus thurifera	Ademuz (JtAD)	40° 04′	1° 15′ W	1518	750

[a]Annual precipitation based on local climatic data and corrected taking into account the site elevation.
[b]Mean values of the referred characteristics were obtained for declining and non-declining sites.

2.2 Field Sampling and Dendrochronological Methods

In each site 8–88 dominant trees were randomly selected and their size (Dbh, diameter at 1.3 m) was measured (Table 2). At least two radial cores per tree were sampled at 1.3 m using a Pressler increment borer. Cores were prepared following standard dendrochronological methods (Fritts, 2001). They were mounted and sanded until tree-rings were clearly visible under a binocular microscope. All samples were visually cross-dated and tree-ring widths were measured to a precision of 0.001 mm using a LINTAB measuring device (Rinntech, Heidelberg, Germany). Cross-dating was evaluated using the program COFECHA (Holmes, 1983).

Each individual series was standardized using a spline function with a 50% frequency response of 32 years to keep high-frequency variability. Standardization involved transforming the measured value into a dimensionless index by dividing it by the expected values given by the spline function. Autoregressive modelling was carried out on each series to remove temporal autocorrelation (Table 2). Then the indexed residual series were averaged using a biweight robust mean to obtain site chronologies for each species using the program ARSTAN (Cook, 1985). In the case of *A. alba* the chronologies were averaged in two groups of sites with common growth trends and similar decline symptoms corresponding to declining (8 sites) and non-declining (25 sites) stands. Declining sites were regarded as those with more than 25% trees with crown defoliation greater than 50% (Camarero et al., 2002). In the case of the raw width series the mean and standard deviation (SD) and the first-order autocorrelation (AR1), which measures the year-to-year persistence in growth, were calculated. The statistical quality of the residual chronologies was evaluated using several dendrochronological statistics (Briffa and Jones, 1990): the mean correlation (r) of individual series with the mean site chronology; the mean sensitivity (MSx) which quantifies the relative change in width among consecutive years; and the Expressed Population Signal (EPS) of residual series which indicates to what extent the sample size is representative of a theoretical infinite population. The common interval of each site and species was selected for EPS values above the 0.85 threshold which is widely used in dendrochronological studies (Wigley et al., 1984).

2.3 NAO and Climatic Data

Monthly and season values of the NAO index were calculated based on the differences between time series of sea-level pressures recorded at Gibraltar and Reykjavik (Jones et al., 1997). NAO data are available in the Climate Research Unit (CRU) homepage (http://www.cru.uea.ac.uk/cru/data/nao.htm). The monthly climatic data used (mean temperature, total precipitation, cloud cover) were also produced by CRU, they are freely available at http://badc.nerc.ac.uk/data/cru/ and correspond to the TS 2.1 and 3.0 gridded (0.5° resolution) datasets (Mitchell and Jones, 2005). The missing data of cloud cover were replaced by the mean values of each monthly variable. In addition to the local climatic datasets compiled at 0.5° resolution, a

Table 2 Dendrochronological statistics of the growth series

Site	N° trees (cores)	Dbh (cm)	RW (mm)	*r*	MSx	AR1	Common interval[a]	Climate R^2_{adj} (%)	NAO R^2_{adj} (%)
QrBE	15 (30)	45.0	2.11 ± 0.76	0.54	0.23	0.74	1924–2008	16.3	3.0
AaIR	14 (29)	32.0	1.83 ± 0.89	0.54	0.17	0.87	1944–2003	31.8	5.1
QfLU	88 (176)	13.4	1.43 ± 0.60	0.61	0.27	0.68	1955–2002	14.1	6.1
PsLU	8 (15)	36.0	2.21 ± 0.83	0.64	0.33	0.77	1946–2004	27.6	10.1
QrMO	12 (24)	23.4	1.45 ± 0.55	0.43	0.26	0.75	1931–2000	71.5	14.4
PuMO	15 (30)	20.5	2.41 ± 0.95	0.58	0.15	0.70	1960–2008	18.2	10.8
FsMR	11 (22)	26.3	1.34 ± 0.09	0.61	0.28	0.71	1920–2009	66.5	3.5
PsMR	11 (23)	40.6	1.50 ± 0.11	0.65	0.29	0.79	1915–2009	41.5	13.0
AadPY	66 (140)	43.3	1.77 ± 0.43	0.58	0.24	0.79	1886–2000	66.0	12.5
AanPY	322 (660)	55.3	2.36 ± 0.67	0.49	0.20	0.82	1889–2000	53.0	10.9
JoAG	8 (21)	12.0	1.07 ± 0.53	0.50	0.27	0.59	1958–2009	38.7	14.1
PtME	24 (41)	8.8	1.06 ± 0.51	0.53	0.40	0.49	1959–2006	70.9	9.9
PhPE	15 (29)	17.2	1.12 ± 0.73	0.73	0.37	0.66	1900–2006	45.0	33.8
JtPE	10 (20)	16.0	1.47 ± 0.78	0.60	0.34	0.74	1956–2006	37.8	25.5
JtRE	15 (25)	17.6	1.00 ± 0.59	0.72	0.35	0.58	1955–2004	51.8	52.1
JtOL	13 (25)	26.8	0.97 ± 0.47	0.63	0.32	0.65	1949–2005	20.0	9.7
JtAD	40 (80)	15.0	1.10 ± 0.37	0.56	0.30	0.42	1960–2004	11.2	36.0

Abbreviations: RW, mean (± SD) tree-ring width for the common interval; r, mean correlation with the mean master site chronology; MSx, mean sensitivity of the residual chronologies; AR1, first-order autocorrelation; Climate R^2_{adj}, adjusted percentage of the variance of growth explained by monthly climatic variables (mean temperature, total precipitation); NAO R^2_{adj}, adjusted percentage of the variance of growth explained by monthly NAO indices.

[a]The common interval is the period regarded as statistically well replicated with EPS > 0.85, where the EPS is the Expressed Population Signal (a measure of the tree-to-tree common growth variance).

regional climatic dataset was obtained considering for the area contained within coordinates 40° 00′–43° 30′ N and 1° 30′ W–0° 30′ E.

2.4 Statistical Analyses

The spatio-temporal of ring-width residual chronologies was described using a Principal Component Analysis (PCA) calculated from their correlation matrix for the common period 1960–1999. The broken stick test was performed to determine the significance of the first three principal components (Holmes, 1992). To quantify the influence of the monthly and seasonal climatic data (mean temperature, total precipitation) and NAO indices on growth, bootstrapped correlation analyses were carried out for the common period 1960–1999 using the program Dendroclim2002 (Biondi and Waikul, 2004). Spatial patterns of climate-growth relationships were explored using the KNMI Climate Explorer (http://climexp.knmi.nl/). The significances of the correlations were based on 999 bootstrapped estimates. The long-term serial correlation in the NAO monthly or seasonal series (winter, December–February; spring, March–May; summer, June–August; autumn, September–November) were removed assuming linear trends. Furthermore, correlation analyses considering all NAO data ($n = 40$) or only positive ($n = 16-27$) or negative ($n = 13-24$) NAO indices were performed to emphasize the effects of different NAO phases on growth. The relationships between climate or NAO data (monthly and seasonal values) and growth (residual indices) were analyzed from the previous September up to the current September. In the case of seasonal data, I focused on the relationships between previous-winter and current-spring NAO indices and growth data based on previous results in nearby areas (Rozas et al., 2009). To estimate the percentage of variance (R^2) and its adjusted value (R^2_{adj}) in growth data explained by climatic (temperature, precipitation) and NAO data, multiple regressions were performed based on the forward selection of significant ($P < 0.05$) monthly predictors. Cloud cover was not used in the climatic model because most dendroclimatic studies are based on temperature and precipitation data (Fritts, 2001). To detect if NAO-growth associations were unstable through time, moving correlations for 30-year periods were performed between NAO monthly and seasonal indices and growth data of the longest chronologies which covered most of the past twentieth century (PsMR, PhPE and the silver fir series AadPY, AanPY).

3 Results

3.1 Growth and Dendrochronological Data

Tree size changed considerably across the study area with mean diameter (Dbh) ranging between 8.8 (*P. terebinthus*) and 55.3 cm (*A. alba*) (Table 1). The mean ring widths varied also notably among sites and species with minimum values of 1.0 mm

(open *J. thurifera* stands under semi-arid and continental conditions) and maximum values of 3.4 mm (young *P. uncinata* mountain forests) (Table 2). High growth values were also observed in mesic temperate forests (*A. alba*, *P. sylvestris*, *Q. robur*), whereas tree rings were usually narrow in sites with a pronounced drought period under Mediterranean conditions dominated by *P. terebinthus*, *Juniperus* species and *P. halepensis*. The maximum correlations between tree series and the mean site chronology were observed in semi-arid sites dominated by *J. thurifera* and *P. halepensis* followed by transitional *P. sylvestris* forests, whereas low correlations were observed in more mesic sites both in temperate (*Q. robur*, *A. alba*) and in Mediterranean conditions (*J. oxycedrus*, *P. terebinthus*). Mesic temperate forest showed the lowest mean sensitivity values, while *J. thurifera* and *P. halepensis* semi-arid sites showed the highest mean relative change in width among consecutive years. Conversely, these last forests and Mediterranean sites (*P. terebinthus*) showed the lowest first-order autocorrelation values, whereas *A. alba* and *P. sylvestris* trees showed the highest year-to-year persistence in growth. Finally, the maximum interspecific correlations between growth series were observed for the Mediterranean sites PtME and PhPE ($r = 0.56, P < 0.001$), separated by 112 km, and for the temperate or transitional sites AadPY and PsMR ($r = 0.53, P < 0.001$), which were located 59 km apart. However, negative associations were detected between Mediterranean continental *J. thurifera* sites and mesic *Q. robur* forests separated by about 200 km (QrMO-JtAD, $r = -0.17, P = 0.40$; QrBE-JtRE, $r = -0.16, P = 0.30$).

Forests with trees of greater diameter showed a higher mean ring-width ($r = 0.68, P = 0.003$) and first-order autocorrelation of tree-ring series ($r = 0.71$, $P = 0.001$) but a lower mean sensitivity ($r = -0.48, P = 0.04$) (Table 2). The percentage of growth variance explained by climatic variables was not significantly related to tree size or to any dendrochronological statistic. However, the percentage of growth variance explained by NAO indices was negatively related to tree-ring width ($r = -0.47, P = 0.05$) and first-order autocorrelation ($r = -0.50, P = 0.04$) but positively associated with the mean sensitivity ($r = 0.48, P = 0.05$).

The first three principal components of the PCA explained, 40.5, 10.9 and 7.1% of the total variance of growth data for all sites (48 series), respectively, being significant ($P < 0.05$) the first two components (*results not presented*). Considering the mean growth series for the two groups of *A. alba* forests based on their decline symptoms and the rest of sites (17 series), the first (PC1) and second (PC2) components were again significant and explained, respectively, 34 and 13% of the total variance (Fig. 1). The PC1 arranged sites according to their main climatic conditions related to precipitation differences since forests located in the more xeric sites (Mediterranean continental climate) showed high scores along this component whereas forests in more mesic habitats (temperate and mountain forests) had the lowest scores. Mountain conifer forests and *Quercus* forests, both mesic and transitional sites, showed high scores in the PC2.

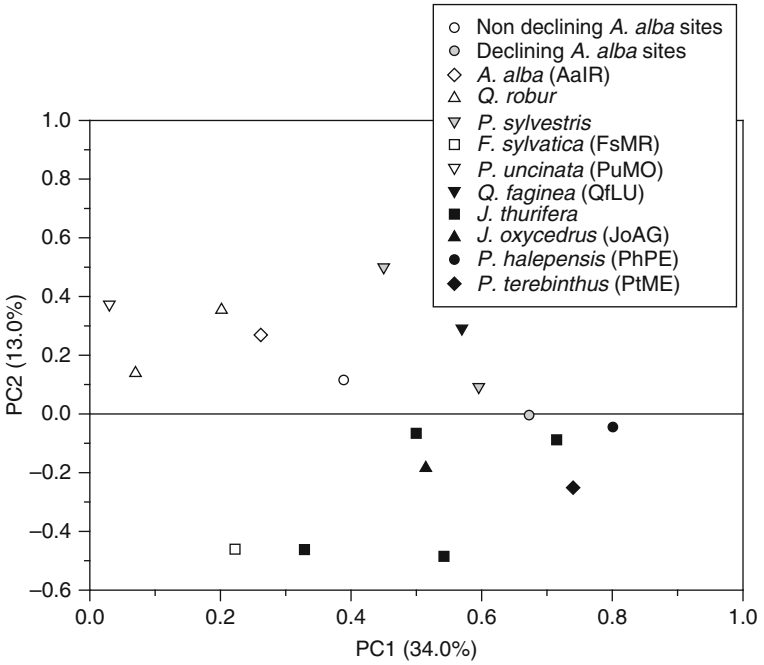

Fig. 1 Scatter diagram of growth chronologies based on the scores of the first two principal components of a PCA considering the mean series of non-declining and declining *A. alba* sites and the rest of study sites (17 series). Codes are as in Table 1

3.2 Relationships Between Growth and Climatic Variables

Tree growth in most study sites was enhanced by warmer April temperatures, wetter and cloudier conditions in June during the year of tree-ring growth (Table 3). In addition, higher February temperatures and more rainfall and cloud cover in May and wet conditions in August of the current year also favored wood formation. However, a previous warm September with low values of cloud cover was usually related to decreased growth. In mesic or transitional sub-Mediterranean sites, a wet January was associated to lower growth the following spring, but in Mediterranean sites tree growth was enhanced by wet conditions in January and the previous December.

The spatial patterns of climate-growth relationships changed according to the climatic variable. For instance, the positive effect of winter precipitation (previous December) on tree growth was stronger in the southern than in the northern part of the study area in Northeastern Spain (Fig. 2). However, the positive effects of late spring and early summer precipitation (current June) on growth did not show such divergence and it was observed near the core of the study area.

Table 3 Significant ($P < 0.05$) correlations (Pearson coefficients) obtained between monthly climatic data (T, mean temperature; P, total precipitation; CC, cloud cover) and growth for the study sites including the first and second principal components (PC1, PC2). Months abbreviated by lower- and uppercase letters correspond to the years before (*t*–1) and during (*t*) tree-ring formation. Codes are as in Table 1

Year *t*–1					Year *t*								
T	s	o	n	d	J	F	M	A	M	J	J	A	S
QrBE								0.32					
AaIR	0.29		0.30					0.42					
QfLU								0.29					
PsLU	–0.39					0.35		0.34					0.32
QrMO			0.29				–0.41						
PuMO								0.29					
FsMR							–0.28						
PsMR	–0.42							0.38	0.29				
AadPY	–0.49					0.34		0.38					
AanPY	–0.50		0.40			0.39		0.40					
JoAG								0.29					
PtME		0.36											
PhPE	–0.33			0.32	0.31	0.29		0.29		–0.29			
JtPE													
JtRE					0.31	0.38		0.42			–0.45		
JtOL				0.29		0.33							
JtAD							0.29	0.30					
PC1	–0.36					0.45		0.46					
PC2	–0.28									0.32			0.29

Table 3 (continued)

Year *t*–1					Year *t*								
P	s	o	n	d	J	F	M	A	M	J	J	A	S
QrBE					–0.30								
AaIR	–0.29											0.31	
QfLU									0.40	0.33			
PsLU									0.46				
QrMO						0.38					0.39		
PuMO												0.33	
FsMR			–0.29		–0.29			0.42		0.36			
PsMR									0.32	0.37		0.29	
AadPY	0.30				–0.33					0.56			
AanPY	0.31				–0.32					0.39			
JoAG			0.38							0.44		0.33	
PtME					0.33			0.45	0.33	0.59			
PhPE				0.29	0.56					0.48			
JtPE					0.40				0.33				
JtRE				0.34	0.40				0.35	0.59			
JtOL				0.39	0.30				0.33			0.30	
JtAD												0.38	
PC1				0.38	0.42				0.47	0.61	0.47		
PC2													

Table 3 (continued)

Year *t*–1					Year *t*								
CC	s	o	n	d	J	F	M	A	M	J	J	A	S
QrBE												0.29	
AaIR	0.31												–0.35
QfLU									0.41	0.31			
PsLU									0.29				
QrMO	0.31		–0.34				0.29						
PuMO								–0.33		–0.30			
FsMR								0.29					
PsMR	0.42												
AadPY	0.42	0.39								0.30			–0.30
AanPY	0.48	0.33			–0.34								
JoAG			0.31							0.44			
PtME								0.30	0.38	0.49			
PhPE				0.51	0.52	0.30			0.34	0.39			
JtPE					0.33				0.46				
JtRE				0.36						0.30	0.30		
JtOL										0.33			
JtAD						–0.32				0.37			
PC1				0.34					0.37	0.46			
PC2						0.29							

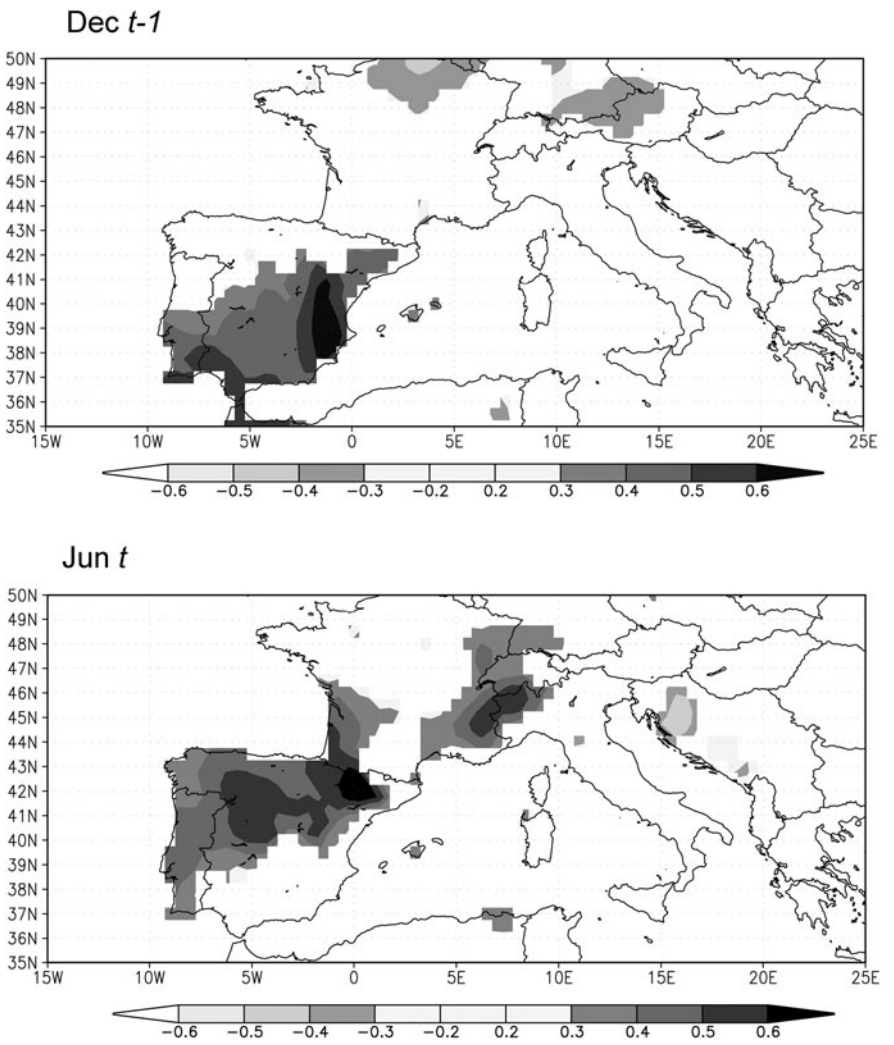

Fig. 2 Spatial patterns of some of the main growth-climate relationships in Northeastern Spain. The maps show correlations between scores of the first principal component (PC1) of growth chronologies and precipitation data (0.5° resolution) for the previous (Dec *t*–1) and the current June (Jun *t*)

The best climatic model for the PC1 scores, capturing the main growth trends of the study sites during the period 1960–1999, explained 78.3% of their variance ($R^2_{adj} = 0.75, F = 24.6, P < 0.001$) and included the following variables: April and late spring-early summer (May, June, July) precipitation, previous October and current April temperature (Fig. 3).

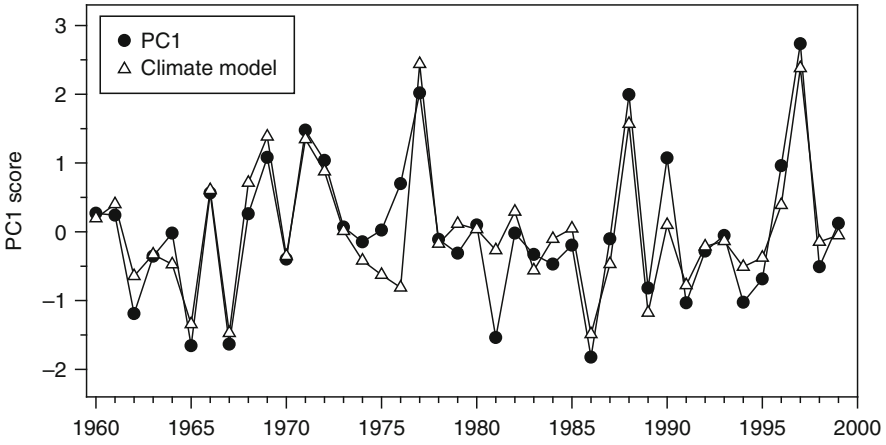

Fig. 3 Temporal patterns of the PC1 scores and modeled values based on a climatic model considering monthly climate variables (mean temperature, total precipitation)

3.3 Relationships Between Growth and NAO Indices

Several xeric sites under Mediterranean and continental conditions showed negative associations between growth and the previous December NAO index, while others showed a similar relationship with the previous September NAO index (Table 4). However, in mesic or transitional sites such as mountain conifer forest or oak woodland it was also detected positive association with the previous November and December NAO indices. Some sites showed positive relationships with the current February index, whereas others showed negative relationships with the current June index.

The scores of the PC1 and PC2 of growth data were negatively and significantly related to the previous December ($P = 0.003$) and January ($P = 0.05$) and to the current August ($P = 0.02$) NAO indices, respectively (Table 4). In the case of the PC1, a slightly stronger association was found with the mean NAO index of the previous December and the current January ($r = -0.47, P = 0.002$). On the other hand, the PC2 was positively but not significantly related to the mean NAO index of the previous November and December ($r = 0.20, P = 0.07$).

The analyses based on positive NAO indices mostly reflected local effects since no significant association was found with the scores of the PC1 (Table 5). Most significant correlations corresponded to previous December and current February NAO indices. Considering only negative NAO indices, several sites and the PC1 showed positive associations with the values of the current February index and negative relationships with the values of the previous December index, whereas the PC2 showed negative associations with the NAO indices of the previous September and the current August and a positive association with the NAO index of the current March (Table 6).

Table 4 Significant ($P < 0.05$) correlations obtained between monthly and seasonal NAO indices and growth for the study sites including the first and second principal components (PC1, PC2). Values in bold are highly significant ($P = 0.001$) and months or seasons without significant values are not presented. Codes are as in Tables 1 and 3

Year t–1					Year t						
Site	Summer	sep	nov	dec	Spring	Jan	Feb	Mar	Apr	Jun	Aug
QrBE			0.22	0.21							
AaIR										–0.30	
PsLU			0.23								
QrMO								–0.41			
PuMO	0.33		**0.45**								
FsMR							–0.29		–0.25	–0.21	
PsMR		–0.30	0.23	–0.28							
AadPY			0.20								
AanPY			0.27				0.28				
JoAG				–0.28				0.32		–0.31	
PtME				–0.32		–0.31					
PhPE				**–0.49**							
JtPE				–0.29	–0.36				–0.33		
JtRE				**–0.49**							
JtOL							0.35			–0.30	0.34
JtAD							**0.54**			–0.35	0.40
PC1				–0.46		–0.31				–0.28	
PC2		–0.28									–0.36

Table 5 Significant ($P < 0.05$) correlations obtained between monthly and seasonal positive NAO indices and growth for the study sites. Values in bold are highly significant ($P = 0.001$). Codes are as in Tables 1 and 4

Year t–1				Year t				
Site	sep	dec	Winter	Spring	Fall	Feb	Mar	Apr
QrBE					0.28			
AaIR								0.35
QfLU							–0.32	
PuMO			0.29					
FsMR			–0.22			–0.39		
PsMR	–0.34							
AadPY		**0.45**		–0.22				
JoAG						0.50		
PhPE		0.26	0.20					
JtRE		**–0.49**						
JtOL	–0.38		0.28			0.43		
JtAD			0.35			**0.53**		

Table 6 Significant ($P < 0.05$) correlations obtained between monthly and seasonal negative NAO indices and growth for the study sites. Values in bold are highly significant ($P = 0.001$). Codes are as in Tables 1 and 4

Year *t*–1						Year *t*						
Site	Summer	Fall	sep	oct	dec	Spring	Summer	Feb	Mar	May	Jun	Aug
QrBE		–0.26		–0.36								
AaIR								0.69				
QfLU					–0.42							
QrMO								0.51				
PsMR			–0.28		–0.32							
AadPY								0.30		–0.27		
AanPY						–0.25				**–0.37**		
JoAG							–0.42					
PhPE					–0.33			0.33				
JtPE						–0.39	–0.31	0.50		–0.33		
JtRE	0.38				**–0.52**			0.44				
JtOL					–0.44			0.39				
JtAD					–0.43			0.53				
PC1				0.45	**–0.58**		–0.35	0.48			–0.39	
PC2			–0.45						0.62			–0.56

The negative associations between the PC1 and PC2 scores and the previous December and the current August NAO indices were more noticeable in the last 2 decades of the past century than before (Fig. 4). In fact, the moving correlations indicated that the negative associations between growth and the previous December NAO index in PhPE and PsMR were unstable and became significant since the 1960s (Fig. 5).

In contrast with the climatic model of the PC1 scores which explained 78% of growth variance (Fig. 3), the best model of the PC1 based on the NAO index explained only 27.9% of their variance ($F = 8.5, P = 0.001$) and contained as predictors the averaged index of the previous December and the current January and the current May index. Actually, only in one study site (JtRE) the NAO indices were able to account for a similar variance of growth as the monthly climatic variables did (Fig. 6). In this *J. thurifera* forest subjected to semiarid and continental Mediterranean conditions, the climatic model explained 51.8% of the growth variance ($F = 11.7, P < 0.001$), whereas the NAO model captured 52.1% of the growth variance ($F = 11.9, P < 0.001$). The climatic model included the following variables (effects between parentheses): June precipitation (+), February, April (+) and July temperature (−) (Table 3; Fig. 6). The NAO indices which were selected in the model corresponded to the previous December (−) and to current February (+) and September (+) (Tables 4, 5 and 6; Fig. 6).

3.4 NAO and Silver Fir Decline

The instability in the NAO-growth relationships was also observed in the case of silver fir forests which showed positive associations with monthly November and

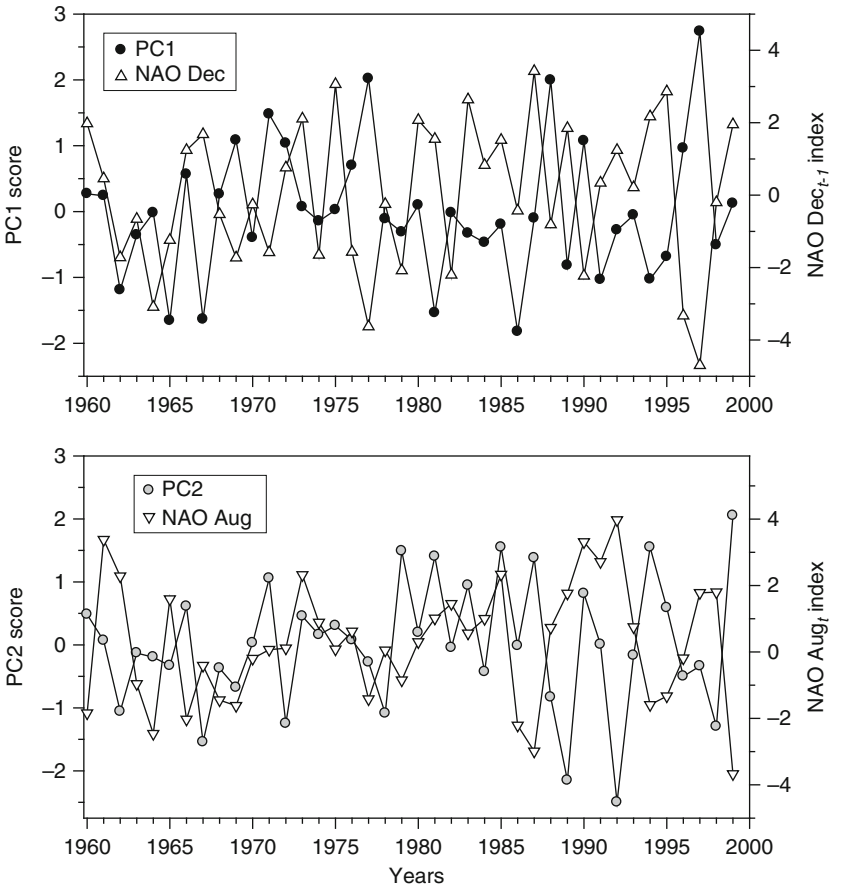

Fig. 4 Temporal patterns of the scores of the first two principal components (PC1, PC2) of growth chronologies and related December and August NAO indices for the years before (t–1) and during (t) tree-ring formation, respectively

February indices of winter before tree-ring growth (Table 4). In some of these forests a decline episode characterised by massive defoliation and mortality was observed in the 1980s after a severe growth reduction in 1986 (Camarero et al., 2002), when the minimum value of the November–February NAO index during the twentieth century was also observed (Fig. 7). The analyses based on moving correlations detected a shift towards positive and significant associations between such index and silver fir growth since the growth reduction in 1986, i.e. the responsiveness of silver fir growth to NAO winter indices increased in the last 2 decades of the past century. Furthermore, this rise in the NAO-growth correlation was greater in non-declining than in declining forests (Fig. 7).

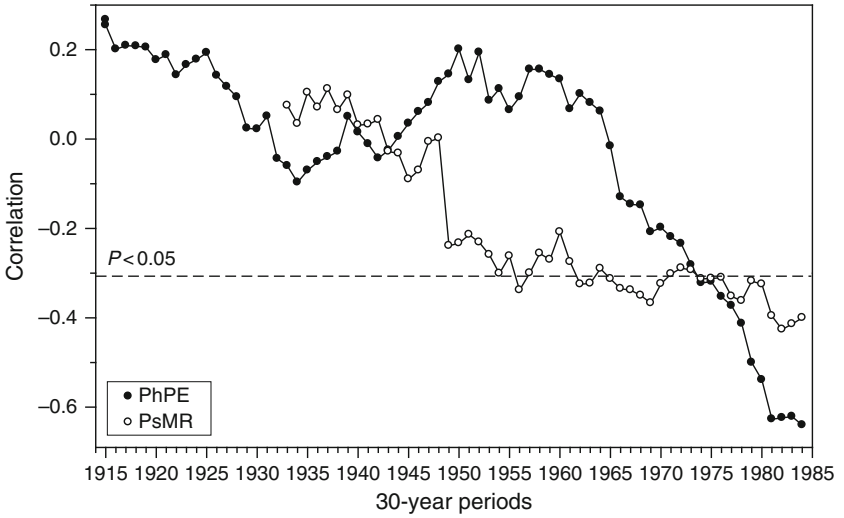

Fig. 5 Moving correlations (30-year periods) between the NAO index of the previous (year *t*–1) December and growth of two selected sites (PhPE, PsMR; see sites codes in Table 1). The years in the *x* axis indicate the mid-point of each 30-year period. The *dashed line* indicates the significance ($P < 0.05$) threshold for negative correlations lower than −0.3

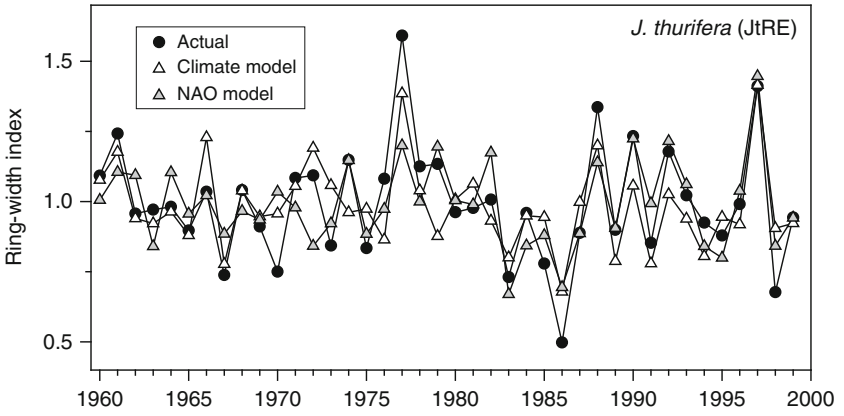

Fig. 6 Temporal patterns of the growth indices of *J. thurifera* in the Retuerta de Pina site (JtRE) as compared with models of tree growth based on climatic (monthly mean temperature and total precipitation) or NAO (indices) predictors

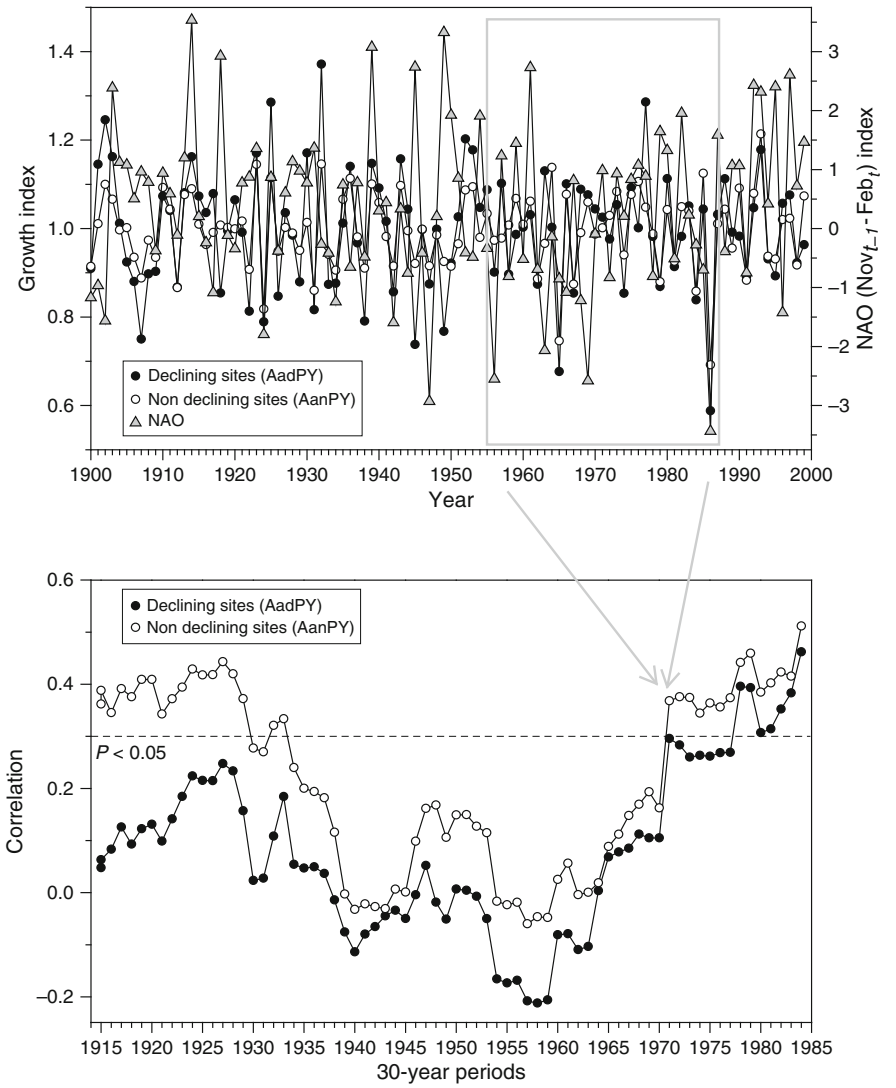

Fig. 7 Growth indices in declining and non-declining silver fir forests (sites codes are as in Table 1) compared with the November–February NAO index of the year before tree-ring growth (*upper graph*) and moving correlations calculated between silver-fir growth and that NAO index (*lower graph*). The years in the *x* axis indicate the mid-point of each 30-year period. The *dashed line* indicates the significance ($P < 0.05$) threshold for correlations greater than 0.3. The *rectangle* delimits the period 1957–1986 and the *arrows* point to the corresponding correlation value when a shift in the NAO-growth correlations was observed

4 Discussion

4.1 Climatic and NAO Influences on Tree Growth

Radial growth of most of the studied tree species responded positively to warm late winters (February) and springs (April) and to wet and cloudy late springs and early summers (May, June), whereas there were both positive and negative responses to wet winters (January) in the case of Mediterranean (e.g., *P. halepensis*) and temperate or cold sites (e.g., *A. alba*), respectively. However, most Mediterranean forests under continental conditions dominated by *J. thurifera* showed positive growth responses to wet conditions in the previous winter (December, January) and were more sensitive to winter NAO indices than temperate forests in mesic sites (e.g., *Q. robur*). The observed responses to spring conditions are in agreement with dendroecological and xylogenesis studies which have inferred or found the maximum radial-growth rates of these species in spring (Camarero et al., 2002, 2010).

The positive responses to previous-winter climatic variables (precipitation, temperature, cloud cover) detected in *P. halepensis* and *J. thurifera* forests under continental Mediterranean climates indicate that warm, wet and cloudy conditions in December and January enhance growth the following spring. In evergreen conifers, earlywood and tree-ring growth depend on the synthesis of carbohydrates during the previous winter (Kagawa et al., 2006). However, results obtained here suggest that the moisture reserves in the soil supplied by winter precipitation may be more relevant to enhance tree growth of these species in spring than temperature-mediated responses which were less important than rainfall effects. In addition, cloudy winter conditions were also linked to enhanced growth indicating that winter photosynthesis and the synthesis of carbohydrate were not constrained by radiation.

In agreement with the main hypothesis of this study, high NAO values during the previous winter are linked to a reduction in precipitation and water availability and a low radial growth the following spring. Previous studies have found that winter NAO indices are negatively associated with tree growth in Southern Europe (Piovesan and Schirone, 2000), whereas the reverse response was detected in Northern Europe (Linderholm et al., 2003; Macias et al., 2004; Schultz et al., 2008). The observed negative relationship between the December NAO index and growth in the study area is also consistent with results from earlier studies of Iberian conifer forests in Northwestern (Roig et al., 2009; Rozas et al., 2009) and Southeastern Spain (Bogino and Bravo, 2008).

Such negative associations between winter NAO and tree growth were not greater in northwestern (e.g., QfLU) than in at southeastern sites (e.g., JtRE), despite the former sites are under stronger influence of Atlantic westerlies than the later ones. Additionally, this results agrees with the spatial patterns of the correlations between the first principal component of growth and previous December precipitation which were higher in southeastern than in northwestern sites. Although the NAO mainly affects the precipitation patterns in southwestern Iberia, the southwest flows are reactivated when they reach the Pyrenees, explaining why tree growth of forests growing in the Middle Ebro Basin (e.g., JtRE) in eastern sites with continental

Mediterranean climates are also greatly affected by NAO patterns (Vicente-Serrano and Lopez-Moreno, 2006). In this *J. thurifera* site, both climatic and NAO-based models were able to capture about half of the growth variance which suggests that long chronologies of this species in semiarid and continental sites may provide a valuable proxy for reconstructions of winter NAO indices. The response of growth to NAO in this and other sites was not related o elevation as suggested Bogino and Bravo (2008) in the case of *Pinus pinaster*. Furthermore, this suggestion agrees with the negative association between the percentage of growth variance explained by NAO indices and tree-ring width, which indicate that series from sites with low growth and high inter-annual variability may reflect well NAO effects on the winter precipitation in the high-frequency domain. It is also noticeable that the average explained variance by climatic variables was much higher (40.1%) than that explained by NAO indices (15.9%), but the NAO-models explained a much higher percentage of growth if only *J. thurifera* and *P. halepensis* forests from semiarid and continental sites were considered (36.8%). Contrastingly, tree growth in mesic and transitional forests was less related to NAO variability as indicated the low growth variance captured by NAO indices (8.6%) (see similar values in Bogino and Bravo, 2008; Rozas et al., 2009). This result was observed even if these sites were located in Western areas near the Atlantic Ocean, probably because of wet conditions, and a low growth responsiveness of dominant tree species to winter precipitation. For instance, sites QrBE (*Q. robur*) and JtRE (*J. thurifera*) are located at linear distances of 32 and 252 km from the Atlantic Ocean, respectively, but NAO indices explained 3.0 and 52.1% of their recent growth variability, respectively.

Most dendroecological studies have focused on the effect of winter NAO on climate and tree growth in the low-frequency domain (Bogino and Bravo, 2008; Roig et al., 2009) because the NAO mainly affects long-term winter and spring climatic variability in Western Europe (Hurrell, 1995). However, several authors have also noted that summer precipitation at high-frequency timescales is related to tree growth in southern Europe where rainfall in the dry season may alleviate drought stress (Piovesan and Schirone, 2000). In this study, it was observed that tree growth was inversely related to current NAO summer indices, a season when growth is mainly enhanced by wet (June, August) and cloudy (June) conditions in xeric and transitional sites. The spatial pattern of the positive effect of June precipitation on growth was centered in Northeastern Spain and resembled related NAO-precipitation associations suggesting that the NAO was involved in this summer effect on growth, but further studies are required to test these assumptions. These results contrast with the positive effect of late-spring and early-summer NAO indices and temperature on tree growth in Fennoscandia (Macias et al., 2004), and even in Northwest Spain (Rozas et al., 2009). In Fennoscandia the positive effect of NAO on growth of Scots pine was mostly observed for negative NAO indices series indicating that these spring NAO values corresponded to climatic conditions (late snowmelt and beginning of the growing season) constraining tree growth whereas positive NAO values did not greatly affect growth (Macias et al., 2004). In this study, a similar effect was observed for February NAO values which were positively related to growth in

temperate (*A. alba*, *Q. robur*) and continental Mediterranean sites (*J. thurifera*, *P. halepensis*). Thus, a warmer early-spring linked to high NAO February values in negative NAO series may be related to an earlier growth resumption in some of these sites where growth was also enhanced by February and April temperatures.

4.2 NAO Variability and Silver Fir Decline

Silver fir growth showed positive associations with monthly November and February NAO indices of the previous winter but such association steeply rose in the mid 1980s when silver fir growth fell abruptly and decline started in xeric sites. Since the 1980s, southwestern Europe has been under the influence of extended periods of warm winters, which were associated with a persistent positive phase of the NAO index for that season (Hurrell, 1995). These results and the growth-climate relationships found for silver fir suggest that high NAO winter indices were possibly linked to warmer late-winter conditions and an enhanced growth through an earlier cambial reactivation of the silver fir xylogenesis, particularly in non-declining sites. However, silver firs produced an extremely narrow ring in 1986 probably because of the previous September 1985 which was very warm and dry (Camarero et al., 2002). Further studies are required to understand if the NAO or other circulation patterns were involved in the climatic determination of such silver fir decline.

One of the main shortcomings of the present study results from the short length of some of the dendrochronological series used. To assess the value of dendrochronological records as a proxy of NAO and as sources of climatic information contained in the NAO index, further analyses are required to investigate the NAO signals in long tree-ring chronologies of different species, particularly in sensitive sites with species whose growth is responsive to NAO variability. These longer dendrochronological records should be analyzed focusing on the temporal instability of NAO-growth relationships on decadal and multidecadal scales (5–15 years) which are the scales of the highest influence of the NAO on climate variability (Hurrell et al., 2003).

5 Conclusions

The proper assessment of the relationships between NAO and tree growth requires an approach based on the analysis of multi-species networks across contrasting geographical and climatic gradients. Regional monthly climatic variables were shown to be usually better predictors of tree growth than large-scale NAO indices. In northeastern Spain, tree growth was enhanced by warm and wet conditions in spring during the year of tree-ring formation. High NAO values during the previous December were linked to a reduction in precipitation and a low radial growth the following spring, but high February NAO values were also associated with warmer early-spring conditions and enhanced growth. Forests growing under xeric

conditions with semiarid and continental climates such as Mediterranean *Juniperus thurifera* sites showed a higher sensitivity in their recent growth patterns to NAO variability than forests growing under more mesic conditions. In fact, only in one *J. thurifera* forest under continental Mediterranean conditions the growth variance explained by NAO indices was high and similar to that explained by climatic data. Further research efforts to monitor the effects of NAO on forest growth and decline should build long *J. thurifera* tree-ring chronologies in continental Mediterranean xeric sites which have proved to be very sensitive to high-frequency changes in winter precipitation and NAO indices of the previous December.

Acknowledgements This work has been supported by the research projects RTA01-071-C3-1 and CGL2008-04847-C02-01/BOS financed by the Spanish Ministry of Science. I thank the support of ARAID and several colleagues for providing samples and driving me to many impressive forests (E. Arrechea, J.M. Gil, R. Hernández, G. Montserrat-Martí, C. Lastanao, N.A. Laskurain, V. Pérez, M.A. Ros, A. Solla).

References

Biondi F, Waikul K (2004) DENDROCLIM2002: a C++ program for statistical calibration of climate signals in tree-ring chronologies. Comput Geosci 30:303–311

Bogino S, Bravo F (2008) SOI and NAO impacts on *Pinus pinaster* Ait. growth in Spanish forests. In: Elferts D, Brumelis G, Gärtner H, Helle G, Schleser G (eds) TRACE – Tree rings in archaeology, climatology and ecology, vol. 6. GFZ Potsdam, Scientific technical report STR 08/05, Potsdam, pp 21–26

Briffa KR, Jones PD (1990) Basic chronology statistics and assessment. In: Cook ER, Kairiuktsis LA(eds) Methods of dendrochronology. Kluwer Academic, Dordrecht, pp 137–152

Camarero JJ, Olano JM, Parras A (2010) Plastic bimodal xylogenesis in conifers from continental Mediterranean climates. New Phytol 185:471–480

Camarero JJ, Padró A, Martín-Bernal E, Gil-Pelegrín E (2002) Aproximación dendroecológica al decaimiento del abeto (*Abies alba* Mill.) en el Pirineo aragonés. Montes 70:26–33

Cook ER (1985) A time series approach to tree-ring standardization. PhD Dissertation, University of Arizona, Tucson, AZ

Fritts H (2001) Tree rings and climate. Academic Press, London

Garfin GM (1998) Relationships between winter atmospheric circulation patterns and extreme tree growth anomalies in the Sierra Nevada. Int J Climatol 18:725–740

Giorgi F, Lionello P (2008) Climate change projections for the Mediterranean region. Glob Planet Change 63:90–104

Girardin MP, Tardif J (2005) Sensitivity of tree growth to the atmospheric vertical profile in the boreal plains of Manitoba, Canada. Can J For Res 35:48–64

González-Hidalgo JC, López-Bustins JA, Štepánek P, Martín-Vide J, de Luis M (2009) Monthly precipitation trends on the Mediterranean fringe of the Iberian Peninsula during the second half of the 20th century (1951–2000). Int J Climatol 29:1415–1429

Hallett TB, Coulson T, Pilkington JG, Clutton-Brock TH, Pemberton JM, Grenfell BT (2004) Why large-scale climate indices seem to predict ecological processes better than local weather. Nature 430:71–75

Hirschboeck KK, Ni F, Wood ML, Woodhouse C (1996) Synoptic dendroclimatology: overview and outlook. In: Dean JS, Meko DM, Swetnam TW (eds) Tree rings, environment, and humanity. Radiocarbon, Tuscon, pp 205–223

Holmes RL (1983) Computer-assisted quality control in tree-ring dating and measurement. Tree-Ring Bull 43:69–78

Holmes RL (1992) Dendrochronology program library. Version 1992-1. Laboratory of Tree-Ring Research, University of Arizona, Tucson, AZ

Hurrell J (1995) Decadal trends in North Atlantic Oscillation and relationship to regional temperature and precipitation. Science 269:676–679

Hurrell J, Kushnir Y, Ottersen G, Visbeck M (2003) An overview of the North Atlantic Oscillation. The North Atlantic Oscillation: climate significance and environmental impact. Geophys Monogr, vol. 134, Amer Geophys Union, pp 1–36

Hurrell J, Van Loon H (1997) Decadal variations in climate associated with the North Atlantic Oscillation. Clim Change 36:301–326

IPCC (2007) Climate change 2007: the physical science basis. Contribution of Working Group I to the 4th assessment report of the Intergovernmental panel on climate change. Cambridge University Press, Cambridge, UK

Jones PD, Jónsson T, Wheeler D (1997) Extension to the North Atlantic Oscillation using early instrumental pressure observations from Gibraltar and south-west Iceland. Int J Climatol 17:1433–1450

Kagawa A, Sugimoto A, Maximov T (2006) $^{13}CO_2$ pulse-labelling of photoassimilates reveals carbon allocation within and between tree rings. Plant Cell Environ 29:1571–1584

Linderholm HW, Solberg BO, Lindholm M (2003) Tree-ring records from central Fennoscandia: the relationship between tree growth and climate along a west-east transect. The Holocene 13:887–895

Macias M, Timonen M, Kirchhefer AJ, Lindholm M, Eronen M, Gutiérrez E (2004) Growth variability of Scots Pine (*Pinus sylvestris*) along a west-east gradient across Northern Fennoscandia: a dendroclimatic approach. Arct Antarct Alp Res 36:565–574

Mitchell TD, Jones PD (2005) An improved method of constructing a database of monthly climate observations and associated high-resolution grids. Int J Climatol 25:693–712

Nahal I (1981) The Mediterranean climate from a biological viewpoint. In: di Castri F, Goodall FW, Specht RL (eds) Mediterranean-type shrublands. Elsevier, Amsterdam, the Netherlands, pp 63–86

Piovesan G, Schirone B (2000) Winter North Atlantic Oscillation effects on the tree rings of the Italian beech (*Fagus sylvatica* L.). Int J Biometeorol 44:121–127

Rodó X, Baert E, Comin F (1997) Variations in seasonal rainfall in Southern Europe during the present century: relationships with the North Atlantic Oscillation and the El Niño-Southern Oscillation. Clim Dyn 13:275–284

Rodríguez-Puebla C, Encinas AH, Sáenz J (2001) Winter precipitation over the Iberian Peninsula and its relationship to circulation indices. Hydrol Earth Syst Sci 5:233–244

Roig FA, Barriopedro D, Herrera RG, Patón Domínguez D, Monge S (2009) North Atlantic Oscillation signatures in western Iberian tree-rings. Geogr Ann 91:141–157

Rozas V, Lama S, García-González I (2009) Differential tree-growth responses to local and large-scale climatic variation in two *Pinus* and two *Quercus* species in northwest Spain. Écoscience 3:299–310

Sáenz J, Rodríguez-Puebla C, Fernández J, Zubillaga J (2001) Interpretation of interannual winter temperature variations over southwestern Europe. J Geophys Res 106:20641–20652

Schultz J, Neuwirth B, Friedrichs DA, Löffler J, Winiger M (2008) Growth responses to NAO along a Central European West-East transect. In: Elferts D, Brumelis G, Gärtner H, Helle G, Schleser G (eds) TRACE – Tree rings in archaeology, climatology and ecology, vol. 6. GFZ Potsdam, Scientific technical report STR 08/05, Potsdam, pp 17–24

Vicente-Serrano SM, Lopez-Moreno JI (2006) The influence of atmospheric circulation at different spatial scales on winter drought variability through a semi-arid climatic gradient in northeast Spain. Int J Climatol 26:1427–1453

Wigley TML, Briffa KR, Jones PD (1984) On the average value of correlated time series, with applications in dendroclimatology and hydrometeorology. J Clim Appl Meteorol 23:201–203

Ecological Impacts of the North Atlantic Oscillation (NAO) in Mediterranean Ecosystems

Oscar Gordo, Carles Barriocanal, and David Robson

Abstract Large-scale climate indices have received much attention in recent years in ecology-climate research due to the advantages they have over typically used local weather variables, such as temperature or rainfall. In the Mediterranean, the North Atlantic Oscillation (NAO) is a major forcing of climate patterns, especially precipitation. More than 60 studies to date have demonstrated the effects of the NAO on both terrestrial and aquatic Mediterranean ecosystems. In terrestrial ecosystems, the NAO affects the phenology and growth of plants and crop yields. It also affects the condition and diet of mammals and disease-related mortality in amphibians. The effects of the NAO are probably better known in marine ecosystems, where the impact on the hydrodynamics of the water column and currents is felt in the dynamics of populations from plankton to fishes in both pelagic and benthonic environments. Additionally, birds are an especially well studied taxon when it comes to effects of the NAO. The NAO has been shown to affect the population dynamics of water birds by impacting the availability and extent of their habitat and by influencing dispersal decisions of individuals. The NAO plays an essential role in the migration of birds throughout the Mediterranean basin, and it is probably a reason for the observed advance of arrival dates during the spring in Europe. In spite of the notable number of studies carried out to date, we are far from knowing accurately the ecological impacts of the NAO on Mediterranean ecosystems. More efforts are needed to understand regional differences in the NAO effects within the Mediterranean basin and how they compare with more northern latitudes of Europe.

Keywords Birds · Climate · Ecosystem · Phenology · Review

1 Why Using Large Scale Climate Indices in Ecology?

We are all aware that environmental conditions, defined as the set of abiotic variables to which organisms are subjected, shape the distribution, abundance, behavior

O. Gordo (✉)
Departamento de Zoología y Antropología Física, Universidad Complutense de Madrid, Madrid, Spain
e-mail: ogordo@bio.ucm.es

S.M. Vicente-Serrano, R.M. Trigo (eds.), *Hydrological, Socioeconomic and Ecological Impacts of the North Atlantic Oscillation in the Mediterranean Region*, Advances in Global Change Research 46, DOI 10.1007/978-94-007-1372-7_11,

and ultimately the evolution of organisms (Begon et al., 2006). Among environmental drivers, climate is recognized as one of the most important abiotic factors. Therefore, one should not be surprised that organisms are responding to the ongoing climate change, even though observed changes in Earth's climate have so far been relatively small (e.g., the global mean annual temperature has increased only by about 0.7°C during the last century (Solomon et al., 2007)). Even though many other factors operate on a long-term temporal scale (e.g., density-dependent processes, land-use transformations, etc.) and may prevent us from establishing unambiguously a causal link between climate change and some responses of organisms (Sala et al., 2000; Forchhammer and Post, 2004), evidence of climate change impacts on organisms is abundant. The impacts are widespread, ranging from the equator to the poles in both terrestrial and aquatic ecosystems and suggesting a climate change imprint on the biosphere at a global scale (Parmesan and Yohe, 2003; Root et al., 2003). Climate-induced responses range from the plasticity of many traits to adapt to weather variability to persistent alterations in ecosystem functioning, community composition and functional interactions among species. Therefore, climate change signals are already apparent on all biological scales (Parmesan, 2006; Rosenzweig et al., 2008).

Given the current global climate change scenario, there is an urgent need to understand better how organisms are affected by climate. This understanding is essential to the accurate prediction of the biological consequences of the ongoing alterations of climate and from this to delineate the necessary actions to ensure conservation of natural populations, communities and ecosystems. One of the main challenges in the study of the effects of climate on organisms is to find the key climate parameter controlling a certain biological phenomenon and its temporal and spatial scales (Hallett et al., 2004; Stenseth and Mysterud, 2005; Gordo, 2007). Temperature is probably the most frequently used climate variable in ecological research. In fact, many biological processes are temperature-dependent (e.g., metabolism, development, activity, etc.), and thus, one may make sound predictions about its effect. In addition, temperature is the climate variable with the most homogeneous and coherent pattern of change across the globe during the last century (i.e., global warming; Solomon et al., 2007). However, temperature is not the only important variable. Other variables, such as precipitation (rainfall and snow), solar radiation, wind, etc., are also essential for individual survival and ecosystem functioning and are, in some cases, as in arid regions, more important than temperature. Therefore, the key climate variable may differ according to the species or the biological process under study. Moreover, the effect of a certain climate variable may vary in space, being more influential for some populations than for others (Forchhammer et al., 2002a, b; Stenseth et al., 2004; Doi and Takahashi, 2008). Such complex responses of organisms to climate are just a reflection of the fact that weather cannot be described simply by temperature or rainfall. Weather is complex to quantify because it results from a collection of physical features of the atmosphere at a certain moment along with their interactions. In addition, weather does not affect organisms in isolation. Climate fluctuations affect all organisms in a certain ecosystem, and it is essential to understand how climate influences organisms and their interactions

with other individuals. In summary, the influence of climate on the individual seems too complex to be described simply by one or a few climate variables.

Large-scale climate indices may help one to deal with these complexities resulting from the heterogeneous influence of climate across taxa and populations. It is obvious that organisms adapt to climate at a local scale by responding to temperature, amount of rainfall, intensity of winds, and so on. However, climate is a paradigm of spatial autocorrelation because sites that are close together resemble each other in their patterns of temporal variability of climate. This feature arises from the fact that local weather is controlled by atmospheric circulatory patterns, which work on a large scale. Climate indices are able to summarize in a single value the weather conditions for a large area. This synthetic nature has been demonstrated to be of great value and use in ecology-climate research, and the application of climatic indices has become increasingly frequent during the last decade (Fig. 1).

Climatologists have defined over a dozen large-scale climate indices that govern most of the observable interannual variability of climate at the planetary scale. Among them, the El Niño-Southern Oscillation (ENSO) and the North Atlantic Oscillation (NAO) are probably the most commonly used by ecologists and are those for which the ecological consequences are best known (Stenseth et al., 2002, 2003; Forchhammer and Post, 2004). As broadly described in other parts of this book, the NAO is a large-scale fluctuation in atmospheric pressure difference along a north-south gradient between the subtropical North Atlantic region (centered on the Azores) and the subpolar region (centered on Iceland). The differences in atmospheric pressure at sea level between the subtropical and the subpolar centers affect the speed and direction of the westerly surface winds across the North Atlantic from North America to Europe (40°N–60°N). As a consequence, the numbers and paths of storms and their associated weather are affected (Hurrell, 1995; Hurrell and van Loon, 1997). Furthermore, there are effects on ocean surface temperature and currents, which in turn have direct effects on heat transport in the North Atlantic and the sea ice coverage in the Arctic region (Ottersen et al., 2001; Stenseth et al., 2003). Although present throughout the year, the greatest interannual and decadal variability is seen during the boreal winter, when the atmosphere is most dynamically active

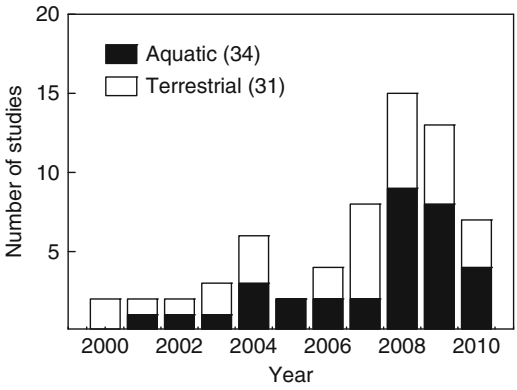

Fig. 1 Number of published studies using the North Atlantic Oscillation as an explanatory variable of any biological phenomena in terrestrial or aquatic ecosystems of the Mediterranean region Source: Isi Web of Knowledge (access date 1-10-2010)

(Hurrell, 1995). The NAO is the most robust mode of recurrent atmospheric behavior in the North Atlantic and has been suggested as the most probable cause for the remarkable changes in the climate over the middle and high latitudes of the Northern Hemisphere during recent decades (Hurrell and van Loon, 1997; Hoerling et al., 2001; Visbeck et al., 2001).

Positive values of the NAO are associated with more frequent and stronger winter storms crossing the Atlantic Ocean on a more northerly track, leading to warmer and wetter conditions in northern Europe and in the eastern coastal areas of the United States (Ottersen et al., 2001; Visbeck et al., 2001; Mysterud et al., 2003; Stenseth et al., 2003; Forchhammer and Post, 2004). In contrast, during negative phases of the NAO, the westerlies are weakened and become less frequent, and the warm and wet winter weather remains over North America, leaving northern Europe cold and dry. The most important feature arising from a comparison between the positive and the negative phases of the NAO is that this large-scale atmospheric circulatory pattern has a geographically marked differential impact on local weather. Correlations between the NAO and other climate variables, such as temperature and rainfall, vary regionally (Hurrell and van Loon, 1997; Ottersen et al., 2001; Visbeck et al., 2001; López-Moreno and Vicente-Serrano, 2008), and thus, the value and interpretation of the NAO as a proxy of climate fluctuations is variable. A paradigmatic example of regional variability is found between northern and southern Europe. During a positive phase of the NAO, the northward track of storms leads to drought anomalies in the Mediterranean basin, while northern latitudes enjoy a wetter climate than average. Unfortunately, the heterogeneous effects of the NAO at the continental scale remain poorly studied in ecology (but see Sanz, 2002, 2003; Jonzén et al., 2006; Gouveia et al., 2008). Moreover, the overwhelming majority of studies about the ecological impact of the NAO have been focussed on central and northern Europe (Ottersen et al., 2001; Mysterud et al., 2003; Forchhammer and Post, 2004), where the intensity and sign of its effect are quite different from other areas.

2 Impacts of the NAO in Mediterranean Ecosystems

Although local climate is also driven by the NAO in the Mediterranean basin, especially precipitation patterns (Lamb and Peppler, 1987; Rodó et al., 1997; Quadrelli et al., 2001; Trigo et al., 2004; Rodrigo and Trigo, 2007; Vicente-Serrano and Cuadrat, 2007), there are few studies describing ecological impacts of the NAO in Mediterranean latitudes. A search in the Web of Science using the next chain "(NAO or North Atlantic Oscillation) and Mediterranean" provided only 65 studies in the fields of Ecology, Biodiversity and Conservation, Zoology, Forestry, Marine and Freshwater Biology, Fisheries, and Agriculture (Fig. 1). Terrestrial and aquatic (both marine and freshwater) ecosystems have received similar attention (31 vs. 34 articles, respectively). Most of the studies have been published in the last few years

in journals such as *Climate Research*, *Fisheries Oceanography*, *Global Change Biology*, *International Journal of Biometeorology*, *Journal of Animal Ecology*, *Journal of Marine Systems*, or *Progress in Oceanography*. Therefore, the study of ecological impacts of the NAO in Mediterranean ecosystems is recent and has occupied many pages in some of the top journals in ecology.

In terrestrial ecosystems, it has been demonstrated that positive NAO values are related to increased growth and advancement of spring phenological events, such as flowering, leaf unfolding or pollen release, of trees (Piovesan and Schirone, 2000; Avolio et al., 2008; Campelo et al., 2009; Rozas et al., 2009; Gordo and Sanz, 2010; Orlandi et al., 2010). Nonetheless, proposed mechanisms for the NAO effect in growth and phenology were different. In the case of plant growth, the main driver is soil moisture, which is dependent mainly on winter rainfalls, which are in turn strongly dependent on the NAO (Piovesan and Schirone, 2000; Campelo et al., 2009; Rozas et al., 2009). However, the effect of the NAO on spring plant phenology would be mediated by its effect on spring temperatures (Gouveia et al., 2008; Gordo and Sanz, 2010). From a more applied point of view, the NAO has been found to affect the yields of wheat and citruses in Spain (Gimeno et al., 2002; Rodríguez-Puebla et al., 2007). Interestingly, wine production and quality were not affected by the NAO in this country (Rodó and Comín, 2000), but they were affected in Portugal (Esteves and Orgaz, 2001). Such differences in crop effects may be due to differences in the regional influence of the NAO on local weather. Therefore, the NAO influence could vary even among areas close together within the Mediterranean basin.

Evidence of NAO effects in terrestrial animals is almost entirely limited to studies with birds. We still lack in depth knowledge on the NAO effect on invertebrate, amphibian, reptile or mammal distributions, abundances and behavior. In a recent study, Martínez-Jauregui et al. (2009) demonstrated that the NAO did not have an effect on seasonal variation of weight in females of red deer (*Cervus elaphus*) in a locality in central Spain. Interestingly, the NAO did play an important role in understanding changes in body weight of females of the same species in populations in Scotland and Norway. Geographical differences in the NAO effect are seen once more, suggesting that one needs to exercise caution in generalizing the NAO effect over broad areas because its effect shows marked regional differences, especially between the Mediterranean and more northern latitudes in Europe. However, the NAO has been an important predictor of the observed changes during the last 3 decades in the diet of the nearly extinct population of Iberian brown bears (*Ursus arctos*; Rodríguez et al., 2007). By altering the phenology and productivity of some plant species (Gordo and Sanz, 2010), the NAO may play an important role in the conservation of this iconic species. The NAO has also been demonstrated to be important to understanding amphibian declines in mountainous lakes of central Spain (Bosch et al., 2007). In this particular case, the NAO has driven increases in local temperatures, which have promoted the spread of a fungus disease that causes mass mortality among amphibians.

The NAO effects in marine ecosystems of the Mediterranean Sea are probably known with greater certainty than in terrestrial ecosystems. The NAO affects the water column hydrodynamics, which in turn affect vertical gradients of mixing, nutrient flow and irradiance, by its control of weather conditions (e.g., temperature, winds, or storms). Knowledge of water column hydrodynamics is essential to an understanding of plankton functioning, abundance, and diversity, so it is not surprising that plankton community dynamics are closely related to the NAO fluctuations in the Mediterranean Sea as well as in other areas (Katara et al., 2008; Kamburska and Fonda-Umani, 2009; Gladan et al., 2010; Pérez et al., 2010). For instance, in the northwestern Mediterranean, dominant zooplankton species vary under positive and negative phases of the NAO because each phase favors different species by imposing different hydrodynamic features (Molinero et al., 2005, 2008; de Puelles et al., 2007; de Puelles and Molinero, 2008). However, the NAO can also show regional differences in its effects in the sea. For instance, *Centropages typicus*, the commonest calanoid copepod in Mediterranean waters, showed a response to the NAO in its abundance in populations in the Gulf of Naples that was opposite to its response in the Bay of Villefranche (Mazzochi et al., 2007).

The NAO effect on hydrodynamics, and consequently on plankton, may have a cascade effect on higher trophic levels. Several studies have found significant associations between the NAO and fish and cephalopod abundances in the Mediterranean (Grbec et al., 2002; Relini et al., 2006, 2010; Bridges et al., 2009; Pérez et al., 2010; but see Ravier and Fromentin, 2004). In the northwestern region of the Mediterranean Sea, the collapse of the sardine *Sardina pilchardus* stocks in the 1990s has been related to the dominant positive phase of the NAO during recent decades (Guisande et al., 2004). Similarly, the collapse of the anchovy *Engraulis encrasicolus* population in 1987 in the Adriatic Sea has been attributed to low recruitment due to the extreme positive value of the NAO during the autumn of 1986 (Santojanni et al., 2006). Along with the cascade effect through hydrodynamics and plankton, fish abundances could also be indirectly affected by water discharge of Mediterranean rivers, which is closely related to the NAO due to precipitation patterns, because the rivers supply nutrients to the sea (Lloret et al., 2001; Cartes et al., 2009).

The NAO has also been related to the strength of some currents within the Mediterranean basin. This relationship has direct effects on the horizontal transport of nutrients from some regions to others of the sea, enhancing productivity and, as consequence, the richness of marine communities. For instance, population dynamics of the hake (*Merluccius merluccius*), an economically important fishery in the Mediterranean, have been linked to the NAO through its effect on currents in the Ligurian and Tyrrhenian Seas (Abella et al., 2008; Massutí et al., 2008).

It is not only the abundance and dynamics of marine organisms that are affected by the NAO. The NAO has also been suggested as the cause of the increase of thermophilic species in the Adriatic Sea as a result of its control over sea temperature (Dulcic et al., 2004; Grubelic et al., 2004).

The NAO fingerprint has also been detected in benthonic communities. For instance, periodical surveys of the benthic macrofauna (especially polychetes) in

the Bay of Banyuls-sur-Mer (France) since the 1960s have shown notable changes that have been partially attributed to NAO fluctuations (Lebrune et al., 2007). This fingerprint can reach even those benthic communities living at depths greater than 1000 m. Off the Catalan coast, it was found that changes in the abundance and composition of deep megabenthos were related to the contrasting values of the NAO between the surveys carried out at the end of the 1980s and the end of the 2000s (Cartes et al., 2009). Similarly, landings of the shrimp *Aristeus antennatus*, which lives at depths between 600 and 800 m, were higher following positive values of the winter NAO (Maynou, 2008a, b). In this case, there was a time lag in the response to the NAO, supporting the idea that the NAO effect may be carried by a population over a number of years following a particular NAO situation (Ottersen et al., 2001).

3 Effects of the NAO on Bird Populations

The NAO has a direct effect on demographic parameters, such as survival, dispersal or fecundity, of many animal species (Ottersen et al., 2001; Mysterud et al., 2003; Forchhammer and Post, 2004). Therefore, one expects to find effects of the NAO on abundances and dynamics of bird populations, and they have indeed been found (Sæther et al., 2004). For instance, a long-term study in a Norwegian population of dippers (*Cinclus cinclus*) demonstrated that year-to-year variations in the population size were positively related to the NAO index, i.e., the population increased under positive NAO values (Sæther et al., 2000). Positive NAO values were related to milder winters, which reduced the duration of the frozen surface of rivers where these individuals forage. These improved conditions for foraging enhanced survival, especially of the younger individuals, which recruited in larger numbers the next spring, leading to an increase in the breeding population.

In the Mediterranean region, the NAO effects on dynamics and demography of bird populations have been studied in a wide variety of species, such as water birds (Almaraz and Amat, 2004a, b; Figuerola, 2007; Bechet and Johnson, 2008; Jiguet et al., 2008), seabirds (Jenouvrier et al., 2009), raptors (Rodríguez and Bustamante, 2003; Costantini et al., 2010), and songbirds (Sanz, 2002, 2003; Grosbois et al., 2006; Rubolini et al., 2007; Balbontín et al., 2009). Such diversity of species demonstrates that NAO signals are apparent in the Mediterranean avifauna as a whole and supports the notion that the NAO effect can be found across all habitats of a large area like the Mediterranean.

Several studies have demonstrated effects of the NAO on water birds, a fact that is not surprising if we take into account the strong dependence of these species on lakes, ponds and marshlands. The occurrence and extent of wetlands in the Mediterranean region are strongly dependent on precipitation patterns, which in turn are driven by the NAO (see other chapters in this book). Almaraz and Amat (2004a, b) showed for the first time that large-scale indices, such as the NAO and the ENSO, were related to population dynamics of the white-headed duck (*Oxyura leucocephala*), a threatened water bird species. Low values of the winter NAO were

linked with increased rainfall, which led to a large expansion of the range of the species during the following breeding season as a result of an increase in wetland surface in Spain (Almaraz and Amat, 2004a). Furthermore, El Niño events (i.e., high ENSO values) were linked with increased rainfall during the summer in the Mediterranean, which reduced breeding densities and increased markedly the recruitment in the next year.

In similar studies, some breeding populations of waders from the Mediterranean showed clear fluctuations in their numbers related to the NAO. In the Doñana National Park (southwestern Spain), the black-winged stilt (*Himantopus himantopus*) breeds in numbers from a dozen pairs up to more than 14,000 pairs (which represents about 30% of the European population). Such extreme variability was related to positive and negative phases of the NAO, respectively, which affect the extent of the Doñana marshlands and consequently the phylopatry and dispersal behavior of this species (Figuerola, 2007). The NAO also drives the hydrological conditions of another major wetland area of the Mediterranean, the Camargue (southern France). Interestingly, the NAO signal is even detected in those populations that use strongly human-managed habitats, such as the commercial salt pans, for breeding, as in the case of the greater flamingo (*Phoenicopterus roseus*; Bechet and Johnson, 2008). Even though the date of the start of salt production determines the potential number of breeding pairs of the species each year, the observed breeding population is also dependent on the water levels in the Camargue lagoons, which are under the NAO influence. A larger extent of marshlands increases the food availability and thus the opportunities for breeding.

Kestrels are small falcons that inhabit open landscapes in Europe and Asia. During the twentieth century, the lesser kestrel (*Falco naumanni*) has shown marked declines, which have led to a threatened status in most European countries and even to extinction in some. Rodríguez and Bustamante (2003) investigated whether recent climatic changes were related to declines in populations from southern Spain. They found significant influences of the winter NAO and annual precipitation patterns on kestrel demography. However, rainfall outperformed the predictive ability of the NAO in demographic models because rainfall probably captured better the environmental variability at the local scale, i.e., at the scale of the breeding colonies of the species. Nevertheless, the rainfall in southern Spain and the NAO showed strong correlations, and thus the NAO influence on bird demography could be shown for this terrestrial species via precipitation amount and seasonal distribution. However, in spite of the drier conditions recorded during recent decades in the kestrel colonies as a result of the prevailing positive phase of the NAO, the authors concluded that the effect was not sufficient to explain the population declines and that causes must be sought in other environmental factors. In Italy, reproductive decisions and reproductive success in a population of kestrels (*Falco tinnunculus*) were also closely related to rainfall, temperature and the NAO index during both the spring and the previous winter (Costantini et al., 2010). Contrary to predictions, this population laid smaller clutches after mild and dry winters (i.e., positive winter NAO index). The authors hypothesized as possible causes for this result a greater survival of low-quality individuals during the winter and/or a disruption in prey phenology.

Nevertheless, the mechanism is unclear, and this fact demonstrated the complexities of the NAO influence on animal population dynamics. The NAO effect can be mediated by conditions in previous seasons, and the balance between current and past weather determines environmental conditions and thus the observable reproductive success.

In a similar way, the NAO effect may be different among different populations (e.g., Sanz, 2002), and this fact may lead to divergent patterns of response to climate change. For instance, barn swallows (*Hirundo rustica*) from Spain are more likely to survive during their first year of life when the winter NAO is positive, while Danish swallows show increased mortality during positive phases of the winter NAO (Balbontín et al., 2009). Unlike the black-winged stilt recruitment (Figuerola, 2007), the recruitment probability of the barn swallows to their natal areas was not affected by the NAO. In these studied populations of swallows, dispersal was explained by another large-scale climate index, the Southern Oscillation Index (SOI), which also showed an opposite effect between the two populations (Balbontín et al., 2009).

4 Effects of the NAO on Bird Migration

Every year millions of individuals move between breeding and wintering areas in one of the most fascinating events of nature: bird migration. Bird migration has long been known to be influenced by weather (Newton, 2008). In fact, the arrival of some migratory species, such as swallows or cuckoos (*Cuculus canorus*), has been traditionally used as an unequivocal signal of spring onset. This sensitivity of bird migratory phenology to weather has led to a renewed interest in this phenomenon in light of the ongoing climate change. If bird migration is sensitive to climate fluctuations, we can use it as a bioindicator of climate change impacts. A plethora of studies has demonstrated shifts in the timing of migration for many species along with significant relationships between climate from departure, passage and arrival areas and bird phenology (see reviews in Gordo, 2007; Lehikoinen and Sparks, 2010). Although climate change seems to be the cause for the alteration of bird migration timing during recent decades, the precise ecological and evolutionary mechanisms by which birds are changing their migratory schedule in response to the new environmental conditions remain to be elucidated.

The arrival date of a migrant to a certain site depends on two factors: (1) the onset date of migration and (2) the speed of progression across the areas between the start and end points of its journey (Gordo, 2007). Experiments with captive birds have demonstrated that the onset of migration is controlled by inflexible endogenous rhythms with a genetic basis (Berthold, 2001; Newton, 2008). However, a growing number of correlative studies have recently suggested some plasticity in the onset of migration; i.e., birds may adjust their departure date according to the prevailing weather or to the ecological conditions found at their departure areas (Saino et al., 2004; Gordo et al., 2005; Saino et al., 2007; Gordo and Sanz, 2008). In addition, many other studies have demonstrated that temperature, precipitation, wind, or vegetation phenology in the passage areas affect bird progression (Gordo, 2007). Overall,

the evidence suggests that climate may influence bird migration both directly and indirectly at several times throughout the year and at several sites. Such complexities of climate effects are not surprising if one takes into account the fact that migrants spend much time moving across vast areas. In this situation, large-scale climate indices become ideal explanatory variables for bird migratory phenology because they are capable of summarizing these complexities of local weather in a single variable that is easy to interpret and obtain (see Section 1).

The NAO index was employed for the first time by Forchhammer et al. (2002a) to explain migratory phenology of some common migrants in Norway. Since then, more than 30 studies have used this variable to explain interannual variability in arrival dates of migrants (Gordo, 2007; Hubálek and Čapek, 2008; Donnelly et al., 2009; Balbontín et al., 2009; Tøttrup et al., 2010). As a norm, most of the time-series of arrival dates show a negative relationship with the NAO; i.e., birds arrive early when the NAO (especially the winter NAO index) is positive (Gienapp et al., 2007). Positive NAO values imply milder winters and thus an advance of the spring (e.g., earlier flowering and leafing of plants, Gordo and Sanz, 2010) and an enhancement of weather conditions during migratory flights (e.g., more tail winds, Hüppop and Hüppop, 2003; Sinelschikova et al., 2007). Therefore, the proposed mechanism for the effect of positive NAO values on migration is the improved environmental conditions for migratory progression across Europe in terms of both food availability and the weather.

However, this picture may be less clear than it seems because most of the studies have been conducted in northern and western Europe, where the NAO effect is stronger and bird populations are subjected along their entire migratory route to the NAO influence. If we focus on the particular case of Mediterranean populations, there are few studied cases, and those studies that do exist usually suggest no effect of the NAO. In Spain, the arrival dates of five common migrants, the white stork (*Ciconia ciconia*), the cuckoo, the swift (*Apus apus*), the barn swallow or the nightingale (*Luscinia megarhynchos*), were not related to the NAO, either for earlier individuals or for later ones (Gordo and Sanz, 2008). In a locality of central Italy, the arrival dates of the first swifts, swallows and nightingales were not related to either the winter NAO (December–March) or the spring NAO (March–May) (Rubolini et al., 2007). Here, only one species, the house martin (*Delichon urbicum*), advanced significantly their arrival in response to positive winter NAO. In a long-term monitoring study of the arrival dates of nightingales in Croatia (Kralj and Dolenec, 2008), the winter NAO did not show any effect. Although the number of studies of Mediterranean bird populations is still small, the evidence suggests that the NAO has little influence on their arrival dates. This fact supports the idea that the NAO effect would be felt mainly from the Mediterranean latitudes northwards and thus, that only those populations breeding in the northernmost regions of the continent, and consequently with extensive migratory routes over Europe, would be significantly influenced by the NAO (Forchhammer et al., 2002a; Hüppop and Hüppop, 2003). Moreover, some studies have demonstrated that the negative

relationship with the winter NAO is stronger in short-distance migrants (i.e., those species overwintering in the Mediterranean basin) than in long-distance ones (i.e., those species overwintering to the south of the Sahara) (Rainio et al., 2006; Tøttrup et al., 2010). If it is considered that positive NAO values are related to drought in the Mediterranean and thus to harsh ecological conditions, it follows that short-distance migrants must benefit from a positive NAO *en route* but not during their wintering stay in the Mediterranean. Unfortunately, the environmental factors operating on the dynamics of wintering populations in the Mediterranean are poorly known, as is the effect of the NAO.

Finally, the Mediterranean basin is an obligatory passage area for all long-distance migrants coming from Africa and moving into Europe for breeding (Newton, 2008). In spite of this key role in the European-African migratory system, only two studies have analyzed the NAO effect on passing migratory bird populations. The *Istituto Nazionale per la Fauna Selvatica* from Italy has been promoting since 1988 the monitoring scheme *Progetto Piccole Isole*. This is a network of ringing sites located in islands and coastal sites, mainly in the central and western parts of the Mediterranean Sea (Italy, Spain, France and Malta), that uses standardized protocols for traping birds (Spina et al., 1993). One of the pioneering and most active ringing stations is located on the Italian island of Capri. There, the passage dates of nine trans-Saharan species were positively correlated to the winter NAO both in early and in late individuals, in opposition to the relationship found between the NAO and passage dates for the same species in ringing sites in Scandinavia (Jonzén et al., 2006). While a positive NAO would enhance migration across Europe (see above), it would impair ecological conditions in northern Africa by droughts in the Mediterranean basin and rainfall deficits during the monsoon season in West Africa (Lamb and Peppler, 1987; Hurrell, 1995; McHugh and Rogers, 2001; Oba et al., 2001; Stige et al., 2006). Therefore, the contrasting effect of the NAO in passage dates of the same species between Mediterranean and Scandinavian latitudes reinforces the idea of the heterogeneous effect of this variable among regions and thus their populations. Populations in Scandinavia have traveled for weeks across Europe and have benefited from enhanced conditions for migratory progression due to positive phases of the NAO. However, in Italy, just after the birds leave Africa, the positive phase of the NAO has the opposite consequences in the environment, and this is reflected in a delayed passage date. However, this is just one study in a single locality. A recent study with 11 migratory species on 3 Spanish islands demonstrated that the NAO did not have any effect on passage dates (Robson and Barriocanal, 2011). Moreover, it was the worst explanatory variable of the timing of migration compared to other predictors, such as temperature, vegetation productivity or the SOI. This extreme contrast in the results of different studies highlights the urgent need to develop more studies in the Mediterranean region to elucidate the true effects of the NAO on migratory bird phenology and the potential regional variability in the effects in relation to each migratory route across the Mediterranean.

5 Conclusions

There is already a notable number of studies that have assessed the effect of NAO fluctuations on a wide variety of species and biological phenomena in the Mediterranean region (Fig. 1). However, after a comprehensive review of the available evidence, we conclude that the impacts of the NAO on Mediterranean ecosystems are still poorly understood, especially on terrestrial ecosystems. We have identified three major non-excluding possible causes for the present state of the art:

(i) There is a considerable heterogeneity in the species and biological phenomena studied, and consequently, there are only one or a few populations studied in each case and usually from a single site. This fact hinders seriously our capacity to make generalizations because the NAO effect on local weather (the relevant scale for organisms) varies among regions (even within the Mediterranean), and we must be very cautious about extrapolating results from one site to others. In addition, many studies, especially in aquatic ecosystems, just report significant associations between the NAO and biological phenomena without providing a mechanistic interpretation of these results. We are firmly convinced that without a biological interpretation, results are of limited use.

(ii) Most of the studies have assessed only the effect of the winter NAO index (December–March), probably imitating the pioneering studies carried out in northern latitudes. Indeed, this phase shows the greater variability (Hurrell, 1995), but the potential influence of the NAO in organisms through climate patterns of other seasons has been completely neglected (but see Gordo and Sanz, 2010). The NAO effect on climate over the whole annual cycle is well-known by the climatologists (e.g., this book), but this is another point where considerably additional progress needs to be made. The climatologic literature is extensive, but unfortunately it is difficult to understand for most ecologists. In addition, the method of studying and defining climate patterns by climatologists is not necessarily the most relevant for organisms (e.g., see Doi et al., 2008). It seems obvious that there is an urgent need to establish multidisciplinary collaborations between climatologists and ecologists to deal accurately with the complex interactions between climate and biosphere.

(iii) Despite the NAO influence on the variability of Mediterranean climate, the NAO may indeed have little effect on Mediterranean ecosystems, especially on terrestrial ecosystems, as the remarkable number of studies reporting non-significant results may demonstrate (e.g., Ravier and Fromentin, 2004; Grosbois et al., 2006; Gordo and Sanz, 2008; Jiguet et al., 2008; Kralj and Dolenec, 2008; Jenouvrier et al., 2009; Robson and Barriocanal, 2011). Moreover, some studies have shown that the NAO effect is overridden by local weather (e.g., Rodríguez and Bustamante, 2003; Gordo and Sanz, 2010). The extremely variable nature of the Mediterranean climate among years as well as the complex balances between temperature and rainfall could be the cause for the poor correlations with the NAO. However, a larger sample of studies would be needed to distinguish unambiguously between a real absence of an effect and a simple lack of evidence.

In view of the current climate change, we need to improve our knowledge about climate effects on organisms. The NAO, as a major driver of climate in the Mediterranean region, may become a keystone to the understanding of past, present and future impacts of climate change on Mediterranean ecosystems. However, the mechanisms by which the NAO influences organisms in Mediterranean ecosystems are different and to some extent more complex than they are in more northern latitudes. These facts demand of the Mediterranean ecologists more original thought and more effort to start long-term monitoring programs of biodiversity and to enhance and maintain those already in progress.

Acknowledgements Oscar Gordo was supported by a Juan de la Cierva contract (ref. JCI-2009-05274).

References

Abella A, Fiorentino F, Mannini A, Relini LO (2008) Exploring relationships between recruitment of European hake (*Merluccius merluccius* L. 1758) and environmental factors in the Ligurian Sea and the Strait of Sicily (Central Mediterranean). J Mar Syst 71:279–293

Almaraz P, Amat JA (2004a) Complex structural effects of two hemispheric climatic oscillators on the regional spatio-temporal expansion of a threatened bird. Ecol Lett 7:547–556

Almaraz P, Amat JA (2004b) Multi-annual spatial and numeric dynamics of the white-headed duck *Oxyura leucocephala* in southern Europe: seasonality, density dependence and climatic variability. J Anim Ecol 73:1013–1023

Avolio E, Pasqualoni L, Federico S, Fornaciari M, Bonofiglio T, Orlandi F, Bellecci C, Romano B (2008) Correlation between large-scale atmospheric fields and the olive pollen season in Central Italy. Int J Biometeorol 52:787–796

Balbontín J, Møller AP, Hermosell IG, Marzal E, Reviriego M, de Lope F (2009) Divergent patterns of impact of environmental conditions on life history traits in two populations of a long-distance migratory bird. Oecologia 159:859–872

Bechet A, Johnson AR (2008) Anthropogenic and environmental determinants of Greater Flamingo *Phoenicopterus roseus* breeding numbers and productivity in the Camargue (Rhone delta, southern France). Ibis 150:69–79

Begon M, Townsend CR, Harper JL (2006) Ecology: from individuals to ecosystems, 4th edn. Blackwell Publishing, Oxford

Berthold P (2001) Bird migration: a general survey. Oxford University Press, Oxford

Bosch J, Carrascal LM, Durán L, Walker S, Fisher MC (2007) Climate change and outbreaks of amphibian chytridiomycosis in a montane area of Central Spain: is there a link? Proc Roy Soc Lond B 274:253–260

Bridges CR, Krohn O, Deflorio M, de Metrio G (2009) Possible NAO and SST influences on the eastern bluefin tuna stock – the in-exfish approach. Collect Vol Sci Papers ICCAT 63: 138–152

Campelo F, Nabais C, García-González I, Cherubini P, Gutiérrez E, Freitas H (2009) Dendrochronology of *Quercus ilex* L. and its potential use for climate reconstruction in the Mediterranean region. Can J For Res 39:2486–2493

Cartes JE, Maynou F, Fanelli E, Papiol V, Lloris D (2009) Long-term changes in the composition and diversity of deep-slope megabenthos and trophic webs off Catalonia (western Mediterranean): Are trends related to climatic oscillations? Prog Oceanogr 82:32–46

Costantini D, Carello L, Dell'Omo G (2010) Patterns of covariation among weather conditions, winter North Atlantic Oscillation index and reproductive traits in Mediterranean kestrels. J Zoology 280:177–184

de Puelles MLF, Alemany F, Jansa J (2007) Zooplankton time-series in the Balearic Sea (western Mediterranean): Variability during the decade 1994–2003. Prog Oceanogr 74:329–354

de Puelles MLF, Molinero JC (2008) Decadal changes in hydrographic and ecological time-series in the Balearic Sea (western Mediterranean), identifying links between climate and zooplankton. ICES J Mar Sci 65:311–317

Doi H, Gordo O, Katano I (2008) Heterogeneous intra-annual climatic changes drive different phenological responses at two trophic levels. Clim Res 36:181–190

Doi H, Takahashi M (2008) Latitudinal patterns in the phenological responses of leaf colouring and leaf fall to climate change in Japan. Glob Ecol Biogeogr 17:556–561

Donnelly A, Cooney T, Jennings E, Buscardo E, Jones M (2009) Response of birds to climatic variability: evidence from the western fringe of Europe. Int J Biometeorol 53:211–220

Dulcic J, Grbec B, Lipej L, Paklar GB, Supic N, Smircic A (2004) The effect of the hemispheric climatic oscillations on the Adriatic ichthyofauna. Fresenius Environ Bull 13:293–298

Esteves MA, Orgaz MDM (2001) The influence of climatic variability on the quality of wine. Int J Biometeorol 45:13–21

Figuerola J (2007) Climate and dispersal: Black-winged stilts disperse further in dry springs. PLoS ONE 2:e539

Forchhammer MC, Post E (2004) Using large-scale climate indices in climate change ecology studies. Popul Ecol 46:1–12

Forchhammer MC, Post E, Stenseth NC (2002a) North Atlantic Oscillation timing of long- and short-distance migration. J Anim Ecol 71:1002–1014

Forchhammer MC, Post E, Stenseth NC, Boertmann DM (2002b) Long-term responses in arctic ungulate dynamics to changes in climatic and trophic processes. Popul Ecol 44:113–120

Gienapp P, Leimu R, Merilä J (2007) Responses to climate change in avian migration time – microevolution or phenotypic plasticity? Clim Res 35:25–35

Gimeno L, Ribera P, Iglesias R, de la Torre L, García R, Hernández E (2002) Identification of empirical relationships between indices of ENSO and NAO and agricultural yields in Spain. Clim Res 21:165–172

Gladan ZN, Marasovic I, Grbec B, Skejic S, Buzancic M, Kuspilic G, Matijevic S, Matic F (2010) Inter-decadal variability in phytoplankton community in the Middle Adriatic (Katela Bay) in relation to the North Atlantic Oscillation. Estuaries Coasts 33:376–383

Gordo O (2007) Why are bird migration dates shifting? A review of weather and climate effects on avian migratory phenology. Clim Res 35:37–58

Gordo O, Brotons L, Ferrer X, Comas P (2005) Do changes in climate patterns in wintering areas affect the timing of the spring arrival of trans-Saharan migrant birds? Glob Change Biol 11: 12–21

Gordo O, Sanz JJ (2008) The relative importance of conditions in wintering and passage areas on spring arrival dates: the case of long-distance Iberian migrants. J Ornithol 149:199–210

Gordo O, Sanz JJ (2010) Impact of climate change on plant phenology in Mediterranean ecosystems. Glob Change Biol 16:1082–1106

Gouveia C, Trigo RM, DaCamara CC, Libonati R, Pereira JMC (2008) The North Atlantic Oscillation and European vegetation dynamics. Int J Climatol 28:1835–1847

Grbec B, Dulcic J, Morovic M (2002) Long-term changes in landings of small pelagic fish in the eastern Adriatic – possible influence of climate oscillations over the Northern Hemisphere. Clim Res 20:241–252

Grosbois V, Henry PY, Blondel J, Perret P, Lebreton JD, Thomas DW, Lambrechts MM (2006) Climate impacts on Mediterranean blue tit survival: an investigation across seasons and spatial scales. Glob Change Biol 12:2235–2249

Grubelic I, Antolic B, Despalatovic M, Grbec B, Paklar GB (2004) Effect of climatic fluctuations on the distribution of warm-water coral *Astroides calycularis* in the Adriatic Sea: new records and review. J Mar Biol Assoc UK 85:599–602

Guisande C, Vergara AR, Riveiro I, Cabanas JM (2004) Climate change and abundance of the Atlantic-Iberian sardine (*Sardina pilchardus*). Fish Oceanogr 13:91–101

Hallett TB, Coulson T, Pilkington JG, Clutton-Brock TH, Pemberton JM, Grenfell BT (2004) Why large-scale climate indices seem to predict ecological processes better than local weather. Nature 430:71–75

Hoerling MP, Hurrell JW, Xu T (2001) Tropical origins for recent North Atlantic climate change. Science 292:90–92

Hubálek Z, Čapek M (2008) Migration distance and the effect of North Atlantic Oscillation on the spring arrival of birds in Central Europe. Folia Zoologica 57:212–220

Hüppop O, Hüppop K (2003) North Atlantic Oscillation and timing of spring migration in birds. Proc Roy Soc Lond B 270:233–240

Hurrell JW (1995) Decadal trends in the North Atlantic Oscillation: regional temperatures and precipitation. Science 269:676–679

Hurrell JW, Van Loon H (1997) Decadal variations in climate associated with North Atlantic Oscillation. Clim Change 36:301–326

Jenouvrier S, Thibault JC, Viallefont A, Vidal P, Ristow D, Mougin JL, Brichetti P, Borg JJ, Bretagnolle V (2009) Global climate patterns explain range-wide synchronicity in survival of a migratory seabird. Glob Change Biol 15:268–279

Jiguet F, Doxa A, Robert A (2008) The origin of out-of-range pelicans in Europe: wild bird dispersal or zoo escapes? Ibis 150:606–618

Jonzén N, Lindén A, Ergon T, Knudsen E, Vik JO, Rubolini D, Piacentini. D, Brinch C, Spina F, Karlsson L, Stervander M, Andersson A, Waldenström J, Lehikoinen A, Edvardsen E, Solvang R, Stenseth NC (2006) Rapid advance of spring arrival dates in long-distance migratory birds. Science 312:1959–1961

Kamburska L, Fonda-Umani S (2009) From seasonal to decadal inter-annual variability of mesozooplankton biomass in the Northern Adriatic Sea (Gulf of Trieste). J Mar Syst 78: 490–504

Katara I, Illian J, Pierce GJ, Scott B, Wang JJ (2008) Atmospheric forcing on chlorophyll concentration in the Mediterranean. Hydrobiologia 612:33–48

Kralj J, Dolenec Z (2008) First arrival dates of the Nightingale (*Luscinia megarhynchos*) to Central Croatia in the early 20th century and at the turn of the 21st century. Cent Eur J Biol 3: 295–298

Lamb PJ, Peppler RA (1987) North Atlantic Oscillation: concept and application. Bull Am Meteorol Soc 68:1218–1225

Lebrune C, Gremare A, Guizien K, Amouroux JM (2007) Long-term comparison of soft bottom macrobenthos in the Bay of Banyuls-sur-Mer (north-western Mediterranean Sea): a reappraisal. J Sea Res 58:125–143

Lehikoinen E, Sparks TH (2010) Bird migration. In: Møller AP, Fiedler W, Berthold P (eds) Effects of climate change on birds. Oxford University Press, Oxford, pp 89–112

Lloret J, Lleonart J, Solé I, Fromentin JM (2001) Fluctuations of landings and environmental conditions in the north-western Mediterranean Sea. Fish Oceanogr 10:33–50

López-Moreno JI, Vicente-Serrano SM (2008) Positive and negative phases of the winter-time North Atlantic Oscillation and drought occurrence over Europe: a multitemporal-scale approach. J Clim 21:1220–1243

Martínez-Jauregui M, San Miguel-Ayanz A, Mysterud A, Rodríguez-Vigal C, Clutton-Brock TH, Langvatn R, Coulson T (2009) Are local weather, NDVI and NAO consistent determinants of red deer weight across three contrasting European countries? Glob Change Biol 15: 1727–1738

Massutí E, Monserrat S, Oliver P, Moranta J, López-Jurado JL, Marcos M, Hidalgo M, Guijarro B, Carbonell A, Pereda P (2008) The influence of oceanographic scenarios on the population dynamics of demersal resources in the western Mediterranean: hypothesis for hake and red shrimp off Balearic Islands. J Mar Syst 71:421–438

Maynou F (2008a) Environmental causes of the fluctuations of red shrimp (*Aristeus antennatus*) landings in the Catalan Sea. J Mar Syst 71:294–302

Maynou F (2008b) Influence of the North Atlantic Oscillation on Mediterranean deep-sea shrimp landings. Clim Res 36:253–257

Mazzochi MG, Christou ED, Di Capua I, de Puelles MLF, Fonda-Umani S, Molinero JC, Nival P, Siokou-Frangou I (2007) Temporal variability of *Centropages typicus* in the Mediterranean Sea over seasonal-to-decadal scales. Prog Oceanogr 72:214–232

McHugh MJ, Rogers JC (2001) North Atlantic Oscillation influence on precipitation variability around the Southeast African convergence zone. J Clim 14:3631–3642

Molinero JC, Ibañez F, Souissi S, Buecher E, Dallot S, Nival P (2008) Climate control on the long-term anomalous changes of zooplankton communities in the northwestern Mediterranean. Glob Change Biol 14:11–26

Molinero JC, Ibañez F, Souissi S, Chifflet M, Nival P (2005) Phenological changes in the northwestern Mediterranean copepods *Centropages typicus* and *Temora stylifera* linked to climate forcing. Oecologia 145:640–649

Mysterud A, Stenseth NC, Yoccoz NG, Ottersen G, Langvatn R (2003) The response of terrestrial ecosystems to climate variability associated with the North Atlantic Oscillation. In: Hurrell JW, Kushnir Y, Ottersen G, Visbeck MH (eds) The North Atlantic Oscillation: climatic significance and environmental impact. American Geophysical Union, Washington, pp 235–262

Newton I (2008) The migration ecology of birds. Academic Press, London

Oba G, Post E, Stenseth NC (2001) Sub-Saharan desertification and productivity are linked to hemispheric climate variability. Glob Change Biol 7:241–246

Orlandi F, García-Mozo H, Galán C, Romano B, Díaz de la Guardia C, Ruiz L, del Mar Trigo M, Domínguez-Vilches E, Fornaciari M (2010) Olive flowering trends in a large Mediterranean area (Italy and Spain). Int J Biometeorol 54:151–163

Ottersen G, Planque B, Belgrano A, Post E, Reid PC, Stenseth NC (2001) Ecological effects of the North Atlantic Oscillation. Oecologia 128:1–14

Parmesan C (2006) Ecological and evolutionary responses to recent climate change. Annu Rev Ecol Evol Syst 37:637–669

Parmesan C, Yohe G (2003) A globally coherent fingerprint of climate change impacts across natural systems. Nature 421:37–42

Piovesan G, Schirone B (2000) Winter North Atlantic Oscillation effects on the tree rings of the Italian beech (*Fagus sylvatica* L.). Int J Biometeorol 44:121–127

Pérez FF, Padín XA, Pazos Y, Gilcoto M, Cabanas M, Pardo PC, Doval MD, Farina-Busto L (2010) Plankton response to weakening of the Iberian coastal upwelling. Glob Change Biol 16:1258–1267

Quadrelli R, Pavan V, Molteni F (2001) Wintertime variability of Mediterranean precipitation and its links with large-scale circulation anomalies. Clim Dyn 17:457–466

Rainio K, Laaksonen T, Ahola M, Vähätalo AV, Lehikoinen E (2006) Climatic responses in spring migration of boreal and arctic birds in relation to wintering area and taxonomy. J Avian Biol 37:507–515

Ravier C, Fromentin JM (2004) Are the long-term fluctuations in Atlantic bluefin tuna (*Thunnus thynnus*) population related to environmental changes? Fish Oceanogr 13:145–160

Relini LO, Mannini A, Fiorentino F, Palandri G, Relini G (2006) Biology and fishery of *Eledone cirrhosa* in the Ligurian Sea. Fish Res 78:72–88

Relini LO, Palandri G, Garibaldi F, Relini M, Cima C, Lanteri L (2010) Large pelagic fish, swordfish, bluefin and small tunas, in the Ligurian Sea: biological characteristics and fishery trends. Chem Ecol 26:341–357

Robson D, Barriocanal C (2011) Ecological conditions in wintering and passage areas as determinants of timing of spring migration in trans-Saharan migratory birds. J Anim Ecol 80:320–331

Rodó X, Baert E, Comín FA (1997) Variations in seasonal rainfall in Southern Europe during the present century: relationships with the North Atlantic Oscillation and the El Niño-Southern Oscillation. Clim Dyn 13:275–284

Rodó X, Comín FA (2000) Links between large-scale anomalies, rainfall and wine quality in the Iberian Peninsula during the last three decades. Glob Change Biol 6: 267–273

Rodrigo FS, Trigo RM (2007) Trends in daily rainfall in the Iberian Peninsula from 1951 to 2002. Int J Climatol 27:513–529

Rodríguez C, Bustamante J (2003) The effect of weather on lesser kestrel breeding success: can climate change explain historical population declines? J Anim Ecol 72:793–810

Rodríguez C, Naves J, Fernández-Gil A, Obeso JR, Delibes M (2007) Long-term trends in food habits of a relict brown bear population in northern Spain: the influence of climate and local factors. Environ Conserv 34:36–44

Rodríguez-Puebla C, Ayuso SM, Frías MD, García-Casado LA (2007) Effects of climate variation on winter cereal production in Spain. Clim Res 34:223–232

Root TL, Price JT, Hall KR, Schneider SH, Rosenzweig C, Pounds JA (2003) Fingerprints of global warming on wild animals and plants. Nature 421:57–60

Rosenzweig C, Karoly D, Vicarelli M, Neofotis P, Wu Q, Casassa G, Menzel A, Root TL, Estrella N, Seguin B, Tryjanowski P, Liu C, Rawlins S, Imeson A (2008) Attributing physical and biological impacts to anthropogenic climate change. Nature 435:353–357

Rozas V, Lamas S, García-González I (2009) Differential tree-growth responses to local and large-scale climatic variation in two *Pinus* and two *Quercus* species in northwest Spain. Ecoscience 16:299–310

Rubolini D, Ambrosini R, Caffi M, Brichetti P, Armiraglio S, Saino N (2007) Long-term trends in first arrival and first egg laying dates of some migrant and resident bird species in northern Italy. Int J Biometeorol 51:553–563

Saino N, Rubolini D, Jonzén N, Ergon T, Montemaggiori A, Stenseth NC, Spina F (2007) Temperature and rainfall anomalies in Africa predict timing of spring migration in trans-Saharan migratory birds. Clim Res 35:123–134

Saino N, Szep T, Romano M, Rubolini D, Spina F, Møller AP (2004) Ecological conditions during winter predict arrival date at the breeding quarters in a trans-Saharan migratory bird. Ecol Lett 7:21–25

Sala OE, Chapin FS, Armesto JJ, Berlow E, Bloomfield J, Dirzo R, Huber-Sanwald E, Huenneke LF, Jackson RB, Kinzig A, Leemans R, Lodge DM, Mooney HA, Oesterheld M, LeRoy Poff N, Sykes MT, Walker BH, Walker M, Wall DH (2000) Global biodiversity scenarios for the year 2100. Science 287:1770–1774

Santojanni A, Arneri E, Bernardini V, Cingolani N, Di Marco M, Russo A (2006) Effects of environmental variables on recruitment of anchovy in the Adriatic Sea. Clim Res 31:181–193

Sanz JJ (2002) Climate change and breeding parameters of great and blue tits throughout the western Palaeartic. Glob Change Biol 8:408–422

Sanz JJ (2003) Large-scale effect of climate change on breeding parameters of pied flycatchers in Western Europe. Ecography 26:45–50

Sæther BE, Sutherland WJ, Engen S (2004) Climate influences on avian population dynamics. Adv Ecol Res 35:185–209

Sæther BE, Tufto J, Engen S, Jerstad K, Rostad OW, Skåtan JE (2000) Population dynamical consequences of climate change for a small temperate songbird. Science 287:855–856

Sinelschikova A, Kosarev V, Panov I, Baushev AN (2007) The influence of wind conditions in Europe on the advance in timing of the spring migration of the song thrush (*Turdus philomelos*) in the south-east Baltic region. Int J Biometeorol 51:431–440

Solomon S, Qin D, Manning M, Chen Z, Marquis M, Averyt KB, Tignor M, Miller HL (eds) (2007) Climate change 2007: the physical science basis. Contribution of Working Group I to the 4th assessment report of the Intergovernmental panel on climate change. Cambridge University Press, Cambridge

Spina F, Massi A, Montemaggiori A, Baccetti N (1993) Spring migration across central Mediterranean: general results from the 'Progetto Piccole Isole'. Die Vogelwarte 37:1–94

Stenseth NC, Ehrich D, Rueness EK, Lingjærde OC, Chan KS, Boutin S, O'Donoghue M, Robinson DA, Viljugrein H, Jakobsen KS (2004) The effect of climatic forcing on population synchrony and genetic structuring of the Canadian lynx. Proc Natl Acad Sci USA 101:6056–6061

Stenseth NC, Mysterud A (2005) Weather packages: finding the right scale and composition of climate in ecology. J Anim Ecol 74:1195–1198

Stenseth NC, Mysterud A, Ottersen G, Hurrell JW, Chan KS, Lima M (2002) Ecological effects of climate fluctuations. Science 297:1292–1296

Stenseth NC, Ottersen G, Hurrell JW, Mysterud A, Lima M, Chan KS, Yoccoz NG, Ådlandsvik B (2003) Studying climate effects on ecology through the use of climate indices: the North Atlantic Oscillation, El Niño Southern Oscillation and beyond. Proc Roy Soc Lond B 270:2087–2096

Stige LC, Stave J, Chan KS, Ciannelli L, Pettorelli N, Glantz M, Herren HR, Stenseth NC (2006) The effect of climate variation on agro-pastoral production in Africa. Proc Natl Acad Sci USA 103:3049–3053

Tøttrup AP, Rainio K, Coppack T, Lehikoinen E, Rahbek C, Thorup K (2010) Local temperature fine-tunes the timing of spring migration in birds. Integr Comp Biol 50:293–304

Trigo RM, Pozo-Vázquez D, Osborn TJ, Castro-Díez Y, Gámiz-Fortis S, Esteban-Parra MJ (2004) North Atlantic oscillation influence on precipitation, river flow and water resources in the Iberian Peninsula. Int J Climatol 24:925–944

Vicente-Serrano SM, Cuadrat JM (2007) North Atlantic Oscillation control of droughts in north-east Spain: evaluation since 1600 A.D. Clim Change 85:357–379

Visbeck MH, Hurrell JW, Polvani L, Cullen HM (2001) The North Atlantic Oscillation: past, present, and future. Proc Natl Acad Sci USA 98:12876–12877

Impacts of the NAO on Atmospheric Pollution in the Mediterranean Basin

Uri Dayan

Abstract There are several inherent problems in attributing pollution concentrations to changes in large-scale atmospheric circulation: (1) the year to year variability being modulated by both, changes in circulation and changes in upwind emissions, (2) the shorter life-time of some pollutants precluding a meaningful relationship with changes in circulation, and (3) the both-ways interaction between trace gases, aerosols and climate. Simulations of transport of anthropogenic CO for high and low phases of the NAO are presented followed by an observational-based study relating the ozone seasonal variability across North Atlantic and the Western Mediterranean to the NAO. Both phases of the NAO controlling dust transport to the Mediterranean are described: the positive phase during summer over the western region and the negative one regulating dust transport over the Eastern Mediterranean in winter. Low NAO indices have been related to a higher cyclonic activity over the western basin. On the contrary, other studies found no correlation between annual wet deposition of African dust-related elements and the NAO. Although, at present, there is no consensus on the process responsible for the observed low-frequency variations in the NAO, most of them predict the continuation of the positive NAO state until the mid twenty-first century implying a predominantly zonal circulation over the western Mediterranean. This imply a reduced import of European trace gases, an enhancement of long range transport of air pollutants from North American sources and conditions in favor of mobilization and transport of North African dust mainly to the western part of this fragile basin.

Keywords Air Pollution · Atmospheric circulation · Environment · Mediterranean Basin · NAO

U. Dayan (✉)
Department of Geography, The Hebrew University of Jerusalem, Jerusalem, Israel
e-mail: msudayan@mscc.huji.ac.il

S.M. Vicente-Serrano, R.M. Trigo (eds.), *Hydrological, Socioeconomic and Ecological Impacts of the North Atlantic Oscillation in the Mediterranean Region*, Advances in Global Change Research 46, DOI 10.1007/978-94-007-1372-7_12,

1 Introduction: Problems in Attributing Pollution Concentrations to Changes in Large-Scale Atmospheric Circulation

The variations of atmospheric pollution concentrations and their relationships to large-scale atmospheric circulation systems have been studied for a while (e.g., Davis and Kalkstein, 1990; Dayan and Lamb, 2008; Dayan et al., 2008; Kalderon-Asael et al., 2009). Secondary pollutants such as ozone are primarily a result of photochemical reactions among anthropogenic precursor emissions and as such, are governed by air mass constituents such as temperature and humidity. Accordingly, variation in trace gases concentrations are modulated by exposure to differing air masses as controlled by changes in atmospheric circulation. Problems rising in attributing pollution concentrations to changes in large-scale atmospheric circulation stem from the fact that changes in upwind emissions and removal processes are not necessarily synchronous with variations in circulation. Some efforts were done, mainly through, coupled climate-chemistry models to treat and analyze simultaneously the changes in general circulation and atmospheric chemistry (Hein et al., 2001; Dastoor and Larocque, 2004).

A second major drawback in trying to relate changes in pollutant concentration to variation in circulation patterns is their different life time and distribution. For example, aerosols are most relevant for short spatial and temporal scales as compared to long-lived greenhouse gases such as CH_4 and CO_2 (Andrea, 2001) for which, various meteorological and emission effects dominate large parts of the globe (Voulgarakis et al., 2009). Radiative forcing of aerosols are of higher spatial variability than Green House Gases (GHG) forcings due to the relatively short aerosol life time of the order of a week (Kostler et al., 2010). Consequently, such short life time of the pollutants preclude a meaningful relationship with changes in large scale circulations.

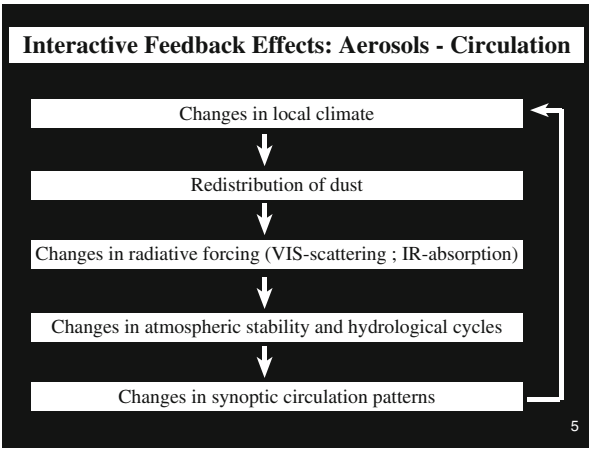

Fig. 1 Flow diagram of the interactive feedback effects: aerosols – circulation

Beside these above mentioned problems, at times, both ways interactions exist between trace gases, aerosols and atmospheric circulation patterns. Tegen et al. (1996) described the interactive feedback effects between mineralogical aerosols and atmospheric circulation emphasizing that: "...both sources and removal of dust are dependent on local climate, changes in radiative forcing by dust may induce changes in regional circulation patterns and therefore to further changes in dust sources and sinks...". Such interactive feedback effects between aerosols and circulation is shown in Fig. 1.

2 Fundamental Approaches Relating Circulation to Environment - Examples

Due to the strong potential for highly interactive feedback effects between typical environmental phenomena related to several modes of the circulation, a methodology consisting of both interactions is needed. This methodology will take into account both approaches: on how the circulation affects the environment (i.e., climatically related variables such as air pollutants) and how the environment affects the circulation. Here, we adopted Yarnal (1993) ideas who addressed these both approaches followed by some examples on studies relating circulation to the environment.

Yarnal explained that in the "Circulation to Environment" classification you first classify the circulation into distinct several patterns and then relate it to the environment, whereas in the second method you classify the circulation data along environment-based criteria (Fig. 2).

The first example demonstrating the impact of circulation on air trace gases is a recent study by Theoharatos et al. (2010) investigating the relationship between synoptic-scale circulation patterns, induced thermal stresses and its possible association to air pollution over Athens, Greece. Here, the authors have shown that poor air quality conditions for SO_2 and O_3 were related to a northward displacement of the Subtropical Jet Stream and large-scale subsidence.

Liu et al. (2009) explained the "Middle East ozone maximum", a summertime enhancement in ozone observed by the Tropospheric Emission Spectrometer satellite instrument as caused by strong descent in the middle and upper troposphere featuring both Arabian and Saharan anticyclones (Fig. 3).

Another study showing the impact of circulation on aerosols was done by Moulin et al. (1998) who used 11-year of daily Meteosat data to develop a satellite-derived climatology of African dust transport. They found that the dust transport patterns are related to cyclogenesis over North Africa.

The last example, this time, depicting the impact of air quality on climate is Lelieveld et al. (2002) study which indicates the influence of elevated European sulfate emissions on cooling of the Mediterranean sea surface temperatures during the mid-1970s. This cooling led to a reduction in evaporation and consequently, less precipitation over the basin.

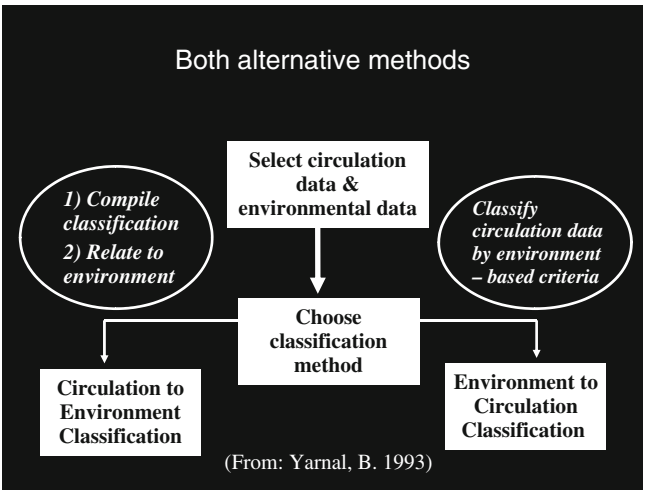

Fig. 2 Both alternative methods to relate environmental phenomena to circulation (adapted from Yarnal, 1993)

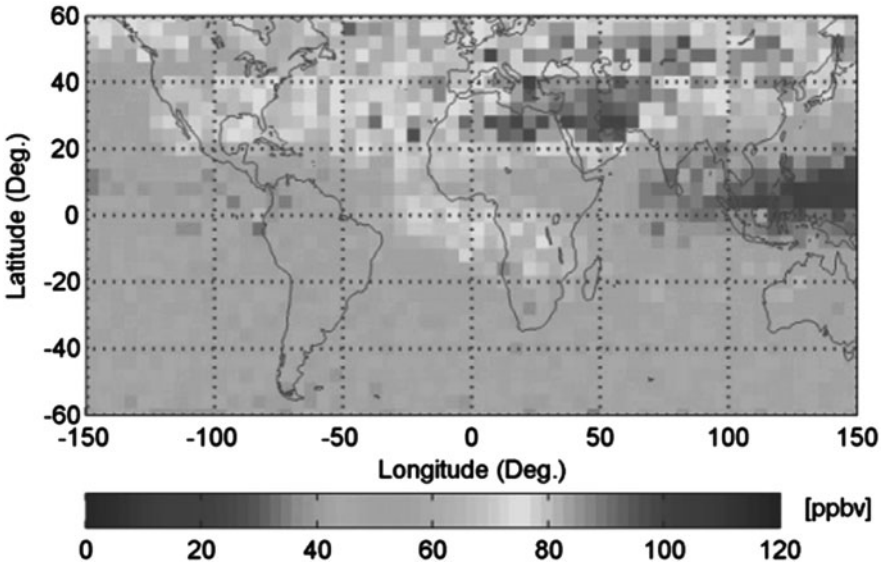

Fig. 3 Monthly mean ozone mixing ratio in July 2005 at 464 hPa from the Tropospheric Emission Spectrometer (from Liu et al., 2009)

3 Circulation to Environment: The Role of the NAO in Controlling the Pathways of Pollution to the Mediterranean

The North Atlantic Oscillation (NAO) index is determined by the intensity and position of the Icelandic low and the Bermuda Azores high. Several studies have identified the NAO as the dominant mode of variability of the surface atmospheric circulation in the Atlantic (Barnston and Livezey, 1987; Kushnir and Wallace, 1989; Hurrell, 1995). The NAO affects not only climatic conditions, but also, climatic-derived conditions such as air pollutant transport and dispersion. Consequently, this is also the oscillation influencing pollution transport over the Northern Hemisphere at large, and more specifically over Western Europe and the western Mediterranean (Eckhardt et al., 2003). Further on, several studies results will be presented to show the strong influence of the NAO on the strengths and locations of the main pollutant transport pathways over the Mediterranean. These changes in these pathways are mainly changes in the mean circulation patterns over Western Europe and the western Mediterranean Basin associated with the NAO and believed to be the main factor for their interannual variations.

Eckhardt et al. (2003) used the Flexpart Lagrangian particle dispersion model to simulate the transport of CO over Europe and the Mediterranean Basin. CO was used as tracer of anthropogenic pollution due to its long life time. The simulation was performed for the 20% lowest and highest NAO for December through February of 1979–1993. They found out that during positive NAO phases, reduced CO outflow from Central Europe to the Mediterranean were obtained due to stronger westerly winds flowing over Europe and most of the pollution was transported northward. These strong westerlies characterizing positive phases of the NAO serve as conveyor belt to transport O_3 formed over the Eastern US to Europe and the Western Mediterranean. This conclusion was reached by Crielson et al. (2003) who used the tropospheric O_3 residual technique which utilizes coincident observations of Total Ozone Mapping Spectrometer (TOMS) and stratospheric O_3 profiles from the Solar Backscatter Ultraviolet instruments to examine the spatial distribution of O_3 and its positive relationship with the NAO (Fig. 4).

NAO controls not only trace gases but particulate as well. Moulin et al. (1997) used Meteosat data from 1983 to 1994 to develop a satellite climatology of African dust transport to the Mediterranean. They found that the interannual variations in dust transport over the Western Mediterranean is well correlated ($R = 0.66$, $p = 0.027$) with the NAO index during summertime. This positive correlation is explained by the frequent passage of cyclones sweeping the western basin during positive phases of the NAO and mobilizing dust from North Africa.

Contrary to the NAO positive phase impact on the dust transport during summer over the western basin, Dayan et al. (2008) presented evidence on the role of the negative phase of the NAO in controlling dust transport during winter to the South Eastern Mediterranean (SEM). In their study, they examined the atmospheric circulation governing dust over the SEM for the "high dust season" (i.e., October–May)

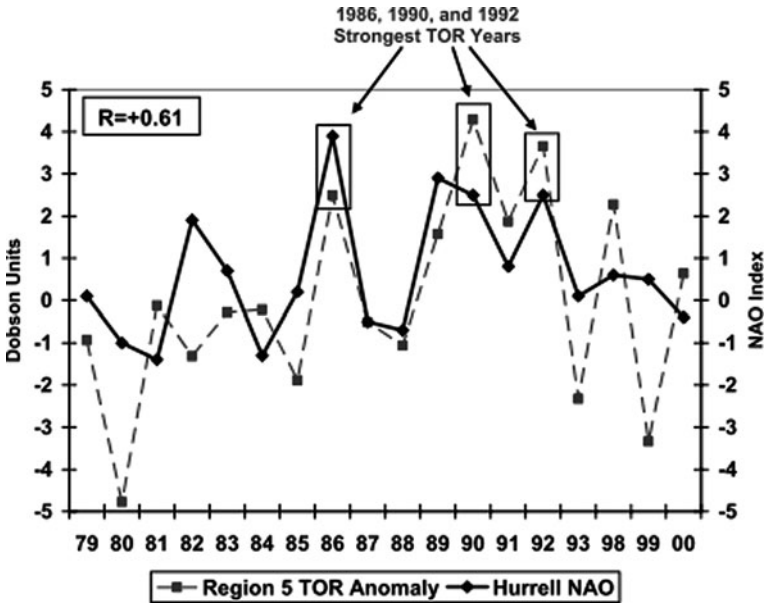

Fig. 4 Springtime depiction showing the interannual variability and positive relationship between springtime tropospheric ozone residual anomaly for Region 5: Eastern North Atlantic and Western Europe and springtime Hurrell NAO index from 1979–2000 (from Crielson et al., 2003)

for 37 years (1968–2004) and found a significant correlation ($R = -0.66$) between the interannual variability of accumulated dust over Beer-Sheba, located in southern Israel which represents the SEM and the NAO modulating the cyclonic activity over the Mediterranean (Fig. 5).

These results indicate that the synoptic system that produces the majority of the dust over the SEM is the Cyprus Low, a cold cyclone, contributing over 2/3 of both, the total yearly dust and rain fields. Namely, the same synoptic system controls both modes of deposition, i.e., wet and dry, and therefore have a similar relationship with the NAO over the SEM.

In another study, Avila and Roda (2002) could not find any correlation between the NAO and wet deposition of African dust over a rural western Mediterranean site in north-east Spain. They suggested that contrary to the Eastern Mediterranean, the two variables controlling wet deposition over the Western Mediterranean vary in an opposite direction with respect to the NAO, i.e., precipitation inversely and dust updraft directly, therefore, canceling each other effects.

In summary we can say that both phases of the NAO have a major role in controlling the transport of particulate matter (mineralogical dust) over the Mediterranean Basin. However, this control is seasonal dependent and differs substantially between the two Mediterranean halves, with the positive phase of the NAO affecting the Western Mediterranean during summertime, whereas, its negative phase produces a larger impact over the Eastern Mediterranean and during winter.

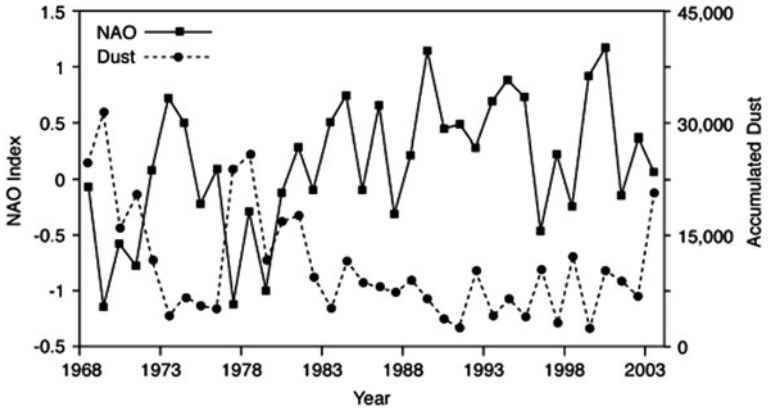

Fig. 5 Annual variation of accumulated dust over southern Israel representing the SEM for October–May (*dashed*) and the NAOI averaged over December–March (*solid*) (from Dayan et al., 2008)

4 Environment to Circulation: Influence of GHG Induced Climate Change on the NAO

In the last section under the "Circulation to Environment" concept, we dealt with the role of the NAO in controlling the export and import pathways of pollution to the Mediterranean Basin based on observations. Here, we will present some studies results, based mainly, on atmospheric model simulations to demonstrate the influence of the increase GHG concentrations on the NAO variability as a sign of global climate change.

Paeth et al. (1999) examined the NAO variability with an observational data set and several model data sets including GHG-induced external forcings. They have shown that the IPCC (BAU) scenario results predict the continuation of the recent positive NAO phase until mid of the twenty-first century. Furthermore, they found statistical evidence that radiative forcing due to increasing GHG concentrations has an impact on the simulated variability of the NAO on time-scale exceeding 60 years. Never the less, such evidence could not be discerned for the real NAO due to its strong interannual variability. The implication of a persisting positive phase of the NAO for the next 30–50 years is a predominantly zonal circulation over Western Europe and less pollution from European sources transported to the Mediterranean Basin.

Osborn (2004) analyzed the simulated response of the winter NAO to GHG forcing using seven coupled climate models. Even though, not all models showed agreement between NAO pattern and regional scale changes expressed as sea level pressure trends for winter atmospheric circulation, a clear correspondence was found for two coupled ocean-atmosphere models, the CCSR (Emori et al., 1999) and the ECHAM-4 (Bacher et al., 1998). All models showed a mean increase of 0.25 hPa/K of global mean temperature increase caused by enhanced GHG forcing

over the Mediterranean Basin. Osborn (2004) main conclusion is that a combination of internal variability and GHG forcing as external variability, has contributed to the NAO increase observed from the 1960s to the 1990s leading to strongest zonal wind over Europe strengthening meridional flow over the Mediterranean.

Based on numerous papers indicating an existing positive relationship between GHG and the NAO (e.g., Paeth et al., 1999; Osborn, 2004; Stephenson et al., 2006), Dayan and Lamb (2005) analyzed the atmospheric circulation that controls wet deposition over Europe and the northern Mediterranean. A positive phase of the NAO is indicative of a predominantly zonal circulation over Europe as compared to a negative phase characterized by relatively strong meridional flows (Paeth et al., 1999). The predominance of the meridional flow and sulfate loaded-deposition years found by Dayan and Lamb (2005) is consistent with the significant negative correlation ($R = -0.43$, $p < 0.005$) obtained between the 16-year time series of the 925 hPa meridional wind and the NAO. A further confirmation of this phenomenon is the significant correlation ($R = -0.39$, $p < 0.005$) found between the meridional wind and sulfate deposition over Europe. The overall downward trend in sulfate deposition observed for the last 16 years over Europe and the northern Mediterranean Basin, the concurrent increases in average temperature (Klein Tank et al., 2002) and the increased frequency of extreme warm-weather events for the summer (Domonkos et al., 2003) suggest, along with the decline in SO_2 emissions, that this period was characterized by predominantly zonal circulation, as indicated by the trend towards greater prevalence of positive NAO. Consequently, Dayan and Lamb (2005) reached the conclusion that negative NAOI years correspond to predominant meridional flow leading to more sulfate deposition over Europe as compared to positive NAO years characterized by a zonal flow and less pollution (Fig. 6). Their conclusion corroborates Duncan and Bey (2004) who emphasized the strong influence of the NAO on the strengths and locations of the export pollution (e.g., O_3) pathways from Europe to the Mediterranean and northern Africa.

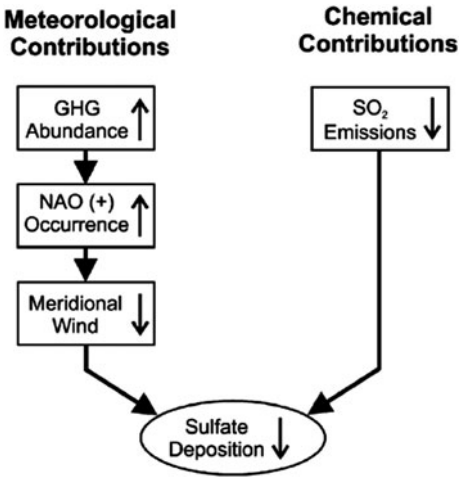

Fig. 6 Block diagram of the meteorological and chemical contributions to changes in sulfate deposition over southern Europe (from Dayan and Lamb, 2005)

5 Future Phases of the NAO and Possible Implications on Air Pollution over the Western and Eastern Mediterranean Basin

Most recent studies point at the difficulty to identify a preferred timescale of variability for the NAO as well as the large amount of its intra-seasonal variability as main reasons for the lack of consensus on the process responsible for its present observed low-frequency variations (Hurrell and Deser, 2010) and, obviously, our inability to predict its trend and variability in the future. Moreover, although this oscillation is natural, it seems to respond to external forcing in addition to its inherent internal variability.

Kuzmina et al. (2005), based on results obtained from 12 coupled climate models, found that the forced model runs resulted in stronger NAO as compared to the control runs. This indicates a possible intensification of the NAO in the future with further increases in GHG concentrations in the atmosphere.

In contrary to Kuzmina et al. (2005) study, Selten et al. (2004) suggest that the strengthening of the westerlies over the North Atlantic is not caused by GHG but rather to a climate variation governed by increased precipitation over the tropical Indian Ocean.

To summarize this section, we can say, with much prudence, that presently there are two opposed scientific views as regarded to the NAO trend and variability, several researchers consider that external climate forcings, such as volcanic eruptions or increased GHG, are the main drivers for a predominance of positive phases of the NAO while other groups consider that physical driven processes internal to the climate system are responsible in driving NAO variations.

Until the scientific community understands better the causes and effects of the observed NAO trend and variability, we should restrict our conclusions on future NAO's implication on air pollution over the Mediterranean Basin by presenting the anticipated impacts of both prevailing modes (positive and negative phases) over this basin as experienced so far. Based on our present limited knowledge, the future NAO's implications are as follow:

A prevailing positive NAO over the Western Mediterranean is likely to:

(1) Reduce the import of European trace gases;
(2) Enhance the long range transport of pollutants from upwind eastward sources, e.g., North America;
(3) Enhance the mobilization and transport of dust from North African sources to the Mediterranean.

A prevailing negative NAO over the Eastern Mediterranean is expected to enhance cyclonic conditions favorizing the passage of more deep cyclones mobilizing and transporting dust from North African sources to this part of the basin.

References

Andrea MO (2001) The dark side of aerosols. Nature 409:671–672

Avila A, Roda F (2002) Assessing decadal changes in rainwater alkalinity at a rural Mediterranean site in the Montseny Mountains (NE Spain). Atmos Environ 36:2881–2890

Bacher S, Oberhuber JM, Roeckner E (1998) ENSO dynamics and seasonal cycle in the tropical Pacific as simulated by the ECHAM4/OPYC3 coupled general circulation model. Clim Dyn 14:1659–1672

Barnston AG, Livezey RE (1987) Classification, seasonality and persistence of low frequency atmospheric circulation patterns. Mon Wea Rev 115:1083–1125

Crielson JK, Fishman J, Wozniak AE (2003) Intercontinental transport of troposheric ozone: a study of its seasonal variability across the North Atlantic utilizing tropospheric ozone residuals and its relationship to the North Atlantic Oscillation. Atmos Chem Phys 3:2053–2066

Dastoor AP, Larocque Y (2004) Global circulation of atmospheric mercury: a modeling study. Atmos Environ 38:147–161

Davis RE, Kalkstein LS (1990) Using a spatial synoptic classification to assess changes in atmospheric pollution concentrations. Phys Geog 11:320–342

Dayan U, Lamb D (2005) Global and synoptic-scale weather patterns controlling wet atmospheric deposition over Central Europe. Atmos Environ 39:521–533

Dayan U, Lamb D (2008) Influence of atmospheric circulation on the variability of wet sulfate deposition. Int J Climatol 28:1315–1324

Dayan U, Ziv B, Shoob T, Enzel Y (2008) Suspended dust over Southeastern Mediterranean and its relation to atmospheric circulations. Int J Climatol 28:915–924

Domonkos P, Kysely J, Piotrowicz P, Petrovic P, Likso T (2003) Variability of extreme temperature events in South-Central Europe during the 20th century and its relationship with large-scale circulation. Int J Climatol 23:987–1010

Duncan BN, Bey I (2004) A modeling study of the export pathways of pollution from Europe: seasonal and interannual variations (1987–1997). J Geophys Res 109:D08301. doi:10.1029/2003JD004079

Eckhardt D, Stohl A, Bierle S, Spichtinger N, James P, Forster C, Junker C, Wagner T, Platt U, Jennings SG (2003) The North Atlantic Oscillation controls air pollution transport to the Arctic. Atmos Chem Phys 3:1769–1778

Emori S, Kozawa T, Abe-Ouchi A, Numaguti A, Kimoto M, Nakajima T (1999) Couple ocean-atmosphere model experiments of future climate change with an explicit representation of sulfate aerosol scattering. J Meteorol Soc Jpn 77:1299–1307

Hein R, Dameris M, Schnadt C, Land C, Grewe V, Kohler I, Ponater M, Sausen R, Steil BB, Landgraf J, Bruhl C (2001) Results of an interactively coupled atmospheric chemistry – general circulation model: comparisons with observations. Annales Geophysicae 19:435–457

Hurrell JW (1995) Decadal trends in the North Atlantic Oscillation: regional temperatures and precipitation. Science 269:676–679

Hurrell JW, Deser C (2010) North Atlantic climate variability: the role of the North Atlantic Oscillation. J Mar Syst 79:231–244

Kalderon-Asael B, Erel Y, Sandler A, Dayan U (2009) Mineralogical and chemical characterization of suspended atmospheric particles over the Eastern Mediterranean based on synoptic-scale circulation patterns. Atmos Environ 43:3963–3970

Klein Tank AMG, Wijngaard JB, Konen JP, Bohm R, Demaree G, Gocheva A, Mileta M, Petrovic P (2002) Daily dataset of the 20th century surface air temperature and precipitation series for the European climate assessment. Int J Climatol 22:1441–1453

Kostler S, Deutener F, Feichter J, Raes F, Lohman U, Roeckner E, Fischer-Bruns I (2010) A GCM study of future climate response to aerosol pollution reductions. Clim Dyn 34:1177–1194

Kushnir Y, Wallace JM (1989) Low frequency variability in the Northern Hemisphere winter – geographical distribution, structure and time-scale dependence. J Atmos Sci 46: 3122–3142

Kuzmina SI, Bengtsson L, Jahannenssen OM, Drange H, Bobylev LP, Miles MW (2005) The North Atlantic Oscillation and greenhouse-gas forcing. Geophys Res Lett 32:L04703. doi:10.1029/2004 GL021064

Lelieveld J, Berresheim H, Borrmann S et al (2002) Global air pollution crossroads over the Mediterranean. Science 298:794–799

Liu JJ, Dylan B, Jones A, Worden JR, Noone D, Parington M, Kar J (2009) Analysis of the summertime buildup of tropospheric O_3 abundances over the Mid-East and North Africa as observed by the Tropospheric Emission Spectrometer instrument. J Geophy Res 114:D05304. doi:10.1029/2008JD010993

Moulin C, Lambert CE, Dayan U, Masson V, Ramonet M, Bousquet P, Dulac F (1998) Satellite climatology of African dust transport in the Mediterranean atmosphere. J Geophys Res 103:13137–13144

Moulin C, Lambert CE, Dulac F, Dayan U (1997) Control of atmospheric export of dust from North Africa by the North Atlantic Oscillation. Nature 387:691–694

Osborn TJ (2004) Simulating the winter North Atlantic Oscillation: the role of internal variability and greenhouse gas forcing. Clim Dyn 22:605–623

Paeth H, Hense A, Glowienka-Hense R, Voss R, Cubasch U (1999) The North Atlantic Oscillation as an indicator for greenhouse-gas induced regional climate change. Clim Dyn 15:953–960

Selten FM, Branstator GW, Dijkstra HA, Kliphius M (2004) Tropical origins for recent and future Northern Hemisphere climate change. Geophys Res Lett 31:L21205. doi:10.1029/2004GL020739

Stephenson DB, Pavan V, Collins M, Junge MM, Quadrelli R (2006) North Atlantic Oscillation response to transient greenhouse gas forcing and the impact on European winter climate: a CMIP2 multi-model assessment. Clim Dyn 27:401–420

Tegen I, Lacis AA, Fung I (1996) The influence on climate forcing of mineral aerosols from disturbed soils. Nature 380:419–422

Theoharatos G, Pantavou K, Mavrakis A, Spanou A, Katavoutas G, Efstathiou P, Mpekas P, Assimakopoulos D (2010) Heat waves observed in 2007 in Athens, Greece: synoptic conditions, bioclimatological assessment, air quality levels and health effects. Environ Res 110:152–161

Voulgarakis A, Savage NH, Braesicke P, Wild O, Carver GD, Pyle JA (2009) Interannual variability of tropospheric composition: the influence of changes in emission, meteorology and clouds. Atmos Chem Phys Discuss 9:14023–14057

Yarnal B (1993) Synoptic climatology in environmental analysis. Bellhaven Press, London

Evaluation of the Relationship Between the NAO and Rainfall Erosivity in NE Spain During the Period 1955–2006

Marta Angulo-Martínez and Santiago Beguería

Abstract Rainfall erosivity is the ability of precipitation to erode soil. Microerosion processes due to the impact of raindrops on the soil – rainsplash – represent an important mechanism of detachment of soil particles, which might be removed thereafter by surface runoff. The annual and interannual patterns of rainfall erosivity are controlled by the variability of rainfall intensity. This study analyses the interannual variability of daily rainfall erosivity due to precipitation in the NE of Spain during the period 1955–2006, and its connection with the North Atlantic Oscillation (NAO). It was found that the erosive power of rainfall is stronger during the negative phase of NAO and weaker during positive NAO conditions, as are the rainfall amounts. Daily rainfall erosivity series were adjusted to a Generalized Pareto probability distribution for positive and negative NAO phases for assessing the effect of NAO on extreme events. Results showed higher values expected for a given return period in most of the area under negative NAO conditions. These findings would be useful in the implementation of soil conservation strategies.

Keywords Rainfall erosivity · EI · North Atlantic Oscillation · R factor · NE Spain

1 Introduction

The concept of rainfall erosivity refers to the ability of any rainfall event to erode soil. It links together the dynamic properties of rainfall as a consequence of rainfall-generating processes and their impact on the soil surface, and involves two main mechanisms: (i) *rainsplash* – the detachment of soil particles due to the kinetic energy of the raindrops –, and (ii) *runoff erosion* – motion of soil particles by shear stress exerted by the surface runoff. Rainfall erosivity is responsible of changes in the soil properties as: crusting, disruption of aggregates, removal of nutrient-rich parcels of soil, etc. Rainfall erosivity represents one of the main mechanisms of degradation in semiarid landscapes where vegetation is scarce. Its influence depends on the characteristics of soil, topography and land use, as well as on other features of

M. Angulo-Martínez (✉)
Estación Experimental de Aula Dei, Spanish National Research Council (CSIC), Zaragoza, Spain
e-mail: mangulo@eead.csic.es

S.M. Vicente-Serrano, R.M. Trigo (eds.), *Hydrological, Socioeconomic and Ecological Impacts of the North Atlantic Oscillation in the Mediterranean Region*, Advances in Global Change Research 46, DOI 10.1007/978-94-007-1372-7_13,

the rainfall regime (D'Odorico et al., 2001). Rainfall erosivity estimates are needed for the estimation of soil erosion amounts through space and time. In the context of climate change the effect of altered rainfall characteristics combined with other aspects as biomass and changes in the soil moisture are some major concerns of soil conservation studies.

Empirical studies have demonstrated an exponential relationship between rainfall intensity and rainfall erosivity (Brown and Foster, 1987; Coutinho and Tomás, 1995; Van Dijk et al., 2002). This relationship allows introducing some important characteristics of the rainfall events as: (i) the raindrop size distribution and their associated kinetic energy, and (ii) the rainfall intensity at detailed time intervals.

Among the several indices developed to estimate rainfall erosivity the most extensively used is the USLE/RUSLE *R* factor, which is calculated from the EI_{30} index (Wischmeier, 1959; Wischmeier and Smith, 1978; Brown and Foster, 1987; Renard et al., 1997). At many sites worldwide the *R* factor has been shown to be highly correlated with soil loss (Van der Knijff et al., 2000; Diodato, 2004; Shi et al., 2004; Hoyos et al., 2005; Curse et al., 2006; Onori et al., 2006; Domínguez-Romero et al., 2007).

One of the main disadvantages of the RUSLE *R* factor is the need for high frequency – typically lower than 15 min or pluviograph data –, long data series. Information of this nature is rarely available with adequate spatial and temporal coverage, and daily records are usually the best available data at most locations. Attempts to estimate rainfall erosivity from daily rainfall records or storm event data have been based largely on exponential relationships (Richardson et al., 1983; Bagarello and D'Asaro, 1994; Petkovsek and Mikos, 2004; Angulo-Martínez and Beguería, 2009). Due to the high temporal and spatial variability of rainfall erosivity (Angulo-Martínez et al., 2009), accurate records based on long data series are required in order to evaluate temporal or spatial trends that may be linked with atmospheric circulation patterns.

Previous work has shown that the spatial and interannual variability of rainfall intensity can be explained by atmospheric circulation patterns (Hurrell, 1995; Jones et al., 1997; Hurrell et al., 2003). The main atmospheric circulation pattern that affects the climate of Europe is the North Atlantic Oscillation (NAO). The NAO is characterized by a north–south sea-level pressure dipolar pattern, with one of the centres located over Iceland and the other one approximately over the Azores Islands. This dipolar pattern reflects the strong contrast in meridional pressure over the North Atlantic region. The positive phase of the NAO reflects below normal heights and pressure across the high latitudes of the North Atlantic, and above-normal heights and pressure over the central North Atlantic. The NAO negative mode produces high-pressure blocking in the northeast Atlantic, and a more meridional circulation than the opposite mode (Jacobeit, 1987; Moses et al., 1987). Upper-air troughs and incursions of polar air over the Mediterranean are more frequent during negative NAO, and the Atlantic storm tracks are displaced south. All these factors are responsible of wetter conditions in the western Mediterranean (Jacobeit, 1987; Moses et al., 1987; Maheras, 1988; Kutiel et al., 1996). In contrast, the NAO positive mode is characterized by moisture transport across the North

Atlantic that has a more southwest to northeast orientation and extends further into northern Europe and Scandinavia. Hence, moisture transport and rainfall are reduced over southern Europe and the Mediterranean (Hurrell, 1995; Hurrell and van Loon, 1997; Moulin et al., 1997; Marshall et al., 2001). The NAO shows a clear signal throughout the whole year, but with stronger intensity and extension during winter due to the stronger meridional gradients.

The influence of the NAO on precipitation over the Iberian Peninsula has been recognized in previous studies (Rodó et al., 1997; Esteban-Parra et al., 1998; Rodríguez-Puebla et al., 1998; Serrano et al., 1999), with a clear difference between the western (Atlantic) and eastern (Mediterranean) areas of the region. It is possible to identify a large part of central and southern Spain and southern Portugal for which the influence of the NAO is dominant. In contrast, the southeastern Mediterranean coast of Spain is dominated by more easterly Mediterranean influences.

There are no previous studies relating rainfall erosivity to atmospheric teleconnection patterns in the Iberian Peninsula. Some works have addressed the influence of the El Niño-Southern Oscillation (ENSO) on rainfall erosivity for some areas of United States (D'Odorico et al., 2001) and Peru (Romero et al., 2007). Since the North Atlantic Oscillation controls the interannual variability of rainfall over the region, there is a need to know in which way rainfall erosivity is related to NAO. Since rainfall erosivity is more related to single extreme precipitation events than to average events, the relationship between the NAO and rainfall erosivity is not necessarily explained by the negative correlation between the NAO and total precipitation amounts. In addition, this knowledge may help agricultural managers to take soil conservation measures to protect the soil.

The aim of this study is to assess the influence of the NAO on daily rainfall erosivity in NE Spain, during the period 1955–2006. A second objective is to identify the changes in the probability of occurrences of extreme daily erosivity events in relation with daily NAO phases.

2 Study Area and Methods

2.1 Study Area

The study area covers the northeast of Spain, encompassing an area of about 147,000 km^2 that corresponds to the administrative territorial province demarks which conform the Ebro Basin. The study area is geographically complex. It encloses several mountain ranges and a main central valley, the Ebro basin. The area is limited to the north by the Cantabric Sea, the Cantabrian Range and the Pyrenees, with maximum elevations above 3000 m a.s.l. At the south and southwest the Iberian Range closes the Ebro valley, with maximum elevations in the range of 2000–2300 m a.s.l. To the east valley is closed by the Catalan Prelittoral Range, with maximum elevations of 1000–1900 m a.s.l., and then continues to the Mediterranean sea.

The climate is influenced by both the Atlantic and the Mediterranean, and the effect of the relief on precipitation and temperature. The bordering mountain ranges isolate the central valley, blocking the maritime influence and resulting in a continental climate with arid conditions (Lana and Burgueño, 1998; Vicente-Serrano, 2005). A climatic gradient in the NW–SE direction is notable, determined by strong Atlantic influences in the north and northwest of the area during much of the year, and the influence of the Mediterranean to the east. The mountain ranges add complexity to the climate of the region, with the Pyrenees extending the Atlantic Ocean influence to the east by increasing precipitation. Precipitation in inland areas is characterized by alternating wet and dry periods as a consequence of the seasonal displacement of the polar front and its associated pressure systems. Inter-annual variability in precipitation can be very high, and prolonged dry periods can be followed by torrential rainfall events that last for several days. The most extreme precipitation events have been recorded along the Mediterranean seaside (Romero et al., 1998; Llasat, 2001; Peñarrocha et al., 2002).

Rainfall erosivity reproduces the characteristics of the precipitation in the study area, as revealed by station-data (Fig. 1). Three different areas can be recognized, following a NW–SE gradient. The NW zone, influenced by the Atlantic, shows the highest monthly rainfall values and minimum rainfall erosivity; the highest erosivity is attained at the beginning of the summer, coinciding with late spring storms. The central zone includes the majority of the observatories, with precipitation amounts that are lower than in the NW zone (although still abundant), though erosivity is

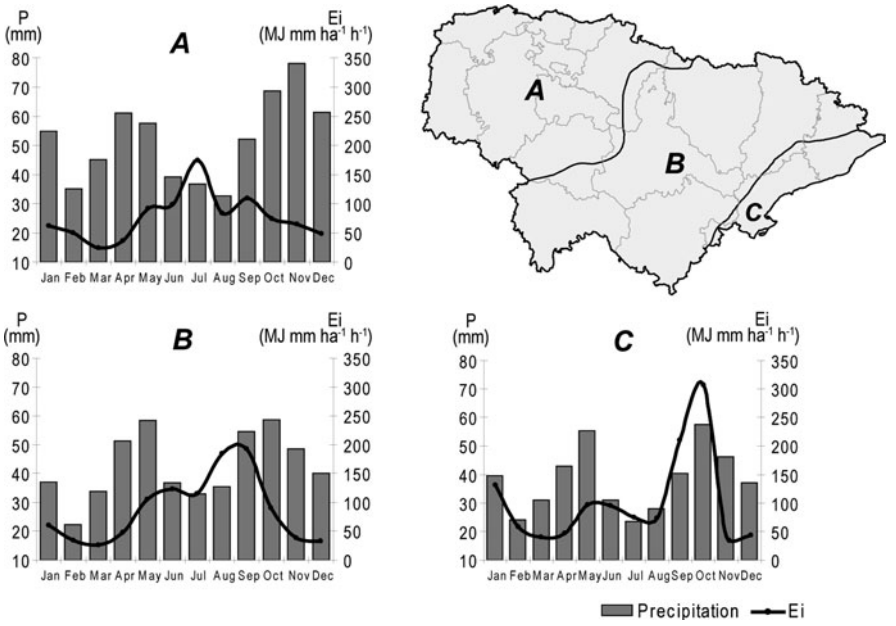

Fig. 1 Homogeneous monthly rainfall erosivity regions in NE Spain (EI index, see Methods, Section 2), and precipitation associated obtained by means hierarchical cluster

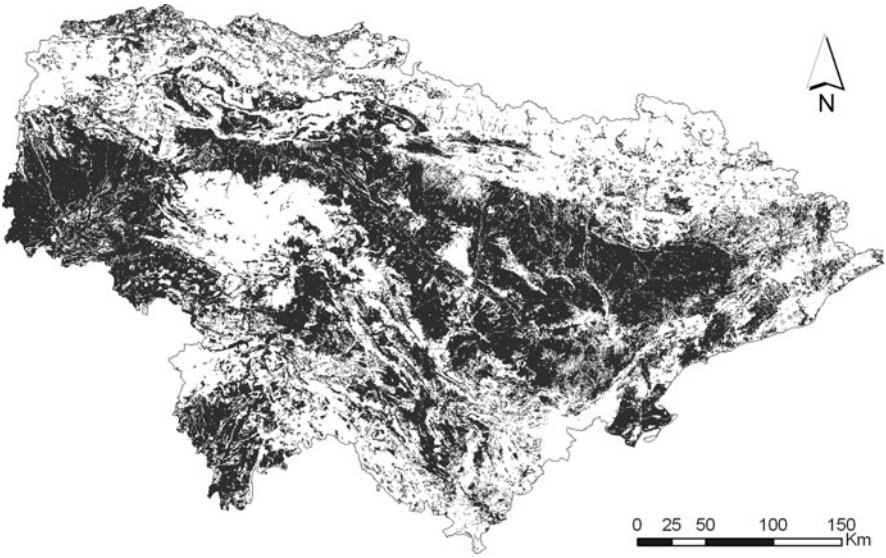

Fig. 2 Spatial surface of the cultivated soil in the NE Spain (68,000 km^2); data: Corine Land Cover version 8/2005 (EEA, 2000)

greater and shows two annual peaks, one in late spring (May–June) and a second (highest) at the end of summer (August–September). The NE zone has a typical Mediterranean rainfall behavior, with maxima in spring and autumn and highest erosivity in autumn. It is important to note that the spring rainfall peaks are not as erosive as those of the autumn, due to differences between these seasons in rainfall generation mechanisms. Spring rainfall events are usually frequent, but tend to have low intensity. In contrast, precipitation in autumn is usually attributable to a few very intense events.

Due to its complex climatology (as a consequence of being a meteorological border region) and the contrasted relief, the Ebro Basin has a long history of social, economic and environmental damage caused by extreme rainfall events (García-Ruiz et al., 2000; Lasanta, 2003; Llasat et al., 2005). The main activity in this area is agriculture, representing approximately 46% of the land use. It is extended around the Ebro valley occupying a broader area close to the Mediterranean coast (Fig. 2). During winter agricultural soils remain uncovered. Consequently, rainfall erosivity is the principal cause of soil erosion with no limiting factor at that time. Mountain areas represent approximately 20% of the study region.

2.2 Daily Rainfall Erosivity Database

The database consisted of 156 daily rainfall series from the Spanish Meteorological Agency (AEMET) for the period 1955–2006 (Fig. 3). Data on cumulative precipitation were taken every day at 0600 LT. The series were obtained via a

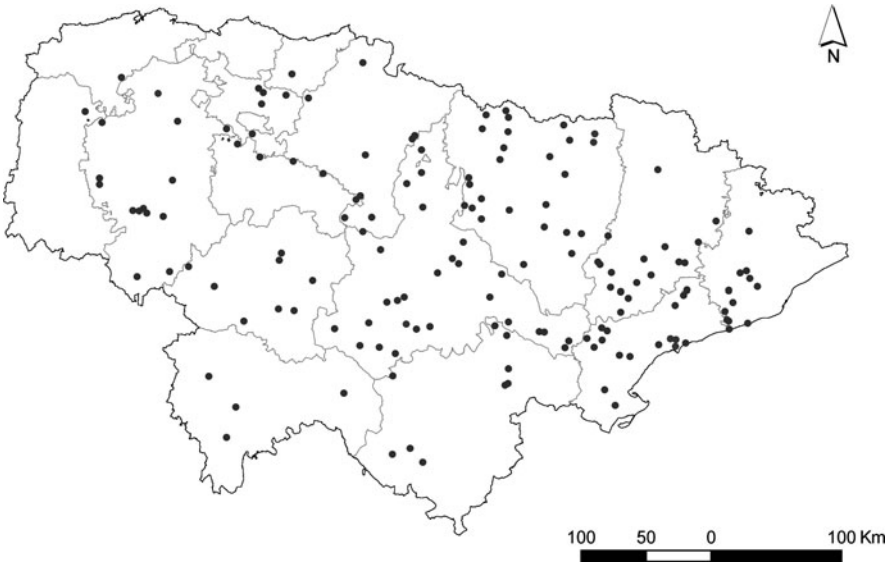

Fig. 3 Spatial distribution of the 156 daily rainfall observatories in the study area for the period 1955–2006

process that included reconstruction, gap filling, quality control and homogeneity testing (Vicente-Serrano et al., 2010).

Daily rainfall series were transformed into daily rainfall erosivity records based on an exponential relationship between the rainfall volume, P (mm/d), and rainfall erosivity index, EI (MJ mm/ha/h/d; Richardson et al., 1983):

$$EI = a\,P^b + \varepsilon, \tag{1}$$

where a and b are empirical parameters and ε is a random, normally distributed error. Parameters a and b are adjusted month-by-month to take account of intra-annual variations in rainfall characteristics. This leads to the more general expression:

$$EI_m = a_m\,P^{b_m} + \varepsilon, \tag{2}$$

where $m = \{1, ..., 12\}$ represents the month of the year. Parameter estimation in the model is achieved by weighted least squares (WLS) regression after a logarithmic transformation of the terms in Equation (2). Weights were assigned to the observations in order to reduce the excessive influence of small erosive events during parameterization (Angulo-Martínez and Beguería, 2009).

For obtaining the values of the parameters a and b it is necessary to count with data on daily EI and P. This data was provided by the automated system for hydrologic information of the Ebro basin water authority (SAIH-Ebro). This dataset

consisted on 110 series of rainfall data with 15 min resolution, covering the period 1997–2007. Daily *EI* values were calculated from these series following the RUSLE methodology, and were used for estimating the parameters in Equation (2). Given the good spatial coverage of the dataset, spatial fields of the parameters *a* and *b* were obtained by spatial interpolation, and their values at the location of the AEMET observatories were recorded. These values where then used to obtain daily series of *EI* for the period 1955–2006, using the AEMET daily rainfall data.

2.3 Atmospheric Circulation Events: North Atlantic Oscillation Index

Following Jones et al. (1997) a North Atlantic Oscillation index (NAOI) was calculated as the normalized difference between time series of sea level pressure recorded at two points in the southwest Iberian Peninsula (Gibraltar, 35°N 5°W) and southwest Iceland (Reykjavik, 65°N, 20°W). Daily sea-level pressure grids from the ds010.0 Daily Northern Hemisphere Sea Level Pressure Grids data set (University Corporation for Atmospheric Research, 1979) were used for calculating the NAOI. We selected those grid points located closest to the mentioned points.

Although the NAO influence is more intense during winter time, in the present study we considered the whole year. Positive and negative events of the NAO index were identified as those days with values of the NAO index higher than 0.5 and lower than –0.5, respectively.

2.4 Differences in Daily Rainfall Erosivity Between Positive and Negative NAO Phases

To evaluate the relationship between the phase of the NAO_i and monthly rainfall erosivity we generated different daily rainfall erosivity (*EI*) series regarding the value of NAO_i – positive (negative) daily EI_{NAOi} series were created with the daily *EI* values which were greater (inferior) of 0.5 (−0.5) NAO_i values, during the period 1955–2006. Daily rainfall erosivity was summed to obtain monthly positive – EI_{NAOi+} – and negative – EI_{NAOi-} – rainfall erosivity for NAO_i. We computed the relative difference EI_{dif} between median annual and monthly and in every observatory by:

$$EI_{dif} = (EI_{NAO-} - EI_{NAO+}) \big/ EI_{NAO+}, \tag{3}$$

where EI_{NAOi-} and EI_{NAOi+} are the median annual and monthly rainfall erosivity during negative and positive days of the NAO_i. Month maps of EI_{dif} were produce to help visualize spatial differences in the effect of NAO_i on rainfall erosivity.

The statistical significance of the relative differences was evaluated using the Wilcoxon-Mann-Whitney (WMW) rank test (Siegel and Castelan, 1988). The non-parametric WMW test, though less powerful than the *t* test, was preferred due to

its robustness against non-normality of the variables (Helsel and Hirsch, 1992). The monthly rainfall erosivity data series during daily negative NAO were compared with the monthly rainfall erosivity data series with the opposite NAO sign, month by month. The significance level was established at $\alpha = 0.05$.

2.5 *Extreme Value Analysis of Rainfall Erosivity During Positive and Negative NAO Phases*

Changes in the probability distributions of extreme rainfall erosivity depending on the NAO phase were analyzed using the extreme value theory (Hershfield, 1973). Peaks-over-threshold (POT) series of daily erosivity (*EI*) were obtained for positive and negative NAO phases, selecting only the observations for which *EI* exceeded a value corresponding to the 95th percentile of the respective series. The resulting series were fitted to a Generalized Pareto (GP) distribution by the maximum likelihood approach. GP is the limit distribution of a POT variable, provided that the POT occurrences fit a Poisson process, i.e. that they are time independent. The appropriateness of the GP distribution to model the daily erosivity POT series was checked visually by means of the L-moment ratios diagram and by a Kolmogorov-Smirnov test (Beguería, 2005; Beguería et al., 2009).

The GP distribution is described by a shape parameter k and a scale parameter α, with probability density function:

$$f(x) = \frac{1}{\alpha}\left[1 - \frac{k}{\alpha}(x - \varepsilon)\right] \tag{4}$$

and distribution function:

$$P(X \leq x) = 1 - \left(1 - \kappa\frac{(x - \varepsilon)}{\alpha}\right)^{\frac{1}{\kappa}}, \tag{5}$$

where x is the daily rainfall erosivity exceeding the threshold value ε, which acts as a location parameter. Estimates of α, κ can be obtained by maximum likelihood (Rao and Hamed, 2000). The highest expected precipitation X_T over a period of T years is obtained as:

$$X_T = \varepsilon + \frac{\alpha}{\kappa}\left[1 - \left(\frac{1}{\lambda T}\right)^{\kappa}\right], \tag{6}$$

where λ is the average number of events per year.

Maps of the extreme events corresponding to return periods of 10 and 50 years were produced for positive and negative NAO phased based on the GP models fitted to the POT series. These maps were compared in order to evaluate differences

in expected extreme events depending on the NAO. Though NAO mostly influences during winter season, some influence can be recognised during autumn and spring. Therefore the POT analysis was applied to the period between October and February.

3 Results

3.1 Differences in Average Daily Rainfall Erosivity Between Negative and Positive NAO Phases

The results of the WMW test comparing the distributions of daily erosivity during positive and negative NAO phases yielded 92 (59%) of significant series globally. Monthly results are shown in Table 1. These differences were present almost all the year, however being especially evident from autumn to early spring (October–March). Most observatories reflected this behaviour. During summer (June–August) the influence of NAO on rainfall erosivity was almost non-existent.

The spatial distribution of the significant relative differences between the daily rainfall erosivity recorded during negative and positive NAO phases for every month are shown in Fig. 4. The NAO influence can be noted from November to April, with different spatial patterns. From June to October we found no influence of NAO in rainfall erosivity, in addition, the relative differences were not significant for most of the area during June to September.

Higher differences were found closer to the Mediterranean. The highest differences between positive and negative NAO phases occurred from November to April, though March did not show any difference, most noticeable in the Mediterranean area where rainfall erosivity under negative NAO phases was between 6 and 30 times higher to the values registered under positive NAO. November showed the highest differences, affecting almost one half of the area extending from the Mediterranean coast to the west towards the centre of the Ebro valley.

Table 1 Difference in monthly erosivity between positive and negative NAO phases (Wilcoxon-Mann-Witney test): number and proportion of series with significant differences

Month	Significant series
Jan	144 (92%)
Feb	136 (87%)
Mar	68 (44%)
Apr	147 (94%)
May	109 (70%)
Jun	27 (17%)
Jul	40 (26%)
Aug	36 (23%)
Sep	11 (7%)
Oct	94 (60%)
Nov	152 (97%)
Dec	145 (93%)

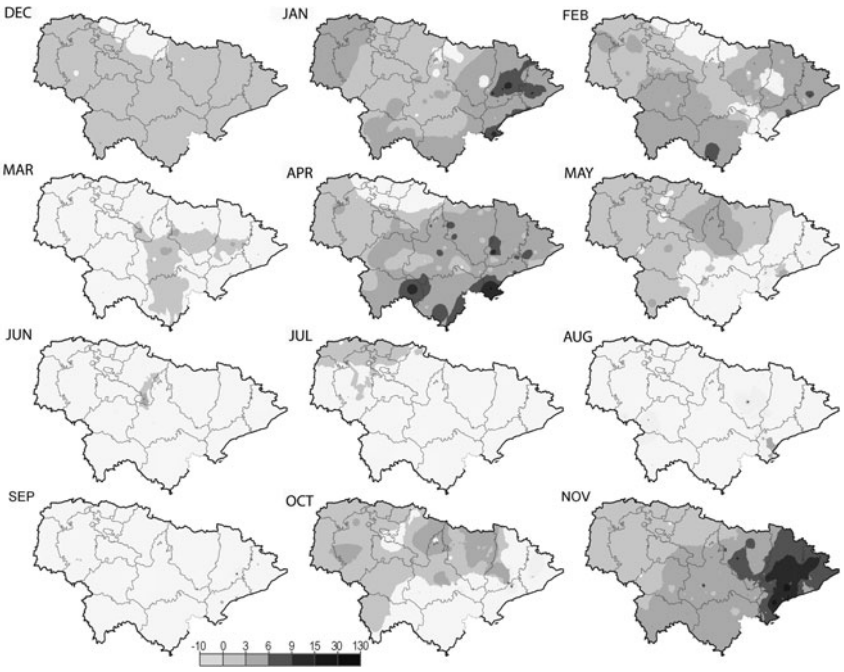

Fig. 4 Relative differences in median monthly rainfall erosivity during negative and positive NAO phases. *White masked areas* indicate no significant difference

3.2 Differences in Extreme Rainfall Erosivity Between Negative and Positive NAO Phases

The GP model provided a very good fit to the POT series of rainfall erosivity, as shown by the L-moment diagrams (Fig. 5). Independently of the sign of the NAO, the empirical L-moments of the rainfall erosivity series plotted closest to the theoretical curve of the GP distribution. The results of the Kolmogorov-Smirnov test allowed accepting the GP distribution for the data, since only in very few cases the null hypothesis that the data came from a GP distribution was rejected. This result agrees with recent studies that demonstrated the high performance of the GP distribution in fitting extreme hydrological variables using partial duration series (Hosking and Wallis, 1987; Madsen and Rosbjerg, 1997; Beguería, 2005). Here we also found that the GP distribution has a good performance in fitting daily rainfall erosivity data.

By adjusting the daily rainfall erosivity series for the selected months to the GP probability distribution we obtained the probability of occurrence of daily rainfall erosivity records associated with negative and positive NAO conditions. Results show greatest rainfall erosivity values expected under negative NAO conditions. Differences could be found between observatories. Those located inland to the south of the region did not show significant differences, however, as expected by results

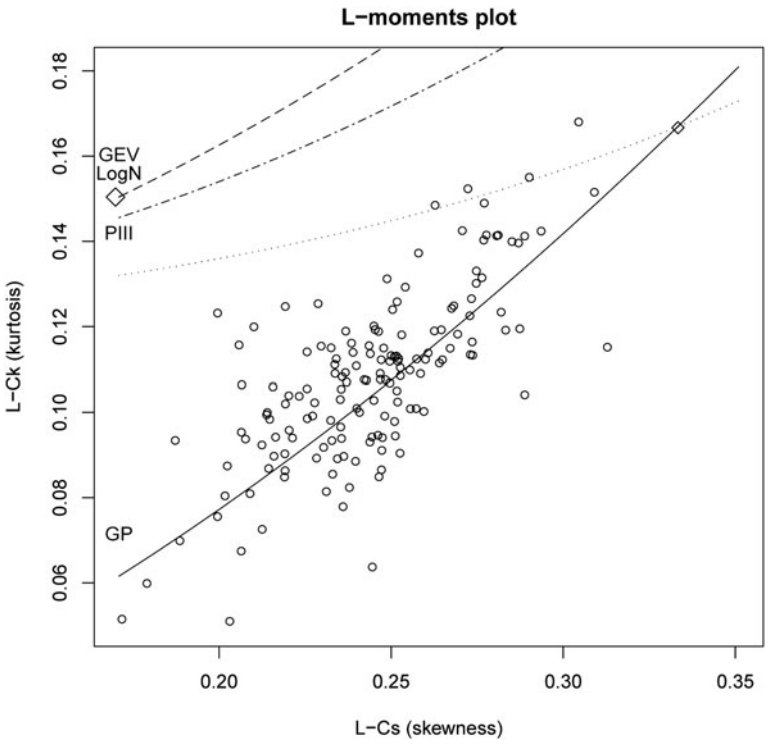

Fig. 5 L-moments ratio diagram, comparing empirical L-moment ratios (L-skewness and L-kurtosis) with the ones of several widely used extreme value distributions: Generalized Extreme Value (GEV), Log-Normal (LN), Pearson III (PIII) and Pareto (GP)

obtained in the precedent section. The mountainous areas and the Mediterranean coast showed a high contrast between the expected rainfall erosivity values under negative or positive conditions.

The rainfall erosivity values expected for a return period of 10 years related to negative and positive NAO conditions during winter and the respective standard error are shown in Fig. 6. Under negative NAO conditions daily rainfall erosivity values of 50 up to 385 (±8 to 22) MJ mm ha/h/d may be recorded in the northern and eastern half of the region. The highest values are concentrated at the north-east perimeter, close to the Mediterranean coast from the Ebro Delta upwards to the north and in the Central Pyrenees. Under positive NAO most of the region shows low daily rainfall erosivity values ranging between 5 and 50 (±0.5 to 8) MJ mm/ha/h/d. High erosivity values are only expected in localized areas such as the Ebro Delta and in the Central Pyrenees.

The results are very similar for a return period of 50 years (Fig. 7), although the spatial pattern of the very high erosivity values excludes the Pyrenees region and the highest erosivity values are thus confined to the Ebro Delta.

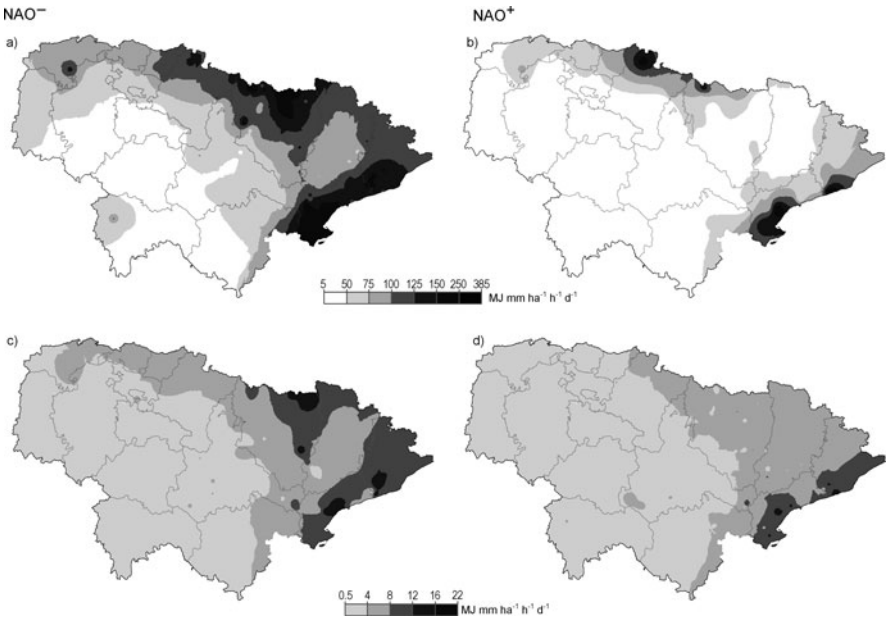

Fig. 6 Spatial distribution of expected daily rainfall erosivity during winter (October–March) corresponding to a return period of 10 years under negative (**a**) and positive (**b**) NAO phases, and their respective standard errors (**c** and **d**, respectively)

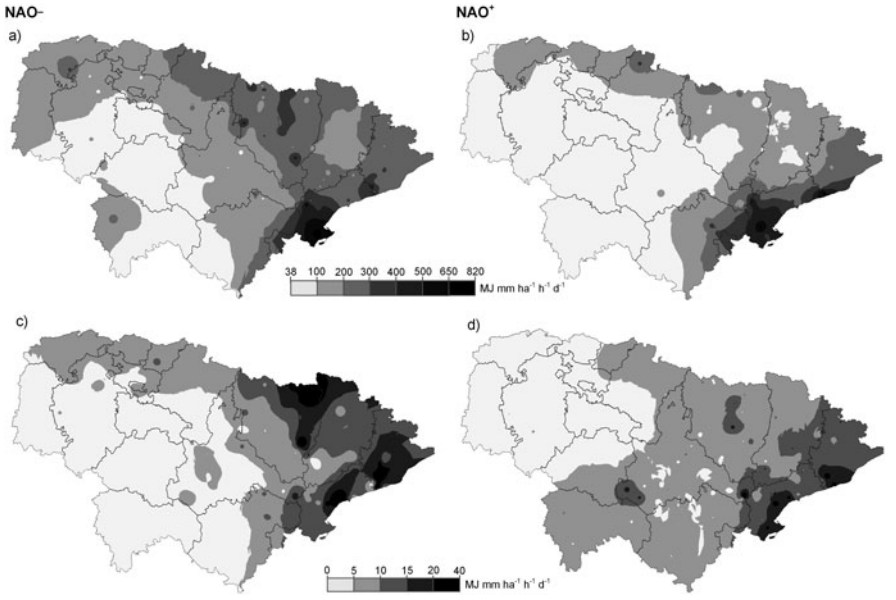

Fig. 7 Spatial distribution of expected daily rainfall erosivity during winter (October–March) corresponding to a return period of 50 years under negative (**a**) and positive (**b**) NAO phases, and their respective standard errors (**c** and **d**, respectively)

4 Discussion and Conclusions

Rainfall erosivity bridges the gap between rainfall dynamics and its direct impact over the surface of the soil, taking into account the energy of the raindrops hitting the soil, and the runoff which will remove the disaggregated soil particles. There is an increasing interest regarding the effects of the climate dynamics, especially in a context of climate change, in the environment. However, very few studies have related the atmospheric circulation patterns to rainfall erosivity due mostly to the lack of accurate rainfall erosivity series long enough to make this analysis possible.

The NAO is responsible for most of the climatic variability in the North Atlantic, modifying direction and intensity of the westerly winds, the track of the polar depressions and the location of the anticyclones. During the negative phase cyclones move southward increasing precipitation on the western Mediterranean. On the contrary, during the positive phases, the Azores subtropical high is reinforced, leading to a drier weather in the Mediterranean region.

This study has shown that atmospheric dynamics, in this case the NAO, have influenced interannual variability of rainfall erosivity at NE of Spain for the period 1955–2006. Higher rainfall erosivity values were related to negative NAO conditions whereas the high pressures associated with positive NAO conditions resulted in lower rainfall erosivity values. This difference was highest towards the east of the study area (Mediterranean region), and the centre of the Ebro valley, and during the winter months (November–April). Agriculture is a major land use in this area, and during this time of the year the agricultural soils are mostly uncovered and exposed to the erosive power of the rain, intensifying the impact of the NAO on soil erosion.

Knowledge of the spatial and temporal patterns of rainfall erosivity will help deepening our understanding of the processes of soil erosion, and might prove helpful for designing soil protection measures.

Acknowledgements We thank the Spanish Meteorological Agency (Agencia Española de Meteorología, AEMET) and the Ebro Basin Water Authority (Confederación Hidrográfica del Ebro, CHE) for providing the data used in this study. The research of M.A. was supported by a JAE-Predoc Research Grant from the Spanish National Research Council (Consejo Superior de Investigaciones Científicas; CSIC).

References

Angulo-Martínez M, Beguería S (2009) Estimating rainfall erosivity from daily precipitation records: a comparison among methods using data from the Ebro Basin (NE Spain). J Hydrol 379:111–121

Angulo-Martínez M, López-Vicente M, Vicente-Serrano SM, Beguería S (2009) Mapping rainfall erosivity at a regional scale: a comparison of interpolation methods in the Ebro Basin (NE Spain). Hydrol Earth Syst Sci 13:1907–1920

Bagarello V, D'Asaro F (1994) Estimating single storm erosion index. Trans Am Soc Agric Eng 37:785–791

Beguería S (2005) Uncertainties in partial duration series modelling of extremes related to the choice of the threshold value. J Hydrol 303:215–230

Beguería S, Vicente-Serrano SM, López-Moreno JI, García-Ruiz JM (2009) Annual and seasonal mapping of peak intensity, magnitude and duration of extreme precipitation events across a climatic gradient, North-east Iberian Peninsula. Int J Climatol 29:1759–1779

Brown LC, Foster GR (1987) Storm erosivity using idealized intensity distributions. Trans Am Soc Agric Eng 30:379–386
Coutinho MA, Tomás PP (1995) Characterization of raindrop size distributions at the Vale Formoso Experimental Erosion Centre. Catena 25:187–197
Curse R, Flanagan J, Frankenberger B, Gelder D, Herzmann D, James D, Krajenski W, Kraszewski M, Laflen J, Opsomer J, Todey D (2006) Daily estimates of rainfall, water runoff and soil erosion in Iowa. J Soil Water Conserv 61:191–199
Diodato N (2004) Estimating RUSLE's rainfall factor in the part of Italy with a Mediterranean rainfall regime. Hydrol Earth Syst Sci 8:103–107
D'Odorico P, Yoo J, Over TM (2001) An assessment of ENSO-Induced patterns of rainfall erosivity in the Southwestern United States. J Clim 14:4230–4242
Domínguez-Romero L, Ayuso Muñoz JL, García Marín AP (2007) Annual distribution of rainfall erosivity in western Andalusia, southern Spain. J Soil Water Conserv 62:390–401
EEA (2000) CORINE land cover 2000. European Environment Agency. http://image2000.jrc.it
Esteban-Parra MJ, Rodrigo FS, Castro-Diez Y (1998) Spatial and temporal patterns of precipitation in Spain for the period 1880–1992. Int J Climatol 18:1557–1574
García-Ruiz JM, Arnáez J, White SM, Lorente A, Beguería S (2000) Uncertainty assessment in the prediction of extreme rainfall events: an example from the Central Spanish Pyrenees. Hydrol Process 14:887–898
Helsel DR, Hirsch RM (1992) Statistical methods in water resources. Elesevier, New York, 522 pp
Hershfield DM (1973) On the probability of extreme rainfall events. Bull Am Meteorol Soc 54:1013–1018
Hosking JRM, Wallis JR (1987) Parameter and quantile estimation for the Generalized Pareto distribution. Technometrics 29:339–349
Hoyos N, Waylen PR, Jaramillo A (2005) Seasonal and spatial patterns of erosivity in a tropical watershed of the Colombian Andes. J Hydrol 314:177–191
Hurrell J (1995) Decadal trends in North Atlantic Oscillation and relationship to regional temperature and precipitation. Science 269:676–679
Hurrell J, Kushnir Y, Ottersen G, Visbeck M (eds) (2003) The North Atlantic Oscillation: climate significance and environmental impacts. Geophys Monogr Ser, vol 134. AGU, Washington, DC
Hurrell JW, van Loon H (1997) Decadal variations in climate associated with the North Atlantic oscillation. Clim Change 36:301–326
Jacobeit J (1987) Variations of trough positions and precipitation patterns in the Mediterranean area. J Climatol 7:453–476
Jones PD, Jónsson T, Wheeler D (1997) Extension to the North Atlantic Oscillation using early instrumental pressure observations from Gibraltar and South-West Iceland. Int J Climatol 17:1433–1450
Kutiel H, Maheras P, Guika S (1996) Circulation indices over the Mediterranean and Europe and their relationship with rainfall conditions across the Mediterranean. Theor Appl Climatol 54:125–138
Lana X, Burgueño A (1998) Spatial and temporal characterization of annual extreme droughts in Catalonia (Northeast Spain). Int J Climatol 18:93–110
Lasanta T (2003) Gestión agrícola y erosión del suelo en la cuenca del Ebro: el estado de la cuestión. Zubía 21:76–96
Llasat MC (2001) An objective classification of rainfall events on the basis of their convective features. Application to rainfall intensity in the North-East of Spain. Int J Climatol 21: 1385–1400
Llasat MC, Barriendos M, Barrera A, Rigo T (2005) Floods in Catalonia (NE Spain) since the 14th century. In: Benito G, Ouarda TBMJ, Bárdossy A (eds) Palaeofloods, historical data & climate variability: applications in flood risk assessment. J Hydrol 313:32–47
Madsen H, Rosbjerg D (1997) The partial duration series method in regional index-flood modeling. Water Resour Res 33:737–746
Maheras P (1988) Changes in precipitation conditions in the western Mediterranean over the last century. J Climatol 8:179–189

Marshall J, Kushnir Y, Battisti D, Chang P, Czaja A, Dickson R, Hurrell J, McCartney M, Saravanan R, Visbeck M (2001) North Atlantic climate variability: phenomena, impacts and mechanisms. Int J Climatol 21:1863–1898

Moses T, Kiladis GN, Diaz HF, Barry RG (1987) Characteristics and frequency of reversals in mean sea level pressure in the North Atlantic sector and their relationship to long-term temperature trends. J Climatol 7:13–30

Moulin C, Lambert CE, Dulac F, Dayan U (1997) Control of atmospheric export of dust from North Africa by the North Atlantic Oscillation. Nature 387:691–694

Onori F, De Bonis P, Grauso S (2006) Soil erosion prediction at the basin scale using the revised universal soil loss equation (RUSLE) in a catchment of Sicily (southern Italy). Environ Geol 50:1129–1140

Petkovsek G, Mikos M (2004) Estimating the R factor from daily rainfall data in the sub-Mediterranean climate of southwest Slovenia. Hydrol Sci J 49:869–877

Peñarrocha D, Estrela MJ, Millán M (2002) Classification of daily rainfall patterns in a Mediterranean area with extreme intensity levels: the Valencia region. Int J Climatol 22: 677–695

Rao AR, Hamed KH (2000) Flood frequency analysis. CRC Press, Boca Raton, FL

Renard KG, Foster GR, Weesies GA, McCool DK, Yoder DC (1997) Predicting soil erosion by water: a guide to conservation planning with the Revised Universal Soil Loss Equation (RUSLE). Handbook #703. US Department of Agriculture, Washington, DC

Richardson CW, Foster GR, Wright DA (1983) Estimation of erosion index from daily rainfall amount. Trans Am Soc Agric Eng 26:153–160

Rodó X, Baert E, Comin FA (1997) Variations in seasonal rainfall in southern Europe during the present century: relationships with the North Atlantic oscillation and the El Niño–Southern oscillation. Clim Dyn 19:275–284

Rodríguez-Puebla C, Encinas AH, Nieto S, Garmendia J (1998) Spatial and temporal patterns of annual precipitation variability over the Iberian Peninsula. Int J Climatol 18: 299–316

Romero CC, Baigorría GA, Stroosnijder L (2007) Changes of erosive rainfall for El Niño and La Niña years in Northern Andean highlands of Peru. Clim Change 85:343–356

Romero R, Guijarro JA, Ramis C, Alonso S (1998) A 30-year (1964–1993) daily rainfall data base for the Spanish Mediterranean regions: first exploratory study. Int J Climatol 18: 541–560

Serrano A, Garcia AJ, Mateos VL, Cancillo ML, Garrido J (1999) Monthly modes of variation of precipitation over the Iberian Peninsula. J Clim 12:2894–2919

Shi ZH, Cai CF, Ding SW, Wang TW, Chow TL (2004) Soil conservation planning at the small watershed level using RUSLE with GIS. Catena 55:33–48

Siegel S, Castelan NJ (1988) Nonparametric statistics for the behavioral sciences. McGraw-Hill, New York

Van der Knijff JM, Jones RJA, Montanarella L (2000) Soil erosion risk assessment in Italy. European Commission—European Soil Bureau, 52 pp

Van Dijk AIJM, Bruijnzeel LA, Rosewell CJ (2002) Rainfall intensity – kinetic energy relationships: a critical literature appraisal. J Hydrol 261:1–23

Vicente-Serrano SM (2005) Las sequías climáticas en el valle medio del Ebro: Factores atmosféricos, evolución temporal y variabilidad espacial. Consejo de Protección de la Naturaleza de Aragón, 277 pp

Vicente-Serrano SM, Beguería S, López-Moreno JI, García-Vera MA, Stepanek P (2010) A complete daily precipitation database for north-east Spain: reconstruction, quality control and homogeneity. Int J Climatol 30:1146–1163

Wischmeier WH (1959) A rainfall erosion index for a universal soil-loss equation. Soil Sci Soc Am Proc 23:246–249

Wischmeier WH, Smith DD (1978) Predicting rainfall erosion losses: a guide to conservation planning. USDA Handbook 537. USDA, Washington, DC

Impacts of the North Atlantic Oscillation on Landslides

José Luís Zêzere and Ricardo M. Trigo

Abstract Western Iberia landslides are mostly triggered by rainfall, as, in fact, are most landslides worldwide. Results obtained using empirical relationships between rainfall amount and duration, and slope instability show that critical rainfall conditions for failure are not the same for different types of landslides. While rapid debris flows are usually triggered by very intense showers concentrated in just a few hours, shallow translational soil slips are most commonly triggered by intense precipitation falls within the 1–15 days long range. On the contrary, activity of the more deeply-seated landslides of rotational, translational and complex types is related to successive weeks of nearly constant rainfall, over periods of 30–90 days. Large-scale patterns such as the El Niño and the North Atlantic Oscillation (NAO) change slowly and have been shown to have an impact in both the precipitation regime and the temporal occurrence of different landslide types in different areas of the world. In this work a particular attention is devoted to the impact of NAO on the landslide events that have occurred in the region located just north of Lisbon between 1956 and 2010. Results show that the large inter-annual variability of winter precipitation observed in Portugal is largely modulated by the NAO mode. The application of a 3-month moving average to both NAO index and precipitation time series allowed the identification of many months with landslide activity as being characterized by negative average values of the NAO index and high values of average precipitation (above 95 mm/month). Landslide activity in the study area is related to both intense, short duration precipitation events (1–15 days) and long-lasting rainfall episodes (1–3 months). The former events trigger shallow translational slides while the later episodes are usually associated with deeper and larger slope movements. The association between the NAO and landslide activity is shown to be more evident for the group of deep seated landslide events.

Keywords Landslides · Rainfall triggering · Thresholds · NAO

J.L. Zêzere (✉)
Centre for Geographical Studies, Institute of Geography and Spatial Planning, University of Lisbon, Lisbon, Portugal
e-mail: zezere@campus.ul.pt

S.M. Vicente-Serrano, R.M. Trigo (eds.), *Hydrological, Socioeconomic and Ecological Impacts of the North Atlantic Oscillation in the Mediterranean Region*, Advances in Global Change Research 46, DOI 10.1007/978-94-007-1372-7_14,

1 Introduction

According to Cruden (1991) a landslide can be defined as the movement of a mass of rock, earth or debris down a slope. Furthermore, the centre of gravity of the affected material in a landslide always moves in a downward and outward direction (Terzagui, 1950). The landslide classification proposed by Cruden and Varnes (1996) is the most widely adopted and it considers five landslide types, distinguished according to the type of rupture and displacement mechanisms: fall, topple, slide, lateral spread and flow.

Landslide factors are multiple and usually occur at the same time making it difficult to define in any particular case "what is the cause of the landslide". Glade and Crozier (2005) based on previous work by Crozier (1986) and Popescu (1994), proposed the classification of landslide causes in the following classes: predisposing factors, preparatory factors and triggering factors. This classification crosses with three different stability states on slopes defined by the same authors: stability, marginal stability and active instability (Glade and Crozier, 2005).

Landslide predisposing factors are those inherent terrain characteristics (e.g., slope geometry, soil and rock characteristics) that can be assumed as static at the short and mid-term and that control the likelihood of landslide occurrence in space. Landslide preparatory and triggering factors are dynamic and can be subdivided in geomorphologic processes, physical processes and anthropogenic processes (Popescu, 1994). When acting as preparatory factors, these processes promote the decrease of the stability margin of the slope without starting the slope movement. When acting as triggering factors, processes are the immediate cause of slope instability, and it is possible to establish a cause-effect relationship between triggering factor occurrence and landslide occurrence. Therefore, it is clear that geomorphologic, physical and anthropogenic factors may act both as landslide preparatory factors and landslide triggering factors depending on process intensity and temporal extent, as well as on the previous stability state of the slope (Glade and Crozier, 2005).

Rainfall is the most important physical process responsible for the triggering of landslides in the Mediterranean region, as in most regions worldwide (Wieczorek, 1996; Corominas, 2001; Guzzetti et al., 2007). Although the decisive role played by rainfall, there is no general "universal rule" regarding rainfall thresholds related to slope instability, despite the enormous effort done with this goal (e.g. Caine, 1980; Fukuota, 1980; Crozier, 1986; Van Asch et al., 1999; Corominas, 2001; Polemio and Petrucci, 2000; Guzzetti et al., 2007).

The control of rainfall on landslides differs substantially depending upon landslide depth and kinematics and the affected material. Shallow soil slips and rapid debris flows are typically activated by short period of very intense rain while deep-seated rotational and translational slides are usually associated with less intense rainfall occurring in period lasting from several weeks to several months (Van Asch et al., 1999). Therefore, even within a single region, different types of slope movements may be associated with different rainfall characteristics that produce different

hydrological triggering conditions (Van Asch et al., 1999; Polemio and Petrucci, 2000; Corominas, 2001; Zêzere and Rodrigues, 2002; Trigo et al., 2005).

Low frequency atmospheric patterns are associated with anomalous precipitation at the seasonal scale, and this is the main rationale to study the relationships between the atmospheric circulation patterns and landslide activity triggered by rainfall. Previous studies have related the Southern Oscillation and landslide activity in different parts of the world (Coe et al., 1998; Godt, 1999; Ngecu and Mathu, 1999). More recently, the authors have found a significant relationship between the North Atlantic Oscillation and the recent landslide-triggered events occurred in the Lisbon Region (Trigo et al., 2005; Zêzere et al., 2005). Apparently, this relationship is associated with the control that the NAO exerts, at the monthly and seasonal scales, on the storms coming from the North Atlantic Ocean that directly affect the Lisbon region (Zêzere et al., 2005, 2008). In this regard we are particularly interested to verify if this link holds for the recent unusual winter of 2009–2010 that has been characterised by high intense precipitation (Vicente-Serrano et al., 2011) and extreme negative NAO values (Cattiaux et al., 2010).

2 Hydrological Triggering Conditions of Landslides and Relation with Rainfall Patterns

Debris flows, shallow soil slips and deep-seated rotational and translational slides are among the most common of landslide types triggered by rainfall.

The generation of surface run-off and high peak discharges in first-order mountain catchments is a critical triggering mechanism for debris flows (Van Asch et al., 1999). This run-off occurs both on saturated and unsaturated soil conditions and provides water to debris material that have accumulated in channels, thus increasing the pore pressure within the debris mass which initiates the debris flow (Van Asch et al., 1999). In such circumstances, the maximum fluid pressure that can be generated in the debris mass is controlled by the infiltration capacity of the soil and the geometry of the slope (gradient, shape and roughness). The activation of debris flow is typically associated with short-duration (minutes to hours) peak rainfall events.

Shallow translational soil slips are failures occurring on steep slopes at a critical depth in general not more than 1–2 m. These landslides are typically triggered by the rapid infiltration and the unsaturated percolation of water in the thin soil material (colluvium deposits) which overlies impermeable rocks. The critical reduction of the soil shear resistance and the consequent slope failure is due to the rapid and temporary rise of the pore water pressure and the loss of soil apparent cohesion resulting from soil saturation (Gostelow, 1991; Iverson, 2000). Activity of rainfall-triggered shallow translational soil slips are usually associated with intense rainfall accumulating within the 1–15 days period.

Deep-seated rotational and translational slides are slope failures occurring along a slip surface located typically at a depth ranging from 5 to 20 m. Materials mobilized by these landslides are soils and rocks that yield small effective hydraulic

diffusivities (Iverson, 2000). Deep-seated landslides are triggered by the reduction of shear strength of involved rocks and soils, resulting from the steady rise on the groundwater level (Gostelow, 1991; van Asch et al., 1999; Iverson, 2000). Therefore, when compared with shallow soil slips deep landslides need larger absolute amounts of water for triggering conditions, and are associated with larger windows of antecedent rainfall (Van Asch et al., 1999). Activity of this type of landslides is usually related to successive weeks of nearly constant rainfall, over periods lasting from 30 to 90 days.

3 Temporal Occurrence of Rainfall-Triggered Landslides in Lisbon Region and Rainfall Triggering Thresholds

3.1 Rainfall Regime and Landslide Events

The rainfall regime in the Lisbon Region is characterized by high variability at the inter-seasonal and the inter-annual scales. The mean annual precipitation (MAP) at the reference rain gauge of S. Julião do Tojal is 730 mm where a daily rainfall data series is available since 1956 (SJT, Fig. 1). Summer months are noticeably dry and rainfall concentrates in the period lasting from October to March (78% of the total amount; 72% of the total rainy days).

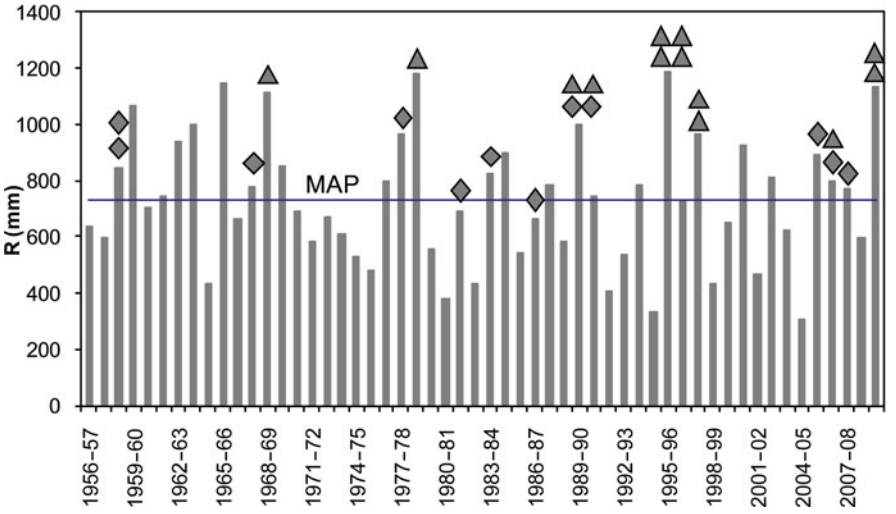

Fig. 1 Annual precipitation (climatological year) at the reference rain gauge of S. Julião do Tojal (period: 1956/1957–2009/2010). *Diamonds*: Shallow landslides events; *triangles*: Deep landslides events

Although the term "landslide event" may be used to characterize the occurrence of a single landslide, this term has a wider connotation as it is used to describe a number of individual landslides triggered in a wide area by a single triggering event, such as an earthquake or an intense rainstorm (Crozier and Glade, 1999). Within this concept, a landslide event in the Lisbon region is a period (a date) for which at least 5 individual landslides are known to have occurred on natural slopes. This number is in accordance with the typical landslide activity observed in the study area (Zêzere et al., 1999).

The dates of landslide activity were reconstructed from field work, archive investigation and interviews with the population living in the study area. A particular attention was given to the particular type(s) of landslide(s) occurred in each event, and a distinction was made between shallow and deep-seated landslides. From 1956–1957 to 2009–2010, 25 landslide events were recognized corresponding to a frequency of one event each 2.16 years, although some years were marked by the occurrence of multiple events (e.g. 1989–1990, 1995–1996, 2009–2010). The total area affected by the above mentioned landslide types within each landslide event

Table 1 Landslide events triggered by rainfall in the Lisbon region from 1956 to 2010

Landslide event #	Date (yyyy/mm/dd)	Critical rainfall amount/duration mm (dd)	Rainfall intensity/ duration mm/day (dd)	Return period (years)	Dominant landslide type
1	1958/12/29	149 (10)	14.9 (10)	2.7	Shallow
2	1959/03/09	175 (10)	17.5 (10)	4.4	Shallow
3	1967/11/15	137 (1)	137.0 (1)	62	Shallow
4	1968/11/15	350 (30)	11.7 (30)	7.6	Deep
5	1978/03/04	204 (15)	13.6 (15)	3.9	Shallow
6	1979/02/10	694 (75)	9.2 (75)	22	Deep
7	1981/12/30	174 (5)	34.7 (5)	14	Shallow
8	1983/11/18	164 (1)	164.0 (1)	194	Shallow
9	1987/02/25	52 (1)	52.0 (1)	2.1	Shallow
10	1989/11/22	164 (15)	11.0 (15)	2.2	Shallow
11	1989/11/25	217 (15)	14.4 (15)	4.7	Shallow
12	1989/12/05	333 (30)	11.1 (30)	6.3	Deep
13	1989/12/21	495 (40)	12.4 (40)	18	Deep
14	1996/01/09	544 (60)	9.1 (60)	11	Deep
15	1996/01/23	686 (75)	9.1 (75)	21	Deep
16	1996/01/28	495 (40)	12.4 (40)	18	Deep
17	1996/02/01	793 (90)	8.8 (90)	27	Deep
18	2001/01/06	447 (60)	7.4 (60)	5.1	Deep
19	2001/01/09	467 (60)	7.8 (60)	6	Deep
20	2006/03/20	156 (4)	39.0 (4)	13	Shallow
21	2006/10/27	219 (10)	21.9 (10)	11	Shallow
22	2006/11/28	427 (40)	10.7 (40)	9	Deep
23	2008/02/18	141 (1)	140.9 (1)	73	Shallow
24	2010/01/14	332 (30)	11.1 (30)	6	Deep
25	2010/03/09	632 (90)	7.0 (90)	8	Deep

was the criterion used to distinguish between shallow and deep landslide events reported in Fig. 1 and Table 1. Shallow (deep) landslide events are characterized by more than 50% of landslide area associated to slip surfaces depth < 1.5 m (depth > 1.5 m). According to this criterion, 13 deep and 12 shallow landslide events were recorded. Interestingly, the nature of the events is non-stationary, with significant changes in frequency of deep and shallow events between the first and second halves of the period considered. Thus, shallow landslide events were more frequent from 1956 until 1989 (9 in 11 cases), while deep landslide events were dominant from 1989 to 2010 (11 in 14 cases).

3.2 Absolute Antecedent Rainfall Threshold

Following the approach used previously by the authors (Trigo et al., 2005; Zêzere et al., 2005), the relationship between rainfall and landslide activity was assessed by computing the cumulative absolute antecedent rainfall for the 1–5, 10, 15, 30, 40, 60, 75, and 90 consecutive days anteceding each landslide event. The Gumbel distribution (Gumbel, 1958) was used to derive the return period for each rainfall amount/duration combination. The critical rainfall combination (quantity-duration) responsible for each landslide event is shown in Table 1, and it was obtained, assuming as critical pair the combination with the higher return period. We acknowledge this assumption lacks a physical basis, nevertheless it provides the best discrimination between landslide events and other rainfall periods not related with slope instability (Zêzere et al., 2005).

The combination between rainfall intensity and critical rainfall duration for the 25 landslide events registered from 1956 to 2010 is shown in Fig. 2. The regression analysis shows that rainfall intensity increases exponentially as duration decreases, following the equation $Ri = 92.03D^{-0.594}$ ($r^2 = 0.902$), where Ri is the rainfall intensity in mm/day and D is the duration of rainfall in days. Figure 2 also shows the maximum yearly values for durations of 1, 5, 10, 15, 30, 40, 60, 75 and 90 days that were computed for those years without landslide activity. The vast majority of these values lie below the fitted curve, thus confirming that regression curve may be used as a reliable rainfall intensity – duration threshold for the study area.

The above mentioned regression model was used to derive the minimum daily rainfall needed to reach the precipitation triggering threshold at the reference rain gauge (S. Julião do Tojal), for any of the following consecutive days: 1–5, 10, 15, 30, 40, 60, 75 and 90 (Zêzere et al., 2008). This calculation accounts for the continuous cumulative absolute antecedent rainfall, and it is shown in Fig. 3 for the time span lasting from 2000 to 2010. During this period, our model correctly predicted 7 landslide events (Landslide events # 18, 19, 20, 21, 22, 23 and 24), and the landslide event # 25 is the solely "false negative" (i.e., unpredicted landslide event). In addition, there is no evidence of "false positives" (i.e., predicted landslide events that did not occur).

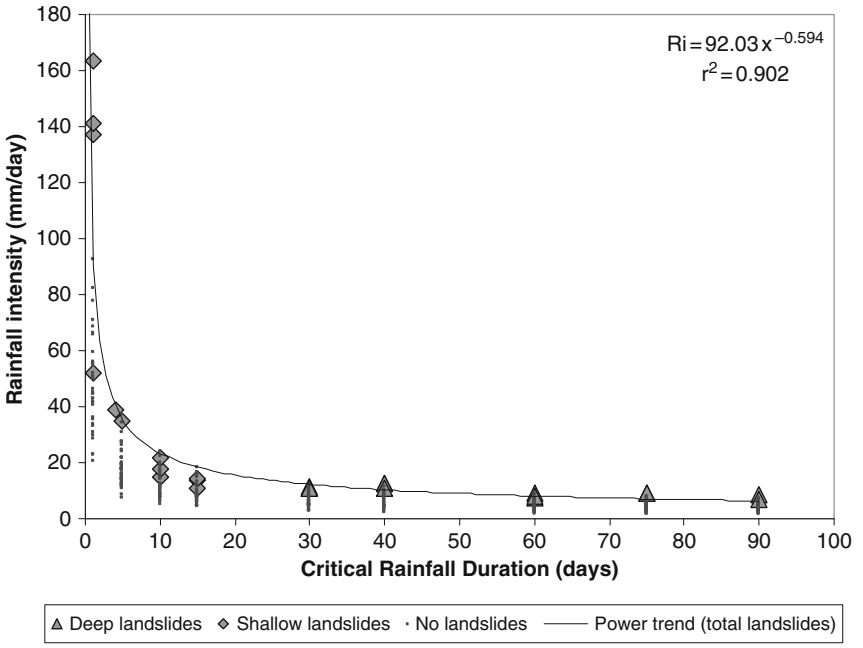

Fig. 2 Regression line between rainfall intensity and rainfall duration for landslide events in the Lisbon region (period 1956–2010)

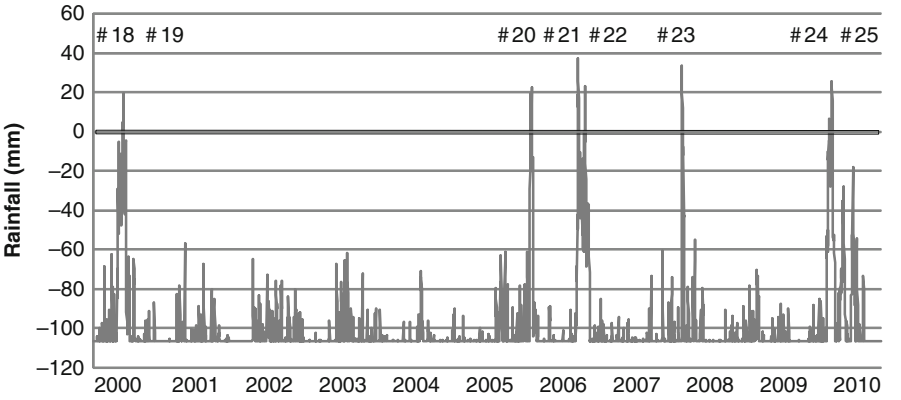

Fig. 3 Daily rainfall needed to reach the rainfall threshold in S. Julião do Tojal for landslide initiation in the Lisbon region (period: September 2000–August 2010)

Table 2 Calibrated antecedent rainfall (CAR) for landslide events in the Lisbon region from 1956 to 2010

Landslide event #	Date (yyyy/mm/dd)	Daily rainfall (mm)	3 days (mm)	5 days (mm)	10 days (mm)	15 days (mm)	30 days (mm)	No. of previous consecutive days with 30-days CAR >50 mm	Dominant landslide type
1	1958/12/29	22.0	54.2	73.6	91.7	99.2	108.5	6	Shallow
2	1959/03/09	45.5	27.5	55.4	82.2	82.2	83.6	4	Shallow
3	1967/11/15	137.0	4.1	4.1	10.3	16.3	25.2	0	Shallow
4	1968/11/15	45.5	43.4	47.3	74.3	92.3	107.7	18	Deep
5	1978/03/04	14.5	43.9	67.1	93.8	105.0	109.8	8	Shallow
6	1979/02/10	26.0	89.3	93.6	110.1	119.7	133.6	17	Deep
7	1981/12/30	78.0	75.5	75.5	102.6	109.5	111.3	3	Shallow
8	1983/11/18	163.7	42.1	59.8	88.2	96.7	103.8	10	Shallow
9	1987/02/25	51.8	22.2	35.4	36.0	46.5	52.1	1	Shallow
10	1989/11/22	33.5	19.9	50.7	62.9	70.9	72.1	4	Shallow
11	1989/11/25	38.0	36.9	42.7	75.7	88.5	89.1	7	Shallow
12	1989/12/05	30.1	58.1	58.1	78.8	93.7	109.7	17	Deep
13	1989/12/21	26.7	29.1	40.5	65.3	78.2	100.9	33	Deep
14	1996/01/09	66.5	17.8	29.5	54.2	79.5	88.4	17	Deep
15	1996/01/23	23.6	36.5	38.7	53.2	78.9	96.8	31	Deep
16	1996/01/28	25.5	9.2	30.9	53.7	62.3	85.6	36	Deep
17	1996/02/01	24.5	34.5	48.6	69.1	79.9	97.9	40	Deep
18	2001/01/06	24.5	22.7	39.1	53.7	79.1	87.4	17	Deep
19	2001/01/09	16.0	22.1	38.6	51.9	67.1	85.3	20	Deep
20	2006/03/20	42.1	89.5	89.6	89.7	95.9	107.4	2	Shallow
21	2006/10/27	26.0	64.4	99.1	126.8	131.4	132.1	6	Shallow
22	2006/11/28	36.5	33.4	58.0	62.8	74.5	79.6	3	Deep
23	2008/02/18	140.9	0.0	0.0	0.3	6.2	6.6	0	Shallow
24	2010/01/14	16.6	55.6	56.1	70.4	78.3	99.7	19	Deep
25	2010/03/09	29.7	36.1	44.8	62.4	72.9	83.4	15	Deep

3.3 Calibrated Antecedent Rainfall Thresholds

Due to superficial and sub-superficial drainage, the impact of a particular rainy event on slope hydrology decreases in time (Canuti et al., 1985; Crozier, 1986). In order to account this effect in the analysis of rainfall-triggered landslide events, we reconstructed the calibrated antecedent rainfall (CAR) for 3, 5, 10, 15 and 30 days using the algorithm proposed by Crozier (1986):

$$CARx = KP1 + K^2P2 + ...K^nPn \quad (1)$$

where CARx is the calibrated antecedent rainfall for day x; P1 is the daily rainfall observed for the day before day x; Pn is the daily rainfall registered for the n-th day before day x; and K (assumed to be 0.9) is the empirical parameter that accounts for the decrease of the impact of a particular rainy event in time due to drainage processes.

Table 2 summarizes the calibrated antecedent rainfall computed with Equation (1) for the 25 landslide events registered in the Lisbon Region. The distinction between shallow and deep landslide events concerning the number of days relevant to the antecedent rainfall was confirmed by combining the daily rainfall and the CAR (Fig. 4). The best result for shallow landslide events was obtained with the combination between the daily rainfall and the 5 days CAR through the exponential rule $Dr = 151.57e^{-0.0336CAR}$ (where Dr is the daily rainfall), whereas deep landslide events are better discriminated by a combined threshold of daily rainfall = 16 mm and 30 days CAR = 80 mm.

Differences on the relevance of antecedent rainfall for shallow and deep landslide events are also remarkable regarding the number of previous consecutive days with 30 days CAR>50 mm (Table 2). This number ranges from 0 to 10 days for dates of shallow movements occurrence, and increases up to a minimum of 15 days for dates characterised by deep landslide activity, with the single exception of landslide event #22.

4 Impact of NAO on Precipitation and on Landslide Occurrence in Lisbon Region

Previous works have shown that the phase of the NAO pattern is the most important to model the temporal precipitation distribution over western Iberia (Hurrell, 1995; Trigo et al., 2004; Zêzere et al., 2005). In fact the authors have shown that the NAO is (statistically) associated with the occurrence of landslide events, particularly those triggered by prolonged periods (up to 3 months) of precipitation (Trigo et al., 2005; Zêzere et al., 2005, 2008).

The NAO index used here was developed at the Climatic Research Unit (University of East Anglia, UK) and is defined, on a monthly basis, as the difference between the normalized surface pressure at Gibraltar (southern tip of Iberian Peninsula) and Stykkisholmur in Iceland (Jones et al., 1997). The NAO index for

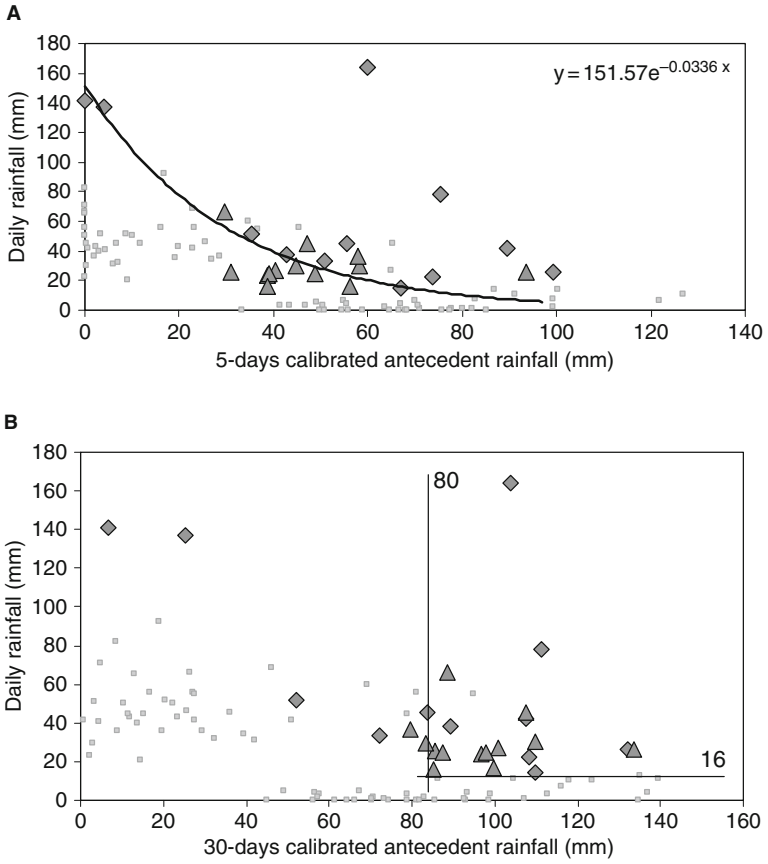

Fig. 4 Relationship between daily rainfall and 5-days (**a**) and 30-days (**b**) calibrated antecedent rainfall (CAR) for landslide events in the Lisbon region (period 1956–2010). *Diamonds*: values associated with shallow landslides events; *triangles*: values associated with deep landslides events; *small dots*: values obtained from the yearly maximum daily rainfall and from the yearly maximum CAR, computed for years without landslide events

winter months presents a positive trend for the last 3 decades of the twentieth century, thus the corresponding distribution is dominated by positive values. In order to remove this positive bias we have normalized all values of NAO index, at the monthly scale, between 1938 and 2010 (the period with precipitation data for the nearby SJT series). We apply the same approach developed previously (Trigo et al., 2005; Zêzere et al., 2008) but updating it to the year 2010. Thus a 3-month moving average was applied to filter the original NAO index and SJT precipitation time series, restricting the analysis to monthly data from the wet season (NDJFM), with the single exception of the landslide event #21 for which October and September values were considered. October values are used to compute November and December averages. Thus, values for February of *year n*, correspond

to the rainfall and NAO index averages computed between December of *year n*–1 and February of *year n*, while values for November of any year are restricted to the October and November values for that same year. For landslides episodes that have occurred in the first 5 days of the month we only considered the NAO index and precipitation values from the previous 2 months (events 5, 12 and 17). The scatter plot obtained with both filtered time series is shown in Fig. 5, being limited to the winter (NDJFM) months. Small open diamonds represent months where landslide events did not occur (or were not reported). Black circles correspond to months with only one recognized landslide event (e.g. February 1996, event 17), while black triangles represent those months with more than one landslide event (e.g. December 1989, events 12 and 13). A number of relevant remarks can be raised in relation to Fig. 5:

1. The linear correlation between both time series is –0.58 (statistically significant at the 1% level) increasing slightly to –0.61 if we restrict the analysis to those months affected by landslide activity represented by the numbered black circles and triangles (regression line is also represented).
2. All months characterized with landslide events are located above the 3-month average precipitation (horizontal line indicating the threshold of 95 mm/month). Furthermore, with the exception of event #23 all cases are characterized by negative values of the averaged NAO index. Interestingly, this event occurred on the 18 February 2008 corresponding to the new all time record of daily precipitation observed in Lisbon (since 1865), Capital of Portugal located just 14 km south of SJT (Fragoso et al., 2010).

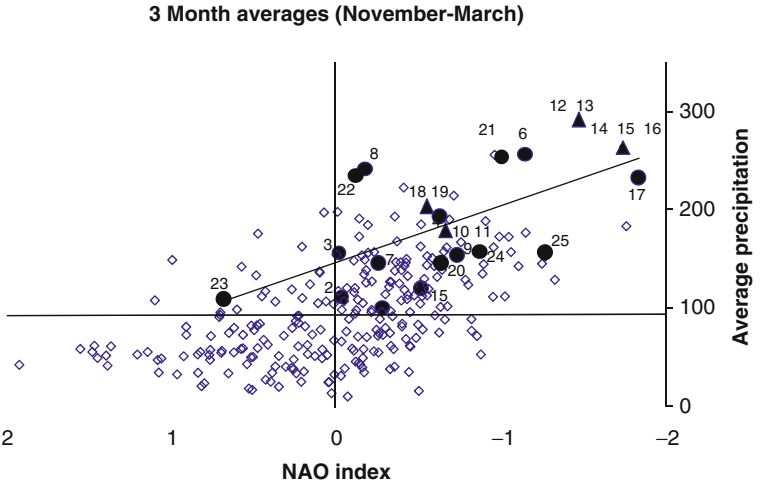

Fig. 5 Scatter plot between 3-month moving average NAO index and SJT precipitation time series (November–March), for the period ranging between 1956 and 2010 (270 months). *Small open diamonds*: months with no landslide events reported. *Black circles*: months with one recognized landslide event. *Black triangles*: months with more than one recognized landslide event. *Numbers* next to *gray symbols* represent the landslide episode number as given in Tables 1 and 2

3. The majority of the multiple landslide events episodes (#12 to #16) are characterized by extremely negative average values of the NAO index (lower than –1) and extremely high values of average precipitation (clearly above 200 mm/month). This prolonged anomalous precipitation regime favors the occurrence of multiple deep landslide events (Table 1).

5 Conclusion

Landslide events occurred since 1956 in the Lisbon region were triggered by rainfall. Events dominated by shallow soil slips have been related to short periods (1–15 days) of intense rainfall, whereas events characterized by the occurrence of deep seated slope movements have been associated to longer periods (30–90 days) of less intense rain. The distinction between landslide types concerning the number of days relevant to the antecedent rainfall was confirmed combining the daily rainfall and the calibrated antecedent rainfall (CAR) from 3 to 30 days for each landslide event. An exponential rule was identified ($Dr = 151.57e^{-0.0336CAR}$) for the 5 days CAR, which is a threshold for shallow landslide events, while deep landslide events were better discriminated by a combined threshold of daily rainfall = 16 mm and 30 days CAR = 80 mm.

These different rainfall triggering conditions are consistent with the different hydrologic processes associated with different types of slope movements. Intense rainfall allows the rapid growth of pore water pressure and the drop of capillarity forces that sustain the apparent cohesion of thin soils. Therefore, shallow soil failures occur within the soil material or at the contact with the underlying less permeable bedrock. Long lasting rainfall episodes enable the steady rise of the groundwater table and the development of positive pore water pressures into the soil. Consequently, deep seated failures occur in relation to the reduction of shear strength of affected materials.

Despite the different relationships existing between the activity of shallow and deep seated landslides and the rainfall triggering conditions, it was possible to derive a single exponential law relating rainfall intensity and the rainfall critical duration for the total set of landslide events occurred in the Lisbon region from 1956 to 2010. The fitting of the curve to the 25 landslide events is impressive ($r^2 = 0.9$) and the vast majority of rainfall episodes that did not cause landslides lie below the curve, thus confirming the curve as a consistent rainfall intensity/duration threshold for the triggering of landslides in the study area.

The linear correlation between the 3 month average NAO index and precipitation is statistically significant (–0.61) for those months characterized by the occurrence of landslide events. The complete set of landslide events lies above the 3-month average precipitation, and 24 in 25 events present negative values of the 3-month average NAO index. Taking into account the different rainfall periods associated with shallow and deep seated landslides events, the association between the NAO and landslide activity is more evident for the group of deep seated landslide events. In addition, the majority of months characterized by the occurrence of

multiple landslide events exhibit extremely high values of average precipitation and extremely negative average values of the NAO index.

However, it must be stressed that it is not so clear-cut to establish the sequence of physical phenomena that link the NAO configuration with local landslide activity. Without pretending to describe the entire chain of physical processes involved these must include; (1) the NAO control of the preferred path for north Atlantic storm tracks, (2) how these low pressure systems influence the precipitation regime of western Iberia, (3) to what extent the precipitation anomalies impact local soil moisture at different temporal scales, and (4) how these changes can be critical for surpassing water pressure thresholds that can trigger landslides.

Acknowledgements This work was supported by Projects Maprisk – Methodologies for assessing landslide hazard and risk applied to municipal planning (PTDC/GEO/68227/2006) and DISASTER – GIS database on hydro-geomorphologic disasters in Portugal: a tool for environmental management and emergency planning (PTDC/CS-GEO/103231/2008) funded by the Portuguese Foundation for Science and Technology (FCT).

References

Caine N (1980) The rainfall intensity–duration control of shallow landslides and debris flows. Geografiska Annaler 62:23–27

Canuti P, Focardi P, Garzonio CA (1985) Correlation between rainfall and landslides. Bull Int Assoc Eng Geol 32:49–54

Cattiaux J, Vautard R, Cassou C, Yiou P, Masson-Delmotte V, Codron F (2010) Winter 2010 in Europe: a cold extreme in a warming climate. Geophys Res Lett 37:L20704. doi:10.1029/2010GL044613

Coe JA, Godt JW, Wilson RC (1998) Distribution of debris flows in Alameda County, California triggered by 1998 El Niño rainstorms: a repeat of January 1982? EOS 79:266

Corominas J (2001) Landslides and climate. Keynote lectures from the 8th international symposium on landslides 4:1–33

Crozier M (1986) Landslides: causes, consequences and environment. Croom Helm, London

Crozier MJ, Glade T (1999) Frequency and magnitude of landsliding: fundamental research issues. Z Geomorph NF Suppl-Bd 115:141–155

Cruden DM (1991) A simple definition of a landslide. Bull Int Assoc Eng Geol 43:27–29

Cruden DM, Varnes DJ (1996) Landslide types and processes. In: Turner AK, Schuster RL (eds) Landslides: investigation and mitigation. National Research Council, Transportation Research Board, Washington, DC, pp 36–75

Fragoso M, Trigo RM, Zêzere JL, Valente MA (2010) The exceptional rainfall episode registered in Lisbon in 18 February 2008. Weather 65(2):31–35

Fukuota M (1980) Landslides associated with rainfall. Geotech Eng 11:1–29

Glade T, Crozier MJ (2005) The nature of landslide hazard and impact. In: Glade T, Anderson MG, Crozier MJ (eds) Landslide hazard and risk. Wiley, Chichester, pp 43–74

Godt JW (1999) Maps showing locations of damaging landslides caused by El Niño rainstorms, winter season 1997–98, San Francisco Bay region, CA. USGS http://pubs.usgs.gov/mf/1999/mf-2325/

Gostelow P (1991) Rainfall and landslides. In: Almeida-Teixeira M et al (eds) Prevention and control of landslides and other mass movements. CEC, Bruxels, pp 139–161

Gumbel EJ (1958) Statistics of extremes. Columbia University Press, New York

Guzzetti F, Peruccacci S, Rossi M, Stark CP (2007) Rainfall thresholds for the initiation of landslides in central and southern Europe. Meteorol Atmos Phys 98:239–267

Hurrell JW (1995) Decadal trends in the North Atlantic Oscillation: regional temperatures and precipitation. Science 269:676–679

Iverson RM (2000) Landslide triggering by rain infiltration. Water Resour Res 36:1897–1910

Jones PD, Jónsson T, Wheeler D (1997) Extension to the North Atlantic Oscillation using early instrumental pressure observations from Gibraltar and south-west Iceland. Int J Climatol 17:1433–1450

Ngecu WM, Mathu EM (1999) The El-Niño triggered landslides and their socioeconomic impact in Kenya. Environ Geol 38:277–284

Polemio M, Petrucci O (2000) Rainfall as a landslide triggering factor: an overview of recent international research. In: Bromhead E, Dixon N, Ibsen M (eds) Landslides in research, theory and practice. Thomas Telford, London, pp 1219–1226

Popescu M (1994) A suggested method for reporting landslide causes. Bull Int Assoc Eng Geol 50:71–74

Terzagui K (1950) Mechanisms of landslides. Geological Society of America (Berkey Volume), pp 83–123

Trigo RM, Pozo-Vázquez D, Osborn TJ, Castro-Díez Y, Gámiz-Fortis S, Esteban-Parra MJ (2004) North Atlantic Oscillation influence on precipitation, river flow and water resources in the Iberian Peninsula. Int J Climatol 24:925–944

Trigo RM, Zêzere JL, Rodrigues ML, Trigo IF (2005) The influence of the North Atlantic Oscillation on rainfall triggering of landslides near Lisbon. Nat Hazards 36:331–354

Van Asch T, Buma J, Van Beek L (1999) A view on some hydrological triggering systems in landslides. Geomorphology 30:25–32

Vicente-Serrano SM, Trigo RM, Liberato ML, López-Moreno JI, Lorenzo-Lacruz J, Beguería S, Morán-Tejeda H, El Kenawy A (2011) The 2010 extreme winter North Hemisphere Atmospheric variability in Iberian precipitation: anomalies, driving mechanisms and future projections. Clim Res 46:51–65

Wieczorek GF (1996) Landslides triggering mechanisms. In: Turner AK, Schuster RL (eds) Landslides: investigation and mitigation. National Research Council, Transportation Research Board, Washington, DC, pp 76–90

Zêzere JL, Ferreira AB, Rodrigues ML (1999) Landslides in the north of Lisbon region (Portugal): conditioning and triggering factors. Phys Chem Earth, Part A 24:925–934

Zêzere JL, Rodrigues ML (2002) Rainfall thresholds for landsliding in Lisbon area (Portugal). In: Rybar J, Stemberk J, Wagner P (eds) Landslides. A.A. Balkema, Lisse, pp 333–338

Zêzere JL, Trigo RM, Fragoso M, Oliveira SC, Garcia RAC (2008) Rainfall-triggered landslides in the Lisbon region over 2006 and relationships with the North Atlantic Oscillation. Nat Hazards Earth Syst Sci 8:483–499

Zêzere JL, Trigo RM, Trigo IF (2005) Shallow and deep landslides induced by rainfall in the Lisbon region (Portugal): assessment of relationships with the North Atlantic Oscillation. Nat Hazards Earth Syst Sci 5:331–344

The Impact of the NAO on the Solar and Wind Energy Resources in the Mediterranean Area

David Pozo-Vazquez, Francisco Javier Santos-Alamillos, Vicente Lara-Fanego, Jose Antonio Ruiz-Arias, and Joaquín Tovar-Pescador

Abstract The influence of the NAO on the solar and wind energy resources in the Mediterranean area, in particular, and over the whole North Atlantic area, in general, has been explored based on the analysis of 20 years of reanalysis and satellite data. The analysis was carried out for the winter and annual periods and proved the existence of a marked influence of the NAO pattern on the spatial and temporal variability of the solar and wind energy resources in the study area. Particularly, the NAO signature on the solar/wind energy resources was found to be a north-south dipolar pattern, with the positive/negative centre over the Mediterranean area. Although the spatial patterns obtained are similar, the nature of the relationship obtained for wind energy was found to be less linear and more complex than that attained for solar energy. A composite analysis revealed that interannual variability of the solar and wind energy resources in the Mediterranean area can reach values above 20% in winter and 10% in the annual case associated with changes in the NAO phase. Finally, the analysis of the spatial patterns of the NAO influence on the solar and wind energy resources revealed the existence of spatial and local balancing between these two energy resources in the study area. Results are of interest regarding the estimation of the expected interannual variability of the wind farms and solar plants production in the study region.

Keywords NAO · Balancing renewable energy · Solar energy · Wind energy

1 Introduction

According to the latest estimates, it is expected that the worldwide primary energy demand will increase by 45% and the demand for electricity will increase by 80% between 2006 and 2030 (IEA, 2008). As a consequence, and without a decisive action, energy-related greenhouse gases (GHG) emissions will more than double by 2050 and the increased oil demand will intensify the concerns over the security of supplies. There are different pathways to stabilize GHG concentrations, but a key

D. Pozo-Vazquez (✉)
Department of Physics, University of Jaén, Jaén, Spain
e-mail: dpozo@ujaen.es

S.M. Vicente-Serrano, R.M. Trigo (eds.), *Hydrological, Socioeconomic and Ecological Impacts of the North Atlantic Oscillation in the Mediterranean Region*, Advances in Global Change Research 46, DOI 10.1007/978-94-007-1372-7_15,

issue in all of them is the replacement of fossil fuels by renewable energy sources. European Union (EU) regulations, for example, set a binding target for 20% of the EU's total energy supply to come from renewable by 2020 (corresponding to a sharp increase from the modest 6.5% observed in 2007). Furthermore, they set a firm target of cutting 20% of the EU's greenhouse gases emissions by 2020 relative to 1990. In this scenario, solar and wind energies -the renewables with the most mature- will necessarily play a key role.

There are three main solar technologies. The first one is the direct conversion of sunlight into electricity (Photovoltaic, PV effect), the concentrating solar power (CSP) and the solar thermal collectors for heating and cooling (SHC). PV and CSP technologies are meant to produce electricity, while SHC can only be used for heating and cooling purposes. PV systems enable direct conversion of sunlight into electricity through semi-conductor devices, through the global horizontal irradiance (GHI) they receive. Today, PV provides 0.2% of total global electricity generation, being Germany the leading country in the world, with 5 GW installed capacity, followed by Spain with above 4 GW (about 4% of the installed capacity). While its use is small today, PV power has a particularly promising future. Actually, global PV capacity has been increased at an average annual growth rate of more than 40% since 2000 and it has significant potential for long-term growth over the next decades. Particularly, PV is projected to provide around 5% of global electricity consumption by 2030, rising to 11% by 2050 (IEA, 2010a). In this context, the Mediterranean area (France, Italy, Greece) are expected to play a major role (IEA, 2010a). The basic concept of CSP is relatively simple: CSP devices concentrate energy from the sun's rays to heat a receiver to high temperatures. This heat is then transformed first into mechanical energy (by turbines or other engines) and then into electricity. The solar energy that CSP plants use is measured as direct normal irradiance (DNI), which is the energy received on a surface tracked perpendicular to the sun's rays. CSP developers typically set a bottom threshold for DNI of about 2000 kWh/m^2/year. Below that, other solar electric technologies that take advantage of both direct and diffuse irradiance, such as PV, are assumed to have a competitive advantage. Good DNI is usually found in arid and semi-arid areas with reliably clear skies, which typically lies at latitudes from 15 to 40° North or South. As a consequence, one of the most favorable areas for the CSP technology is the Mediterranean basin. In 2010, the global stock of CSP plants neared 1 GW capacity, mainly in Spain (about 0.5 GW). Projects now in development or under construction in more than a dozen countries (including China, India, Morocco, Spain and the United States) are expected to totalize 15 GW, and CSP is expected to contribute about 5% (1500 GW) of the annual global electricity production in 2050 (IEA, 2010b). Particularly, potential in the Middle East and North Africa would cover about 100 times the current consumption of the Middle East, North Africa and the European Union combined (IEA, 2010b). Finally, wind energy is probably the most cost-effective of the renewable energy technologies. It must be stressed that wind energy was the renewable source with the fastest growing rate: since 2000, cumulative installed capacity has grown at an average rate around 30% per year (Global Wind Energy Council, 2007). In 2008, wind energy provided nearly 20% of electricity consumption in Denmark,

more than 11% in Portugal and Spain, over 4% of all EU electricity and nearly 2% in the United States (IEA, 2009). By 2030, wind electricity is estimated to be produced annually from over 1000 GW of wind installed capacity, corresponding to 9% of global electricity production with an expected rising to 12% in 2050 (IEA, 2009).

The Mediterranean area presents some special features regarding the transition from a fossil era to a greener one. In fact the region presents considerable wind and outstanding solar energy resources that would make this transition easier. According to different studies (DLR, 2007; DESERTEC, 2010; Price Water House Cooper, 2010), Europe and North Africa together could produce by 2050 about 80% of their electricity needs from renewables, if their respective grids were sufficiently interconnected.

1.1 Energy and Meteorology

The expected huge development of the renewable energies in the coming decades will demand a corresponding development of the so-called *energy meteorology* science. Energy meteorology includes all the aspects of the meteorology and climatology relevant for the renewable energies. In fact, the meteorological and climate information is a key issue at the various stages of a renewable energy project, as outlined in Fig. 1. Particularly, in the first stages (project development), the climate information is required in terms of the resource evaluation. This evaluation includes data obtained based on direct measurement, satellites and models

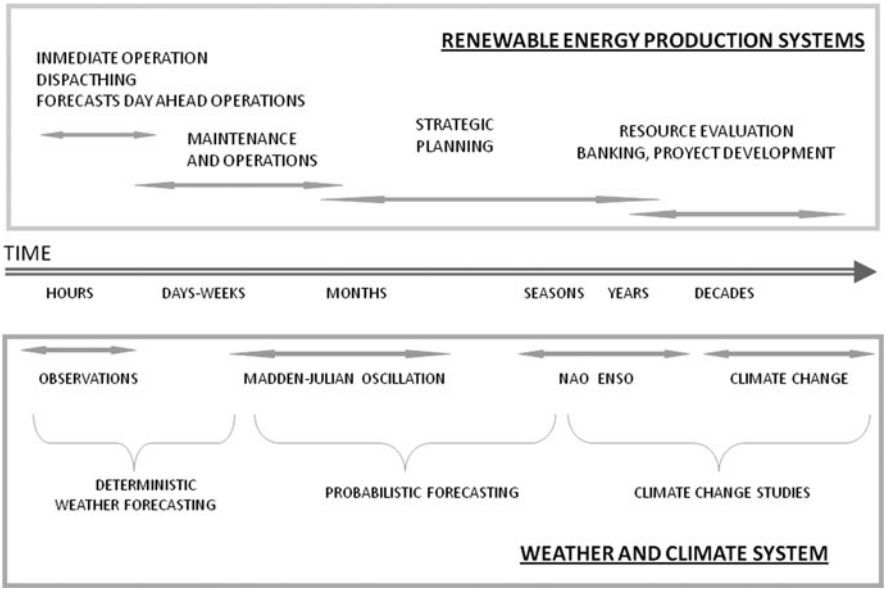

Fig. 1 The relationship between the weather and climate and different activities related to the renewable energy

estimations. Once operating, weather forecasts are needed for the yield integration in the power grid. This requires information from both satellite (nowcasting) and forecasts from Numerical Weather Prediction models (forecasting) (Lara-Fanego et al., 2011). Accurate information on expected solar irradiance or wind speed is used for the management of the electricity grids, the scheduling of conventional power plants and also for decision making on the energy market. Monthly and seasonal forecasts are also of interest for maintaining operation and strategic planning, as they can potentially allow the electricity system operators to estimate the energy production availability and the electric network operator to conveniently adapt demand and resources (Weisser and Foxon, 2003).

Accurate resource evaluation is a key issue in the first stages of a renewable energy project. Particularly, as the life span of wind farms or solar plants (both PV and STPP) is about 20 years, the economic feasibility study of the project should be considered an adequate estimation of the interannual variability of the resources. Usually, the resource evaluation is mainly based on field measurements collected at meteorological stations. Since these measures are expensive and time consuming, typically only a few years of data are available for the investment decision making (Barbour and Walker, 2008). However, a few years of measurements do not generally account for the natural climate variability of the resources. Consequently, the projected production could significantly vary from 1 year to another and through decades. Therefore, some complementary studies, usually based on satellite estimates or model simulations, are necessary for a reliable renewable energy resources evaluation. Aside from these very important economic aspects, the evaluation of interannual variability is crucial regarding the reliability of a power system with a high penetration of renewable energy. Particularly, an important area of research regarding the resources evaluation is the analysis of the balancing between different renewables. There are two different types of balancing: spatial and local balancing. Spatial balancing takes place if the combined output of many variable renewable energy plants, based on same or different resources (mainly wind and solar), at different locations over a wide area, is smoother than the output of individual power plants (von Bremen, 2008). Note that the spatial balancing is a consequence of the different weather and climate conditions over large regions. On the other hand, local balancing takes place when, within the same location, the combined output of two different renewable energy plants, based on different resources (wind and solar), is smoother along time than the output of each individual plant. Several studies show that the existence of spatial or local balancing allows increasing the reliability of solar and wind plants yields, provided the grid are sufficiently interconnected (von Bremen, 2008; Cassola et al., 2008; Kempton et al., 2010).

Although other phenomena, as aerosols or solar cycles, may play a significant role, interannual variability of the solar radiation is mainly related to changes in the cloud cover associated with changes in the large scale circulation patterns (Sanchez-Lorenzo et al., 2008, 2009; Chiacchio and Wild, 2010; Papadimas et al., 2010). Concerning the wind resources, surface winds are also mainly driven by large scale circulation. Nevertheless, local features such as surface roughness, local thermal

contrast and orography can modify their spatial and temporal features, especially in areas of complex topography as the Mediterranean region (Burlando, 2009; Li et al., 2010). On the other side, the North Atlantic Oscillation (NAO) is recognised as a major actor regarding the interannual variability of the large scale circulation in the Mediterranean area, especially during winter (Hurrell et al., 2003). Particularly, the impact of the NAO on the cloud cover variability and on solar radiation at the surface at the whole North Atlantic area has been previously described (Trigo et al., 2002; Pozo-Vázquez et al., 2004; Lohmann et al., 2006; Sanchez-Lorenzo et al., 2008, 2009; Chiacchio and Wild, 2010; Papadimas et al., 2010). However, the NAO impact on the wind and, therefore, wind energy resources is almost unexplored. Therefore, the NAO can plausibly have significant effects on the wind and solar energy resources in the Mediterranean basin which are worth to be analyzed.

In this work we present an analysis of the impact of the NAO on the solar and wind energy resources in the Mediterranean area. Particularly, the study aims to evaluate the role of the NAO in the interannual variability of the wind and solar energy. Monthly means of daily integrated wind and solar energy data, covering the whole North Atlantic and the Mediterranean area, including the north of Africa, are analyzed. The dataset was derived from satellite retrievals (solar energy) and meteorological reanalysis (wind energy and cloud cover) and extends over a period of about 20 years. We first carried out a correlation analysis to explore the linear relationship between the NAO and the solar and wind energy. An analysis of the cloud cover-NAO correlation is also undertaken. In a second part, the composite analysis is used to study the linear and non-linear component of the solar and wind energy anomalies response to the NAO phases. Finally, the eventual existence of balancing between the wind and solar energy resources associated with the NAO cycle is explored. The work is organized as follows: Section 2 describes the dataset and the processes used to derive the wind and solar energy data. Section 3 deals with the results. Finally, in Section 4 some concluding remarks are outlined.

2 Data Description

Two datasets have been used in this work. Firstly, the ERA-Interim reanalysis dataset was used to derive cloud cover data and the wind energy resources. The ERA-interim global reanalysis are the third generation of reanalysis of the European Center for Medium Range Weather Forecasting (ECMWF). Original data have a spatial resolution of about 0.7º and a temporal step of 3 h (Simmons et al., 2007). In this work we have analyzed the period 1989–2008. Wind speed at 10 m above the surface at 3 h interval was used to estimate daily integrated values of the wind energy based on:

$$E_{daily-wind} = \sum_{1}^{8} \left(\frac{1}{2} \rho v^3 \right) 3, \tag{1}$$

where v is the wind speed every 3 h and ρ is the density of the air at sea level. Note the energy units are (W·h). Based on these daily integrated wind energy estimates, monthly means values were computed. Finally, winter season and annual mean values were computed based on the monthly values. December through February were used for winter, while annual values were computed from December of the preceding year to November of the considered year. Regarding the cloud cover, daily mean values were computed based on the 3 h interval values. Then, monthly mean values and winter and annual mean values were computed based on the same procedure that for the wind data.

Solar energy was derived from the Irradiance at the Surface derived from ISCCP cloud (ISIS) dataset (Lohmann et al., 2006). It consists of 3-hourly values of direct normal and global irradiances at the surface that have been derived by means of one-dimensional radiative transfer computations. The ISIS dataset covers the time period 1984–2004, with a spatial resolution of 280 by 280 km. Note that 3-h temporal resolution of ISIS enables the study of daily cycles. The daily integrated solar energy estimates were obtained along the period 1985–2004 based on the global irradiance data:

$$E_{daily-solar} = \sum_{1}^{8} GHI \times 3, \tag{2}$$

where GHI is the global irradiance every 3 h. As for the wind energy, and based on these daily integrated solar energy estimates, monthly means values were computed and, then, winter season and annual mean values were obtained.

Both the ERA-interim and the ISIS dataset have a global coverage. In this work, although the analysis has been focused in the Mediterranean region, the study area has been extended to the whole North Atlantic region, including the north of Africa, from latitude 20º northward.

Finally, the winter and annual NAO index as defined by Hurrell et al. (2003) was used to monitor the NAO.

3 Results

3.1 NAO-Solar Energy Correlation Analysis

Figures 2a and 2b show the sample correlation coefficients between the NAO index and the solar energy for the winter and annual cases, respectively. During the winter, a dipolar pattern can be observed: while almost the whole Mediterranean region presents positive correlations, most part of central and northern Europe presents negative values. The highest positive correlation values (0.8) are located over the southwest of the Iberian Peninsula. Also over most part of the central and eastern Mediterranean area high positive values (0.6) are observed. On the other hand, the highest negative correlations are located over the north west of Russia (–0.6) and British Islands (–0.4). Note also the relatively weak, but significant, negative

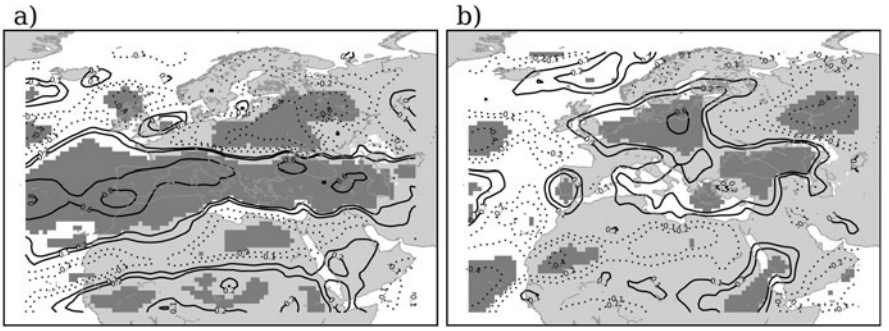

Fig. 2 (**a**) Correlation between the NAO index and the solar energy for the winter season. The period of analysis covers 2005–2004. *Dots* indicate negative correlation while *continuous line* indicates positive correlation. *Shading* indicates local statistical significance of the difference at 90% confidence level based on a t-test. (**b**) as in (**a**) but for the annual data

correlation obtained over Egypt. Results are in agreement with those recently presented by Papadimas et al. (2010), which showed the existence of a Mediterranean solar radiation spatial variability mode associated with the NAO during the winter. Regarding the annual correlation map, it resembles winter case but displaced north-eastward and with weaker values. Particularly, the highest positive correlations (0.6) are found over Poland and the Baltic area. Regarding the Mediterranean area, weak but statistically significant positive correlations (0.2) are found over the southwest of the Iberian Peninsula and the eastern Mediterranean area and weak negative correlations over the north of Egypt.

Since interannual variability of the solar radiation is mainly associated with cloud cover, the former NAO-solar energy correlation patterns should resemble the NAO-cloud cover spatial correlation over the study area. Figures 3a and 3b shows the correlation between the NAO index and the total cloud cover for the winter and

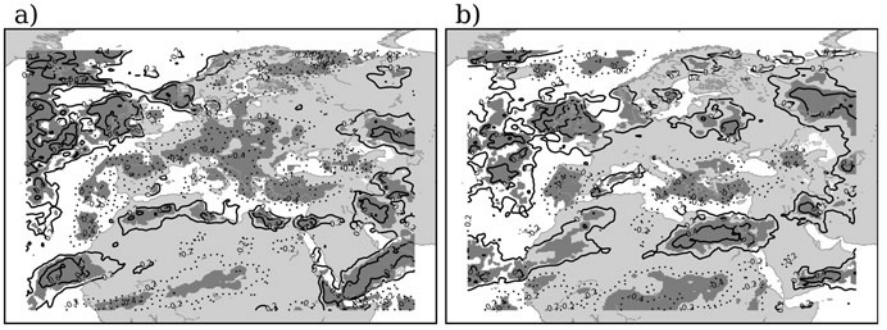

Fig. 3 (**a**) Correlation between the NAO index and the cloud cover for the winter season. The period of analysis covers 1989–2008. *Dots* indicates negative correlation while *continuous line* indicates positive correlation. *Shading* indicates local statistical significance of the difference at 90% confidence level based on a t-test. (**b**) as in (**a**) but for the annual data

annual cases, respectively. As expected, both the winter and annual patterns are in agreement with those observed in Fig. 2. In particular it should be noted the negative correlation pattern covering the majority of the Mediterranean area during winter (Fig. 3a), with the maximum negative values (–0.3) located over the central and eastern sectors. On the other hand, positive correlation values (0.6) are found over Ireland. These results are in agreement with the analysis of the cloud-cover NAO relationship of Trigo et al. (2002). Concerning the annual case (Fig. 3b), negative correlation values (about –0.3) are observed over the west of the Iberian Peninsula and the eastern Mediterranean area, in agreement with the patterns observed in Fig. 2b. In any case, correlations are, both for the winter and annual case, weaker than those obtained for the solar energy.

3.2 NAO-Wind Energy Correlation Analysis

Figure 4a, b show the correlation between the NAO index and the wind energy for the winter and annual cases, respectively. In both cases, a dipolar pattern can be observed, with negative correlation values over the whole Mediterranean region and positive correlations concentrated over central and northern Europe. Noteworthy, the correlations are weaker than those obtained for the solar energy, indicating a weaker linear relationship between the NAO and the wind energy. Note that annual dipolar pattern seems to be shifted south-eastward compared to the winter case. Particularly, for winter, the maximum positive correlations (0.6) are found over the north of the British Islands and the Scandinavian Peninsula. For the annual case, these high positive values are also observed in central Europe. On the other hand, the maximum negative values are found over Greece in winter and over the north of Algeria in the annual case. Note the striking feature over the Gibraltar Strait area during winter. Over this area, high positive correlation values (0.6) are found while

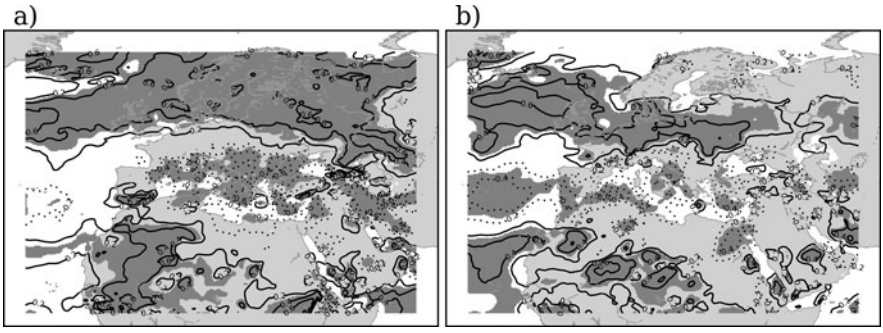

Fig. 4 (**a**) Correlation between the NAO index and the wind energy for the winter season. The period of analysis covers 1989–2008. *Dots* indicate negative correlation while *continuous line* indicates positive correlation. *Shading* indicates local statistical significance of the difference at 90% confidence level based on a t-test. (**b**) as in (**a**) but for the annual data

negative values are found in the rest of the Mediterranean area. This feature, which deserves more research in the future, is probably related to the special topographic characteristic of this area.

3.3 Solar Energy Composite Analysis

In this section, composite patterns of winter solar energy anomalies are obtained as a function of the state of the NAO. Data are represented as anomalies (in percentage) from the mean of complete study period (1985–2004). Figure 5a shows the composite of solar energy anomalies for winters in which the value of NAO index was positive (NAO>1) and Fig. 5b for winters in which the NAO index was negative (NAO<–1). The differences between positive NAO and normal NAO (i.e., –1<NAO<1) winters (Fig. 5c) and negative NAO and normal NAO winters (Fig. 5d) are also shown. Finally, the differences between the anomalies during positive and negative NAO winters (i.e., the differences between Fig. 5c, d) are represented in Fig. 5e. Note that Fig. 5c, d, f represent the spatial patterns of the maximum interannual changes (from one winter to other) that can be expected in the solar energy resources. During positive NAO winters (Fig. 5a), the solar energy presents positive anomalies over the whole Mediterranean area and negative anomalies over central Europe and the north of the British Islands. The spatial pattern of anomalies observed during negative NAO winters are similar but of reverse sign (Fig. 5b). Both patterns are in agreement with the correlation patterns presented in Fig. 2a. When comparing the anomalies during positive NAO and normal NAO winters (Fig. 5c), the whole Mediterranean area presents statistically significant positive anomalies. The maximum values (10–15%) are observed over the Iberian Peninsula, Greece and Turkey. On the other hand, the north of the British Islands presents the highest negative anomalies (about –10%). The comparison between negative and normal NAO winters (Fig. 5d) shows the existence of statistically significant negative anomalies (–4 to –8%) over the Iberian Peninsula, the south of France and over certain areas of Greece and Turkey. In addition, statistically significant positive anomalies (+4 to +8%) are found over eastern and northern Europe. By comparing the anomalies during positive and negative NAO winters (Fig. 5d), noticeable interannual changes in the availability of solar energy during the winter season can be expected in certain areas of the study region. Particularly, over the Iberian Peninsula, the northern part of Greece and Turkey, central Europe and the British Islands, interannual changes in the solar resources of values up to 15% can be expected associated with interannual changes in the NAO phase.

Similarly to Figs. 5 and 6 presents the solar energy anomalies associated with the NAO phases but on annual basis. In general, the annual spatial patterns of anomalies resemble their winter counterparts but with weaker anomalies. As for the winter case, statistically significant positive anomalies are found over the whole Mediterranean area when comparing positive NAO and normal NAO years (Fig. 6c), but anomalies are considerable weaker (about 4% compared to 10% of the winter case). When comparing negative and normal NAO years (Fig. 6d) statistically

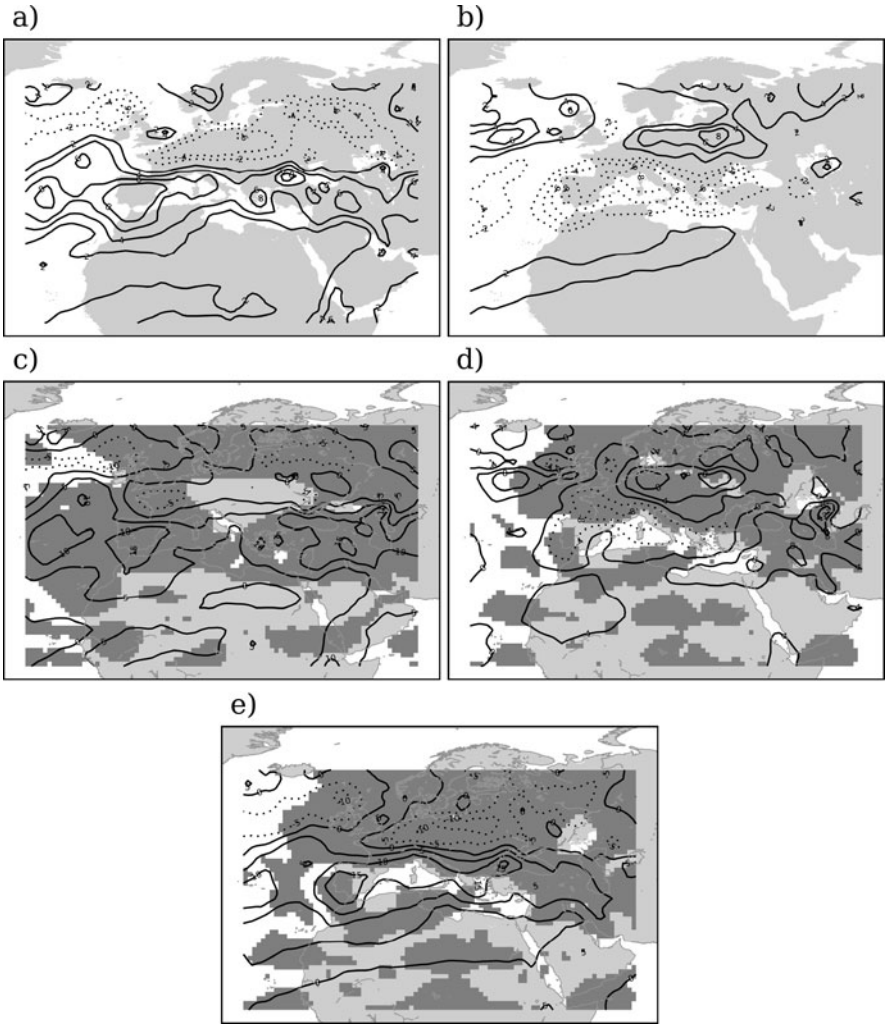

Fig. 5 Composites of winter season observed solar energy anomalies as a function of the NAO phase. (**a**) During the positive phase (NAO>1). (**b**) During the negative phase (NAO<–1). (**c**) Difference between the positive phase and the normal phase (–1<NAO<1). (**d**) Difference between the negative phase and the normal phase. (**e**) Differences between the positive and negative phase. Data are anomalies in percentage from the long term mean. *Continuous line* indicates positive or zero anomalies and *dotted line* indicates negative anomalies. *Shading* indicates local statistical significance of the difference at 90% confidence level based on a t-test

significant negative anomalies (about –3%) are found over the South of France and Italy and positive anomalies (about 2%) over the southeast of the Iberian Peninsula, Tunis and the east of Turkey. The differences between positive and negative NAO years (Fig. 6e) show that important interannual changes in the availability of solar energy can be expected in certain areas of the study region, but of a lower magnitude

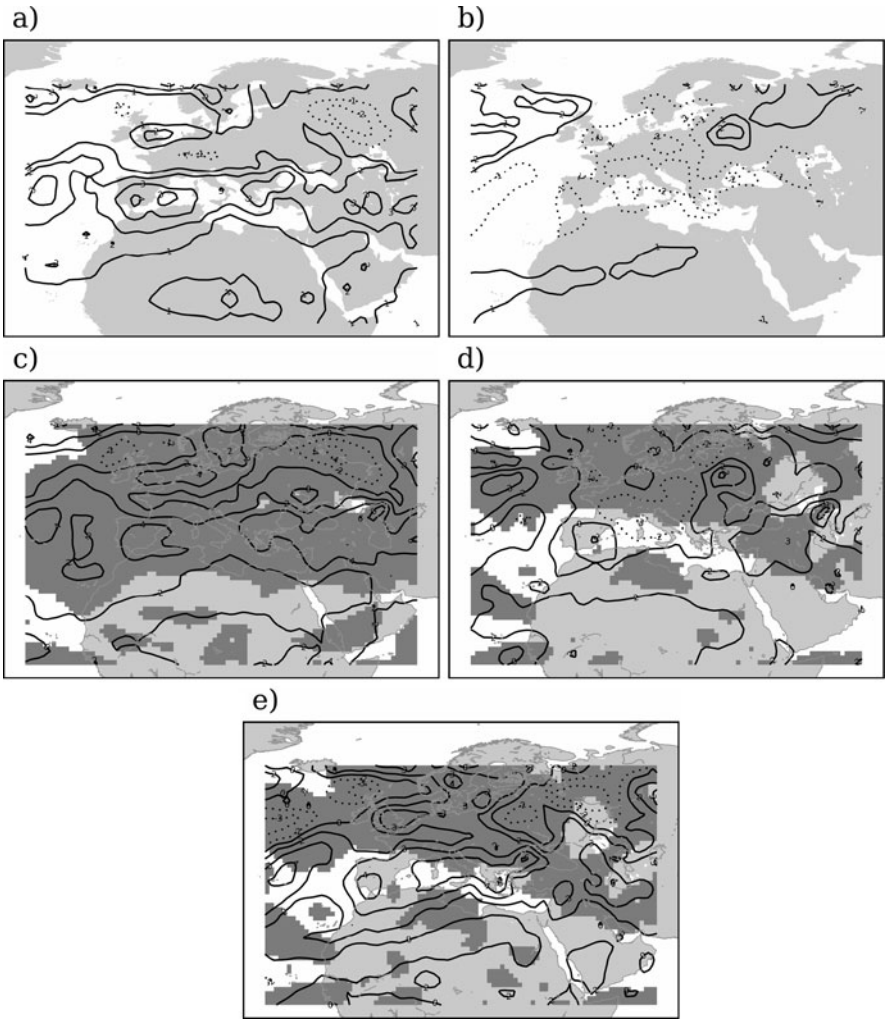

Fig. 6 As in Fig. 5 but for the annual data

than those observed for the winter case. Particularly, in the Mediterranean region, interannual changes of values, between 4 and 8%, can be expected associated with interannual changes in the NAO. Results are in agreement to Lohmann et al. (2006) analysis of the interannual variability of the GHI in the Mediterranean area.

3.4 Wind Energy Composite Analysis

As in Fig. 5 for the solar energy, Fig. 7 presents the composite patterns of wind energy anomalies during the winter associated with the different phases of the NAO.

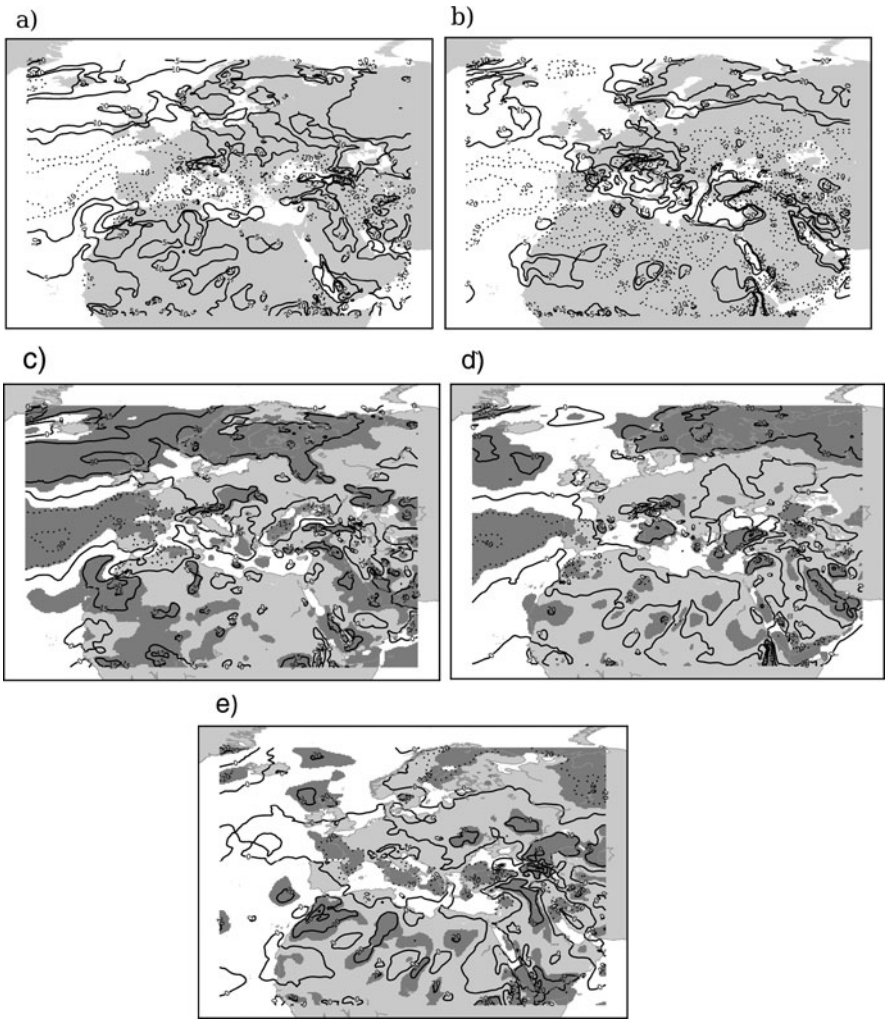

Fig. 7 As in Fig. 5 but for the wind energy anomalies

During positive NAO winters (Fig. 7a), positive anomalies are observed over the British Isles and the Scandinavian Peninsula, reaching up to 20%. Also positive anomalies but weaker (+10%) are observed over central Europe, the northwest of Morocco/Gibraltar Strait area, the north of Egypt and the eastern of Turkey. On the other hand, over the Iberian Peninsula, the central Mediterranean and the Black Sea areas, negative anomalies of values between –5 and –10% are found. When comparing these anomalies with those observed during normal NAO winters (Fig. 7c), some interesting features are obtained. Particularly, statistically significant and positive values of up to 30% are observed over the British Islands and the Scandinavian

area. Positive differences of values between 15 and 30% are observed also over the northwest of Morocco, central Europe and certain areas of the south and north of Turkey. On the other hand, statistically significant negative differences (–15 to –30%) are found over the Iberian Peninsula, north of Algeria and the northwest of Turkey. The pattern observed during negative NAO winters (Fig. 7b) is not the opposite of that observed during the positive NAO winters. This result is indicative of an important non-linear relationship between the wind energy and the NAO in the study area during winter. Particularly, during negative NAO winters, positive anomalies are observed over the whole Mediterranean basin (10–20%) and the Scandinavian area (about 20%), while negative anomalies are observed over the Iberian Peninsula (–10 to –20%). When comparing these anomalies with those found during normal winters (Fig. 7d), statistically significant positive differences are observed over Italy, Greece and Turkey (+20%) and over the Scandinavian area (+40%). On the other hand, negative differences are observed over the Iberian Peninsula and the north of Morocco (–20 to –40%). Finally, the patterns in Fig. 7e indicate that interannual changes in the winter NAO from positive to negative phase (or vice-versa) may lead to important changes in the wind resources availability. Particularly, over the central Mediterranean expected changes from one winter to other can reach about 20%, while over Turkey and the northwest of Morocco these changes can reach up 40%. Remarkably, and as a consequence of the non-linear influence of the NAO on the wind resource, anomalies observed in Fig. 7e in the Mediterranean area are of the same order of magnitude of those of Fig. 7c, d. Therefore, it can be concluded that in many areas of this region, as Turkey, Greece or the northwest of Morocco, interannual variability of the wind resources from one winter to other can be really high. This reflects the marked interannual variability of the NAO: over these areas, wind resources experiment noticeable changes from one winter to another. This happens not only when the NAO changes from the positive to the negative phase, but also when the NAO changes from a positive or negative phase to a normal phase or vice-versa (Fig. 7c–e).

The composite anomaly patterns for the annual case (Fig. 8) are similar to their winter counterparts but displaced south-eastward and with weaker anomalies. Particularly, as for the winter case, and as may be expected from Fig. 4b, the annual case also presents an important non-linear relationship between the NAO and the wind energy resources. Notably, Fig. 8a, b do not present opposite patterns. Statistically significant negative anomalies (about –8%) are found over the central Mediterranean area when comparing positive NAO and normal NAO years (Fig. 8c). Positive anomalies are observed over central and northern Europe and over the Iberian Peninsula, with values in the order of 8%. When comparing negative and normal NAO years (Fig. 8d) statistically significant and positive differences (with values about 10%) are found over the central and eastern Mediterranean areas, the north of the Iberian Peninsula and some areas in central and northern Europe. On the other hand, statistically significant negative differences are observed over the south of the Iberian Peninsula and the north of Morocco and Algeria. Finally, Fig. 8f indicates the existence of an important interannual variability of the wind resources in the study region associated with interannual changes in the NAO from

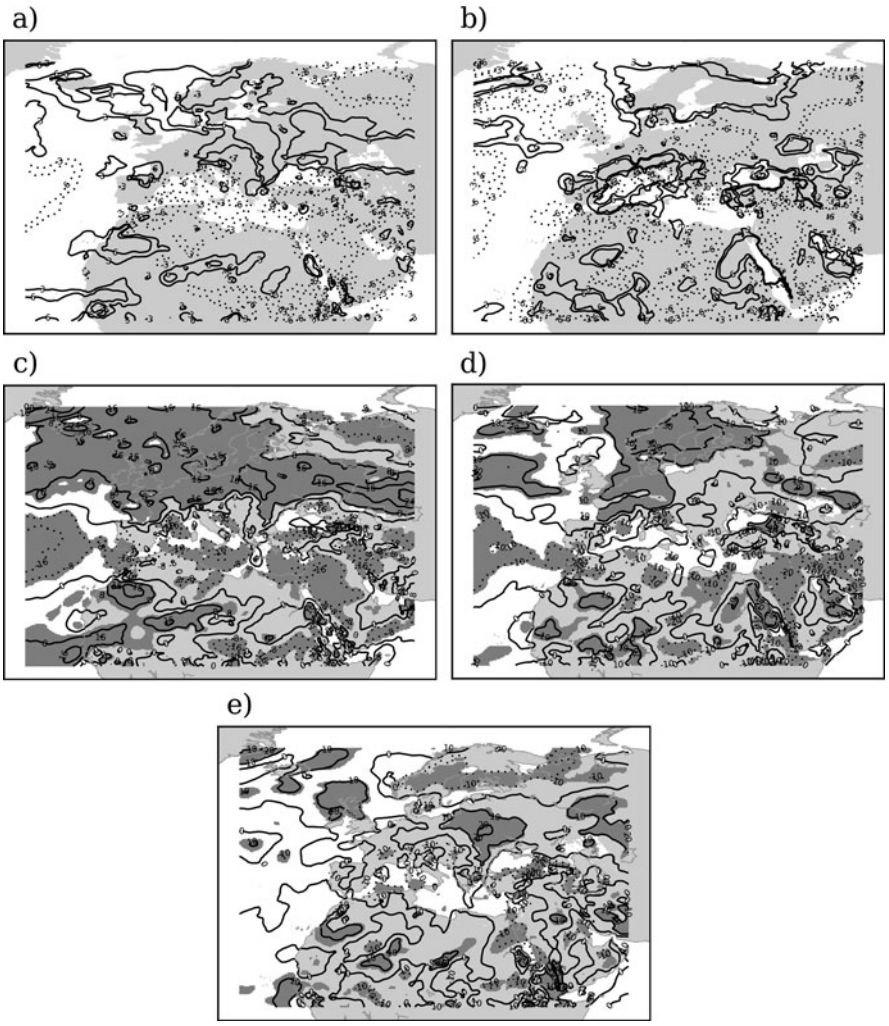

Fig. 8 As in Fig. 7 but for the annual data

positive to negative phase (or vice-versa). Particularly, in the central and eastern part of Mediterranean region, over the Gibraltar Strait area and over the northwest of Morocco, these changes can reach up to 10%. Nevertheless, and as a consequence of the important non-linear relationship between the wind energy resources and the NAO, these changes are of a lower magnitude than the changes observed when the NAO changes from a positive or negative phase to the normal phase (or vice-versa) (Fig. 8c, d). Similarly to the winter analysis, it can be concluded that in certain areas of the Mediterranean (namely the northwest of Morocco, the Gibraltar Strait and Greece), interannual variability of the wind resources can be really high. This situation reflects the fact that wind resources over these areas experiment marked

changes from 1 year to other not only when the NAO changes from the positive to the negative phase, but also when the NAO changes from a positive or negative phase to a normal phase or vice-versa (Fig. 8c–e).

3.5 The NAO and the Balancing of the Solar and Wind Energy Resources

The previous sections revealed that the variability of the solar and wind energy resources in the study region associated with the NAO presents considerable spatial differences. Notably, the spatial patterns of the NAO influence on the solar and wind resources reveal in some cases the existence of spatial balancing. For instance, the dipolar pattern of the spatial correlation in Fig. 2a indicates the existence of spatial balancing of the solar resources between the central and northern Europe, on one side, and the Mediterranean basin, on the other. Even more, there exists also a weaker but more interesting (because of the availability of the solar resources) balancing between the north of Egypt and the rest of the Mediterranean area. Unfortunately this spatial balancing is not present in the annual analysis (Fig. 2b). Regarding the wind, the dipolar pattern in Fig. 4a also reveals the existence of spatial balancing between northern Europe and the Mediterranean area as earlier highlighted by Pryor et al. (2006). Compared to the winter solar energy case, the strength of this balancing seems to be weaker. In addition, during winter, there exists also spatial balancing between the western Mediterranean (Gibraltar strait) and the rest of the Mediterranean region. Regarding the annual case, and unlike the solar resources, the spatial balancing is also present but displaced southwest-ward (Fig. 4b). Finally, the comparison of Figs. 2a and 4a reveals that the NAO impact on the solar and wind resources over the study area presents a similar north-south dipolar pattern but the sign of the dipoles are just opposite. Therefore, it can be concluded the existence of a notably local balancing between the solar and wind resources almost over the whole study region during winter. Regarding the Mediterranean region, the strength of this balancing seems to be especially high in the central part, over Greece, where correlation between the NAO and the solar energy is higher than 0.6 (Fig. 2a) and between the NAO and the wind energy with *circa* –0.6 (Fig. 4a). For the annual case (Figs. 2b and 4b) the balancing is also present but weaker. Concerning the Mediterranean area, the southwest of the Iberian Peninsula, Greece and Turkey present a remarkable balancing. For instance, over the southwest of Iberian Peninsula the NAO-solar energy correlation reaches about 0.2 while NAO-wind energy correlation is about –0.4.

4 Summary and Conclusions

The influence of the NAO on the solar and wind energy resources in the Mediterranean area has been explored based on the analysis of 20 years of reanalysis and satellite data. Particularly, the role of the NAO cycle in the interannual

variability of the solar and wind energy resources was analyzed based on correlation and composite analysis. Although the study is focused on the Mediterranean area, for the sake of completeness, the analysed data covered the whole North Atlantic and Mediterranean area, including the north of Africa. The analysis was carried out twice for the winter and annual periods and aimed to contribute to a better understanding of renewable energy resources in the study region.

Regarding the winter solar energy, a north south dipolar pattern of correlation was found, with the positive centre of the dipole over the Mediterranean and the negative one over central and northern Europe. Correlation coefficient over the whole Mediterranean area reached values above 0.6, with the highest value (0.8) over the Iberian Peninsula. The annual case presented a correlation map resembling the winter case but displaced north-eastward and with weaker values. A similar analysis for the cloud cover instead of for the solar energy was able to explain the former results. In any case, the NAO-cloud cover correlation was found, both for the winter and annual case, to be weaker than those obtained for the solar energy. The composite analysis revealed some additional features of the NAO-solar energy relationship. Particularly, positive anomalies (10–15%) were found over the Iberian Peninsula, Greece and Turkey associated with the positive phase NAO winters. On the other hand, during negative NAO winters, negative anomalies (–4 to –8%) were found over the Iberian Peninsula, the south of France, Greece and Turkey. As a consequence, over these areas, interannual changes in the winter solar energy resources of values of up to 15% can be expected associated with interannual changes in the NAO phase. Regarding the annual analysis, the composite analysis showed similar results but anomalies were considerable weaker. For instance, the positive NAO years were found associated with positive anomalies (4%) over the whole Mediterranean area. Negative NAO years were found associated with negative anomalies over the South of France and Italy (–3%) and positive anomalies (2%) over the southeast of the Iberian Peninsula, Tunis and the east of Turkey. As a consequence, for the entire Mediterranean region, interannual changes of values between 4 and 8% were found associated with interannual changes in the NAO phase.

The NAO-wind energy relationship was found to be considerably more complex than the NAO-solar energy one. Particularly, the winter correlation analysis proved the existence of north-south dipolar pattern, with positive values over central and northern Europe and negative values over the Mediterranean area. For the latter area, negative correlation values (–0.4 to –0.6) were observed, except over the Gibraltar Strait area, where positive correlation values were found. The annual correlation analysis showed a similar pattern, but shifted south-eastward. Thus over the Mediterranean area, the maximum negative values were observed over Greece (–0.6) in the winter case and over Algeria (–0.6) in the annual case. Noteworthy, in general the correlations were weaker than for the solar energy case, indicating a weaker linear relationship between the NAO and the wind energy. The composite analysis revealed additional features regarding the complex relationship between the NAO and the wind energy in the study area. For instance, the winter analysis proved the existence of positive anomalies (15–30%) over the northwest of Morocco and the south and north of Turkey, and negative anomalies (–15 to –30%)

over the Iberian Peninsula, north of Algeria and the northwest of Turkey associated with the positive phase of the NAO. The composite pattern observed during negative NAO winters was not the opposite of the observed during the positive NAO winters. Particularly, the main features during this negative phase were the presence of positive anomalies (+20%) over Italy, Greece and Turkey and negative anomalies (–20 to –40%) over the Iberian Peninsula and the north of Morocco. As a consequence, notable interannual changes in the winter wind energy resources associated with interannual changes in the NAO phase were found over the central Mediterranean (20%), Turkey and the northwest of Morocco (+40%). The annual composite patterns showed to be similar to their winter counterparts but the patterns were displaced south-eastward and the anomalies were weaker. Particularly, over the central Mediterranean, negative anomalies (–8%) were found associated with the positive phase of the NAO. During the negative phase, positive anomalies (10%) were found over the central and eastern Mediterranean area and the north of the Iberian Peninsula, while negative anomalies (–10%) were found over the south of the Iberian Peninsula and the north of Morocco and Algeria. Consequently, interannual changes in the annual wind resources of values over 10% were found in the central and eastern part of Mediterranean region, over the Gibraltar Strait area and over the northwest of Morocco associated with interannual changes in the NAO phase.

Finally, the analysis of the spatial patterns of the NAO influence on the solar and wind energy resources revealed the existence of spatial and local balancing. Among others, the dipolar pattern of the spatial correlation obtained for the solar energy during winter indicated the existence of spatial balancing of the solar resources between the central and northern Europe and the Mediterranean. However, it should be noted that this spatial balancing was not present in the annual analysis. The dipolar pattern of the winter NAO-wind energy relationship also revealed the existence of spatial balancing between northern Europe and the Mediterranean area for the wind energy. Nevertheless, compared to the winter solar energy case, the strength of this balancing was found to be weaker. In addition, during winter, spatial balancing between the western Mediterranean (Gibraltar Strait) and the rest of the Mediterranean region was also found. Regarding the annual case, and unlike the solar resources, the spatial balancing was also present but displaced south-westward. In addition to the spatial balancing found for the wind and the solar energy, a significant local balancing between the solar and wind resources almost over the whole study region was found associated with the NAO cycle. Regarding the Mediterranean region and during winter, the strength of this balancing was found to be especially high in the central section. In the annual case the most important local balancing was found over the southwest of the Iberian Peninsula, Greece and Turkey, although the magnitude was weaker than in the winter case.

The authors believe that the results above summarized are of interest regarding the solar and wind energy resources evaluation in the Mediterranean area. In this regard we would like to emphasise that, in the light of results obtained here, a more in depth assessments of solar and wind resources should be required and that measuring solar and wind data covering only a few years should be avoided. This will

provide a better estimation of the expected interannual variability of the renewable resources and, therefore, of the plant production interannual variability.

Acknowledgements The Spanish Ministry of Science and Technology (grant ENE2007-67849-C02-01) and the Andalusian Ministry of Science and Technology (grant P07-RNM-02872) and FEDER funds financed this study. Support is also obtained from the Plan Andaluz de Investigación (Grupo TEP-220). The DLR-ISIS data images were obtained from the Institute of Atmospheric Physics, German Aerospace Center (DLR) (Lohmann, 2006).

References

Barbour P, Walker S (2008) Wind resource evaluation: Eola Hills. Technical report, Energy Resources Research Laboratory, Department of Mechanical Engineering, Oregon State University, Corvallis, OR

Burlando M (2009) The synoptic-scale surface wind climate regimes of the Mediterranean Sea according to the cluster analysis of ERA-40 wind fields. Theor Appl Climatol 96:69–83

Cassola F, Burlando M, Antonelli M, Corrado FR (2008) Optimization of the regional spatial distribution of wind power plants to minimize the variability of wind energy input into power supply systems. J Appl Meteorol Climatol 47:3099–3116

Chiacchio M, Wild M (2010) Influence of NAO and clouds on long-term seasonal variations of surface solar radiation in Europe. J Geophys Res 115:D00D22. doi:10.1029/2009JD012182

DESERTEC (2010) DESERTEC Red paper. An overview of the DESERTEC concept. DESERTEC organization. http://www.desertec.org/

DLR (2007) TRANS-CSP. DLR-ITT technical report, Köln, Germany

Global Wind Energy Council (2007) Global wind energy council report. http://www.gwec.net/uploads/media/Global_Wind_2007_Report_final.pdf

Hurrell JW, Kushnir Y, Visbeck M, Ottersen G (2003) An overview of the North Atlantic Oscillation. In: Hurrell JW et al (eds) The North Atlantic Oscillation: climate significance and environmental impact. Geophys Monogr Ser, vol 134. AGU, Washington, DC, pp 1–35

IEA (2008) World energy outlook. International Energy Agency, OECD Publication

IEA (2009) Technology roadmap. Wind energy. International Energy, OECD Publication

IEA (2010a) Technology roadmap. Solar photovoltaic energy. International Energy, OECD Publication

IEA (2010b) Technology roadmap. Concentrating solar power. International Energy, OECD Publication

Kempton W, Pimenta FM, Veron DE, Colle BA (2010) Electric power from offshore wind via synoptic-scale interconnection. Proc Natl Acad Sci 107:7240–7245

Lara-Fanego V, Ruiz-Arias JA, Pozo-Vázquez D, Santos-Alamillos F, Tovar-Pescador J (2011) Evaluation of the WRF model solar irradiance forecasts in Andalusia (southern Spain). Sol Energy, doi:10.1016/j.solener.2011.02.014

Li X, Zhong S, Blan X, Hellman WE (2010) Climate and climate variability of the wind power resources in the Great Lakes region of the United States. J Geophys Res 115:D18107. doi:10.1029/2009JD013415

Lohmann S, Schillings C, Mayer B, Meyer R (2006) Long-term variability of solar direct and global radiation derived from ISCCP data and comparison with reanalysis data. Solar Energy 80:1390–1401

Papadimas CD, Fotiadi AK, Hatzianastassiou N, Vardavas I, Bartzokas A (2010) Regional co-variability and teleconnection patterns in surface solar radiation on a planetary scale. Int J Climatol 30:2314–2329

Pozo-Vázquez D, Tovar-Pescador J, Gámiz-Fortis SR, Esteban-Parra MJ, Castro-Díez Y (2004) NAO and solar radiation variability in the European North Atlantic region. Geophys Res Lett 31. doi:10.1029/2003GL018502

Price Water House Coopers (2010) 100% *Renewable electricity: a roadmap to 2050 for Europe and North Africa*. Price Water House Coopers, London

Pryor S, Barthelmie R, Shoof JT (2006) Inter-annual variability of wind indices across Europe. Wind Energy 9:27–38

Sanchez-Lorenzo A, Calbó J, Brunetti M, Deser C (2009) Dimming/brightening over the Iberian Peninsula: trends in sunshine duration and cloud cover and their relations with atmospheric circulation. J Geophys Res 114:D00D09. doi:10.1029/2008JD011394

Sanchez-Lorenzo A, Calbó J, Martin-Vide J (2008) Spatial and temporal trends in sunshine duration over Western Europe (1938–2004). J Clim 21:6089–6098

Simmons A, Uppala S, Dee D, Kobayashi S (2007) ERA-I: new ECMWF reanalysis products from 1989 onwards. ECMWF Newsletter 110:25–35

Trigo RM, Osborn TJ, Corte-Real JM (2002) The North Atlantic Oscillation influence on Europe: climate impacts and associated physical mechanisms. Clim Res 20:9–17

von Bremen L (2008) Large-scale variability of weather dependent renewable energy sources. In: Troccoli A (ed) Management of weather and climate risk in the energy industry. Springer, The Netherlands, pp 189–205

Weisser D, Foxon T (2003) Implications of seasonal and diurnal variations of wind velocity for power output estimation of a turbine: a case study of Grenada. Int J Energy Res 27:1165–1179

Index

S.M. Vicente-Serrano, R.M. Trigo (eds.), *Hydrological, Socioeconomic and Ecological Impacts of the North Atlantic Oscillation in the Mediterranean Region*, Advances in Global Change Research 46, DOI 10.1007/978-94-007-1372-7,